DEVELOPMENT OF RAPID CHARACTERIZATION METHODS AND STABILIZATION OF EXPANSIVE SOIL

A THESIS

submitted by

ASHOK KUMAR T

for the award of the degree

of

DOCTOR OF PHILOSOPHY

GEOTECHNICAL ENGINEERING DIVISON

DEPARTMENT OF CIVIL ENGINEERING

INDIAN INSTITUTE OF TECHNOLOGY MADRAS

NOVEMBER 2019

Dedicated to

God

my mother,

my brother-Nagarajan,

my sister – Parameshwari,

THESIS CERTIFICATE

This is to certify that the thesis entitled **DEVELOPMENT OF RAPID CHARACTERIZATION METHODS AND STABILIZATION OF EXPANSIVE SOIL**, submitted by **ASHOK KUMAR T**, to the **Indian Institute of Technology Madras**, for the award of the degree of **Doctor of Philosophy**, is a bonafide report of the research work done by him under our supervision. The contents of this thesis, in full or parts, have not been submitted to any other Institute or University for the award of any other degree or diploma. This research was carried out at Indian Institute of Technology, Madras.

Dr. T. Thyagaraj
Research Advisor
Associate Professor
Geotechnical Engineering Division
Department of Civil Engineering
IIT Madras, Chennai

Prof. R. G. Robinson
Research Advisor
Professor
Geotechnical Engineering Division
Department of Civil Engineering
IIT Madras, Chennai

Date: 18/11/2019

Place: Chennai - 600036

ACKNOWLEDGMENTS

I would like to express deep sense of gratitude to my research guides **Dr.T. Thyagaraj** and **Prof. R. G. Robinson** for their valuable guidance, invaluable suggestions and constant encouragement and support during my research. I would like to thank for being the best teacher and guide during my course of study at IIT Madras.

I express my sincere thanks to **Prof. K. Ramamurthy** Head, Department of Civil Engineering and to my Doctoral Committee members **Prof. Manu Santhanam, Dr. Subhadeep Baneerjee , and Dr. Abhijit Chaudhuri** for the their time and effort in reviewing my progress and for their valuable suggestions.

I would like to thank **Prof. K. Rajagopal, Prof. A. Boominathan, Prof. G. R. Dodagoudar, Dr. V. B. Maji, Dr. Dali Naidu Arnepalli**, **Dr. Subhadeep Baneerjee**, and **Dr. K. Ramesh Kannan** faculty members of Geotechnical Engineering Division, for their critical comments and invaluable suggestions at various stages of the research work.

I express my sincere thanks to **Mr. Murali, Mr. Prince, Mr. David Mr. Balasubrahmanian,** and **Mr. Nagarajan** Civil Engineering workshop, for their immense help to fabricate experimental setups with great care. I would like to thank **Mr. K. Om Prakash, Mr. P. Suresh, Mr. Madhan Vel Narayanan, Mr. Gothanda Raman, Mr. Dhasthageer** and **Mr. Aravind Raj**, for their help while doing experiments in the Geotechnical Engineering Laboratory. I would like to thank the staffs of Head of Department office for their help in academic related matters.

I thank my friends and lab mates for their timely help and support, **Sundaravel, Senthilkumar, Lini, Saranya, Julina, Shivasamy, Sriram, Swagatika, Raheena, Sabari Ramesh, Kumar, Azneb, Amal and Raja**.

I would also thank to my friends, **Subramaniam, Ganesh Kumar, Sridhar, and Prasanna** for supporting me during my stay in IIT Madras

Ashok Kumar T

ABSTRACT

KEYWORDS: Expansive soils, Swell pressure, back pressure saturation, compensating material, stabilization, fly ash, swell-shrink cycles, infiltration, leaching

Expansive soils are known for their volume change behaviour due to hydration of hydrophilic minerals present in them. To identify and classify the degree of soil expansion, both qualitative and quantitative methods are followed in the current practice. The qualitative methods include the Atterberg limits, free swell index tests, free swell ratio, etc., but these methods do not incorporate the placement conditions in the swell values obtained from these tests as they are carried out on remoulded or powdered soils. Swell potential and swell pressure tests provide the quantitative swell parameters in the current practice, but these tests are time-consuming. Factors such as stress path, dry density, water content, degree of saturation, wetting sequence and method of testing affect the volume change and swell parameters. Therefore, an attempt is made in the present study to include the placement conditions in the free swell tests using small compacted or undisturbed soil specimens instead of the powdered soil samples used in the conventional free swell tests.

Literature demonstrates the evolution of several treatment methods for controlling the detrimental volume change of expansive soils. Among them, the soil replacement technique finds its place due to its simplicity and economy. However, the mechanisms of replacement technique in specific were not explored in detail. Previous research reported that the mechanisms of cohesive non-swelling (CNS) material in controlling the volume change of expansive soils are cohesive force and surcharge pressure. However, the understanding of the mechanisms of soil replacement technique in controlling the volume change of expansive soils was mainly based on the mechanical behaviour. As the compensating materials are expected to control the infiltration of water into the expansive soils, it is also expected to change their swell-shrink behaviour.. Therefore, it becomes important to understand the mechanism of replacement material from the hydraulic perspective, and thus forms the focus of the present study. Further, the availability of CNS materials near the construction site remains as a great challenge. In such cases, the locally available soils are chemically modified using lime and fly ash for preparing the chemically stabilized soil (CSS) cushion as an alternate. Therefore, an attempt is made in

the present study to understand the mechanism of stabilization of underlying expansive soil through leaching of lime from the overlying CSS material.

The depth of active zone in some arid and semi-arid regions extends to 6-11m. In such cases, the in-situ deep stabilization techniques like lime column, lime pile and lime slurry injection techniques are being used for controlling the volume change. Little (1995) and Thyagaraj and Suresh (2012) reported that the lime slurry injected soil showed significant improvement in the engineering behaviour of expansive soils. However, the effectiveness of lime, fly ash (Class F) and lime-fly ash slurry injection in deep stabilization of expansive soils when subjected to wet-dry cycles is not known. Therefore, the present research also examines the wet-dry durability of lime, fly ash and lime-fly ash slurry injected expansive soil in desiccated state.

In order to achieve the above stated objectives, series of experiments were carried out on different soils. First series of experiments were carried out on 28 natural soils for the development of rapid characterization methods which led to the development of new classification chart and table for soil expansivity. This method consists of performing free swell tests in 100 ml measuring jars as in the conventional free swell index tests but using undisturbed or compacted soil specimens instead of powdered soils in order to include the placement conditions in the measurement. Another series of experiments were carried out to accelerate the testing time using constant rate of strain (CRS) apparatus for obtaining the swell parameters – swell potential and swell pressure. The acceleration in swelling was achieved through back pressure saturation instead of conventional method of submergence. Constant rate of strain consolidation testing was carried out during consolidation stage for the determination of swell pressure.

For shallow stabilization of expansive soils, four series of experiments were carried out using four different compensating materials – sand, non-swelling soil, CNS and CSS materials – with a special emphasis on understanding the mechanisms from both mechanical and hydraulic perspectives. The hydraulic response was studied through both infiltration and hydraulic conductivity tests using oedometric-infiltrometer cells and flexible wall permeameters. Further, the mechanism of stabilization of underlying expansive soil through leaching of lime from the overlying CSS material was studied using a flexible wall permeameter under the effective confining pressure of 40 kPa. The effectiveness of compensating materials was also evaluated during wet-dry cycles.

The effectiveness of slurry injection technique in deep stabilization of expansive soils using lime, fly ash and lime-fly ash slurries was brought out in the laboratory test tanks. The expansive soil was compacted to 95% of maximum dry density at 2.5% wet of optimum moisture content in the test tanks and then desiccated in direct sunlight. Then, lime/ fly ash/ lime-fly ash slurry was injected through a central hole and cured for 28 days. The water-binder ratios of the fly ash and lime-fly ash slurries were evaluated using the mini-slump tests and the same were adopted for the slurry injection in desiccated expansive soil. After 28 days of curing, the slurry treated expansive soils were subjected to wet-dry cycles in the test tanks under a seating pressure of 6.25 kPa. Further, the undisturbed specimens were obtained from the test tanks after four wet-dry cycles for further evaluation of treated soils.

The experimental results demonstrate that there exists a good correlation between the proposed method of desiccated state free swell (DSFS) values and oedometer swell potential values. Based on this correlation a classification chart and table are proposed for expansive soil identification and classification of degree of expansivity of soils. Further, this proposed classification chat is also validated using additional data obtained from10 undisturbed soil specimens collected from the field. Further, the accelerated method using CRS apparatus decreased the testing time by 7-13 times for obtaining the swell parameters with reference to the conventional oedometer method. Compared to the conventional method, the swell potential and swell pressure values obtained with the back pressure saturation were found to be higher by about 19-34% and 6-28 %, respectively. This is attributed to the attainment of greater saturation using back pressure saturation technique.

The top inundation of two-layer system of different compensating materials and expansive soils showed that the compensating materials delayed the activation of swelling and time required for equilibrium due to the impervious nature of the compensating materials. The time delay for swell activation was very short for the sand, and it was very long for the CNS material. The impervious nature of the compensating materials was further studied with hydraulic conductivity studies which showed that the hydraulic conductivity of CNS material varied from 10^{-6} to 10^{-8} cm/s, whereas it varied from 10^{-3} to 10^{-5} cm/s for the sand, NSS and CSS material. As the hydraulic conductivity of CNS material was low, the infiltration tests were carried out on CNS material. The infiltration rates of CNS material were found to be 6.25×10^{-7} cm/s and 5.0×10^{-7} cm/s at standard and modified Proctor placement conditions, respectively. Therefore, placement of impervious material like CNS over the expansive soil slows down the moisture migration into the CNS layer and reduces the active zone depth, and thereby, controls the swell-shrink potentials. The mechanisms controlling the volume change of expansive soils stabilized with compensating materials are summarized as – removal and replacement of expansive soil in the active zone, overburden stress of compensating materials, impervious nature of compensating materials, variation in depth of active zone and mechanism of chemical stabilization due to leaching in the case of CSS stabilized expansive soil. Among the above mechanisms, the removal and replacement mechanism and impervious nature were found to be the major mechanisms contributing to the control of swell-shrink movements of expansive soils.

Deep stabilization of expansive soil using both lime and lime-fly ash slurry injected expansive soils in desiccated state showed a significant improvement during the first wetting cycle owing to the greater pH values of lime and lime-fly ash slurries (12.76-12.65), which produced a conducive environment for the pozzolanic reactions to occur. However, the fly ash slurry injected soil behaviour was almost similar to the untreated soil behaviour as the pH of the fly ash slurry solution was low (7.50). During successive wet-dry cycles, the volumetric deformation of both lime and lime-fly ash slurry treated expansive soils increased due to deterioration of cementitious bonds and leaching of lime with wet-dry cycles.

The present experimental work reveals that both shallow stabilization of expansive soil using CNS material and deep stabilization of expansive soil using lime and lime-slurry injection definitely controls the volume change of expansive soils even during wet-dry cycles as the fluctuations in moisture content with depth within the active zone are far lower than that are simulated in the laboratory conditions.

TABLE OF CONTENTS

LIST OF TABLES

LIST OF FIGURES

NOMENCLATURE

English Symbols

d	diameter of central injection hole
D_r	Relative Density
k	Hydraulic conductivity
I_{inflow}	Inflow Infiltration rate
h	Ponding depth
L	Depth of wetting front
e_{comp}	Initial void ratio at compacted state
Δe	change one void ratio form compacted to desiccated state
Z	depth of active zone
σ_v’	Average effective stress
u_b	Pore pressure
A_T	Total surface area of soil specimen
A_S	Area of soil surface
A_C	Area of cracks

Greek Symbols

θ_S	Saturated volumetric water content
θ_i	Initial volumetric water content
ψ_f	Matric potential at wetting front

Abbreviations

CNS	Cohesive Non-Swelling

NSS	Non Swelling Soil
CSS	Chemically Stabilized Soil
OMC	Optimum Moisture Content
MDD	Maximum Dry Density
CRS	Constant Rate of Strain Loading
FSI	Free Swell Index
FSR	Free Swell Ratio
FSV	Free Swell Value
DSFS	Desiccated State Free Swell
CSFS	Compacted State Free Swell
TR	Thickness Ratio

CHAPTER 1

INTRODUCTION

1.1 BACKGROUND

Construction of lightly loaded structures over expansive clays is always an issue owing to their high swell-shrink movements due to seasonal moisture fluctuations. The high swell-shrink potentials of these soils are attributed to the presence of the montmorillonite mineral which is also called as smectite (Chen, 1975). In India, these soils are commonly called as black cotton soils and cover about 20% of land area. The high swell-shrink movements of these soils cause distress to the lightly loaded structures and lead to the development of cracks in buildings, failure of pavements, runways, sewer lines, water lines and irrigation structures, etc. (Nelson *et al.*, 2015). Therefore, identification and classification of degree of expansion of soils becomes equally important to treatment method as it aids in selection of suitable treatment method.

In order to determine the degree of expansion of soils both qualitative and quantitative methods are used in geotechnical engineering practice. Even though qualitative methods like free swell index are attractive, simple and extensively used, they suffer from their own limitations. The quantitative methods are effective, but they are time consuming. As improper characterization may lead to failure of structures founded on them, the characterization becomes important and calls for new methods which quantify the degree of expansion and at the same time they should be easy to carry out. Therefore, the present research aims at developing new methods of characterization for identifying the expansive soils and evaluating the degree of expansivity.

Owing to the effectiveness and availability, the waste materials like fly ash are used as an additive for chemical modification. Fly ash is a product obtained by combustion of sub-bituminous coal which is collected in electrostatic precipitators. The fly ash particles are spherical in shape and often covered with calcium, and it initiates the formation of the cementitious products when it reacts with water in soil (Das and Yudhbir, 2005). In India, nearly 75% of electricity is obtained by the mode of thermal power plants and hence the fly ash generation has increased to about 196.14 million tons during the year 2017-2018 (Central Electricity Authority, India 2018). Since the fly ash is provided in large quantity, the disposal of fly ash is a great problem. Since the quantity is large, there is a problem in disposing the fly ash. The utilization of fly ash in large quantities is possible in various engineering applications as partial replacement of cement, embankment or fill materials, stabilizing agent, and as mineral filler in asphalt paving mixtures, etc. (ACAA, 1998).

The selection of method of treatment of expansive soil depends on swell pressure and depth of active zone. For shallow active depths, the volume change of expansive soils can be controlled by various methods, such as moisture control, compensating material (sand cushion, cohesive non-swelling (CNS) layer) and chemical modification (Chen, 1975; Nelson and Miller, 1992). Among these methods, the use of compensating material is more attractive for shallow stabilization (Bharadwaj, 2013). Earlier studies reported different compensating materials like CNS and chemically stabilized soil (CSS) in controlling the volume change of expansive soils (Katti, 1978; Sivapullaiah *et al*., 2004). However, previous researchers have studied only the mechanical behaviour of compensating material, and the studies related to the hydraulic properties of compensating materials and mechanisms of impervious barrier are limited.

In places where the active zone depth ranges from 6-11 m (Nelson *et al*., 2015), the methods like lime column, lime pile and lime slurry injection are effective in controlling the volume change. Little (1995) and Thyagaraj and Suresh (2012) reported that the lime slurry injected soil showed significant improvement in the engineering behaviour of expansive soils. However, the effectiveness of fly ash (Class F) and lime slurry injection in the deep stabilization of expansive soils is not known. Therefore, the present research also aims at stabilizing the expansive soil at both shallow and deep depths.

1.2 NEED FOR THE STUDY

The following points emerge from the detailed literature review:

1. Among the various available qualitative method for the characterization of expansive soils, the differential free swell test is extensively used to classify the expansive clay because of its determination is simple. However, this method does not include the factors like dry density and moisture content of natural soil deposits and compacted soils on the measured swell values. Therefore, there is a definite need to develop new methods of characterisation of expansive soils which includes the effects of moisture content and dry density.

2. The measurement of swell parameters using conventional methods is often tedious and time consuming. Hence, there is a need for alternate methods for swell characterization which consume less time and easy to perform
3. CNS material is being used as a cushion in controlling the heave. However, understanding of the mechanism of CNS with respect to the hydraulic response is lacking. Further, the availability of CNS material near the construction sites remains as a challenge. In such cases, the locally available soils are chemically modified using lime and fly ash for preparing the CSS cushion as an alternate. Therefore, the behaviour of CNS and CSS cushions during wetting and drying cycles needs examination.
4. Numerous studies were reported in the literature where lime slurry is used for the deep stabilization of expansive soil. However, the behaviour of lime slurry, fly ash slurry and lime-fly ash slurry treated expansive soil during wetting and drying is not known and need examination.

1.3. OBJECTIVES

The main objectives of the present study are as follows:

1. To develop a rapid method of characterization for classification of expansive soils which incorporates the effect of dry density and moisture content, adopting the free swell concept.
2. To develop an accelerated method for swell potential and swell pressure measurement using CRS apparatus.
3. To understand the mechanism of CNS technique in stabilizing the expansive soils with the aid of hydraulic conductivity and infiltration studies.
4. To evaluate the efficacy of chemically stabilized soil (CSS) cushion using class C fly ash and lime in stabilizing the expansive soil and
5. To examine the efficacy of lime slurry, fly ash slurry and class F fly ash-lime slurry in stabilizing the expansive soil subjected to wetting and drying cycles.

1.4. SCOPE OF THE WORK

The scope of the work includes the following:

1. Basic characterization of expansive soils with varying swell potentials. It also includes the determination of physico-chemical, index and engineering properties.

2. Performing free swell index tests and swell potential tests on different soils covering a wide range of plasticity index in both compacted and undisturbed states. The soils containing different clay minerals, such as kaolinite, illite and montmorillonite minerals were chosen and tested. Correlating the experimental results obtained from new method with the existing methods of characterization for the development of a new classification chart and table.
3. The study of chemically stabilized soil (CSS) cushion and deep stabilization of expansive soils using fly ashes are limited to the laboratory scale model tests and evaluation of the physico-chemical, index and engineering properties of untreated and treated samples collected from different radial distances and depths will be evaluated.
4. Fly ash materials were limited to Class C fly ash from Neyveli and Class F fly ash from Chennai.

1.5. ORGANIZATION OF THE THESIS

This thesis is organized into eight chapters with five contributing chapters. A brief summary of individual chapter is given here.

Chapter 1: Introduction

This chapter brings out the importance of the problem being studied. Then the need for the study, objectives and scope of the present study are presented. It also provides a brief write up about how the chapters are organized in this thesis.

Chapter 2: Literature review

A detailed literature review covering the methods available for the characterization of expansive soils using both qualitative and quantitative methods are presented first. Then, the works reported in the literature pertaining to the shallow and deep stabilization of expansive soils using compensating materials and chemical additives are also discussed. Finally, the problem statement is elaborated in this chapter.

Chapter 3: Development of rapid method for characterization of expansive soils

This chapter presents detailed laboratory studies carried out on the proposed desiccated state free swell (DSFS) method for identification and classification of the degree of soil expansion with limited efforts and testing accessories. It also presents the classification chart and table development based on DSFS method for expansive soil identification and classification from the experimental results obtained from 21 soil samples covering wide range of swelling potentials. This section also validates the proposed classification chart and table with existing methods by testing additional undisturbed samples collected from field.

Chapter 4: Accelerated method for measurement of swell potential and swell pressure of expansive soil using constant rate of strain apparatus

This chapter deals with the proposed accelerated methods for measuring the swell potential and swell pressure of the expansive soils. The effective use of back pressure application for saturation of the soil specimen is presented in this chapter. It also compares the results obtained from the conventional method without back pressure application with the results obtained using the proposed method with back pressure application.

Chapter 5: Distress of an industrial building constructed on an expansive soil – a case study

This chapter presents the detailed site investigation carried out on the distressed industrial building founded on expansive soil deposits. It also covers the laboratory tests conducted on undisturbed soil samples collected from the field. Further, the discussions on the causes for the initiation of distress and recommendations are also summarised here.

Chapter 6: Mechanisms of compensating material in controlling the volume change of expansive soil

This chapter presents the laboratory test results of expansive soil stabilized with different compensating materials like sand, Cohesive Non-swelling oil (CNS), Non-Swelling soil (NSS) and Chemically Stabilized Soil (CSS). It also presents the preparation of CSS material using expansive soil, class C-fly ash and lime. The test results of hydraulic conductivity and infiltration characteristics of compensating materials are presented in this section. Based on the present experimental results using all the compensating materials, an effort is made to bring out the mechanism of compensating materials in controlling the volume change of expansive soils subjected to wet-dry cycles.

Chapter 7: Deep stabilization of expansive soil using lime, fly ash and lime-fly ash slurry injection

This chapter presents the laboratory tank studies on the stabilization of desiccated expansive soil using lime, fly ash and lime-fly ash slurry injection. It also discusses the method developed for the preparation of fly ash slurry and lime-fly ash slurry solution. Swell-shrink behaviour of both untreated and treated expansive soils is compared in this chapter. It also reports the index, physico-chemical properties and unconfined compressive strength of soil samples subjected to four wet-dry cycles.

Chapter 8: Summary and Conclusions

This chapter summarises the major conclusions drawn from the present experimental work

CHAPTER 2

LITERATURE REVIEW

2.1 INTRODUCTION

Expansive soils undergo volume change (shrinkage and swelling) due to change in moisture content. The volume change in these soils depends on moisture content, the degree of compaction (dry unit weight), imposed stress and degree of saturation (Chen, 1988; Nelson and Miller, 1992; Coduto, 2013). Significant volumetric expansion of the soils affect the long-term performance of lightweight structures which includes pavements, runways, canal lining, sewer lines and other irrigation structures. In order to overcome such problems, proper characterisation of expansive soils and adaptation of suitable stabilization methods becomes essential. In view of this, a detailed literature review is carried out on identification and characterization of expansive soils including direct and indirect methods and shallow and deep stabilization methods are presented in this chapter.

2.2 DISTRIBUTION OF EXPANSIVE SOILS

Problems with expansive soils have been reported in nearly forty countries worldwide, particularly in countries like India, China, Australia, Mexico, USA, Cuba, Great Britain, Argentina, Spain, Burma, Ethiopia, Ghana, Iran, Israel, Kenya, Morocco, South Africa and Venezuela (Chen, 1975; Fredlund and Rahardjo, 1993, Nelson *et al.* 2015). The cost of damages to engineering structures due to expansive clays increases every year in USA and it was evaluated as $15 billion (Lee and Ian, 2012). In USA, every year 2,50,000 new residential buildings are constructed on swelling soils. Among them, 60% of the houses are damaged with minor cracks in the walls and foundations, and 10% of houses are severely damaged (Keller, 2007). In the year 2000, the Association of British Insurer has estimated that the average cost of £400 million was claimed as subsidence damage related to the swell-shrink movement of soils (Freeman *et al*. 2002).

In India, these soils are commonly called as black cotton soils because of its colour and it suitability for growing cotton plants. These soils cover about 20 % of total land area of India, particularly in states like Gujarat, Maharashtra, Madhya Pradesh, Utter

Pradesh, Karnataka, Rajasthan, Andhra Pradesh, Telangana and Tamil Nadu (Katti, 1978; Patil *et al.* 2012). The distribution of expansive soil in Indian peninsula is shown in Figure 2.1.

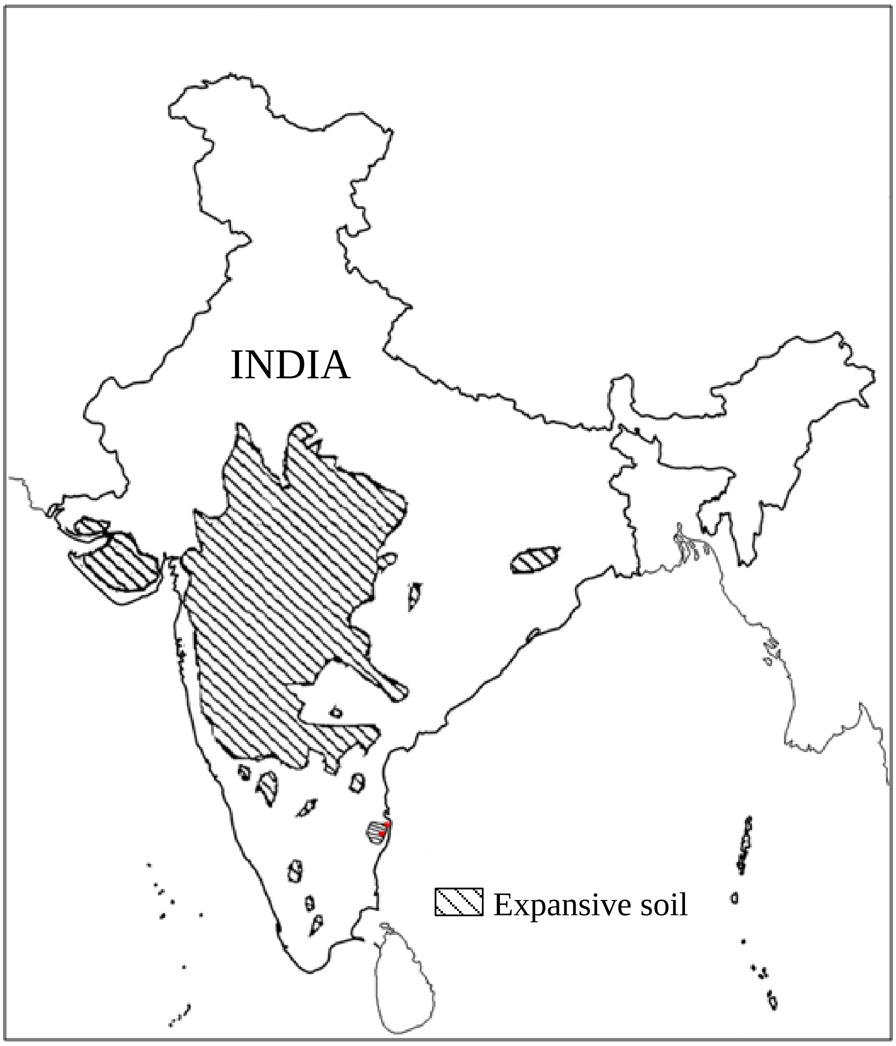

Figure 2.1: Regions covered with expansive clay formation in India (from Maps of India, 2018)

2.3 EXPANSIVE SOILS

The soils which are dominated with Montmorillonite clay mineral generally exhibit swell-shrink properties. The mineral montmorrillonite was named after the village in France called montmorrillon where it was first discovered (Holtz *et al.* 2011). This mineral comes under smectite group and is categorised by its high electrolyte content, high pH and more Ca^{2+} and Mg^{2+} ions than K^{+} and Na^{+} ions (Mitchell and Soga, 2005).

Figure 2.2 shows the stacking of tetrahedral and octahedral sheet for 1:1 and 2:1 clay minerals. The common 1:1 mineral is kaolinite and during hydration the separation of clay particle is restricted due to the strong hydrogen bonding between the interlayers. For 2:1 mineral, the bonding between the combined sheets is the weak vander waals force and exchangeable cations, and this bonds can be easily destroyed or separated due to adsorbed water or any polar liquids (Mitchell and Soga, 2005). Chemically the clay particles are identified as platelets (layered structures) with negative charges at the surfaces and positive charges on their edges. The presence of cations in the soil water gets attracted towards the negative surfaces of the clay platelets and the negative charges towards the edges of clay particles. During hydration of clay minerals, the water molecules enter between the single crystals, and also it begins to enter between the individual layers and changes the thickness of the structure ranging from 9.6 Å to maximum separation (Mitchell and Soga, 2005).

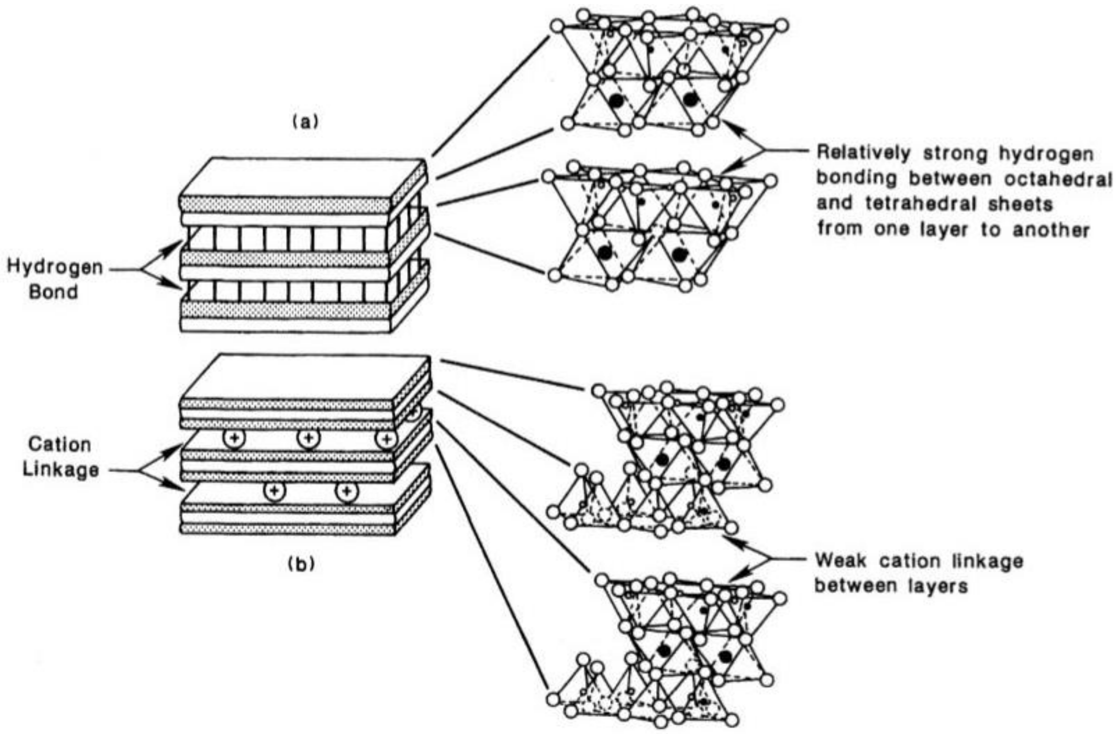

Figure 2.2: (a) 1:1 Kaolinite mineral with strong hydrogen bonding between the interlayer, and (b) 2:1Smectite mineral with weak cation bonding between the interlayer (after Little, 1995)

2.4 METHODS OF CHARACTERISATION OF EXPANSIVE SOILS

Expansive soils are problematic due to high swell-shrink potential. For identification and characterisation of expansive soil, mineralogical, physical and engineering properties of the soils are used in practice. Chen (1975) reported that expansive soil identification through mineralogical studies like X-ray diffraction (XRD), differential thermal analysis (DTA), dye adsorption and chemical analysis may provide reliable results. But these methods require specialized and sophisticated instruments, which are costly and needs interpretation of the results by the experts. Therefore, the characterisation through physical and engineering properties are popular and it could be evaluated as direct and indirect methods which are listed in Table 2.1

Table 2.1 Methods to determine the degree of expansivity of expansive soil

Direct methods	Indirect methods
Oedometer tests, X-ray diffraction (XRD), Differential thermal analysis (DTA),	Free swell tests, Free swell index tests, Modified free swell index, Free swell ratio, Liquid limit, Plasticity index, Shrinkage limit, Shrinkage index, Activity tests, Colloidal content tests

2.4.1 Attterberg Limits and Colloidal Content

Indirect methods are simple laboratory methods but these tests have their own limitations. Earlier studies tried to identify the expansive soil through colloidal content, liquid limit, plastic limit and shrinkage factors. Skemptom (1953) proposed the term activity by relating plasticity index and percentage of clay fraction and concluded that the soils with activity value of more than 1.25 experience more volume change. Holtz and Gibbs (1956) used colloidal content (particle size < 0.001 mm) to estimate the potential of soil expansion, as shown in Table 2.2. However, Seed *et al.* (1962) believed that the amount of clay fraction cannot be related to swell potential, but they proved that for the given clay type, the degree of expansion increases with increase in percentage of clay size fraction. Later, the works of Chen (1965), Raman (1967) and Chen (1988) highlighted the usage of liquid limit (w_L), plasticity index (I_P) and shrinkage index (I_S) in predicting the soil expansion and their classification system are summarised in Table 2.2.

The liquid limit of the clay containing montmorillonite as a clay mineral is a function of diffuse double layer (DDL) thickness. However, soils with higher liquid limit may not be a sign of expansive clay (Sridharan *et al*. 1986). Some experimental studies were carried out by Sridharan and Rao (1988) to use the index properties for the prediction of the soil expansion of soils enriched with montmorillonite. They concluded that DDL thickness which governs the swelling force also governs the index properties of the soil, and hence the prediction of soil expansion of montmorillonite soils gives reliable results. However, these prediction methods may not hold good for soils containing kaolinite-rich soils. Later, the findings of Seed *et al*. (1962), Sridharan and Prakash (1998) and Fityus *et al*. (2005) showed that shrinkage limit is a function of initial water content and grain size distribution of the soils, and hence it could not be used as a tool to identify the swelling potential of the expansive clay.

Table 2.2 Prediction of soil expansion through colloidal content, w_L, I_P and I_S

Degree of expansion	Colloidal content; % minus 0.001 mm (Holtz and Gibbs, 1956)	W_L (%)		I_P (%)		I_S (%)	
		Chen 1965	IS 1498: (1970)	IS 1498: (1970)	Chen (1988)	Raman (1967)	IS 1498: (1970)
Low	< 15	< 30	20 - 35	< 12	0 -15	<15	<15
Medium	13 - 23	30 - 40	35 - 50	12 - 23	10 - 35	15-30	15-30
high	20 - 31	40 - 60	50 - 70	23 - 32	20 - 55	30-40	30-60
Very high	> 28	> 60	70 - 90	> 32	> 35	>40	>60

2.4.2 Sediment Volume Methods

Holtz and Gibbs (1956) developed a sediment volume test for measuring the free swell value (FSV) of soils, which is presently used for classification. 10 cm^3 of dry soil is placed in 100 ml jar. Distilled water was poured and the sediment volume was recorded. FSV is defined as the ratio of change in volume from dry to wet state over the initial volume of the soil (10 cm^3), expressed as percentage as given in equation 2.1. They stated that the soil with FSV of 100% or less may cause considerable damage for light weight structures. The attraction of this method is that the results can be obtained within a period of 24 hours. The free swell value is given by the equation (2.1):

$$FSV = \left[\frac{V_f - V_i}{V_i} \right] \times 100 \tag{2.1}$$

where V_i is the initial volume of the soil (10 cm^3 of soil passing through 425 µm sieve) and V_f is the final volume of soil sediment after reaching equilibrium condition.

In FSV test, the preparation of exactly 10 cm^3 volume of soil is difficult and also it depends on the personal judgement, and hence this test became obsolete. In order to overcome this problem, the free swell index (FSI) (IS 2720-40: 1977) is used. In FSI method, 10 grams of oven dried soil passing through 425 µm sieve is poured into two separate 100 ml jars. One cylinder is filled with water and another cylinder is filled with kerosene up to 100 ml. After complete removal of entrapped air, the soil-water suspension is allowed to settle until it reaches the equilibrium state. The difference in final volumes in the both cylinders will give the differential free swell value. Since kerosene is a non-polar liquid it will not cause any swell in the soil. The free swell index is given by the following equation

$$FSI = \left[\frac{V_d - V_k}{V_k}\right] \times 100 \tag{2.2}$$

where V_d = final sediment volume of soil in distilled water and V_k = final sediment volume of soil in kerosene

FSI is followed in many countries for the identification and classification of expansive soils. However, soils which are rich in kaolinite mineral shows a negative free swell index (Sridharan *et al.*, 1985). Later, methods like modified free swell index (MFSI) (ratio of difference between volume of soil in distilled water and volume of soil solids to the volume of soil solids) (Sivapullaiah *et al.* 1987) and the free swell ratio (FSR) (ratio of volume of soil in distilled water to the volume of soil in kerosene) (Sridharan and Prakash, 2000) were developed to overcome the limitations and to predict the expansivity of soils and type of minerals present in it. Table 2.3 summarises the methods and their classification system for expansive soils. The modified free swell index is given by the follwing equation

$$MFSI = \left[\frac{V_d - V_s}{V_s}\right] \tag{2.3}$$

where V_s = volume of soil solids, $V_s = \frac{W_s}{G_s \gamma_w}$, W_s = weight of solids, G_s = specific gravity of soil, γ_w = unit weight of water. The free swell ratio is given by the equation

$$FSR = \left[\frac{V_d}{V_k}\right] \tag{2.4}$$

Table 2.3 Prediction of soil expansion from sediment volume methods

Degree of soil expansion	FSI (%) (IS -1498)	MFSI (Sivapullaiah *et al*. 1987)	FSR (Sridharan and Prakash, 2000)
Negligible	-	< 2.5	< 1.0
Low	< 50	-	1.0 - 1.5
Medium	50 - 100	2.5 - 10.0	1.5 - 2.0
High	100 - 200	10.0 - 20.0	2.0 - 4.0
Very high	> 200	> 20.0	> 4.0

2.4.3 Oedometer Methods

Swell potential (*SP*) and swell pressure (p_s) are the most widely used parameters for the identification and classification of expansive soils (Shuai, 1996; Tu, 2015). Seed *et al.* (1962) defined the swell potential as the percent swell of a soil specimen, compacted to the standard Proctor maximum dry unit weight at its optimum moisture content, upon inundation with free water under a seating pressure of 6.9 kPa (1 psi). If the volume change of the expansive soils is prevented, the soils exert pressure on the structures founded on them, which is quantified in terms of swell pressure. Swell pressure is defined as the minimum pressure required to prevent the volume change of expansive soils upon inundation with water (Holtz and Gibbs, 1956; Sridharan *et al.* 1986; Holtz *et al*. 2011).

Several methods were developed in the literature to evaluate the swell potential and swell pressure using the conventional oedometer apparatus (Sridharan *et al*. 1986; Nelson and Miller, 1992; Vanapalli and Lu, 2012). The following oedometer methods are widely used to determine the swell pressure of expansive soils:

(a) Loading after wetting also called as swell-consolidation test (ASTM D4546-14; IS 2720:41-1997)

(b) Wetting after loading test (ASTM D4546-14)

(c) Zero swell or constant volume method (BS 1377-5-1990; IS 2720-41-1997)

(d) Single point wetting after loading test (ASTM D4546-14)

a) Loading after wetting (or) Swell-consolidation method (ASTM D4546-12; IS 2720:41-1997) (Method - A)

The compacted soil specimen is inundated and allowed to swell until the dial reading becomes constant under a minimum seating pressure. The specimen is then loaded incrementally with a load incremental ratio of 1.0 to consolidate the swollen specimen to its initial void ratio/ thickness. The pressure corresponding to zero volume change (initial void ratio) is taken as the swelling pressure and it is shown in Figure 2.3. The limitation of this method is that it does not represent the normal sequence of load application in the field. In the field the soil swells by absorbing water under the existing structural loads. But in the laboratory condition, the sample was allowed to swell first under minimum seating pressure and then the load is superimposed. Hence, this method does not simulate the field condition. However, this method quite reflects the site condition where the soil is subjected to prewetting treatment.

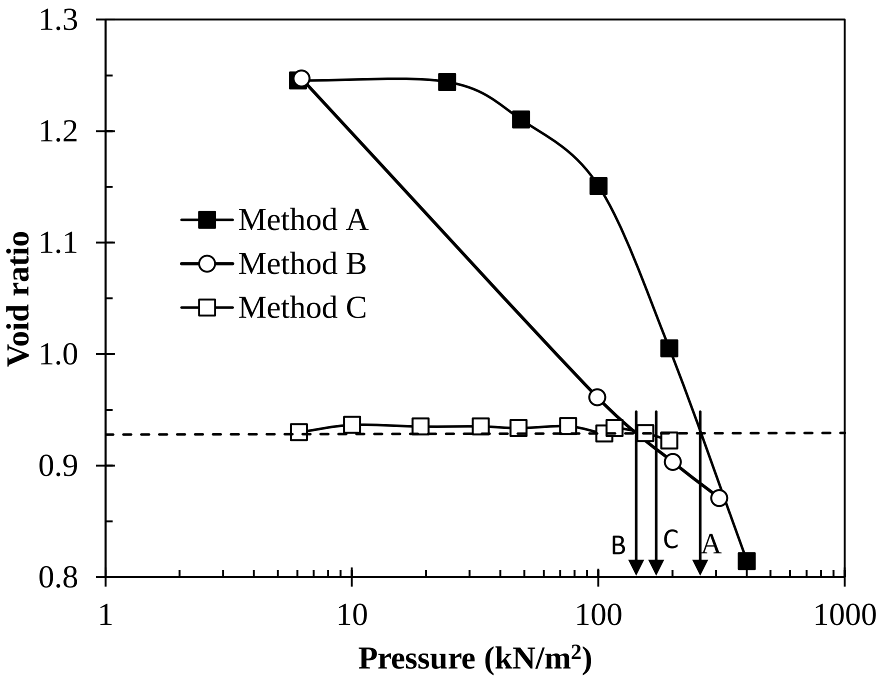

Figure 2.3: Comparison of swell pressure of soil determined from three methods (after Soundara and Robinson, 2009)

b) Wetting after loading tests (ASTM D4546-12) (Method - B)

In this method, three to four identical specimens are loaded in an oedometer with different seating pressures which is closer to the expected swelling pressure. The specimens are left until they reach the equilibrium in the initial state under the applied load. The specimens are then inundated with distilled water and the volume change with time is recorded. The final vertical deformations of the specimens are plotted against the applied pressure and the connecting line which intersects the X-axis represents the swelling pressure of the soil, as shown in Figure 2.3. This method simulates the field condition more closely.

c) Zero swell or constant volume method (BS 1377-5-1990; IS 2720-41-1997) (Method - C)

In this method, the specimen is not allowed to undergo any vertical swell during inundation and it is maintained by varying the vertical pressure. The swelling pressure is recorded as the maximum stress required for maintaining its initial thickness, shown in Figure 2.3. In IS 2720-41(1997) it is suggested to use a proving ring to maintain constant volume. This method also simulates the in-situ condition where the applied load form the super-structure in service condition does not change with time. However, this method is very sensitive to measurement, because even a small amount of swell is allowed to expand, it may under-estimate the swell pressure.

d) Single point wetting after loading test

This method is as similar to wetting after loading tests (Method-B) but only one specimen will be used for the testing. The specimens may be from the field or prepared in the laboratory prepared. For selecting the seating pressure, the thickness of overburden soil and super structural load could be used. The measured heave will be the reflection for the given seating pressure and to measure the swell pressure, two more identical specimens with different seating pressure should be tested.

Among all the methods, the swell-consolidation method is widely used as it measures both swell, swell pressure and consolidation characteristics and due to its simplicity. Factors such as stress path, dry unit weight, water content, degree of saturation, wetting sequence and method of testing affects the swell pressure (Chen, 1975; Justo *et al.* 1984; Sridharan *et al.* 1986; Dhowain, 1990; Villar and Lloret, 2008; Soundara and Robinson 2009). Nagaraj *et al*. (2009) observed that the expansive soil specimens in oedometer cells do not reach full saturation on wetting in swell pressure tests. They also observed that the water content within the soil specimens is not uniform, with lower water content in the middle portion and higher water contents in the top and bottom portions close to the wetting fronts which are in direct contact with water. In order to overcome the limitation of saturation and non-uniform water content, Nagaraj *et al.* (2009) proposed a technique of introduction of sand drains in the compacted specimens for easy access of free water throughout the specimens. They reported that five to nine sand drains of 2.8 mm diameter, in specimens of 60 mm diameter, are sufficient to saturate the specimens. The particle size of sand used for the drains was less than 425 μm. The specimens with holes and after filling with fine sand in the oedometer specimen are shown in Figure 2.4. The results showed that the introduction of sand drains increased the degree of saturation, which in turn resulted in an increase in swell potential by about 17-20%. The swell pressure also increased by about 24% due to greater saturation. Nagaraj *et al.* (2009) also reported that the installation of sand drains was not successful in expansive soils characterized with low dry unit weight due to the sample disturbance. Moreover, filling of 2.8 mm diameter holes with sand is also difficult. The presence of sand drains may also affect the subsequent consolidation after swelling.

Recently, Nelson (2016) studied the effect of duration of submergence and method of inundation on swell measurement and concluded that an increase of 33% of swell was observed when the specimen was properly saturated.

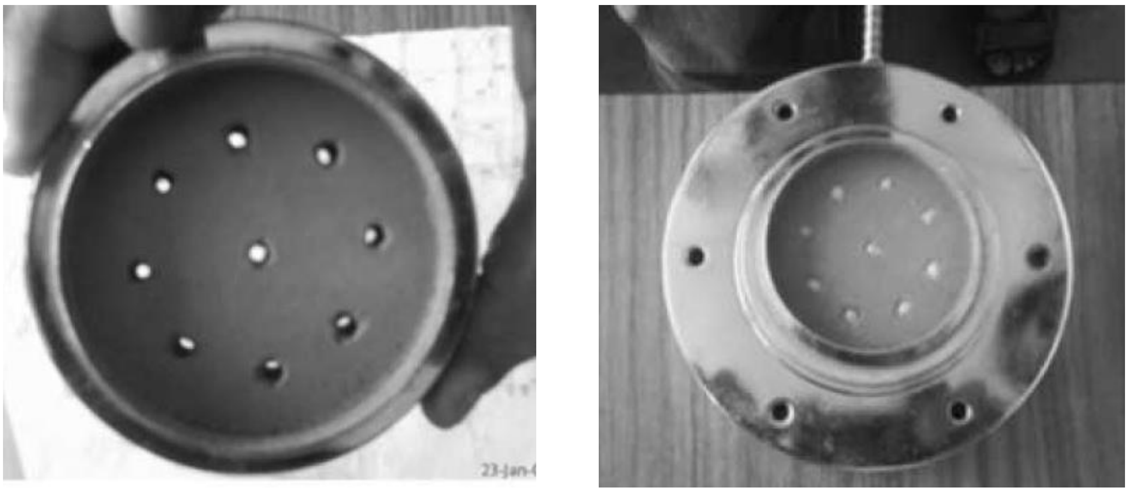

Figure 2.4: (a) 2.8 mm diameter holes in oedometer specimen and (b) holes filled with fine sand for better saturation (after Nagaraj *et al*. 2009)

Table 2.4 summarises the classification system for expansive soils based on oedometer tests developed by different authors. The classification chart proposed by Holtz and Gibbs (1956) was reported to underestimate the swelling capacity of Indian expansive soils (Sridharan and Prakash, 2000).

Table 2.4 Prediction of soil expansion using oedometer apparatus

Degree of expansion	Swell pressure (kPa)(Chen 1975)	Percent swell (Holtz and Gibbs 1956)*	Percent swell (Seed *et.al* 1962)$^{\psi}$
Low	50	< 10	< 1.5
Medium	150 - 250	10 - 20	1.5 - 5.0
High	250 - 950	20 - 30	5.0 - 25.0
Very High	> 950	> 30	> 25.0

* Swell measured from dry to saturated sate under seating pressure of 6.9 kPa

$^{\psi}$ Swell measured from compacted to saturated sate under seating pressure of 6.9 kPa

2.4.4 Factors Affecting Swelling

The following parameters govern the volume change in expansive soils during inundation:

(i) Type of clay mineral,

(ii) Initial moisture content

(iii) Initial dry unit weight

(iv) Overburden stress.

i) Type of clay mineral

The most common minerals present in the soils are kaolinite, illite and montmorillonite. Soils containing the clay mineral montimorillonite generally exhibit high swell-shrink properties. For illite, the volume change is about 15% of its original volume, but when it is intermixed with montmorillonite, it may increase to 60-100%. Similarly, for calcium montmorillonite, it is about 50-100%, but it increases to 2000% for sodium montmorillonite (Bell, 1993). The volume change in kaolinite is limited or zero due to strong interlayer hydrogen bonding (Mitchell and Soga, 2005).

ii) Initial moisture content

Holtz and Gibbs (1956) reported that the soils compacted on wet of optimum showed less amount of swelling when compared to the soils compacted at dry of optimum. The initial water content controls the volume change for remoulded soil specimens. Usually, the soil specimens at the driest state could be used to perform the test (Chen, 1975). More attention should be provided during the time lapse between sample preparation to setting up the specimen in oedometer frame and application of seating load to inundation period.

iii) Initial dry unit weight

The most important parameter which governs the swelling capacity of the expansive soil is the dry unit weight (Chen 1975). The works of Holtz (1956) and Chen (1988) also highlighted that the swelling capacity of the soil increases with the increase in dry unit weight and this is due to the denser packing of soil particles.

iv) Overburden stress

Holtz (1959) reported that the total overburden stress which acts over the soil mass determines the magnitude of volume change for the corresponding moisture content and dry unit weight. For laboratory determination of swell potential a seating pressure of 6.9 kPa (Seed *et al.* 1962) was used and this minimum pressure may lead to erratic results. Hence, Chen (1975) suggested an average seating pressure of 48 kPa which is a common pressure exerted by most foundation systems.

2.5 DEPTH OF ACTIVE ZONE

Due to the cyclic process of precipitation and evapotranspiration, the water content fluctuates at the surface level of expansive soil deposit and it decreases or increases with depth according to the environmental condition (summer and winter). Nelson *et al*. (2001) defined the active zone as the zone of soil that contributes to the heave due to soil expansion at any particular time. The selection of the method of treatment to the expansive soils depends on the depth of active zone and swell pressure. It is essential to evaluate the active zone for a given site, because almost 60-80% of volume change occurs in the top 50% of active zone depth (Rao *et al.* 1988; Fityus *et al*. 2004).

Figure 2.5 shows the water content variation with depth in a uniform soil profile (Durkee, 2000). The plot A shows the variation in dry condition and plot B shows the idealised pattern in which the soil surface is covered to minimise the loss of moisture. Similarly, the plots C and D show the variation of moisture in winter and summer seasons, respectively. The depth to which water fluctuates between the plot C and D is referred as the zone of moisture fluctuation (H_S), and below this depth, moisture will be in the equilibrium condition. And for this soil profile, the zone of seasonal fluctuation is less than or equal to Z_S.

The depth of active zone depth changes with time and also it depends on the soil profile, hydraulic conductivity and other environmental factors. In places, where the soil profile is stratified, the depth of active zone can be determined by plotting w/w_L or I_P versus depth (Nelson and Miller 1992). Typically in India, the depth of active zone was found to be 3.5 to 5 m in Madhya Pradesh, 1.5 m in Maharashtra and NIT Warangal campus, Telangana (Murthy and Praveen, 2008; Soni, 2009). The maximum depth of active zone was found in the place Colorado (USA) and it was obtained as 16 m (Holtz, 1969). In general, the soil profile with deeper active zone will swell more than the active zone founded at shallow depth (Coduto, 2013)

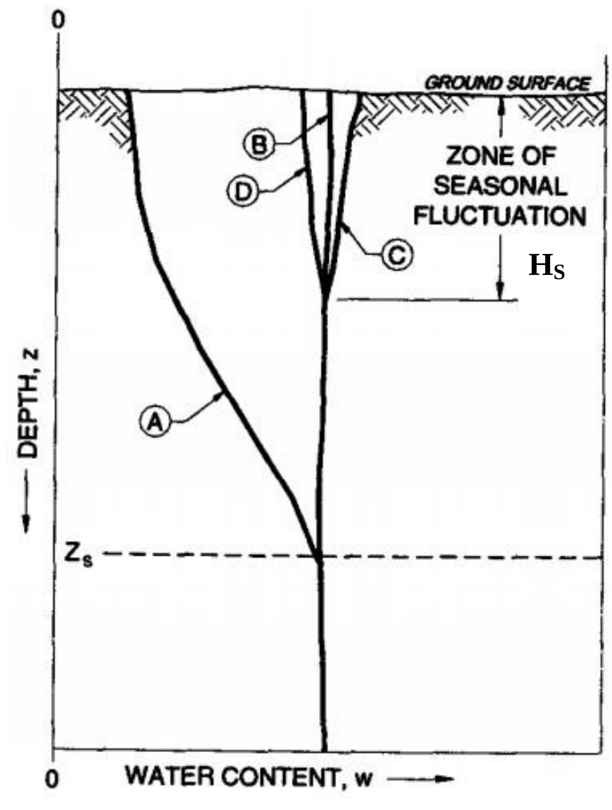

A = idealised water content variation in dry condition.
B= drying and saturation is prevented by impervious cover
C= water content variation in winter season
D= water content variation in dry condition
H_s = Active zone
Z_s = Maximum active zone variation

Figure 2.5: Variations of moisture content with depth for different environmental conditions (after Durkee, 2000)

The depth of active zone (H_S) gets shifted or altered because of external factors like watering of the landscape, planting of shrubs and trees, breakage of utility lines, discharge of water from roof drains, *etc*. (Chen, 1975; Coduto, 2013). Fityus *et al*. (2004) studied the influence of vegetation and presence of impervious layer on the depth of the active zone through pilot field study. The change in the field water content was continuously monitored for seven years of duration. Figure 2.6 compares the variation in the active zone due to different environmental conditions. From Figure 2.6(b), it can be observed that the presence of trees has extended the active zone to deeper depth .i.e. the active zone has reached to 2.5 m when compared to 1.6 m measured at the open ground surface. Similarly, for the ground surface covered with a flexible cover, the water content fluctuation was observed only in the top 0.4 m depth, as shown in Figure 2.6(c). The depth of active zone at a given site is difficult to determine, and this creates significant uncertainty in the prediction of heave in the soil profile (Coduto, 2013).

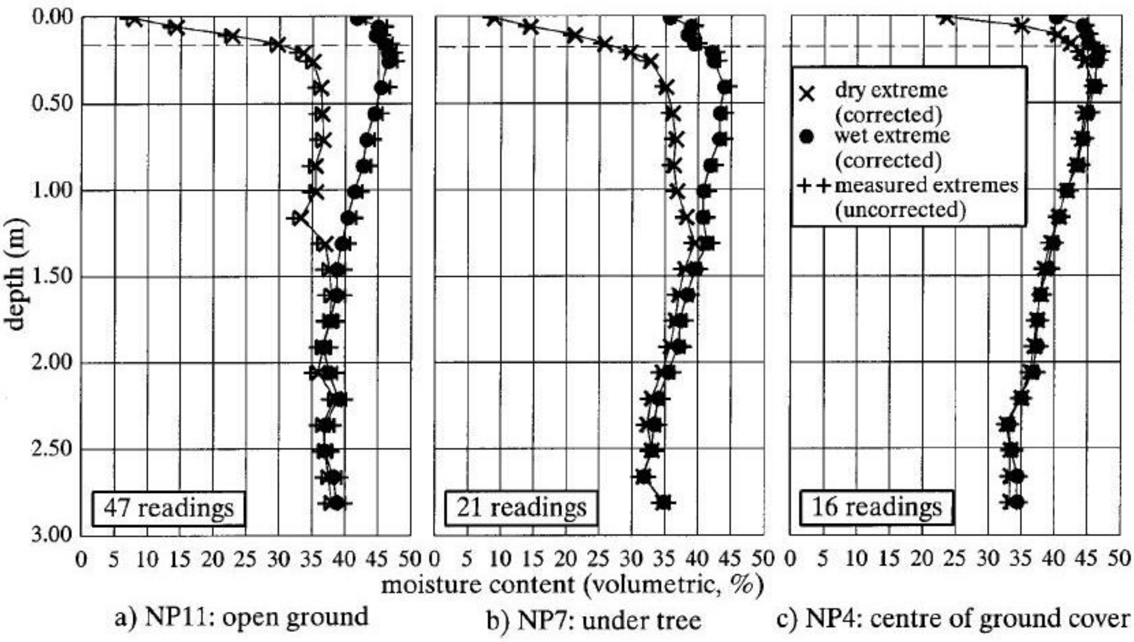

Figure 2.6: Influence of field conditions on the changes in active zone depth based on 7 years of field observations (after Fityus *et al*. 2004)

2.6 TREATMENT OF EXPANSIVE SOILS

Treatment methods for expansive soils can be classified into four groups based on the mechanisms involved, namely, mechanical, chemical, thermal and electrical methods (Puppala *et al*. 2003). Among these methods, mechanical and chemical methods are commonly adopted stabilization methods which include prewetting, moisture control, compaction control, surcharge loading, removal and replacement and chemical stabilization.

2.6.1 Prewetting

Prewetting treatment is performed by flooding expansive soil with water and allowed to swell prior to the start of construction work. It should be ensured that the water content remains constant with varying depth because this gets reflected on the safety of structures after construction. Van der Merve *et al.* (1980) conducted a field study by providing a sand blanket layer over the expansive soil for quicker saturation and they end up with 50% of total heave in 50 days of ponding. However, in case of high plastic clays, it may take long time for saturation owing to its low hydraulic conductivity. In addition, the volume change during inundation leads to significant reduction in shear strength (Nelson and Miller, 1992).

2.6.2 Moisture Control

The extent of soil swelling depends on the initial moisture content and if it is maintained constant by preventing it from additional ingression of water, the initiation of non-uniform heave could be minimised. The migration of water can be prevented by providing horizontal and vertical barriers. These barriers can be used for both pre-construction and remedial works. Membranes, asphalt and rigid or flexible barriers are some of the materials used in the construction of horizontal barriers. Prefabricated asphalt sheet with thickness less than 12 mm and 4 feet wide also have been used (Chen, 1975).

Vertical barriers are generally better than horizontal barriers in controlling the swell-shrink movement of the soil. Polyethelene membrane, concrete and other durable impervious material can be used in the construction (Chen, 1975). The desired depth of the vertical barrier should be at least one-half to two-third of the active zone depth (Nelson and Miller, 1992).

2.6.3 Compaction Control

In order to reduce the volume change in expansive soils, the soils can be compacted to lower dry densities (Holtz, 1959). Better results can be obtained when soils are compacted at wet side of optimum with minimum density (Chen, 1975). However, in case of stiff clays, it is difficult to compact the soils with moisture content of 4-5% above the optimum moisture content (Chen, 1975). But the adjustment of compaction characteristics of the soil has the following limitations (Nelson and Miller, 1992),

a) Reduction in dry density leads to low bearing capacity and hence, this method may be applicable only for lightly loaded structures,
b) For high swelling soils, the compaction control is less effective, and
c) Proper quality control measures should be taken to ensure that the specified density and water content are achieved.

2.6.4 Surcharge Loading

Swell can be controlled by providing a surcharge load equivalent to the swell pressure of the soil. This method is applicable only for low to medium swelling soils. For example, a swell pressure of 28 kPa can be controlled by a 4 ft thickness (1.2 m) of compacted fill or concrete foundation (Chen, 1975). This method may not be economical and less effective for soils with higher swell pressures because of the magnitude of surcharge pressure required varies non-linearly with swell pressure (Nelson and Miller, 1992).

2.6.5 Removal and Replacement

A simple way to control the problem of expansive soil is to remove the soil and replace it with non-swelling soils. Katti (1978) conducted a laboratory and field study on cohesive non swelling (CNS) behaviour of granular soil. The thickness of the compensating material depends on the magnitude of swell pressure and it normally varies from 0.75 to 1.0 m. Based on the practical applications, Chen (1988) recommends a minimum depth of replacement as 0.9 - 1.2 m (3 to 4 ft) because the surcharge due to the thickness of higher density granular soil and self-weight of the structure is important in governing the volume change of underlying expansive soil.

2.7 CHEMICAL STABILIZATION

Modification of expansive soils using chemical stabilization is the most preferred method among the field engineers due to its workability and efficiency in controlling the swell (Bell, 1993). Chemical stabilization finds its advantages as it controls the swell-shrink potentials of the expansive soils, and makes the soils less plastic. The chemical stabilization can be achieved using calcium-based additives (cement, lime, fly ash, etc).

2.7.1 Lime Stabilization

Among the chemical admixtures, lime is the widely used admixture for controlling the detrimental swell-shrink potentials of expansive soils. Bell (1993) reported that lime stabilization is quite applicable for plastic clays and heavy plastic clays, but it is not suitable for soil with plasticity index less than 10%. And to initiate the reactions in soils with less fines, addition of pozzolanic materials like fly ash may be required.

For stabilization of soil, quicklime (CaO), hydrated lime ($Ca(OH)_2$) are the most used commercial products. However, the degree of improvement depends on the purity of lime and pozzolanic property of the soils to be improved. In general, clays are rich in pozzolanic property due to the presence of siliceous and aluminous materials which can form cementitious products with lime treatment in the presence of water.

Four basic reactions occur when lime is mixed with soils namely cation exchange, flocculation or agglomeration of fine clay particles, carbonation and pozzolanic reactions. The first two reactions reduce the plasticity of the soils, which are rapid and called as short-term modification reactions. The other two reactions are termed as long term soil-lime pozzolanic reactions. Carbonation is an undesirable reaction because of the formation of weak cementing agents whereas the pozzolanic reactions produce the major increase in strength (Holtz, 1969; Bell, 1988). Figure 2.7 presents the formation of pozzolanic products for soil stabilized with lime and other calcium based stabilizers.

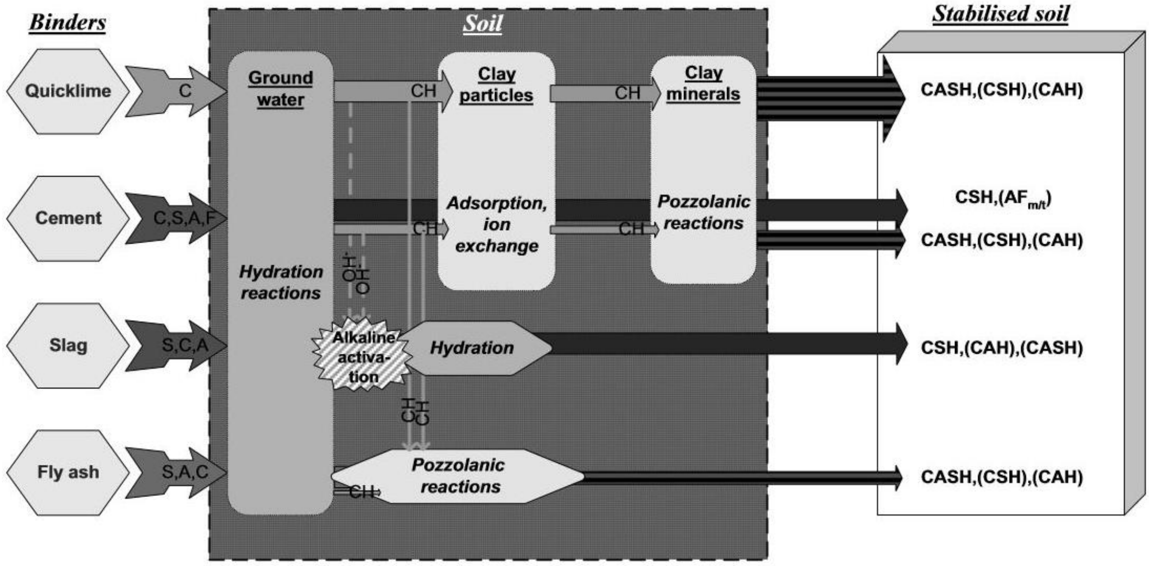

Figure 2.7: Formation of cementitious products for soils stabilized with different chemical binders (after Ahnberg and Johansson, 2005)

2.7.2 Factors Influencing Soil-Lime Reactions

Lime stabilization is governed by many factors such as type of clay, percentage of clay fraction, exchangeable ions, pH of soil, curing period, temperature and quantity of lime. (Nelson and Miller, 1992)

i. Type and amount of clay minerals

The percentage increase in the strength of lime admixed soils depends on the pozzolanic nature of the soil and generally clay soils are more reactive than the other soils. The highly plastic clays are more reactive with lime than the low plasticity soils (Herrin and Mitchell, 1961). Sivapullaiah *et al.* (2000) investigated the role of type and amount of clay on the soil-lime reactions and mechanism involved. The lime treatment was more effective in altering the index properties of montmorillonitic soil in comparison to kaolinite.

ii. Curing period

Curing is one of the major parameters affecting the engineering properties of lime stabilized soil. Its effect on the strength gain dependd on relative humidity, temperature and time. Herrin and Mitchell (1961) found that the strength increases rapidly at first, but subsequently the increase is very slow. Curing alters the Atterberg limits by increasing the liquid limit and shrinkage limit at various percentages of lime. This is because of the water occupying the larger void spaces of the flocculated arrangement and the random arrangement mobilized by cementitious products formed due to pozzolanic reactions respectively (Prakash *et al*. 1989). Rao and Shivananda (2002) studied the strength increment in lime treated soil with increase in curing periods. The pozzolanic reactions did not occur during the first day of curing but it increased with curing periods. It also reported that with increase in curing periods, the pH of the soil starts decreasing and it is due to the involvement of hydroxyl ions (OH) in the dissolution of silica and alumina from the soil.

iii. Temperature

Lime treated soils attain strength mainly due to the pozzolanic reactions and the rate of pozzolanic reactions can be increased by increasing the curing temperature which in turn increases the strength. The strength can be increased rapidly by increasing the temperature with time (Herrin and Mitchell, 1961). Al-Mukhtar *et al*. (2010) showed an increase in rate of pozzolanic reactions by 6 times when temperature is increased from 20˚ to 50˚. However the reactions between the soil-lime are retorted if the temperature falls below 4˚ C.

iv. Quantity of lime

Herrin and Mitchell (1961) showed that the addition of lime reduces the volume change occurring in soils up to an optimum lime content and beyond which there is no significant reduction. Quantity of lime to be added to achieve the desired volume stability is given by initial consumption of lime (ICL). ICL is the minimum amount of lime required to bring the pH of soil to 12.4 which is determined by Eades and Grim test. If lime added to the soils is less than ICL, only modification reactions occur whereas the pozzolanic reactions occur on addition of lime in excess of ICL value (Boardman *et al*. 2001).

Harrison and Davidson (1960) gave the minimum lime percentage or "lime fixation point" by the following empirical expression:

$$\text{Lm} = \frac{\text{Clay content} < 2\ \mu\text{m}}{35} + 1.25 \qquad (2.5)$$

Further Ingles and Metcalf (1972) suggested that addition of 1% lime for every 10% of clay content of the soil may be sufficient for soil modification. In general the optimum lime content will be in the range of 4-8% with respect to dry weight of soil mass and higher percentage of lime content is related to the increase in percentage of clay content (Bell, 1993).

2.7.3 Properties of Lime Stabilized Soils

i) Index properties

The addition of lime to the expansive soil increases the plastic limit and decreases the liquid limit and hence the plasticity index of soil (Herrin and Mitchell, 1961; Bell, 1988; Rao *et al*. 1993). This is because of the reduction in diffused double layer thickness caused by short-term modification reactions. The shrinkage values tend to increase significantly with the increase in percentage of lime. The consequence of flocculation brought about by cation exchange and particle agglomeration reactions on addition of lime increases the shrinkage limit (Prakash *et al*. 1989). The free swell index increases with addition of lime which is because of the dominating effect of flocculation over the depressed double layer (Sivapullaiah *et al*. 2000).

ii) Compaction characteristics

The addition of lime decreases the maximum dry density and increases the optimum moisture content. The flocculent fabric formed due to lime modification reactions offer resistance to the mechanical energy which decreases the maximum dry density and the additional water held in the flocculated structure increase the optimum moisture content (Bell, 1988; Prakash *et al*. 1989).

iii) Swell characteristics

The volume change in the lime stabilized expansive soil decreased with the increase in lime content (Rao *et al*. 2001; Guney *et al*. 2007). Rao and Venkataswamy (2002) studied the changes in swell potential for untreated and lime treated specimens. The treated specimens stabilized at optimum lime content (OLC) showed zero volume change when compared with the untreated specimens.

iv) Strength and deformation characteristics

The addition of lime increases the shear strength of soil gradually with time (Broms and Boman, 1979; Bell, 1988). The California Bearing Ratio (CBR) of clay soil increases with the addition of lime and it continues to increase with time if the is lime content is more than the lime fixation point (Bell, 1988). Rajasekaran and Rao (1996) improved the soft marine clay using lime column technique where the strength of the soil was found to increase significantly by 8 to 10 times that of untreated soil.

2.7.4 Cement Stabilization

The reaction products formed in the soil-cement stabilized mixtures are similar to that of lime. Croft (1967) reported that with the addition of cement to the soils, the shear strength and shrinkage limit has increased and it also reduced the liquid limit, plasticity index and potential volume change. But with increase in clay content (high plastic clay), the consumption of cement content has increased and hence it may not be economical (Croft, 1967; Bell, 1976). However, for soils with 5 - 35% of fines may yield economical cement content and soils with liquid limit > 45% and plasticity index > 18% are not advisable for cement stabilization (Bell, 1993).

The required quantity of cement based on dry weight of soil will be in the range of 3-16% and it is optimised based on soil type and expected soil properties (Bell, 1993). Table 2.5 presents the typical range of cement content required for stabilization of different types of soil. The strength gain of cement treated soils will be higher than the lime treated soils during the earlier stage and it is due to the formation of cementitious products within few hours (Ahnberg and Johansson, 2005). Figure 2.8 shows the estimation of reaction products and compressive strength for different binders with time. The time delay in formation of reaction products in lime mixed soil slows down the rate of strength development.

Table 2.5 Typical range of percentage of cement required for different soil types (after Bell, 1993)

ASTM Soil Classification	% of Cement content based on dry wt of soil (ACI ,1990)*	% of cement for moisture-density test (ASTM D 558-1992), based on dry wt of soil
GW, GP, GM, SW, SP,SM	3 - 5	5
GP, GM, SP,SM	5 - 8	6
GM, GC, SM,SC	5 - 9	7
SP	7 - 11	9
CL, ML	7 - 12	10
ML, MH,CH	8 - 13	10
CL,CH	9 - 15	12
MH,CH	10 - 16	13

*These guidelines may not be applicable for non-reactive soils and organic soils

The presence of organic matter and sulphate can prevent the hydration of cement stabilized soils. And this is due to the fact that it absorbs calcium present in the cement. Hence, the soils with organic content more than 2% and pH less than 5% are not desirable for cement stabilization (Bell, 1993).

2.7.5 Fly Ash Stabilization

Fly ash is a waste product produced from the thermal power plants and it is utilized in various geotechnical field applications such as backfill material, flowable fill, soil stabilizing admixture, clay liner, cushion material and sub-base construction material (pavement) (Cokca, 2001; Sridharan and Prakash, 2007). The generation and productive usage of fly ash across the World is presented in Figure 2.9

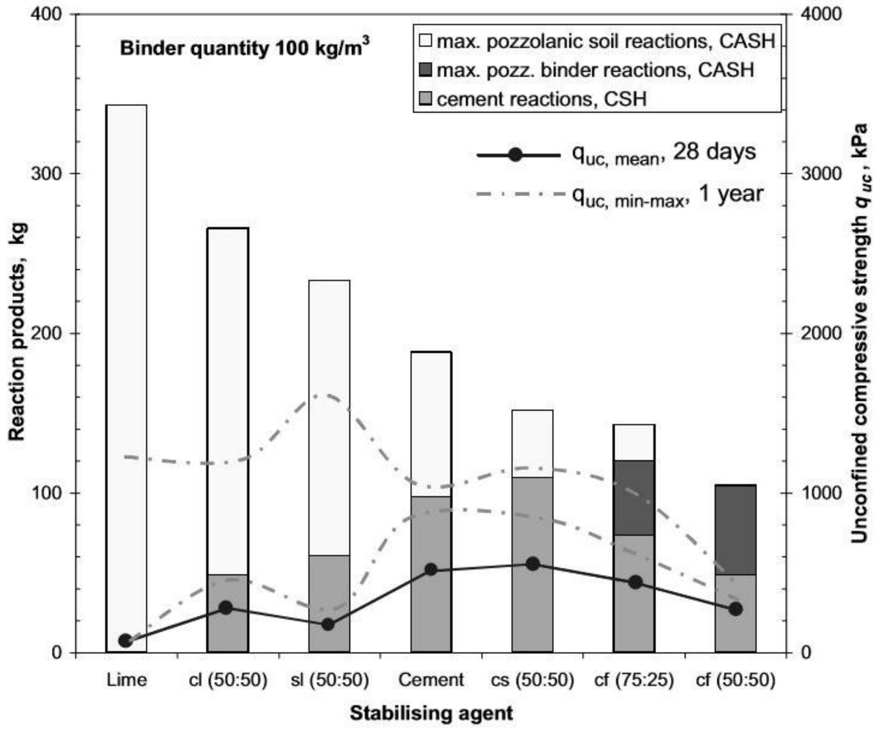

Figure 2.8: Formation of reaction products for different binders with time (after Ahnberg and Johansson, 2005)

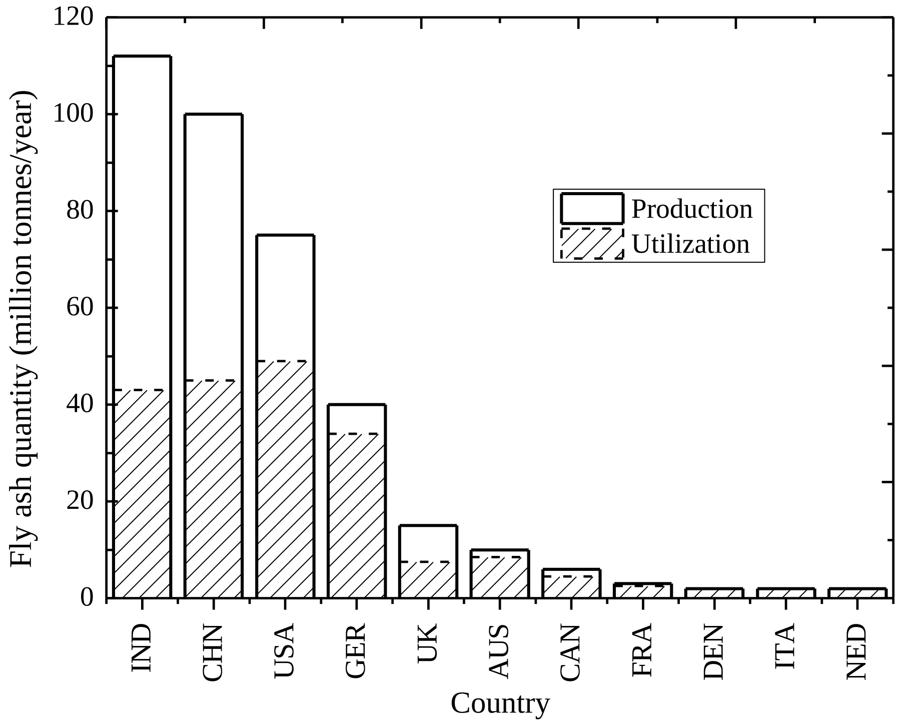

Figure 2.9: Production and utilization of fly ash in various countries (after Pandey and Singh, 2010)

Similar to lime and cement, fly ash has a tendency to form cementitious products (CSH and CAH) owing to its pozzolanic properties. It is a by-product obtained by combustion of coal which is collected in an electrostatic precipitator. Based on the source of coal used for burning and the chemical composition (SiO_2+Al_2O_3+Fe_2O_3), the fly ash can be classified as Class C and Class F (ASTM-C618). Mehta (1979) classified low calcium fly ash (CaO < 5%) and high calcium fly ash (CaO > 15%) based on the calcium oxide content. The incineration of lignite or sub-bituminous coal produces Class C fly ash and these are naturally pozzolanic, which often does not require any activator (lime or cement) for reactions due to its self-cementitious property (Sridharan and Prakash, 2007). Class F fly ashes are produced by burning anthracite and bituminous coal. Class F fly ash requires an activator to initiate the cementitious reactions. Figure 2.7 shows the chemical reactions of fly ash stabilized soil.

Physical mixing of fly ash with soil shows significant changes in the index and engineering properties of soil, but its improvement depends on particle size distribution, pozzolanic reactivity of fly ash and free lime content (Sivapulliah *et al*. 1996; Mir and Sridharan, 2013). Das and Yudhbir (2005) carried out research on the geotechnical characterisation of Indian fly ashes, and their study revealed that the Neyveli fly ash is rich in calcium with cementitious properties, and it used as an additive for improving the engineering properties of soil.

i) Class C Fly ash stabilized soil

Cokca (2001) studied the swelling characteristics of fly ash-soil mixes, lime-soil mixes, and cement-soil mixes and concluded that high-calcium and low-calcium class C fly ashes were effective in stabilizing the expansive soil. Nalbantoglu and Tuncer (2001) have reported the beneficial use of Soma fly ash (CaO = 16%) in reducing the swell potential and increasing the hydraulic conductivity of the calcareous expansive soil. The study highlighted the pronounced changes in the soil properties on the addition of fly ash in conjunction with small quantities of lime. Erdem *et al*. (2011) reported that the unconfined compressive and resilient modulus of organic soil improved with Class C fly ash (CaO >10%) owing to the pozzolanic reactions.

ii) Class F Fly ash stabilized soil

Kumar and Sharma (2004) reported the improvement in undrained cohesion and decrease in hydraulic conductivity with the increase in fly ash content. They have also reported that there is a reduction in a free swell index, swell potential and swell pressure by about 50% at 20% fly ash. Sivapullaiah *et al*. (2009) found that addition of 25-50% fly ash is useful in controlling the alkali induced volume change in the soil. Edil *et al*. (2006) made an attempt to study the effectiveness of self-cementing properties of fly ash in stabilizing the fine-grained soil. The CBR value increased with increase in fly ash content of 10% and 18% at the compaction water content of 7%. At the same time, resilient modulus also increased with an increase in fly ash content of about 25-30%.

2.7.6 Swell-Shrink Behaviour of Lime and Calcium Based Stabilizer Treated soil

In the field conditions, the expansive soils undergoes swelling due to uptake of water from precipitation, leaks in sewer and water lines, and in an similar way the soils may shrink due to evaporation, withdrawal of water by the vegetation (plants and trees), etc. The cyclic behaviour in the field has been explored by many researchers (Aitchinson and Homes, 1953; Johnson, 1980). These cyclic movements in turn results in severe distress to structures founded on them. The treatment of the expansive soils with chemical additives is the viable option to reduce the adverse effects due to the cyclic behavior. But the cyclic movements do not remain constant immediately on stabilization of the expansive soils. The type of stabilizer, amount of stabilizer and period of curing affects the cyclic behavior. Therefore, it is essential for the geotechnical engineers to consider these movements even after the stabilization of soils. The stabilizer not only has to reduce the swelling but should be effective over the designed life period of the structure. Some of the additives are soluble in water which may cause them to leach during wet-dry cycles.

Several studies had been carried out to analyse the cyclic behaviour of the virgin expansive soils. The works of Dif and Bluemel (1991), Day, (1994), and Thyagaraj and Zodinsanga (2014) showed that the magnitude of swelling measured from the completely dried specimens increased and the swell-shrink deformation process was irreversible. Conversely, the swelling measured from the partially dried specimens resulted in the reduction of swelling capacity and water absorption. Generally in wet-dry cycles, the void ratio and water content at the second swelling was higher and hence it was considered as most critical case among the N number of cycles (Tripathy *et al.* 2002). The cyclic swelling and shrinkage continues for four or five cycles and a level of fatigue is reached, with equilibrium in the magnitudes of swelling and shrinkage (Dif and Bluemel, 1991; Al-Homoud *et al*. 1995).

Rao and Shivananda (2002) also reported a decrease in the efficiency of lime treated soil after the first cycle of wetting and drying. They reported an increase in the swell potential after the first cycle and slight decrease in swell potential during the subsequent cycles and attained equilibrium in the fifth cycle. They found that the detrimental behavior was due to the breakage of the cementation bonds, reduction in void ratio and water content after the first wetting and drying cycles.

Guney *et al.* (2005) carried out the experiments to study the impact of cyclic wetting and drying on lime stabilized clayey soils using the oedometer cells. The specimens were treated with lime contents of 3% and 6%. It was reported that the maximum swell reduction was observed in the first cycle and then the swell increased with increase in number of wet –dry cycles. According to Guney, the lime was effective only in the first wetting and the beneficial effects of lime stabilization in controlling the swelling potential of treated soils are partially lost, and this is attributed to the destruction of the cementitious compounds, in the subsequent cycles.

Khattab *et al.* (2007) studied the wet-dry cycles of lime stabilized bentonite with the addition of 4% lime in specially designed oedometers. The stabilized soil specimens were subjected to wetting and drying cycles by adopting two types of procedures. In one series, the specimens were subjected to drying at 60^{o} prior to subjecting it to wetting and drying cycles. In the other series, samples were first subjected to wetting followed by the drying process. The lime treatment influences the wetting and drying cycles and shows a reduction in the swelling behavior compared to the untreated soil. But with increase in number of cycles, the swelling magnitude was observed to increase. Similar behaviour was observed with the other series also. The pre-dried sample exhibited comparatively higher swelling and shrinkage. The authors have attributed such behaviour to the interruption of the lime-clay reactions during the initial drying.

The studies by Cuisinier and Deneele (2008) indicated that the treatment efficiency decreases with time, the decrease may be linked to particular environmental conditions (weather, drainage, etc.) or the lime soil reactions. Estabragh *et al.* (2013) conducted laboratory study on the cyclic vertical deformations of pond ash stabilized expansive soil, as presented in Figure 2.10. It was concluded that swell reduction was effective only in the first cycle and its efficacy was lost in subsequent cycles due to the destruction of pozzolanic products. Recently, Chittoori *et al*. (2017) compared the swell-shrink cycles of lime and cement treated expansive soils. It was observed that the soils with less montmorillonite content survived for higher number of cycles than soils with more montmorillonite content. And the study also reported that the cement stabilized soil showed better performance than the lime stabilized under swell-shrink condition.

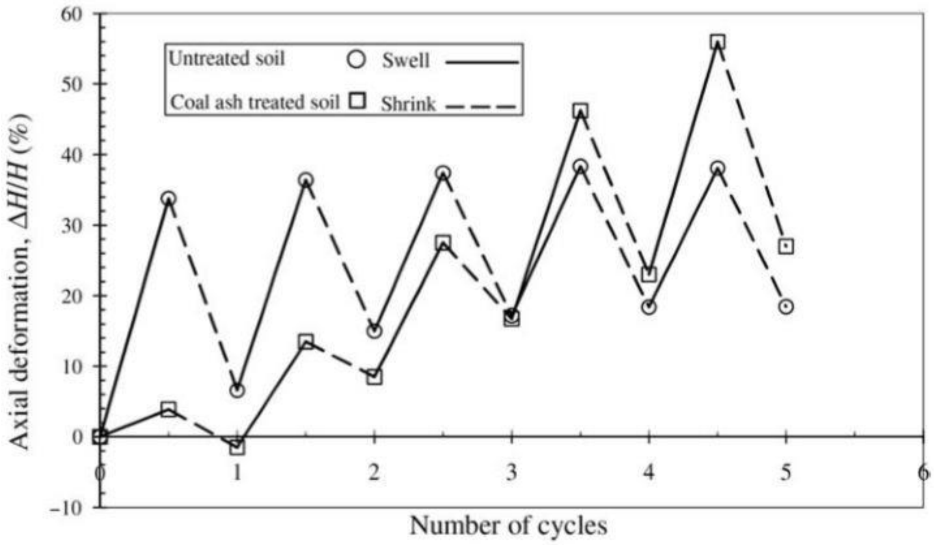

Figure 2.10: Variation of vertical strain with wet-dry cycles for expansive soil and soil treated with 20% coal ash (after Estabragh *et al*. 2013)

2.7. 7 Resilient Modulus of Stabilized Soil

The engineering properties of the earth materials for the pavement applications can be evaluated through the resilient modulus test. Resilient modulus is an appropriate test to measure the stiffness of the subgrade layer in a pavement structure. The specimen is initially exposed to an all-round confining pressure which produces an initial strain as shown in Figure 2.11 Then the cyclic axial stress is applied at a constant magnitude σ_d, which induces the cyclic resilient axial strain, ε_r. The resilient modulus M_R is defined as the ratio of the cyclic deviatoric stress to recoverable axial strain and it given by the equation

$$M_R = \left[\frac{\sigma_d}{\varepsilon_{rt}} \right] \tag{2.6}$$

where σ_d is the repeated deviatoric stress (σ_1-σ_3), and ε_{rt} is the recoverable axial strain

Figure 2.12 show the simulation of axial loading through the wheel load in the field. The magnitude of resilient modulus depends on loading condition (confining pressure, deviatoric stress and repeating load), type of soil (find grained or coarse grained soil), soil physical state (unit weight and water content) and method of compaction (Li and Selig 1994; Lee *et al*. 1997). Studies carried out by several researchers have shown that the resilient modulus of cohesive soils is greatly influenced by the deviatoric stress. Studies carried out by Wilson *et al.* (1990), Drumm *et al*. (1990) and Thompson and Robnett (1979) have shown that at low stress levels (stress values < 27.6 kPa), the M_R values show a decreasing trend with increasing deviatoric stress. At greater levels of deviatoric stress (stress values > 41.4 kPa), the resilient modulus values either decreases or reaches constant value. Figure 2.13 show the variation of resilient modulus with confining stress and deviatoric stress for a typical fine grained soil.

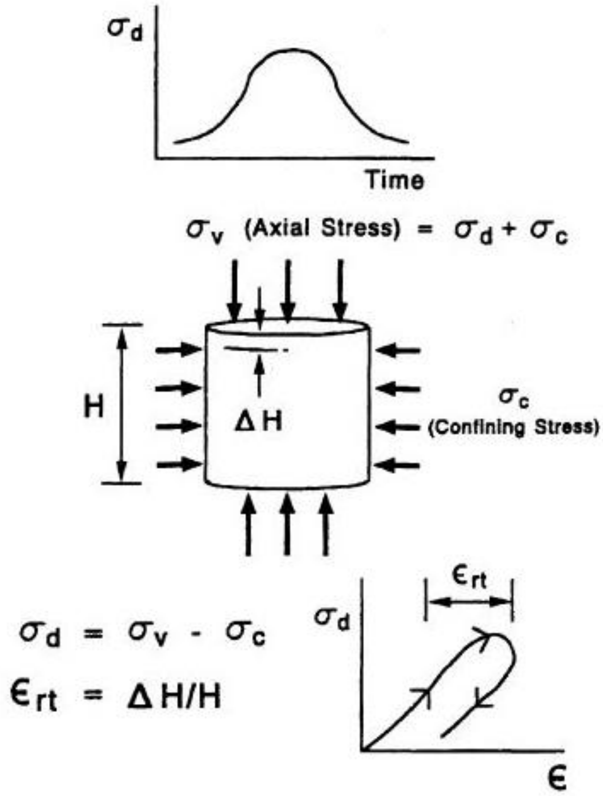

Figure 2.11: Laboratory condition of stress application for resilient modulus test (after Little, 1995)

To overcome the limitations of problematic soils as a pavement layers, many researchers (Robnett and Thompson 1976; Little 1995; Puppala *et al*. 1996) worked on chemical stabilization to improve its engineering properties. Puppala *et al.* (2007) carried out cyclic triaxial tests using the AASHTO T-294 protocol to determine the resilient modulus of lime treated soils. The resilient modulus testing indicated a 20 to 50% increase of M_R values and there was a decrease in plastic deformation. Recently, Bhuvaneshwari *et al.* (2019) studied the effect of moisture ingression on the resilient modulus of lime stabilized expansive soil. It was reported that soaked specimen showed higher resilient modulus than the unsoaked specimens for 6% lime treated specimens.

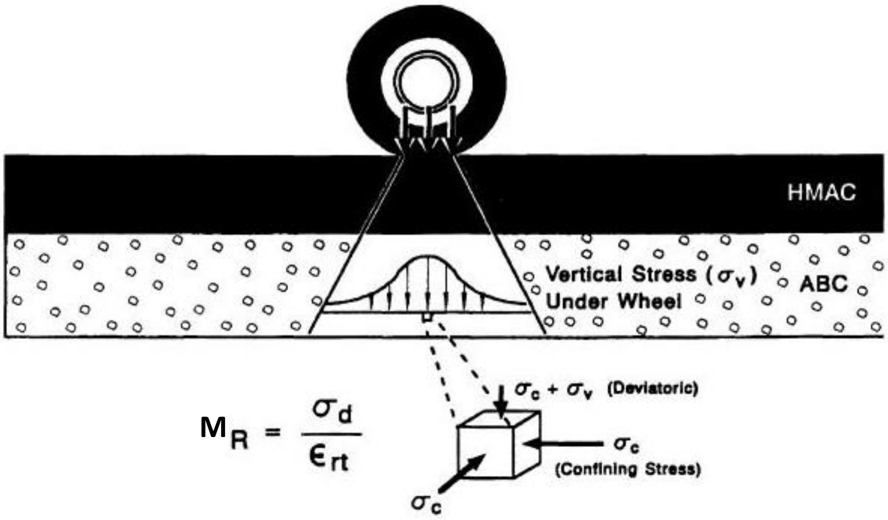

Figure 2.12: Stress distribution in typical pavement subjected to traffic load (after Little, 1995)

2.7.8 Models for resilient modulus

From the above discussion, it is seen that the important factors that govern the magnitude of resilient modulus are deviatoric stress and confining pressure. But the researchers (Barksdale 1975; Townsend and Chisolm 1976) also found that confining pressure has less influence on the resilient modulus of fine grained soils. Hence, many works were carried to establish the constitutive models to predict the resilient modulus of fine grained and coarse grained soils. The following are the models widely used for the prediction of resilient modulus

a) Power model

This model was adopted by Witczak and Uzna (1981) mainly based on the works on fine grained soils.

$$\frac{M_R}{\sigma_{atm}} = k\left[\frac{\sigma_d}{\sigma_{atm}}\right]^n \tag{2.7}$$

where n and k are soil model parameters depends on soil type and soil physical state (n value is usually negative). This model considers only the applied deviatoric stress and the effect of confining stress was not included. Hence this model could not predict the correct M_R value if there is an increase in the confining stress resulting from heavy traffic loads.

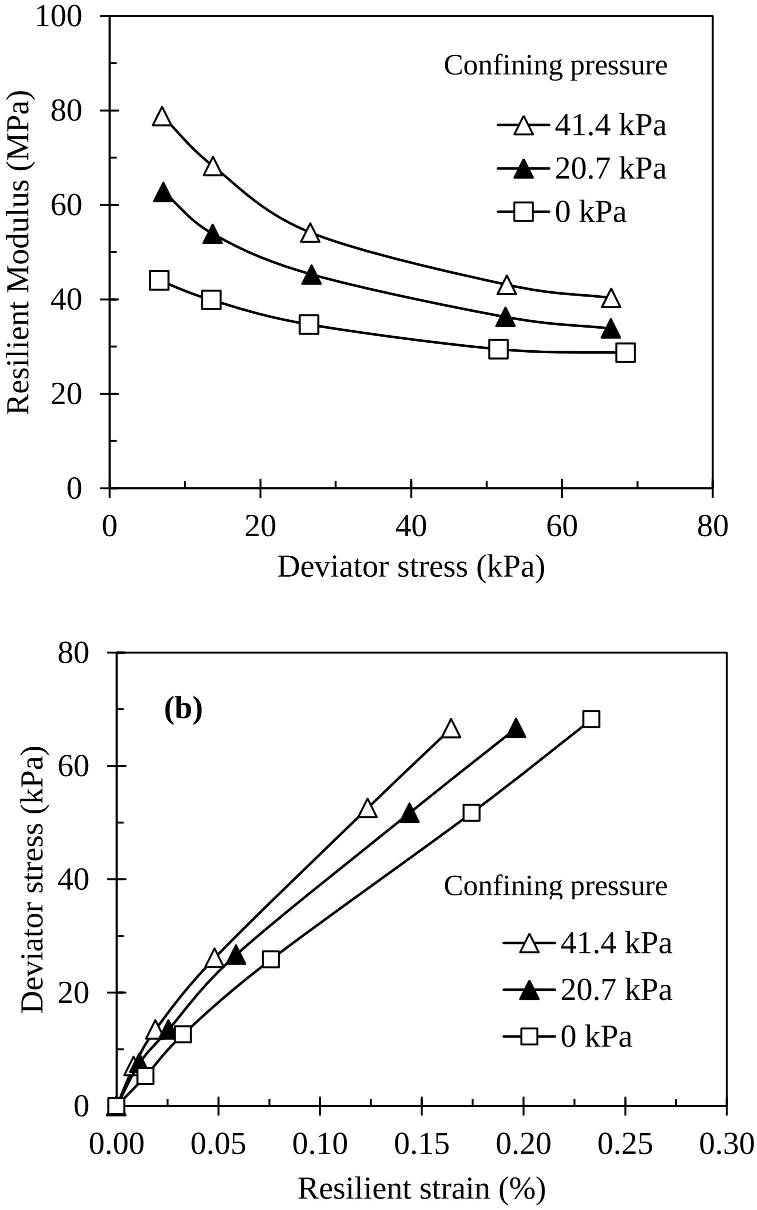

Figure 2.13: Resilient modulus tests on fine grained soils (a) deviator stress versus. resilient modulus and (b) resilient strain versus deviator stress (after Lee *et al*. 1997)

b) Bulk stress model

The resilient modulus from bulk stress model is given by the equation

$$\frac{M_R}{\sigma_{atm}} = k_1 \left[\frac{\theta}{\sigma_{atm}} \right]^{k_2} \qquad (2.8)$$

Where k_1 and k_2 are model constants and θ = bulk stress ($\sigma_1+\sigma_2+\sigma_3$)

This model includes the effect of both confining pressure and deviatoric stress. AASHTO-T 307 (2003) also suggests the bulk stress model for the determination of resilient modulus of granular soil. But this model does not consider the development of shear stress and shear strain during the cyclic loading (Witczak and Uzan, 1988)

c) Universal model

This model is the extension of power and bulk stress model and also it includes the effect of both confining pressure and deviatoric stress. The universal model is given by the equation

$$\frac{M_R}{\sigma_{atm}} = k_1 \left[\frac{\theta}{\sigma_{atm}} \right]^{k_2} \left[\frac{\sigma_d}{\sigma_{atm}} \right]^{k_3} \qquad (2.9)$$

d) Octahedral stress model

Mohammad *et al*. (1999) proposed this model as to overcome the limitations of bulk stress model and deviatoric stress model. This model includes the effect of stress states and soil physical sate (moisture content and dry density).

$$\frac{M_R}{\sigma_{atm}} = k_1 \left[\frac{\sigma_{oct}}{\sigma_{atm}} \right]^{ki} \left[\frac{\tau_{oct}}{\sigma_{atm}} \right]^{k2} \qquad (2.10)$$

Where σ_{oct} is octahedral normal stress, $\sigma_{oct} = \frac{\sigma_1 + 2\sigma_3}{3}$

τ_{oct} is octahedral shear stress, $\tau_{oct} = \frac{\sqrt{2}}{3}(\sigma_1 - \sigma_3)$

2.8 SHALLOW STABILIZATION

Shallow stabilization is effective but it can be carried out to a limited depth. Stabilization methods like prewetting, compaction control, cohesive non-swelling soil (CNS) and chemical stabilization are effective for shallow applications. Chemical stabilization is the most widely used technique and it can be used for shallow and deep stabilization.

Chemical stabilization is carried out by scarifying/ the shallow soil and stabilizer (lime/cement/fly ash) in the powder or slurry form is spread and mixed with the soil using a rotovator and then compacted. The depth of treatment of soil through physical mixing is limited to 1.5 m and beyond this depth it may require special equipments (Bowles, 2012).

2.8.1 Replacement with Non-Swelling Soil

The partial or full replacement of expansive soil strata with non-expansive fill materials reduces the volume change upon soil wetting. Holtz (1959) suggested the soil replacement as a retrofitting technique for Mohawk and Welton canal constructed over expansive soil. Lightly compacted gravel and sand was used as a compensating material. Since it is a remedial measure, the material was placed over the partially swollen sample, and the replacement material not only provides the surcharge effect but also it minimises the differential movement. Satyanarayana (1969) and Moussa *et al*. (2008) suggested sand cushion as a compensating material to control the volume change. It works on the principle that during monsoon the wet sand consumes less volume and hence it accommodates the excess volume change of underlying expansive soil. Similarly, during the shrinkage process of expansive soil, the excess voids are compensated by bulking nature of sand in a partially saturated condition. Table 2.6 summarises the different types of compensating materials and their function in volume change control.

Based on the field observations Chen (1975) reported that a structure resting on 5 feet (1.5 m) of granular soil (SP - SC) followed by expansive soil did not result any distress. But the mechanism behind the control of swell was not clear i.e. whether the seepage water did not reached the expansive soil or it was because of the uniform heave of expansive soil that did not result in any distress of the structure. And he also suggested that the degree of compaction of the compensating material should be in the range of 90 to 100% of standard proctor density. The continuous works of Katti *et al.* (1969); Katti and Kate (1975); Katti (1978) proposed cohesive non swelling (CNS) soil as a compensating material and showed that the swelling was controlled due to the development of cohesive forces in the CNS material. Figures 2.14 and 2.15 show the application of CNS technique in canal lining and pavement construction adopted by Katti (1978). Based on the laboratory and field investigations, Katti (1978) proposed the specifications, field conditions and thickness of CNS material to minimise the heave of expansive soil during saturation. Table 2.7 presents the specifications for CNS material reported by Katti (1978). IS-9451: 1994 also suggested the specification proposed by Katti (1978) for swell control in expansive soils in particular for canal applications. Bharadwaj (2013) carried out the numerical study to predict the heave in expansive soil stabilized with non-swelling soil. Figure 2.16 compares the predicted heave in expansive soil for varying thickness of 0.5 to 4 m thickness of non-swelling soil.

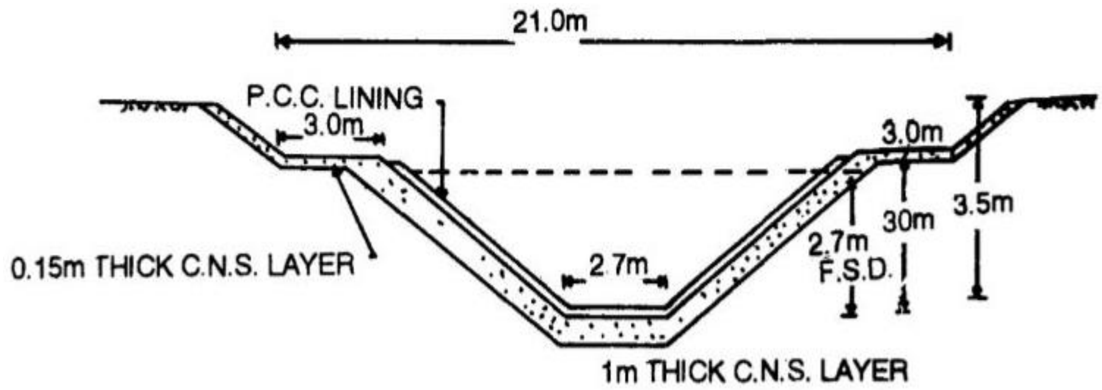

Figure 2.14: Cross section of canal with CNS material in expansive soil (after Katti, 1978)

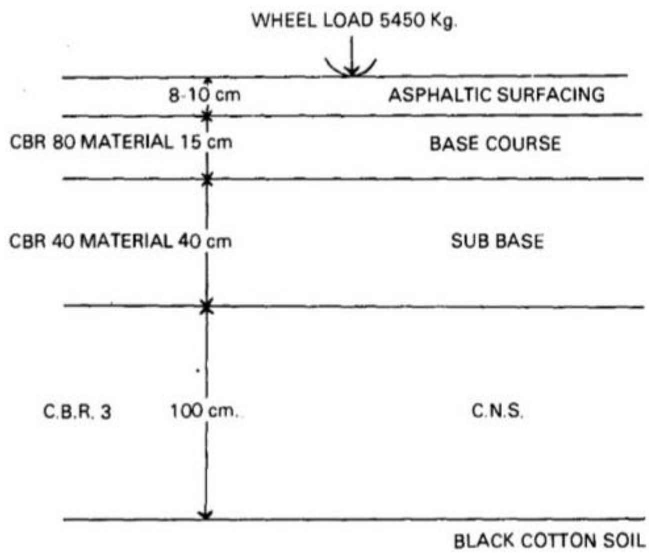

Figure 2.15: Cross section of flexible pavement with CNS material in expansive soil (after Katti, 1978)

Practically it is difficult to obtain the soils with the exact specification of CNS material in the vicinity of the construction site (location), and this makes the designer to choose alternate methods (Katti, 1978; Rao *et al.* 1994). Later researchers tried to get a CNS material using industrial wastes like fly ash and rice husk ash by using directly or blending with cement or lime as cushion. Few experiments were conducted to study the possibility of using native expansive clay as CNS material by mixing with suitable admixtures and called this material as chemically stabilized soil (CSS) cushion (Katti, 1978; Katti and Katti, 1994).

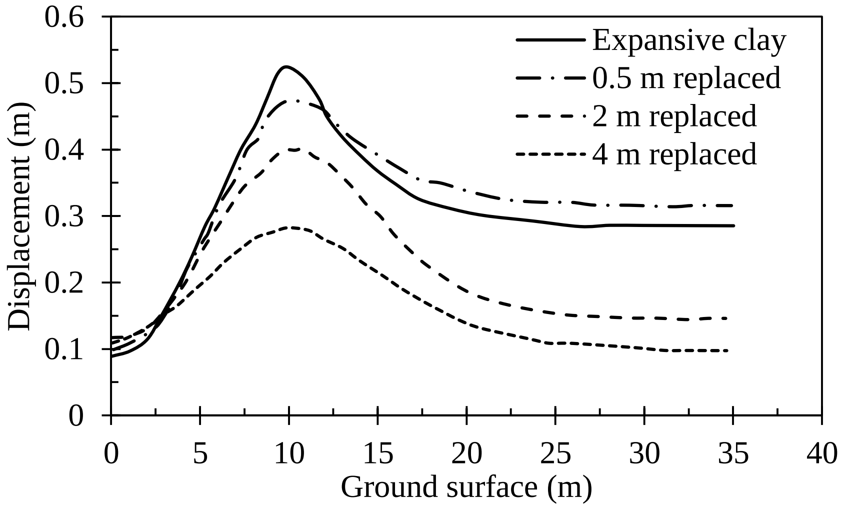

Figure 2.16: Predicted heave at the ground surface (after Bharadwaj, 2013)

Sivapullaih *et al*. (2004) performed the laboratory-based studies to use the rice husk ash as a cushion material by mixing with lime and cement. The results showed that the 6% of lime along with rice husk ash which was cured for a week was suitable for a lime cushion material (LSC). The swell potential of LSC (lime stabilized cushion) stabilized expansive soil was effective not only in the first cycle, but also its efficacy continuous for the subsequent cycles. And the swell potential decreases further with increase in thickness ratio. Rao *et al*. (2008) recommended the use of lime admixed fly ash as a cushion material. They also suggested that the thickness of the cushion should be half the depth of active zone for efficient functioning. Murthy and Praveen (2008) suggested that the expansive clay blended with 0.5% $CaCl_2$ and 8% rice husk ash can also be used as CNS material.

2.8.2 Cyclic swell-shrink behaviour of CNS/ CSS stabilized expansive soil

Few studies were carried out on natural, cement/ lime stabilized murrum as a CNS material and subjected to wetting and drying cycles (Sahoo *et al*. 2008; Sahoo and Pradhan, 2010). Rao and Rao (2010) performed swell-shrink studies to evaluate the suitability of cement and lime stabilized fly ash as a cushion material. They found that the cement stabilized fly ash cushion was more effective than the lime stabilized fly ash cushion in controlling the swell-shrink movements.

Table 2.6: Summary of different compensating materials used for the volume change control in expansive soils

Literature	Depth of excavation in active zone (AZ) (m)	Thickness of material to be compacted (m)	Soil suggested for replacement	Governing factor/ mechanism controlling swelling
Satyanarayana (1969)	-	-	Sand	✓ Due to change in thickness of sand upon wetting ✓ Loss of adhesion between clay particles
Chen, (1975)	-	0.9 to 1.5 (depending on swell pressure)	Soils with LL= 30% to 50% , Fines(<75 μm) - 5 to 50%	Material should be impervious
Katti, 1978	-	0.75 to 1.0 (depending on swell pressure)	Summarised in Table 2.7	Cohesive forces in CNS material
Moussa *et al*. (1985)	-	-	Sand	✓ Loss of adhesion between clay particles ✓ Due to change in void ratio of sand upon saturation
Rao *et al* (1988)	✓ Swell decreases with removal of soil in active zone ✓ Half the Depth of removal in active zone reduces the swell by 85%	-	Any non-swelling soil	-

Literature	Depth of Excavation in Active zone (AZ), m	Thickness of material to be compacted (m)	Soil suggested for replacement	Governing factor/mechanism of controlling swelling
Nelson and Miller (1992)	-	Suggested based on the works of Chen (1988)- 0.9 to 1.2	-	Replacement may control the moisture variation of underlying expansive soil
Fityus *et al.* (2004)	✓ 50% swell occurs in top 20-50% depth of active zone ✓ 80% swell occurs in top 60% depth of active zone	-	-	-
IS 9451-1994	-	0.75-1.15(depends on swell pressure)	As similar to Katti (1978)	Not explained
Rao *et al.* (2008)	Half the depth of swelling region can be excavated	-	CSS	Development of cohesive forces in CSS material
Murty and Praveen (2008)		0.5 to 1.0	CSS	Overburden stress and cohesive bonds in CSS
Bharadwaj (2013)	-	-	Non-swelling soil	✓ Partial removal of soil in heave zone ✓ Surcharge stress ✓ Hydraulic properties of replacement material

Note: CNS: Cohesive non swelling; CSS: Chemically stabilized soil

Table 2.7: Specifications for cohesive non-swelling soil (CNS) (after Katti, 1978)

S.No	Properties	Specifications range
1	Gradation (%) Clay (<0.002 mm) Silt (0.06 mm - 0.002 mm) Sand (2 mm - 0.06 mm) Gravel (>2.0 mm)	 15 - 25 30 - 45 30 - 40 0 - 10
2	Atterberg limits (%) Liquid limit Plastic limit Plasticity Index Shrinkage limit	 30 - 50 20 - 25 10 - 25 15 and above
3	a) Swelling pressure when compacted to standard Proctor optimum maximum dry density at moisture content and with no volume change condition (kg/cm^2) b) Swelling pressure when compacted to standard proctor dry denisty at optimum moisture content and with no volume change condition (kg/cm^2)	Less than 0.1 Less than 0.05
4	Clay minerals	Kaolinite or illite
5	Shear strength of compacted sample at standard Proctor maximum dry density and optimum optimum content after saturation a)1/2 UCS (kg/cm^2) b) consolidated drained direct shear test at 0.0125 mm/min C_u (kg/cm^2) ϕ_u (degree)	 0.12-0.35 0.1-0.3 8-15
6	Approximate thickness of CNS layer Swelling pressure (kg/cm^2) 1 - 1.5 2 - 3 3.5 - 5.0	 75-85 90-100 105-115

2.9 DEEP STABILIZATION

In-situ deep stabilization of clay soils using lime has been mainly pioneered in Sweden, Japan and USA to improve the engineering properties of soft soils (Tsytovich *et al*. 1971; Broms and Boman 1979; Kitsugi and Azakami 1982; Bell, 1988; Chew et al. 1993; Porbaha 1998). The in-situ deep stabilization using lime can be divided in to three main groups: lime columns, lime piles and lime slurry injection (Glendinning and Rogers 1996). Lime columns are used primarily as an alternative to stone columns for stabilizing soft clays. Lime piles are used for similar applications, while lime slurry has its main application in slope stability.

2.9.1 Lime Column Technique

Columns refer to creation of deep vertical columns of lime/ cement stabilized material in-situ. The most commonly used method is Deep Soil Mixing (DSM) and it is constructed by in-situ mixing of lime and soft clay. The schematic view of deep soil mixing blade and stabilized soil columns are shown in Figure 2.17. Deep mixing has been adopted in various applications like foundation improvement, seepage control, heave control, liquefaction mitigation, marine applications, etc. (Porbaha 1998). The columns are generally formed through mechanical mixer in which admixtures are mixed with the soil by mixing blades and method like jet mixing is also used (Porbaha 1998). Figure 16(b) shows the formation and completed deep soil mixing column. The deep soil mixing with designed guidelines was first implemented for the stabilization of marine clay for the construction of the Tokyo port in 1975 (Terashi, 2002a). The diameter of the stabilized soil column varies from 0.5 to 1 m and the depth of treatment of soil ranges from 3 to 50 m (Moseley and Kirsch, 2004). Figure 2.18 show different patterns of installation of DSM columns.

In early 1970's, the lime was used as a principal binder for stabilization, but later usage of other admixtures like cement, slag, fly ash has also gained its importance. Figure 2.19 shows the alternatives in chemical binders for soil stabilization with time. For stabilization of soft clay, cement has been preferred over lime is not only due to its availability and low cost, but also because of its better efficacy than lime (Broms, 1984). The chemical reactions between the soil and lime/ cement produce material of greater shear strength and reduced compressibility than the untreated soil.

Bergado *et al.* (1999) reported that engineering behaviour of cement-stabilized soils is mainly influenced by the percentage of cement added and curing period. The cement content (A_w) is defined as

$$A_W = \frac{\text{weight of cement}}{\text{dry weight of soil}} \tag{2.11}$$

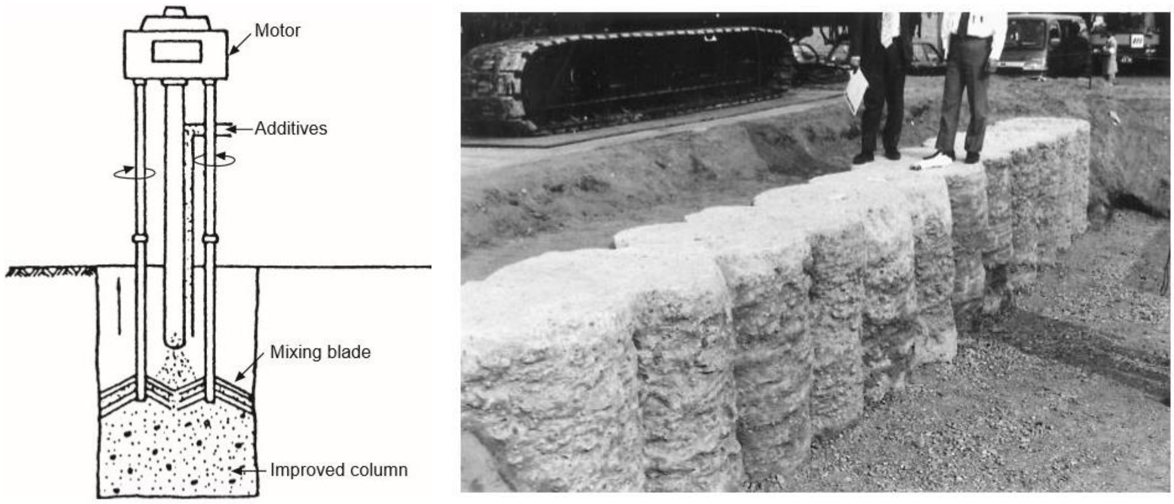

Figure 2.17: (a) Formation of deep mixing column and (b) stabilized ground by deep mixing technique (after Porbaha, 1998)

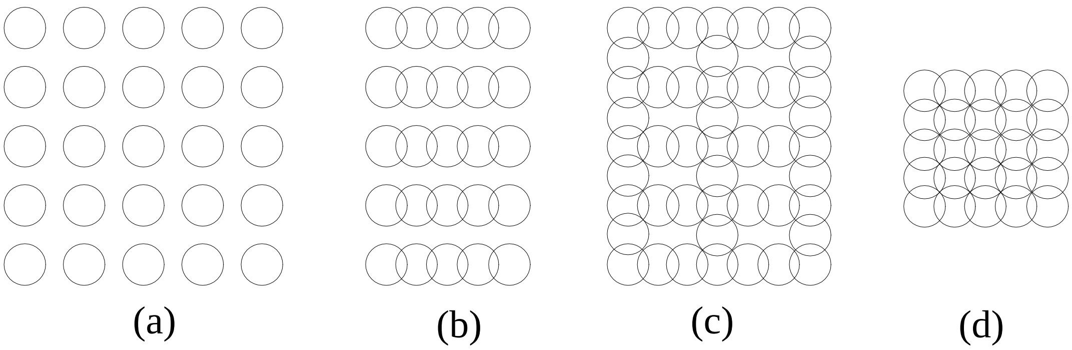

Figure 2.18: DSM patterns (a) Column type (b) overlapped walls (c) grid type (d) block type (after Moseley and Kirsch, 2004)

But later Muira *et al.* (2001) demonstrated that engineering characteristics of soil-cement brahviour is also influenced by clay water content of soil-cement paste. They developed a new factor (C_w/A_w), ratio of total clay water content to cement content.

$$C_w = w + \frac{W}{C} A_w \tag{2.12}$$

where C_w = total clay water content (%), w = remoulding water content (%), W/C = water-cement ratio and A_w = cement content

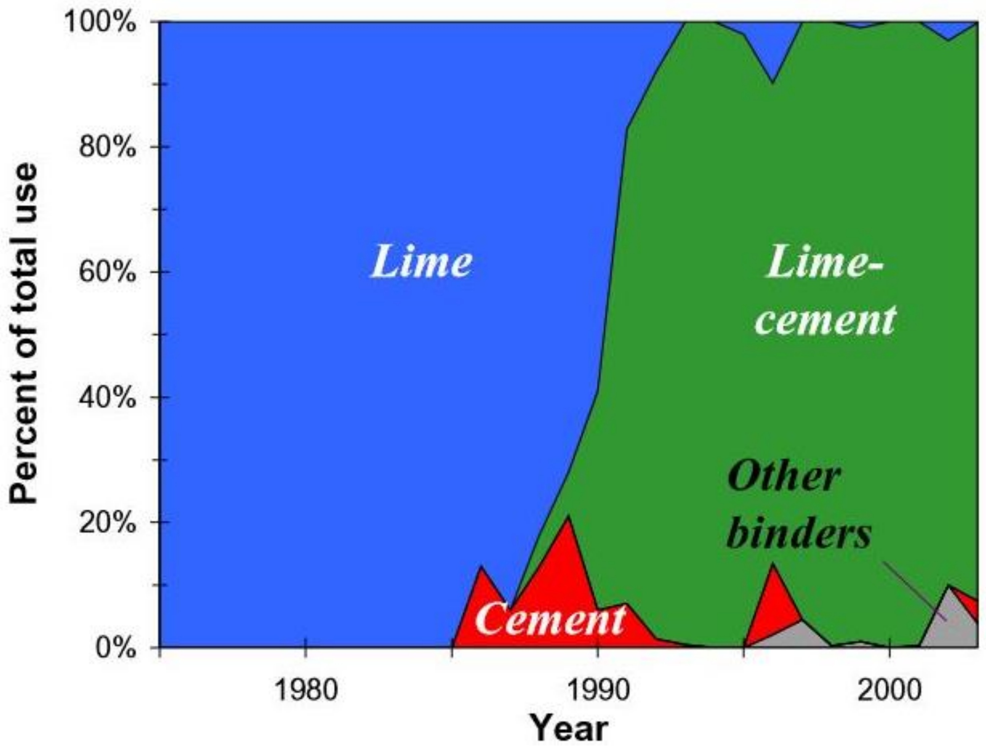

Figure 2.19 Changes in chemical binders with time for deep soil mixing applications (after Ahnberg, 2006)

Recently, Bushra and Robinson (2013) performed laboratory based studies to improve the engineering properties of low plasticity marine clay through cement-fly ash mixture. They found that the optimum dosage of fly ash as 20% along with 10% cement, with the total clay water content as 1.25 times the liquid limit water content.

Hewayde *et al*. (2005) conducted a laboratory-scale experimental investigation on the efficiency of unreinforced and reinforced lime columns in controlling the swelling of expansive soils. The unreinforced and reinforced lime columns reduced the swelling potential of expansive soil by 33% and 69%, respectively, as compared to untreated expansive soil. The swelling reduction in reinforced lime column is attributed to both physico-chemical changes occurring due to lime and development of resistive adhesive forces at the interfaces of lime column and surrounding soil and the reinforcement and lime column.

Puppalla *et al*. (2008) evaluated the effectiveness of lime-cement deep soil mixed (DSM) column in controlling the swelling of medium stiff expansive soils through pilot field studies at Haltom City, USA. The results showed that the swell-shrink movements and swell pressures in both vertical and lateral directions were remarkably lower in sections treated with DSM columns as compared to the untreated soil sections. Madhyannapu *et al*. (2010) performed a quality assessment to compare the stiffness and strength achieved in the laboratory and field tests. They found that the field stiffness and strength reduced by 30% to 60% and 20% to 30%, respectively, when compared to the laboratory conditioned specimens.

2.9.2 Lime Pile Technique

Lime piles are used as an alternative for stabilizing soft saturated soils (Bell, 1988; Glendinning and Rogers, 1996). Lime piles are usually holes created in the ground and filled with lime. Generally, the lime piles are 0.3-0.5 m in diameter and spaced at 1-2 m center to center. In China and Japan relatively large diameter (0.5-1 m) quicklime piles have been used as a ground improvement technique for soft soils (Tsytovich *et al*. 1971; Kitsugi and Azakami, 1982). When lime in contacts with water, it will expand 30-70% of its original volume and generates heat as a result of exothermic reaction and this makes the pore water to evaporate (Bell, 1993). The improvement is primarily attributed to expansion of pile, dehydration of clay and soil-lime reactions. However, migration of lime into the soil is restricted to small radial distances of about one to two times the diameter (1-2D) of the lime piles. Rao *et al*. (1993), Rajasekharan and Rao (1997) and Mathew and Rao (1997) have extensively investigated the use of lime piles to improve the engineering behaviour of Indian marine clays. Their laboratory test results showed that lime migrated up to radial distances of 2 to 4 times the diameter of the lime piles. The results indicated a significant improvement in the plasticity characteristics of the marine soil due to lime treatment. The lime seeping from the column reacted with the soft soil to form cementation compounds that reduced the compressibility and improved the shear strength of the soil.

Rao and Venkataswamy (2002) conducted laboratory scale experiments to study the efficiency of the lime piles in altering the physico-chemical and engineering properties of compacted expansive soil. Their study indicated that the lime pile treatment promoted short-term lime modification reactions, but not the soil-lime pozzolanic reactions. The results showed that the lime pile treatment reduced the plasticity index, swell potential and slightly increased the unconfined compressive strength of the expansive soil.

2.9.3 Lime Slurry Technique

Lime slurry injection, as the name suggests, involves the introduction of lime slurry into the ground through the drilled holes made at regular intervals. Sometimes there may be secondary and tertiary injection based on the type of soil and project. The depth of treatment normally ranges from 1 to 3 m and for some projects it was even extended up to 12 m (Little, 1995). Figure 2.20 show typical pattern of lime slurry injection under pressure for stabilization of soil. This method can be adopted for both pre- and post-treatment of the soil.

In this technique, slurry is introduced into the pores and fissures in the clay, causing the treatment by migration due to permeation of the slurry (Rajasekharan and Rao 1997). The lime slurry can be injected under gravity or pressure and in particularly for deeper depth pressure injection may be useful. The injection pressure generally ranges from 345 kPa to 1380 kPa and also it depends on the type of soil and its refusal (Bell, 1993). Usually, the lime migration in expansive soil is very slow because of its impervious properties, but still soil stabilized with slurry injection showed lower percent swell (Chen, 1988). Davidson *et al*. (1965) gave an equation for the laboratory condition to know the diffusion rate of lime,

$$L = 0.081\, t^{\left(\frac{1}{2}\right)} \tag{2.13}$$

where L= lime penetration distance (inches), and t = time (days)

Thyagaraj (2001) performed laboratory-scale experiments to evaluate the effectiveness of in-situ lime slurry stabilization technique in controlling the volume change potential of expansive soils in the desiccated state. The study indicated that desiccation induced extensive shrinkage cracks in the expansive soil and greatly assisted the migration of lime slurry into the expansive soil mass. The migrated lime slurry promoted strong lime-modification and pozzolanic reactions to occur in the soil mass, which in turn reduced the swell potentials, and increased the unconfined compressive strength of the lime slurry treated specimens.

Wilkinson *et al.* (2010) studied the effect of pressure injection of lime slurry on improvement of expansive soil through pilot field testing. The observation shows that the formation of hydraulic fracture due to pressure injection paves way for the channelling of lime slurry in to large volume of soil. Figure 2.21 show the formation of hydraulic fracture in the soil profile.

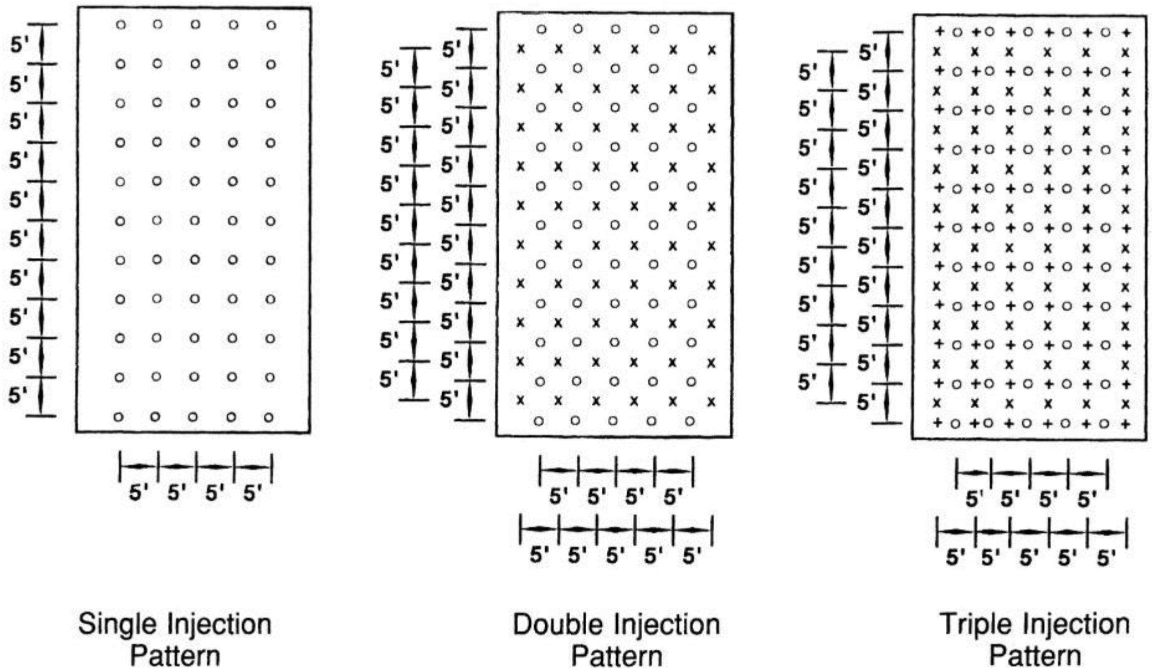

Figure 2.20: Grid systems for primary, secondary and tertiary injection of lime slurry under pressure (after Little, 1995)

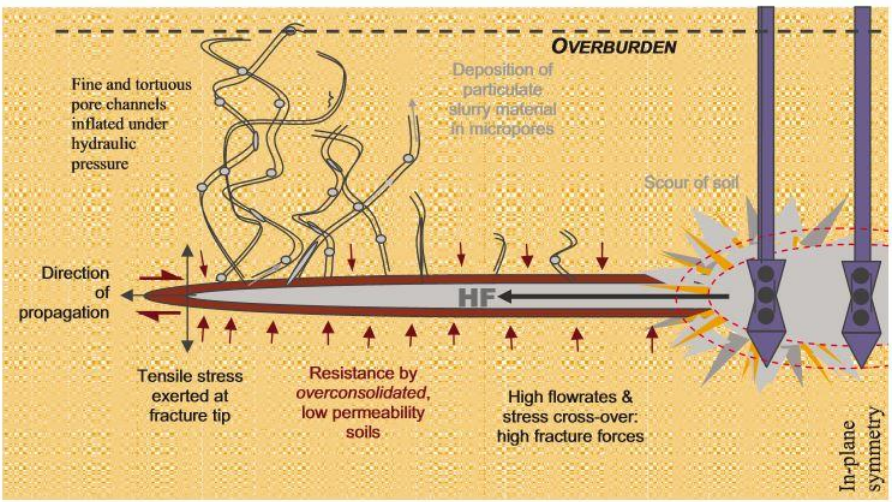

Figure 2.21: Injection of lime slurry into the soil under pressure (after Wilkinson *et al.* 2010)

Thyagaraj and Suresh (2012) conducted pilot scale field studies to evaluate the efficacy of in-situ lime slurry stabilization technique in controlling the swell-shrink potentials of expansive soils in desiccated state. Their field test results indicated that the lime slurry migrated through extensive shrinkage cracks in desiccated state and promoted strong lime-modification and pozzolanic reactions in the soil mass. The lime slurry treatment increased the soil $pH \approx 12$ to the levels that are conducive for the pozzolanic reactions to occur. The soil-lime reactions reduced the swelling potential and increased the unconfined compressive strength of lime slurry treated expansive soil. The test results encourage the application of lime slurry technique to expansive soil deposits during dry season upon development of shrinkage cracks.

Even though this method is cost effective and easy for field applications, it has some limitations. This technique provides less degree of improvement for soils with low permeability and fewer shrinkage cracks because this will obstruct the migration of lime slurry (Nelson and Miller, 1992). During the injection of slurry, there will be an increase in moisture content of the surrounding soil and this result in pre-swelling of overburden soil and loss of bearing strength of the soil (Little, 1995). Further, Wilkinson *et al*. (2004) reported that it was difficult to determine the degree of improvement after the completion of soil treatment. Hence, it may require secondary treatment if the primary treatment was not able to produce the expected results.

2.10 STATEMENT OF PROBLEM

It is evident from the above literature review that in the current practice, both qualitative and quantitative methods are practised to identify and classify the expansivity of the soil. The qualitative methods include the liquid limit, shrinkage limit, activity, differential free swell and free swell ratio. The soil sample collected from the field is oven dried, pulverised and sieved through a 425 µm sieve prior to testing. *Since the powdered sample are used for testing, these methods are independent of field placement conditions. Therefore, there is a need to develop new methods of characterisation of expansive soils which include the effects of moisture content and dry density of the soil.*

Swell potential (SP) and swell pressure (p_s) tests are the direct methods used for the determination of swell parameters quantitatively, but these methods are time-consuming and tedious (Sridharan *et al*. 1986). Factors, such as stress path, dry unit weight, water content, degree of saturation, wetting sequence and method of testing, affect the volume change and swell pressure measurement. *There are limited works available in the literature that discusses the effect of method of inundation on the estimation of swell using the conventional oedometer tests.*

Several methods have been evolved in the literature to control the free field heave in expansive soils. Methods such as moisture control, surcharge control, soil replacement technique and chemical stabilisation are more popular among field engineers. Among them, soil replacement technique could be the first choice in particular for shallow active zone because of its feasible field procedure and economical aspect. Earlier works available in the literature detailed the possible mechanism of CNS material in controlling the field heave through mobilisation of cohesive force, surcharge pressure, impervious property. *But the function of compensating material in volume change control is not explored in the literature by relating it with hydraulic characteristics of compacted CNS material.*

Fly ash has been used in various geotechnical engineering applications through physical mixing to improve the index and engineering properties. *Even though the chemically stabilized soil cushion (CSS) was explored recently by few researchers, the mechanism of stabilization and the design aspects of CSS cushion are not understood completely and thus needs further examination.*

The literature shows that many experimental works were carried out on deep stabilization of soft clay using lime and cement slurry. But limited works were conducted on expansive soils. Moreover, the deep stabilization of expansive soils using lime and fly ash is not explored in detail. *Therefore, there is a need to study the effectiveness of Class F fly ash along with lime in stabilizing the thick expansive soil deposits using slurry technique.*

CHAPTER 3

DEVELOPMENT OF RAPID METHOD FOR CHARACTERIZATION OF EXPANSIVE SOILS

3.1 INTRODUCTION

In this chapter a method is proposed to classify the degree of soil expansion with minimum effort in short time duration. In practice, to identity and classify the nature of soil expansivity, index properties like liquid limit, plasticity index, shrinkage index, colloidal content and free swell index (FSI) tests are used. However, these test methods do not include the field conditions as the powdered soils are used for the testing. In order to include the placement conditions, a new method – desiccated state free swell (DSFS) method – is proposed in this chapter. In DSFS method, first the small compacted soil specimens were desiccated and then the volume was measured and placed in a 100 ml jar and allowed to swell in distilled water, similar to FSI method. The percentage increase in volume of the desiccated soil specimen is measured and the same is used for the classification of degree of soil expansion. The proposed DSFS method is more reliable than the conventional FSI as this method includes the effect of placement moisture content and dry density in its measurement. A total of 21 soils covering a wide range of plasticity characteristics and swell potentials were used in the present study. From the experimental results it was observed that the prediction of soil expansion using DSFS method is better in comparison to the conventional qualitative methods. Finally, based on experimental results obtained from 21 soils a new classification chart is proposed based on DSFS method for the prediction of the degree of soil expansion.

3.2 EXPERIMENTAL PROGRAM

The present study aims to propose a new method for the identification of expansive soil and its degree of soil expansively. For expansive soil identification, both qualitative methods (like free swell index, modified free swell index and free swell ratio) and quantitative methods (swell potential) are used, and the same methods are compared with the proposed method. The experimental program followed is presented in the flow chart shown in Figure 3.1.

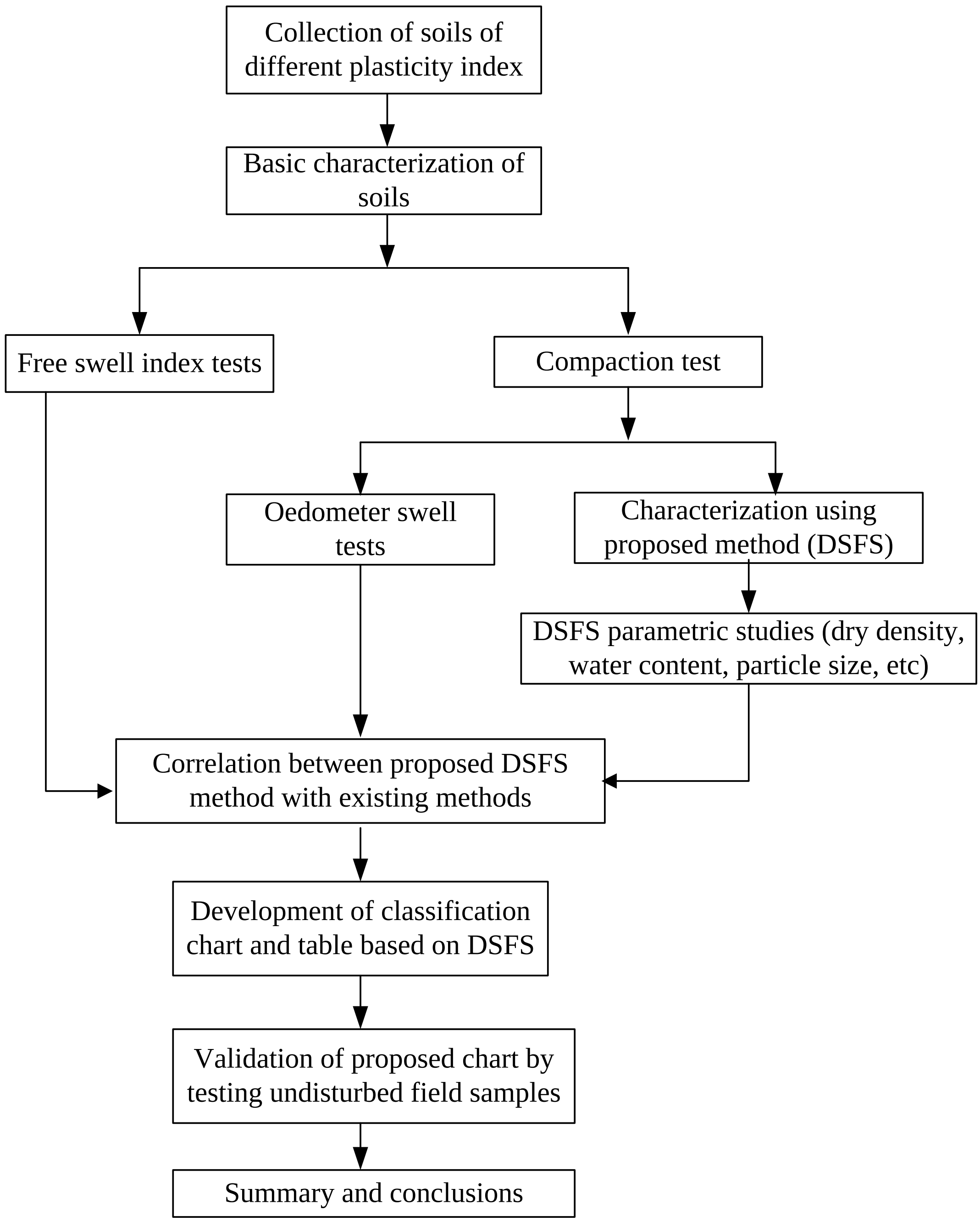

Figure 3.1 Flow chart depicting the experimental program followed in the present study

3.2.1 Materials and Properties

To perform the tests on soils with a wide range of plasticity index, expansive soils, red soils and laterite soils were obtained from the field. Commercially available kaolinite was also used for testing. The field soil samples were air-dried, pulverised and passed through the 425 μm sieve before using them for testing. Basic characterization tests were performed as per Indian Standards (IS) and the properties are compiled in Table 3.1. The liquid limit and shrinkage limit of the soils vary from 35% to 95% and 8.5% to 22.5%, respectively. From the Atterberg limits and sieve analysis, the soils were classified as CH, CL, SC and SM as per Unified Soil Classification System. As the objective of the present chapter is to incorporate the placement conditions in free swell measurements, the standard Proctor compaction tests were also carried out on all the soils.

The placement conditions of soils were selected from the compaction curve, such that it considers dry of optimum, optimum and wet of optimum conditions of the soils (Figure 3.2). To study the degree of soil expansivity, one-dimensional swell potential tests were also carried out on all the soil samples. The tests were conducted in rings of 75 mm diameter and 30 mm thickness stainless steel rings. The pre-wetted soil was statically compacted to 20 mm thickness. After fixing the oedometer ring with the compacted soil specimen in the oedometer cells, the assemblies were fixed in the loading frame and the surcharge pressure of 6.25 kPa was applied. The oedometer cells were flooded with distilled water and allowed to swell until it reaches the equilibrium condition. The expansive nature of the soil was classified based on the chart proposed by Seed *et al.* (1962) and it varies from 0% to 23%, as summarised in Table 3.3. Figure 3.3 shows the time-swell plots of low, medium, high and non-swelling soils used for the present testing.

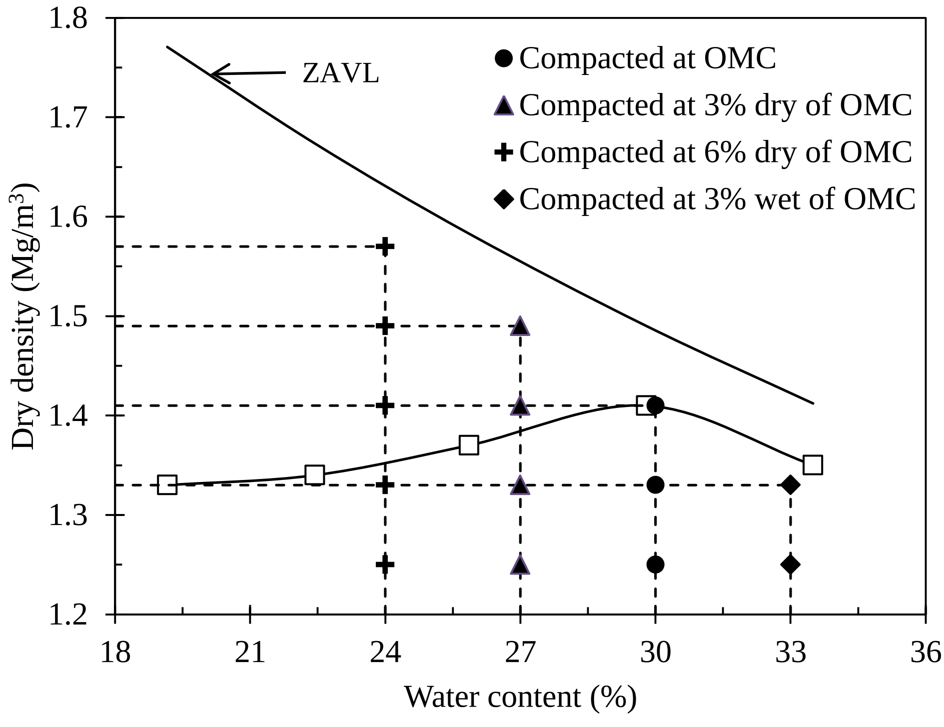

Figure 3.2: Placement conditions adopted for DSFS and oedometer swell potential tests on Trichy soil-2 (Standard Proctor curve)

Table 3.1 Properties of soils used for testing

S. No	Soil description	Grain size distribution (%)				G_s	Atterberg limits (%)			I_P (%)	USCS	DFS (%)	FSR	MFSI
		Gravel	Sand	Silt	Clay		w_L	w_P	w_S					
1	Chemmenchery	-	42	17	41	2.7	97	20	11.0	77	CH	300	4.0	9.80
2	Trichy soil-1	-	33	17	50	2.74	90	22	8.0	68	CH	280	4.0	9.41
3	NIT Warrangal	1	22	24	53	2.72	85	25	9	60	CH	240	4.0	8.25
4	Kishkinta	-	3	15	82	2.71	74	30	9.0	44	CH	110	2.1	4.69
5	Siruseri	-	7	18	75	2.78	78	30	9.0	48	CH	100	2.0	4.56
6	Trichy soil-2	-	3	29	68	2.68	95	33	8.5	62	CH	95	1.9	4.09
7	Gummudipoondi	-	8	34	58	2.60	59	25	8.0	34	CH	91	1.91	3.94
8	Padianallur	-	12	30	58	2.68	59	28	9.5	31	CH	95	1.95	-
9	NIOT chennai	-	43	20	37	2.71	59	24	10.5	35	CH	73	1.82	3.74
10	AP soil	1	5	41	53	2.67	57	28	11.0	29	CH	50	1.5	3.01
11	Kenya soil	-	21	48	31	2.73	69	23	14.5	46	CH	45	1.4	2.96
12	L&T Ford	-	3	44	53	2.72	52.5	23	-	29.5	CH	75	1.8	-
13	Anna nagar	-	10	36	54	2.7	46	22	8.7	24	CL	82	1.82	4.0

14	Kaolinite	-	39	28	33	2.67	40	25	22.5	15	CL	Negative	-	2.20
15	Laterite soil	-	-	-	-	2.75	32	16.5	11.5	14.5	CL	0	1	1.75
16	Red soil (1)	15	56	19	10	2.7	35	17	15.0	18	SC	20	1.2	2.24
17	Red soil (2)	4	54	33	9	2.7	43	17	16.0	26	SC	20	1.2	2.24
18	20% FS + 80% SS	-	27	15	58	2.75	64	26	9.0	38	CH	86	1.91	4.09
19	40% FS + 60% SS	-	47	11	42	2.73	52	22	9.5	30	CH	74	1.82	3.78
20	60% FS + 40% SS	-	67	7	26	2.7	37	18	15.0	19	SC	73	1.82	3.73
21	80%FS + 20% SS	-	87	3	10	2.66	-	-	18	-	SM	0	1.0	1.66

Note. FS: Fine sand; SS: Siruseri soil, USCS: Unified Soil Classification System, w_L : liquid limit, w_{PL} : plastic limit, w_{SL} : shrinkage limit, I_P : plasticity index, FSR : Free swell ratio, MFSI: modified free swell index

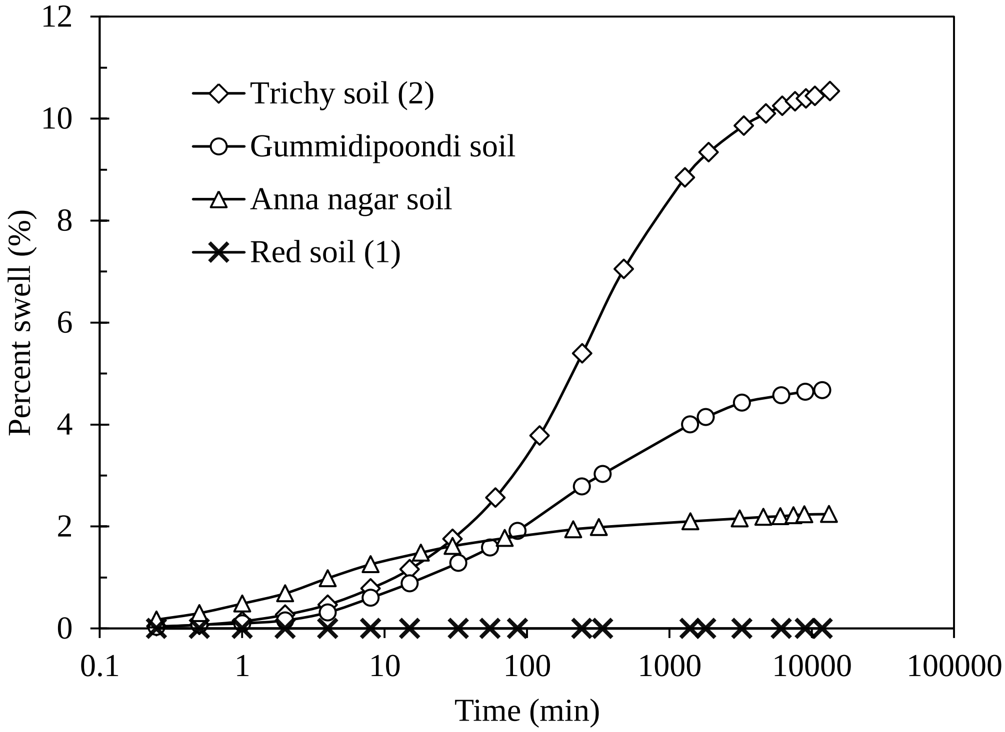

Figure 3.3: Time-swell plots of high, medium, low and non-swelling soils

3.2.2 Accessories for Preparation of Compacted Soil Specimens

Figure 3.4 shows the ring and necessary accessories fabricated for the preparation of small compacted soil specimens for the proposed DSFS method. It consists of a base plate, ring, spacer and ejector. The diameter and thickness of stainless steel ring is fixed as 27.5 mm and 20 mm, respectively. The dimensions of the ring were chosen such that the inner diameter of the ring is equal to or slightly lower than the inner diameter of the conventional 100 ml jars used for free swell index tests. The thickness of the soil specimens was fixed as 14 mm as it represents the height corresponding to volume of 10 cm^3 in 100 ml jars.

3.2.3 Specimen Preparation

The pulverised soil passing through 425 μm was oven dried at 105˚C for 24 hours and mixed with a predetermined amount of distilled water to get the desired initial moisture content. For the estimated dry density, known weight of pre-wetted soil was placed into the ring of 27.5 mm diameter and 20 mm height. It was then statically compacted to the required thickness of 14 mm corresponding to the required density. In order to get reliable results, three or four identical specimens were prepared with the same moisture content and dry density. For obtaining the desiccated soil specimens, the compacted soil specimens were air-dried, followed by oven drying at 105˚C.

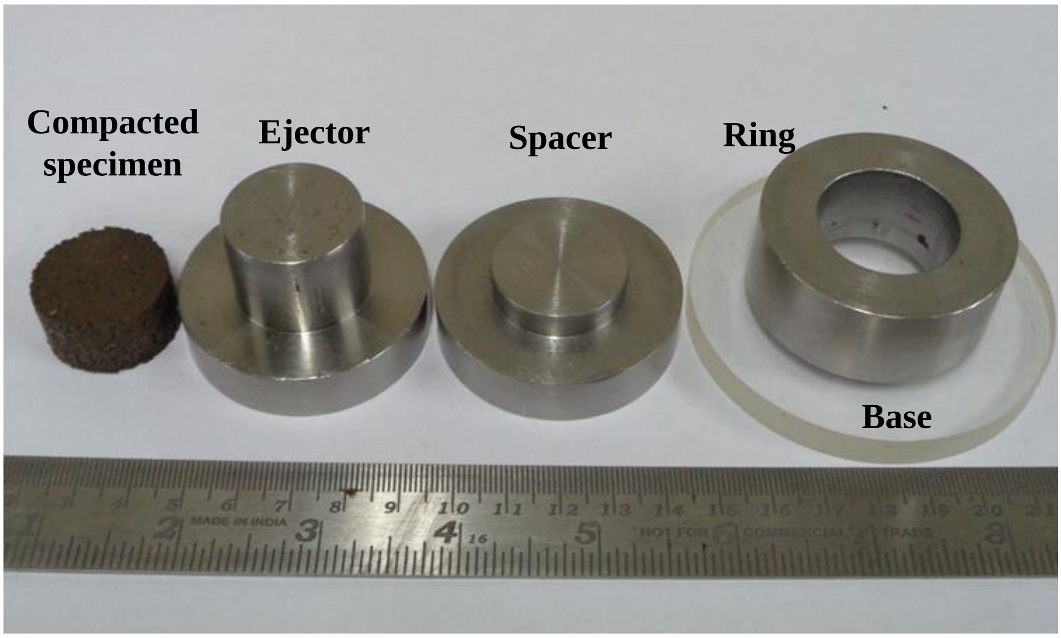

Figure 3.4: Accessories fabricated for preparation of compacted soil specimens for DSFS testing

3.2.4 Testing Procedure

The compacted soil specimens were inserted carefully into the 100 ml jar and filled with distilled water. The testing procedure is similar to that of conventional free swell index method; however in the proposed method the compacted specimens were used instead of powdered soil sample. Upon pouring the water, the as-compacted or desiccated soil specimens swelled laterally and then vertically. Hence, the swell is reported as volumetric free swell. The volume change was observed with time till it reached the equilibrium volume. The initial and final swollen volumes of the specimens were used for calculating the free swell values. The free swell values measured using as-compacted specimens is reported as CSFS and it is calculated using Equation 3.1.

$$\text{Compacted state free swell (CSFS)} = \left[\frac{Vs - V_i}{V_i}\right] \times 100 \quad (3.1)$$

where V_s is volume of swollen soil specimen (cm^3) and V_i is volume of as-compacted or desiccated soil specimen (cm^3) (V_i = 8.315 cm^3)

Free swell tests were conducted on as-compacted and desiccated soil specimens to bring out the effect of placement conditions on swelling. In as-compacted state, the initial volume of the compacted specimen is equal to the volume of the ring corresponding to 14 mm thickness. However, the volume of the desiccated soil specimen is measured manually by taking the average diameter and thickness using vernier caliper. Similarly, the free swell value measured using desiccated soil specimen is reported as desiccated state free swell (DSFS) and it is calculated using the Equation (3.2)

$$\text{Desiccated state free swell (DSFS)} = \left[\frac{Vs - V_d}{V_d}\right] \times 100 \tag{3.2}$$

where V_s is swollen volume in 100 ml measuring jar and V_d is desiccated volume of the oven dried soil specimen.

3.2.5 Parametric Studies Using Desiccated Specimens

One-dimensional oedometer test setups were used for the determination of swell potential. The desiccated state free swell (DSFS) was carried out using the fabricated accessories (Figure 3.4). The following parametric studies were carried out to evaluate the efficacy of the proposed method.

a) Initial moisture content (*w*) using Trichy soil-2. The water content was varied from 27 to 33%
b) Initial dry density using Trichy soil-2 and with varying dry density from 1.25 to 1.57 Mg/m^3
c) The effect of particle size using NIOT soil, the soil passing through 4.75 mm, 2mm, 425 µm sieve were used
d) Soil gradation effect using Siruseri soil where the fine sand was added to the swelling soil and the fine sand content varied from 20 to 80%.

For all the soils, the swell potential tests were carried out at their respective optimum moisture content and maximum dry density.

3.3 RESULTS AND DISCUSSION

3.3.1 Effect of Placement Conditions on Compacted State Free Swell (CSFS)

Figure 3.5 brings out the effect of moisture content on compacted state free swell (CSFS) of Trichy soil-2 at different dry densities. As expected, the compacted state free swell of the Trichy soil-2 decreased with increase in the moisture content at all dry densities. The compacted state free swell values at different placement conditions of Trichy soil-2 are summarized in Table 3.2. With increase in the water content, the initial degree of saturation increases at a given dry density, and hence the soil specimens tested at wet-side of optimum moisture content resulted in lower compacted state free swell values. The results obtained from the CSFS tests were compared with the one-dimensional oedometer swell potential values for evaluating the ability of CSFS method in capturing the swell potential (Table 3.2). Both methods have the same kind of behaviour under similar conditions (Table 3.2). Puppala *et al*. (2013) also showed that the soil specimens compacted at dry side of optimum water content exhibited higher volumetric swell than the specimens compacted at optimum and wet side of optimum water contents and these results were substantiated using three-dimensional free swell tests.

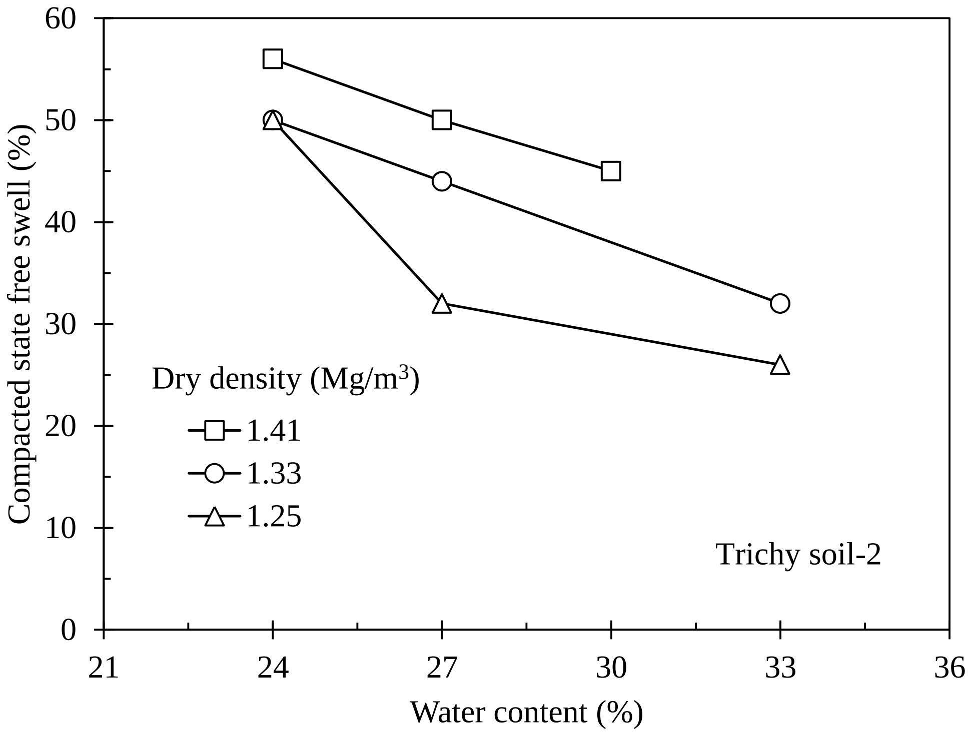

Figure 3.5: Effect of water content on compacted sate free swell (CSFS) of Trichy soil-2 at different dry densities

Further, it is evident that the compacted state free swell values of expansive soils were in the range of 25 to 150%. Similarly, for as-compacted non-expansive soils were around 35 to 60%. As there is an overlap between the magnitude of CSFS values, it is difficult to differentiate high swelling expansive soils from non-expansive soils. Therefore, the tests were also conducted on desiccated soil specimens. Moreover, the use of desiccated soil specimens for the tests could capture the effects of both shrinkage and swelling including the effect of placement condition all at one go. Further, in case of undisturbed specimens which are close to saturation the CSFS cannot capture the soil expansion owing to their high degree of saturation. Chen (1975) also suggested that it is better to measure the volume change of the soil specimens in its driest state in order to capture the extreme swelling property of the expansive soil. Thus, it becomes advantageous and easy to differentiate the expansive and non-expansive soils using desiccated soil specimens.

Table 3.2 Summary of free swell tests of Trichy soil-2 from compacted state and desiccated state at different placement conditions

S. No.	Placement conditions		Free swell (%)		Swell potential (%) (as-compacted)
	w (%)	ρ_d (Mg/m^3)	As-compacted state	Desiccated state	
1	33	1.33	32	219	8.5
		1.25	26	201	7.5
2	30.5	1.41	44	222	9.8
		1.33	32	202	8.8
		1.25	26	188	8.0
3	27	1.49	56	214	-
		1.41	50	194	14.2
		1.33	44	179	12.3
		1.25	32	164	11.2
4	24	1.57	80	214	-
		1.49	68	199	-
		1.41	56	183	16.5
		1.33	50	168	13.8
		1.25	50	152	12.0

3.3.2 Desiccated State Free Swell Method

As highlighted by Briaud *et al.* (2003), the rate of drying may enhance or reduce the possible formation of shrinkage cracks in the soil specimens. The rapid oven drying reduces the testing time but induces extensive shrinkage cracks, while the slow drying increases the testing time but reduces the shrinkage cracks. Further, the slow drying produces relatively homogenous specimens. Therefore, tests were carried out using both rapid and slow dried soil specimens to evaluate if the rate of drying has any significant effect on the DSFS values. Few specimens were rapidly dried immediately after compacting the soil specimens to the desired placement conditions. Due to rapid drying, the shrinkage cracks were developed both on the surface and inside the specimens. The rapid drying resulted in the entrapment of air in the swollen specimens. Entrapped air could not escape from the specimens as depicted in Figure 3.6. This overestimate the DSFS values of rapidly dried specimens, Therefore, the soil specimens were gradually air dried at the room temperature until the volume change becomes constant and used for the determination of DSFS.

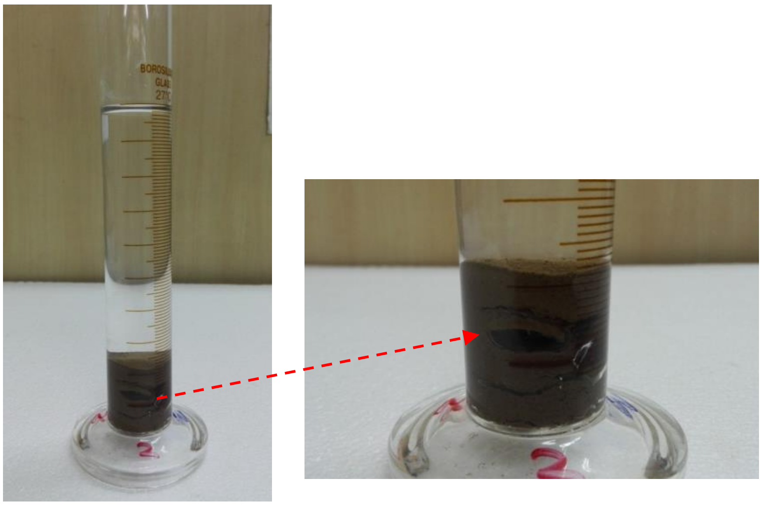

Figure 3.6: Depiction of entrapped air pockets in the swollen specimens using rapid dried soil specimens for the DSFS tests

The rate of drying and final air-dried water content depends on the room temperature. In the present study, the specimens were air-dried at room temperature of 27-29 ˚C. Figure 3.7 compares the variation in the vertical deformation (ΔH/H), lateral deformation (ΔD/D) and volumetric deformation (ΔV/V) with time during the drying process of Trichy soil-2 soil specimens. From Figure 3.6, it is clear that Trichy soil-2 required almost 47 hours to reach a water content of 15.8% from the initial water content of 30.5% where the vertical, lateral and volumetric strain reached equilibrium values. The vertical and lateral strains were almost equal as the suction acts equally in all the directions. Subsequently, the soil specimen was allowed to dry at 105˚C in hot air oven. The same procedure was adopted for all the other soils. All the specimens were oven dried before using them for the DSFS testing. Further, the DSFS method captures the initial placement conditions of specimens before drying.

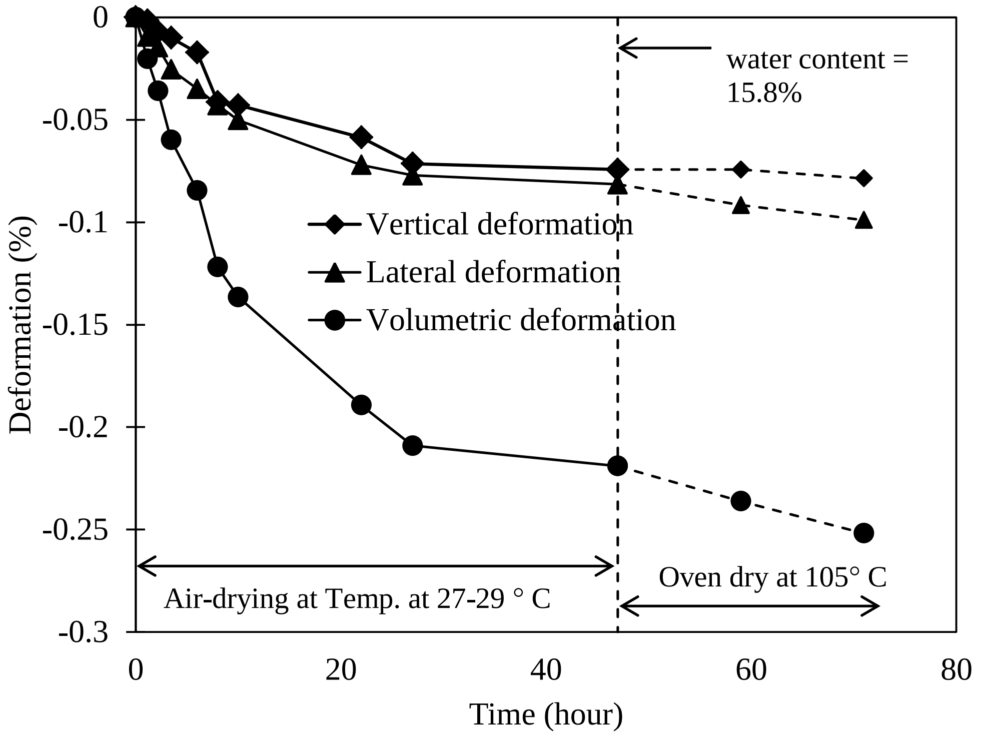

Figure 3.7: Comparison of vertical, lateral and volumetric deformation with time during drying process of Trichy soil-2

Figure 3.8 pictorially compares the final swollen volume of identical soil specimens in the 100 ml measuring jars tested using as-compacted and desiccated state. As the volume change was measured from the completely dry condition in case of DSFS value, the magnitude of desiccated state free swell was far greater than the volumetric free swell measured from the as-compacted state for a given placement condition (Figure 3.8).

Figure 3.9 presents the variation of desiccated state free swell with initial placement water content at different dry densities. With increase in initial water content, the DSFS increased. The greater DSFS value on the wet side of optimum is mainly attributed to decrease in the desiccated volume of the soil specimen. Mishra and Sridharan (2017) also reported similar observation that the soil specimens compacted on wet of optimum water content underwent more volumetric shrinkage. Further, the DSFS tests were also conducted to bring out effect of dry density at constant water content. From Figure 3.10, it can be observed that with increase in dry density the DSFS increased. This is due to the fact that the denser packing of soil particles at higher densities resulted in the higher DSFS value.

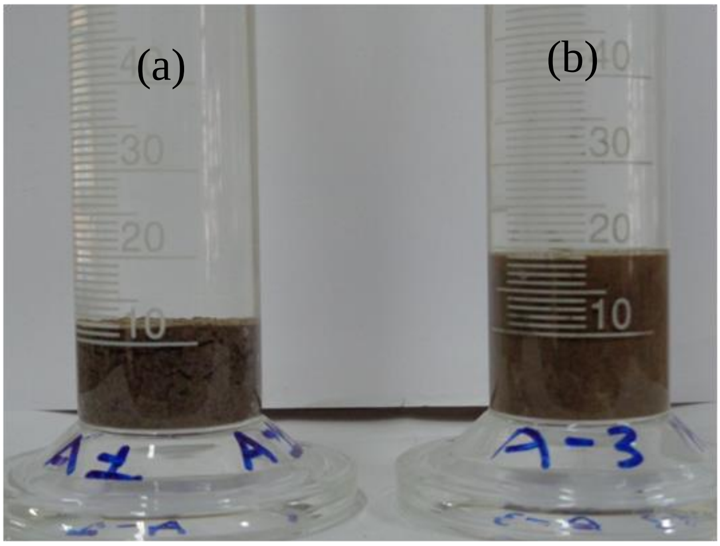

Figure 3.8: Pictorial comparison of final swollen values of: (a) as-compacted and (b) desiccated soil specimen at a given placement conditions of Trichy soil-2

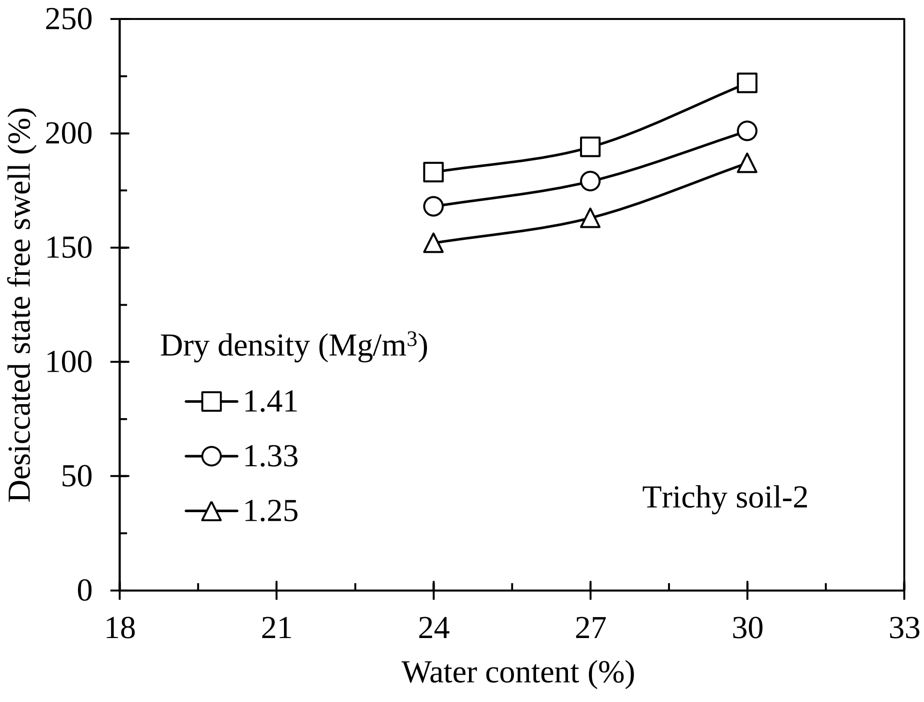

Figure 3.9: Effect of water content on DSFS of Trichy soil-2 at different dry densities

Figure 3.11 shows a correlation between percentage reduction in cross-sectional area of the desiccated soil specimens and desiccated state free swell for Trichy soil-2 compacted at different moisture content conditions. Percent reduction in cross-sectional area is calculated by Equation 3.3. From Figure 3.11, it is evident that the specimen with greater reduction in cross-sectional area underwent greater volumetric desiccated free swell. These results were comparable with the works of Rao *et al*. (2000) where they performed oedometer volumetric swell on desiccated soil specimens under a surcharge pressure of 6.25 kPa.

$$\text{Percentage reduction in c/s area} = \frac{A - A_d}{A} \times 100 \qquad 3.3$$

where A = compacted cross-sectional area of the soil specimen and A_d = cross-sectional of the same soil specimen in the desiccated state.

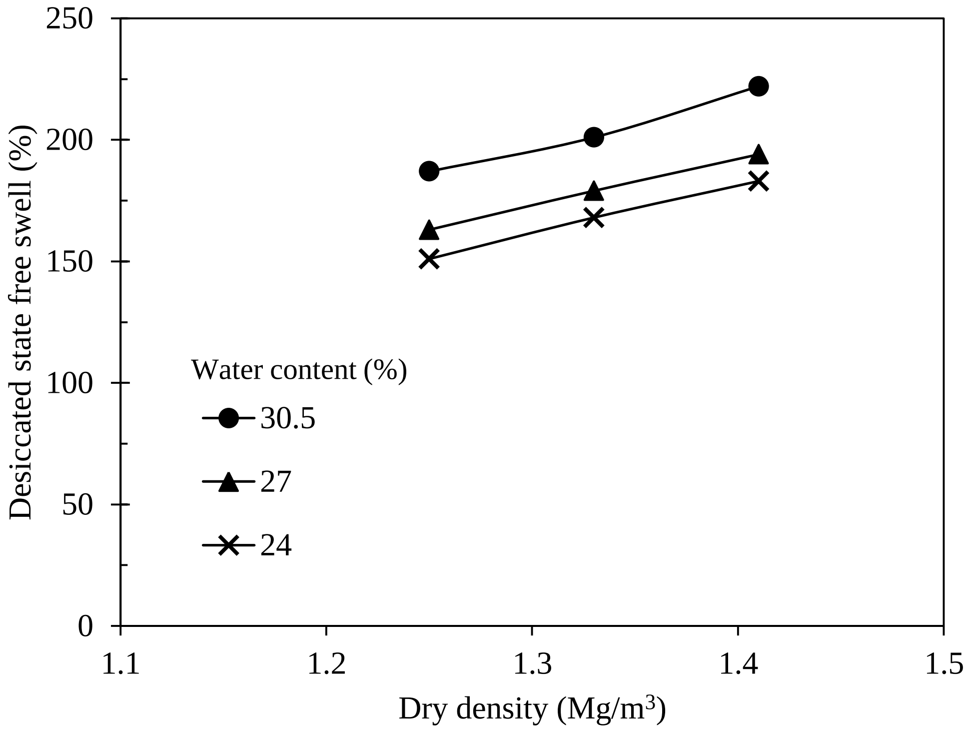

Figure 3.10: Effect of dry densities on DSFS of Trichy soil-2 at different water content

Figure 3.12 compares the variation of ($\Delta e/w$) with respect to initial compacted void ratio of soil specimens compacted at different moisture contents. The change in void ratio was calculated as difference in void ratio between compacted and desiccated state i.e. Δe = ($e_{compacted}$ - $e_{desiccated}$). From Figure 3.12, it is noticed that the soil specimens with higher initial void ratio experience greater change in void ratio (Δe). Further, the soil specimen which has undergone greater change in void ratio (Δe) showed higher free swell (Figure 3.13). From Figure 3.13, it is also noticed that the higher magnitude of free swell is mainly influenced by the initial compacted void ratio rather than the initial placement water content.

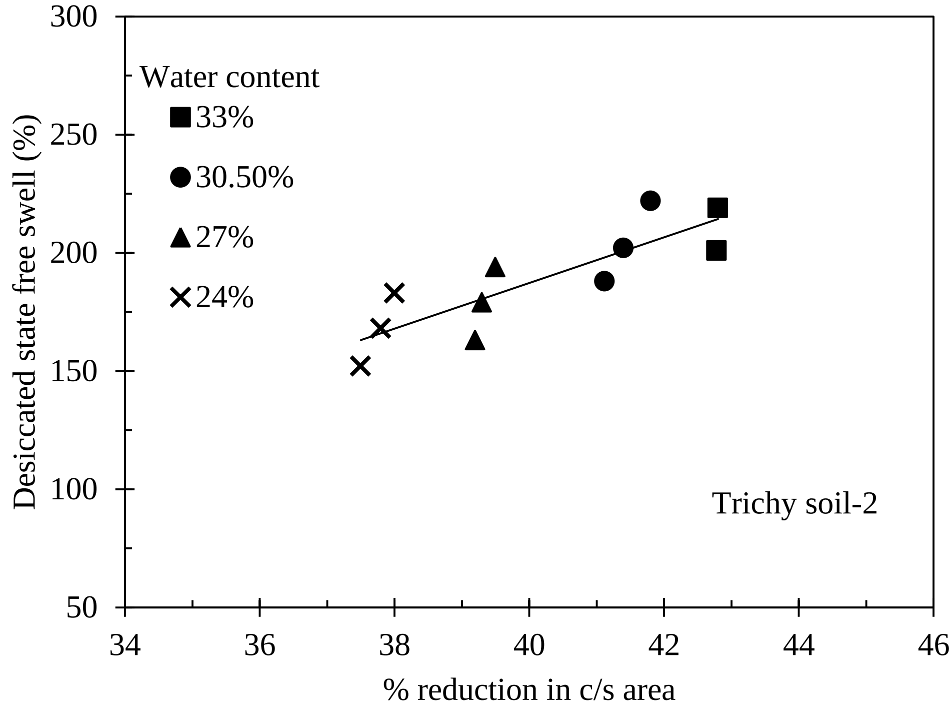

Figure 3.11: Correlation between desiccated state free swell and % reduction in the c/s area of the desiccated soil specimens of Trichy soil-2

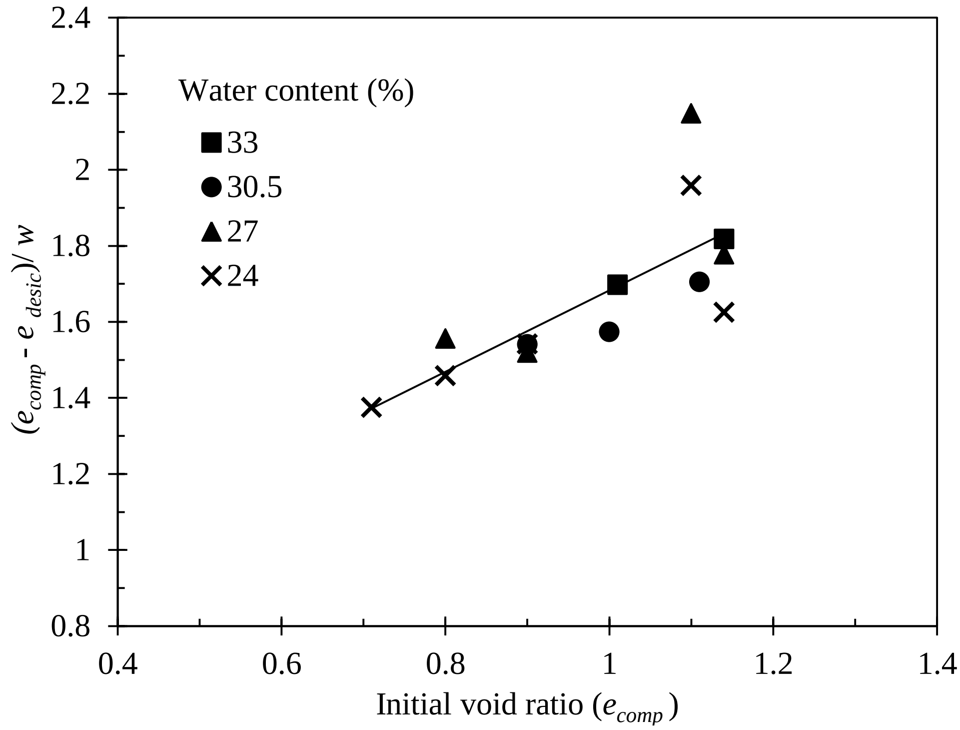

Figure 3.12: Correlation between change in void ratio and initial void ratio of the desiccated soil specimens of Trichy soil-2

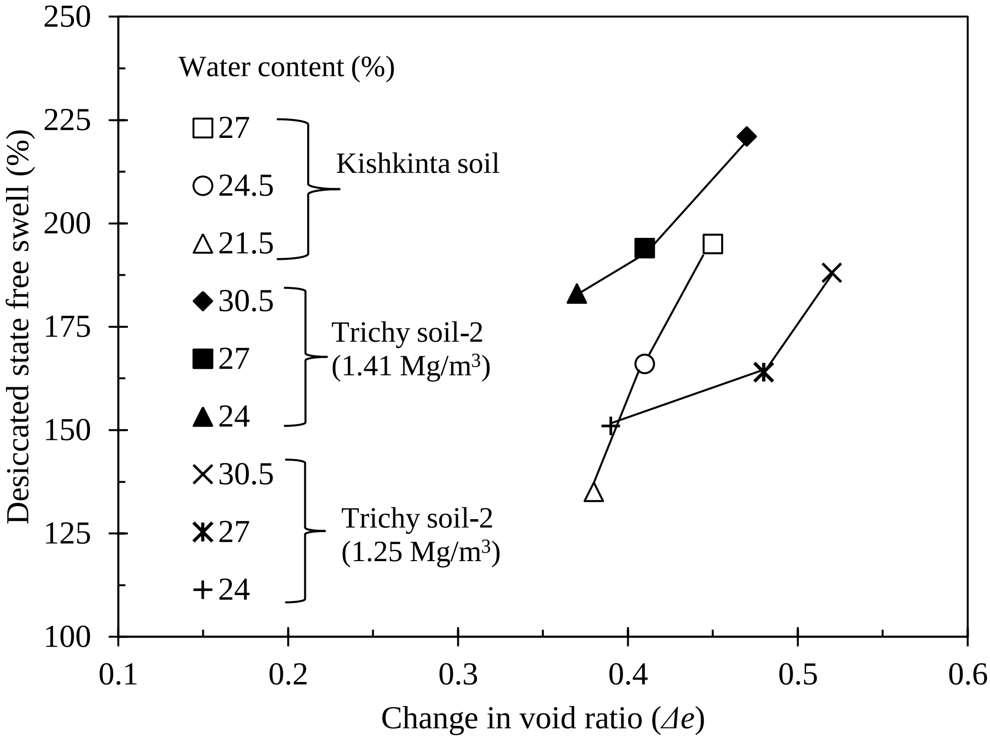

Figure 3.13: Variation of desiccated state free swell with change in void ratio (Δe) of the desiccated soil specimens

Additional DSFS tests were also conducted on soil specimens prepared from slurry state as in the shrinkage limit tests to check the validity of the proposed DSFS method. Trichy soil-2 was prepared from slurry condition similar to the shrinkage limit tests (i.e. water content = 1.0 times of liquid limit). A shrinkage mould of 27.5 mm diameter and 14 mm thickness was used for this test. These dimensions of the mould are same as the compacted specimen size. The slurry in the mould was air-dried for two days and then oven-dried at 105˚C to reduce the water content to a value lower than the shrinkage limit value of the soil. Mercury displacement method was used to measure the desiccated volume of the soil specimens. Then the free swell test was conducted using the desiccated soil specimen in the 100 ml jar and the DSFS was found to be 312%. The DSFS of Trichy soil-2 from the slurry state is greater than the DSFS value of same soil from the compacted state (222%; ρ_d = 1.41 Mg/m^3, w = 30.5%). This is as expected as the specimen reconstituted from slurry undergoes more shrinkage than the compacted specimen owing to differences in soil structure.

3.3.3 Comparison of DSFS of Swelling and Non-Swelling Soils

Figure 3.14 compares the variation of DSFS with dry density at constant water content of both swelling and non-swelling soils. In order to compare the DSFS of swelling and non-swelling soils, experiments were also carried out on non-swelling soils like kaolinite, red soil and laterite soil. As detailed in the above section, the oven dried soil specimens were used for the testing. For non-swelling soils, as-compacted or desiccated soil specimens did not show much variation in the free swell values. Figure 3.14 shows that the desiccated state free swell remains almost constant with increase in dry density. However, the DSFS of Trichy soil-2 increased with dry density. In some cases, the soils enriched with kaolinite mineral may also show residual swelling due to the elastic rebound of soil particles when inundated with distilled water (Yong and Warkentin, 1966). For non-swelling soils, the desiccated state free swell values were in the range of 30% to 60%, and hence, the soils with a DSFS value of less than 75% could be considered as non-critical or low-swelling soils (Table 3.3). Figure 3.15 presents the DSFS measurement on non-swelling soils in 100 ml measuring jars.

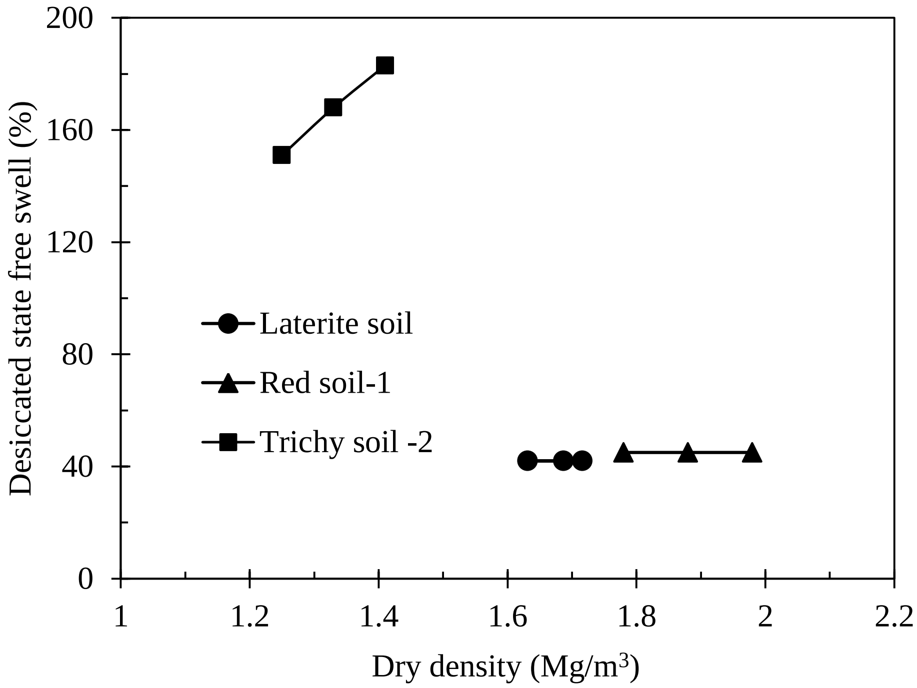

Figure 3.14: Comparison of variation of desiccated state free swell with dry density (at constant water content) of swelling and non-swelling soils

Table 3.3 Summary of DSFS and swell potential values of 21 soils

Description	OMC (%)	MDD (Mg/m^3)	DSFS (%)	SP (%)	Volumetric free swell (%)
Chemmenchery	19	1.7	382	23	150
Trichy-1	19.5	1.68	270	17.0	130
NIT warrangal	24.5	1.57	350	18.5	100
kishkinta soil	27	1.34	194	10.4	32
Siruseri	28	1.41	215	11.5	60
Trichy-2	30.5	1.41	222	10.5	45
Gummdipoondi	18.5	1.72	141	5.0	40
Padianallur	21	1.62	120	5.4	40
NIOT clay	17.5	1.76	140	6.30	44
AP soil	23	1.47	131	6.00	44
Kenya soil	17	1.68	190	11	60
L& T	16	1.76	140	7.5	55
Anna nagar	20	1.55	112	2.50	32
Kaolinite	20.4	1.61	45	0.0	40
Laterite soil	14	1.83	42	0.0	40
Red soil (1)	12	1.98	40	0.0	35
Red soil (2)	12	1.89	42	0.0	36
20% FS + 80% SS	23	1.59	168	9.50	44
40% FS + 60% SS	19	1.66	134	5.0	38
60% FS + 40% SS	17	1.75	102	2.0	20
80% FS + 20% SS	14.5	1.82	60	0.0	20

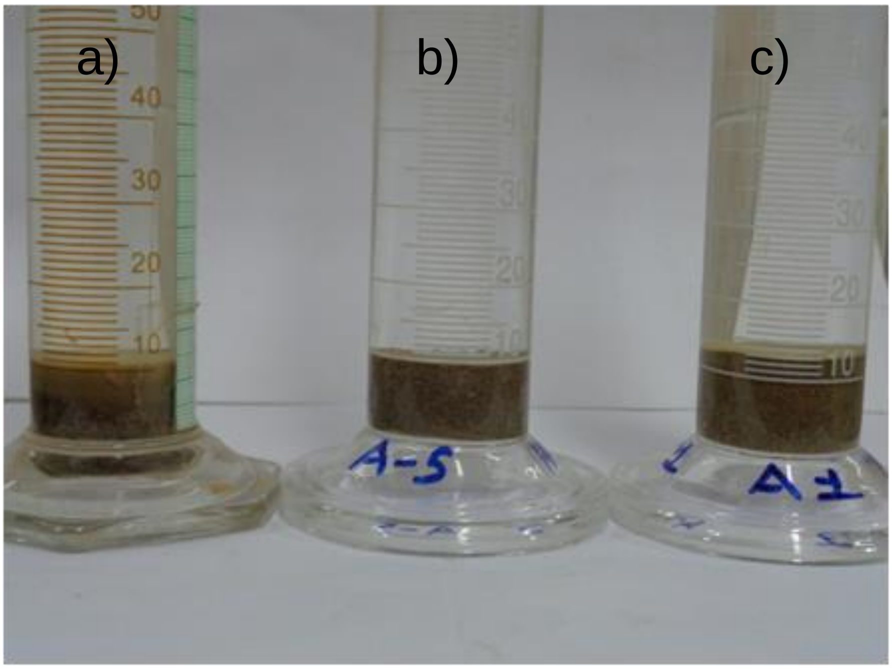

Figure 3.15: Pictorial comparison of free swell measurement of non-swelling soil using: a) FSI test using powdered soil specimen, b) CSFS test on as-compacted soil specimens and c) DSFS test on desiccated soil specimen

3.3.4 Time Duration of DSFS Test

In case of free swell index method, most of the soils reach their equilibrium sediment volume condition within 24 hours. However, the soils which are highly expansive may take longer time (24-216 hours) to reach the equilibrium state using distilled water as an inundating fluid (Sridharan *et al*. 1990). To overcome this problem, 0.025% NaCl solution could be used as an inundating fluid instead of distilled water (Sridharan and Prakash, 2000). However, the proposed method required 24-48 hours to reach the equilibrium swell conditions for most of the as-compacted soil specimens. Further, it is interesting to note that the time required for reaching equilibrium from desiccated state reduced drastically to 4-12 hours. Almost 90 to 95% of swell occurred within a period of 30 minutes. Figure 3.16 presents the approximate time required for Siruseri soil and Chennai Airport soil (undisturbed soil specimen collected from the field) in 100 ml jars. However, the expansive soils with higher densities like Chemmenchery and Trichy soil-1 required 7-14 days to reach swell equilibrium, similar to that of swell potential tests.

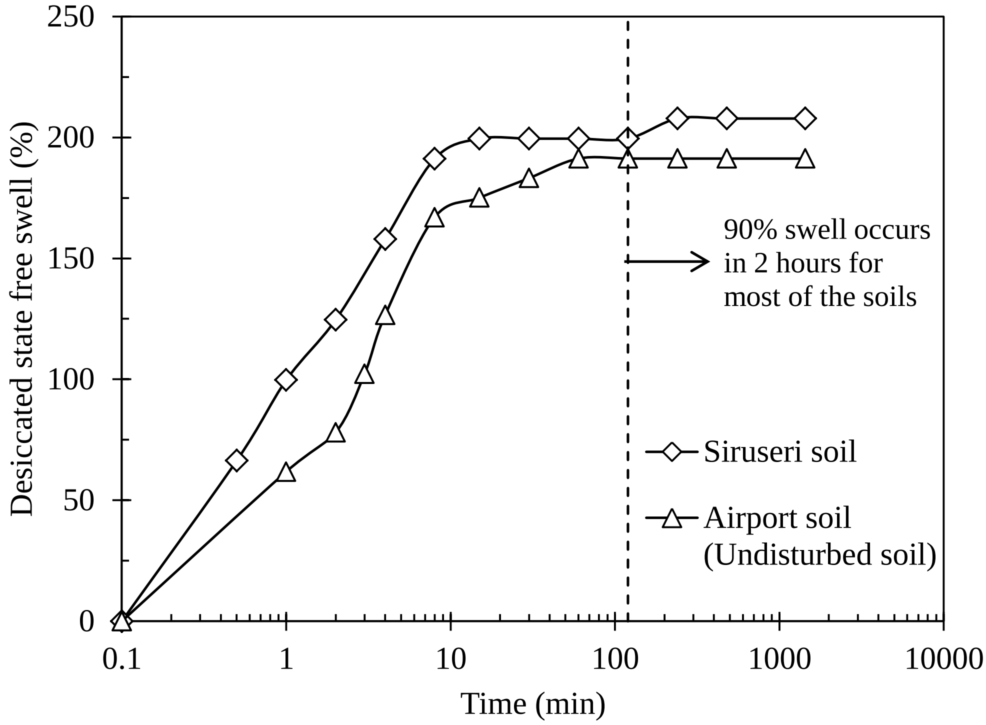

Figure 3.16: Variation of desiccated state free swell with time of Siruseri and Chennai airport soils (undisturbed soil collected from field)

3.3.5 Effect of Maximum Particle Size and Sand Content on DSFS

For the proposed DSFS method, the diameter of the soil specimens used was 27 mm and the diameter to thickness ratio of the specimen was maintained as 2.0. For the conventional oedometer tests, the ASTM-D4546 and IS 2720-41 recommended a minimum diameter to thickness ratio of 2.5 and 3.0 respectively. Further, the thickness of the soil specimen should not be less than 6 to 10 times the maximum particles size. In the present study, it was observed that soil specimens with lower percentage of sand did not show too much variation in DSFS value even though the tests were conducted on soil specimens prepared using 2 mm or 0.425 mm passing soil. However, this may not be the case if the soil contains appreciable amount of sand. Hence, in order to understand the effect of maximum particle size on DSFS values, the tests were conducted on soils with appreciable amount of sand content as swell. NIOT soil was selected for the tests as it comprises of 49% sand, 23% silt and 28% clay fractions. Three soils specimens were prepared using NIOT soil – soil fraction passing through 4.75 mm sieve, soil fraction passing through 2 mm sieve and soil fraction passing through 0.425 mm sieve. This changes the proportion of sand, silt and clay content in the soils. Figure 3.17 brings out the effect of clay content on DSFS value of NIOT soil. It is evident from Figure 3.17 that as the sand content increased; the DSFS value decreased at all dry densities. Based on DSFS tests conducted on processed soils, the NIOT soil could be identified as medium swelling soil using 2 mm and 4.75 mm passing soils and as high swelling soil using 0.425 mm passing soil. One-dimensional swell potential tests were also conducted on NIOT soil, and the swell potential was found to be 11.2% and 6.0% for the soil fraction passing 0.425 mm and 4.75 mm sieve, respectively. However, the swell potential of both 4.75 mm and 0.425 mm passing soils classify the soil as high swelling soils. Therefore, in order to get reliable results from the proposed method, it is better to use compacted soil specimens prepared using the soil passing through 0.425 mm sieve.

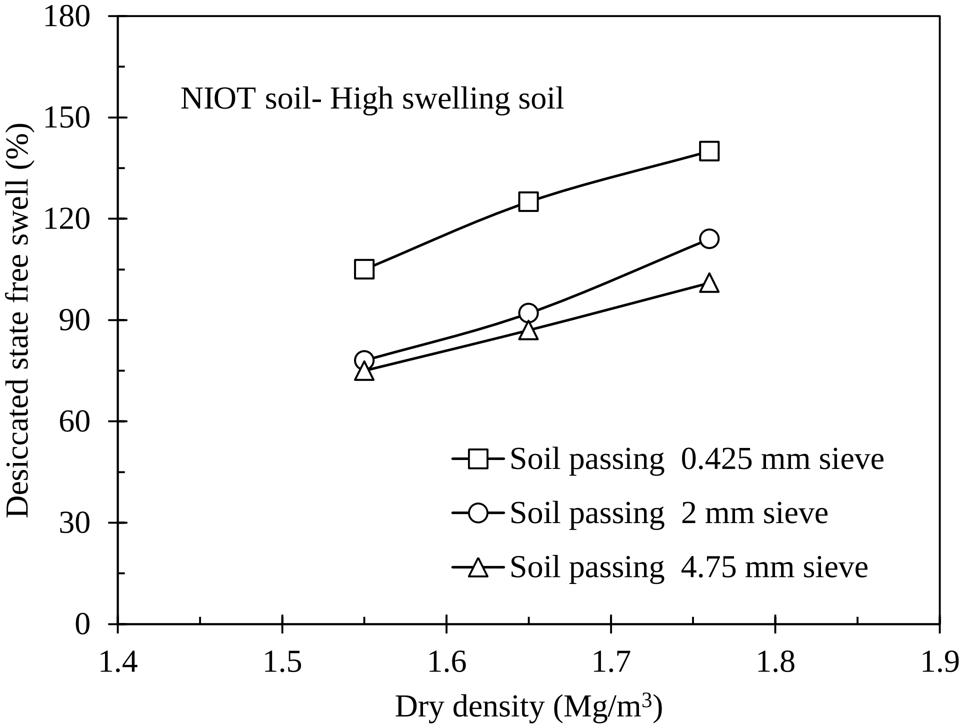

Figure 3.17: Effect of clay content on the DSFS of NIOT soil

From the above discussion it is clear that the maximum particle size for the DSFS tests is restricted to 0.425 mm. In this section, 0.425 mm processed swelling soil was mixed with fine sand in different proportions (20%/ 40%/ 60%/ 80%) and a series of DSFS tests were conducted to bring out the effect of sand content using soil fraction passing through 0.425 mm sieve. DSFS test results were compared with swell potential results. Siruseri soil which is classified as high compressible clay (CH) with 7% sand, 18% silt and 75%

clay fractions was used for the test. The river sand passing through 0.425 mm sieve and retained on 0.075 mm sieve was used for the tests. As expected the inclusion of fine sand to soil reduces the liquid limit of soil from 76% to 28% and increases the shrinkage limit to 18% from 9%. Similarly, the dry density of the soil mixture increased from 1.41 Mg/m^3 to 1.82 Mg/m^3, and the optimum moisture content decreased to 14.5% from 28%. Further, when the sand content is increased to 80%, the free swell index of the soil is reduced to 0% (Table 3.1).

Figure 3.18 compares the variation of desiccated state free swell and swell potential with increase in sand content of Siruseri soil. With addition of sand to the soil, both swell potential and DSFS decreased but the decrease in swell potential is relatively rapid. Moreover with addition of 80% sand to the soil the swell potential has decreased to 0%, whereas the DSFS was in the range of 60%. This clearly shows that DSFS value can be never reach a value of 0%. The reduction in swell value is mainly due to the replacement of plastic fines by non-plastic fine sand and lower volumetric shrinkage of desiccated specimen. Sivapullaiah *et al.* (1996) reported that the presence of fine sand (< 425 μm) in a soil-sand mixtures alter the swell-shrink behaviour because the swell occurs only after filling the voids of non-swelling finer fractions.

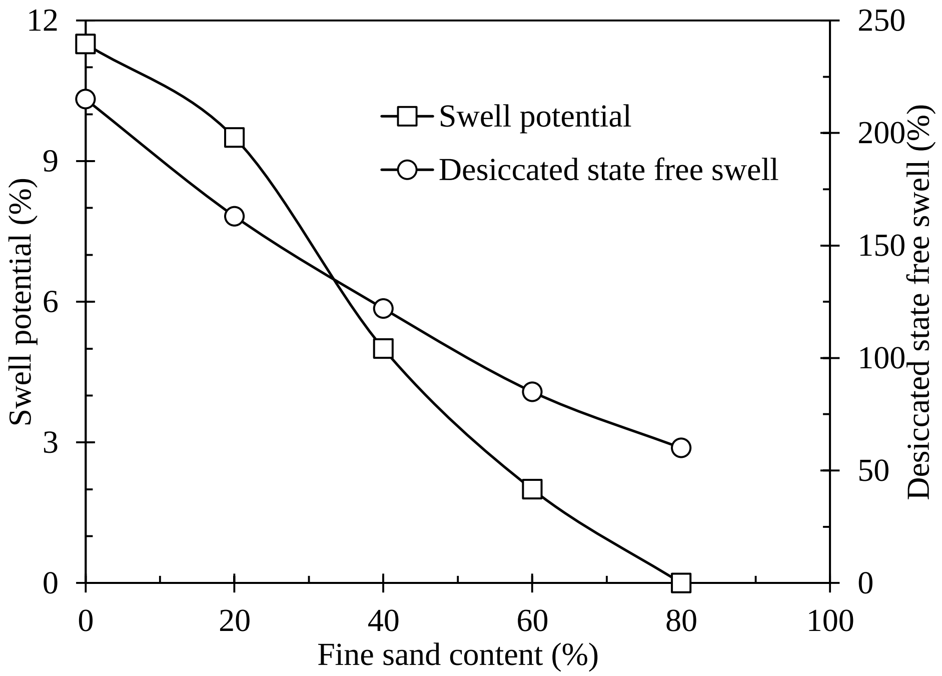

Figure 3.18: Comparison of variations in swell potential and desiccated state free swell of Siruseri soil

3.4 DEVELOPMENT OF CLASSIFICATION CHART AND TABLE FOR EXPANSIVE SOILS

An attempt is made in the present study to develop a classification chart and table for soil expansivity based on the DSFS tests carried out on 21 different soils. First, the DSFS was correlated with liquid limit, plasticity index, shrinkage index and free swell index in Figure 3.19. From Figure 3.19, it is evident that a good correlation exists between DSFS and liquid limit, plasticity index and free swell index, whereas the correlation between DSFS and shrinkage index is poor. Among these correlations, the correlation between DSFS and plasticity index is good with a R^2 value of 0.89 (Figure 3.19 b). Further, the range of w_L, I_P and FSI pertaining to different degree of soil expansivity are mapped to DSFS values. The range of w_L, I_P and FSI pertaining to different degree of soil expansivity along with corresponding DSFS values are presented in Table 3.4. From Table 3.4, it is clear that for most of the degree of soil expansivity using DSFS values arrived using w_L, I_P and FSI are only partially matching.

Table 3.4 Degree of soil expansion based on DSFS

Degree of soil expansion	DSFS based on LL* (%)	DSFS based on PI *** (%)	DSFS on FSI# (%)
Low	<40	<40	<110
Medium	40-115	40-85	110-165
High	115-200	85-130	165-270
Very High	>200	>130	>270

Note: *: DSFS values arrived from Figure 6.19a,
**: DSFS values arrived from Figure 6.19b,
#: DSFS values arrived from Figure 6.19d.

Further, the DSFS values were correlated with swell potential values obtained from compacted specimens (at MDD and OMC placement conditions) as presented in Figure 3.20. The R^2 value was found to be 0.96 for this correlation. The range of swell potential values pertaining to different degree of soil expanisvity using Seed *et al*. (1962) table are mapped to DSFS values from Figure 3.20. These DSFS values are also partially matching with the the DSFS values obtained using w_L, I_P and FSI correlations. Since the correlation between DSFS and swell potential (quantitative method) is good, it is reasonable to freeze the DSFS ranges obtained using swell potential for classifying the different degree of soil expansivity. Therefore, a classification table for degree of soil expansivity based on DSFS for specimens compacted to MDD and OMC is herein proposed in Table 3.5.

Table 3.5 Prediction and classification of expansive soil based on DSFS

Desiccated State Free Swell (%)	Degree of Soil Expansion
< 75	Low swelling
75-125	Medium swelling
125 - 400	High swelling
> 400	Very high swelling

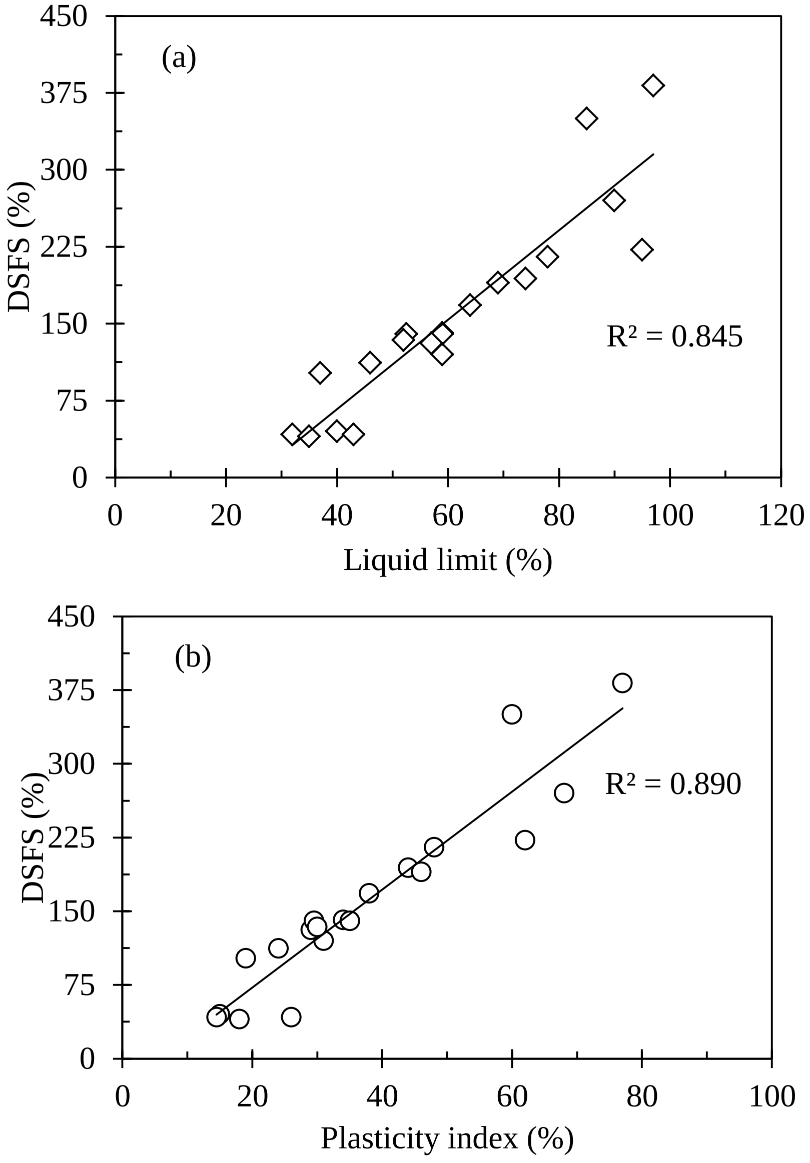

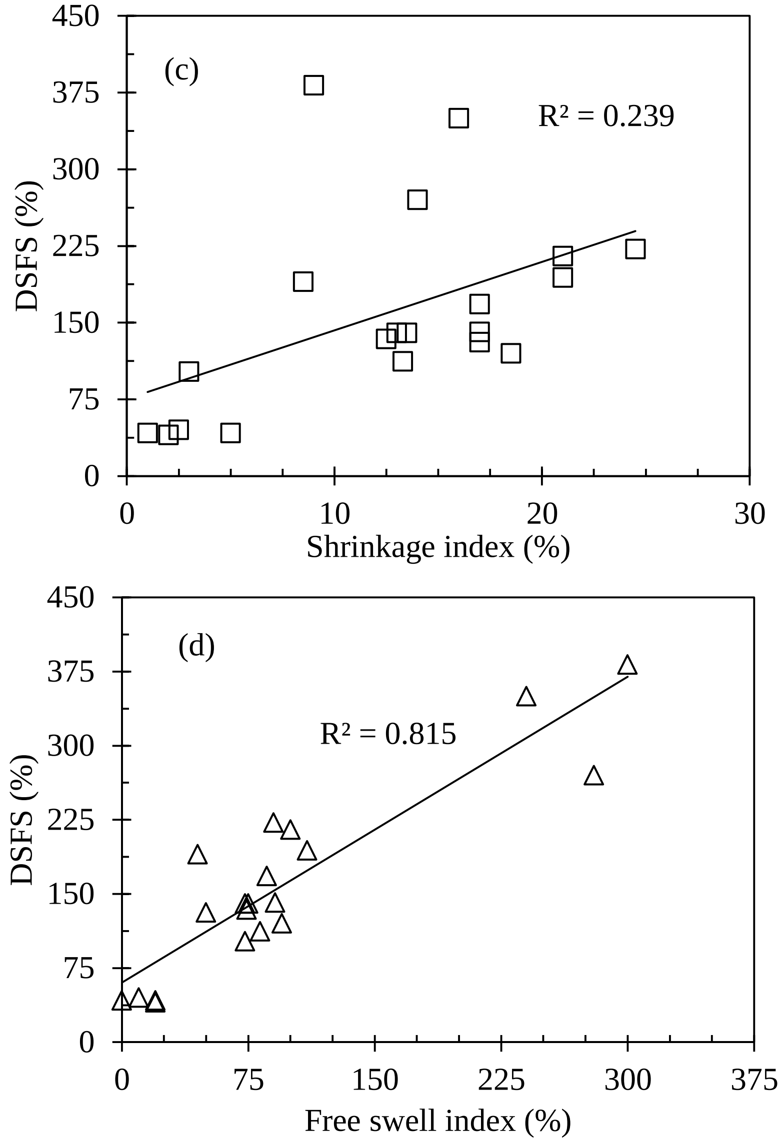

Figure 3.19: Correlation of DSFS with: (a) liquid limit (b) plasticity index (c) shrinkage index and (d) free swell index

As the main objective of the present study is to develop a new method for soil expansivity chart or table to include the placement condition in the free swell measurement and the proposed table (Table 3.5) includes the placement condition pertaining to MDD and OMC, it is necessary to develop a prediction chart or table which includes the different placement conditions in the free swell measurement. Therefore, the data in Figure 3.20 is re-plotted as a relationship between DSFS and desiccated volume in Figure 3.21. Based on the swell potential values, the prediction chart is divided into three regions, namely Zone I - low swelling, Zone II - medium swelling and Zone III – high swelling.

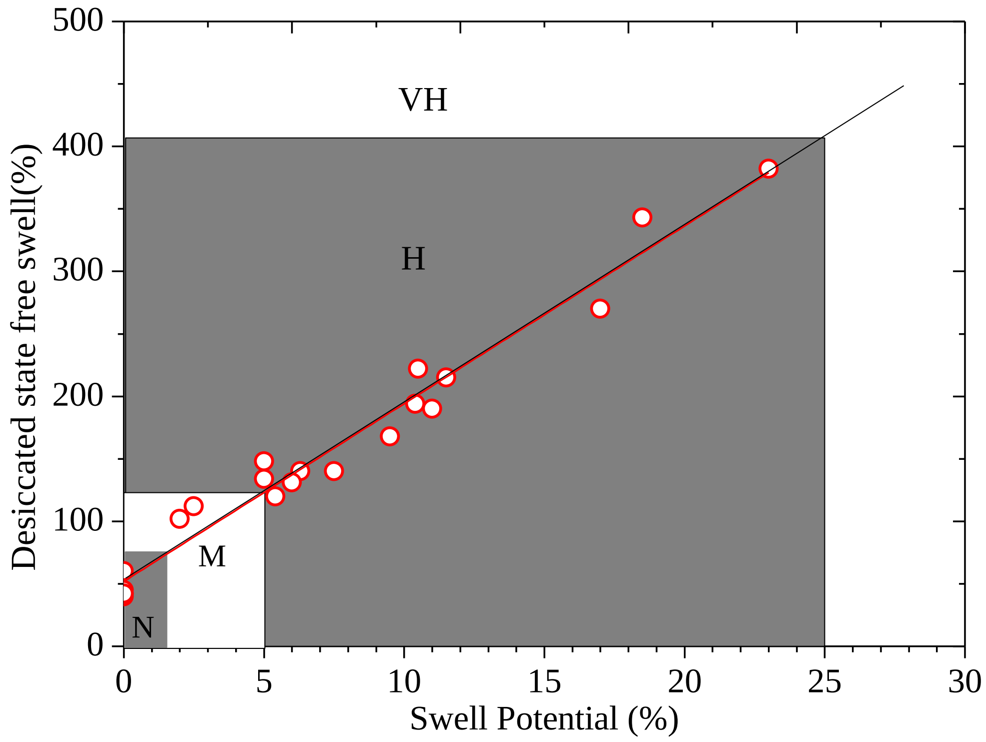

Figure 3.20: Classification chart for expansive soils based on desiccated state free swell method with swell potential as a control test method

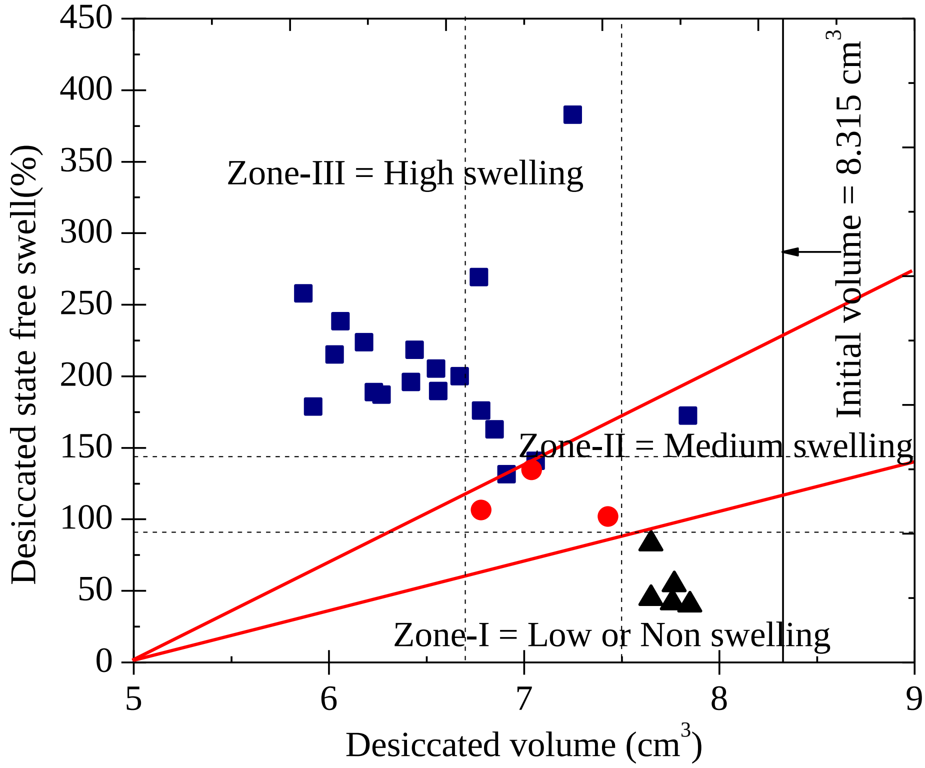

Figure 3.21: Proposed classification chart for expansive soil based on desiccated volume and DSFS value of soil specimens

3.4.1 Swell Measurement of Field Soil Samples Using DSFS Method

In order to check the suitability of the proposed degree of expansivity chart (Figure 3.21) for field applications, ten undisturbed soil samples were collected from the field from seven different site locations. Figure 3.22 shows the sampling tube with inner diameter of 27.5 mm and height of 50 mm in order to obtain soil samples from the field. This diameter is equal to the diameter of the free swell jars used for testing. Before sampling, the inner and outer sides of the sampling tubes were lubricated with silicon grease or oil to reduce the friction during sample ejection. Then, in the field, the top surface of the soil was removed for any debris and then the sampling tubes were pushed gently into the soil at the required depth to obtain the samples. The sample extrusion from the sampling tube was carried out as per the procedure detailed in IS-1892: 1979 (i.e.) from cutting edge to the head of the tube. After the soil samples were extruded, the above protocol was followed to get the desiccated state free swell values. A minimum of two to three specimens were tested for measuring the volume change of one field sample. In order to check the predicted soil expansivity from DSFS values, swell potential and free swell index tests were also carried out on additional samples collected from same location.

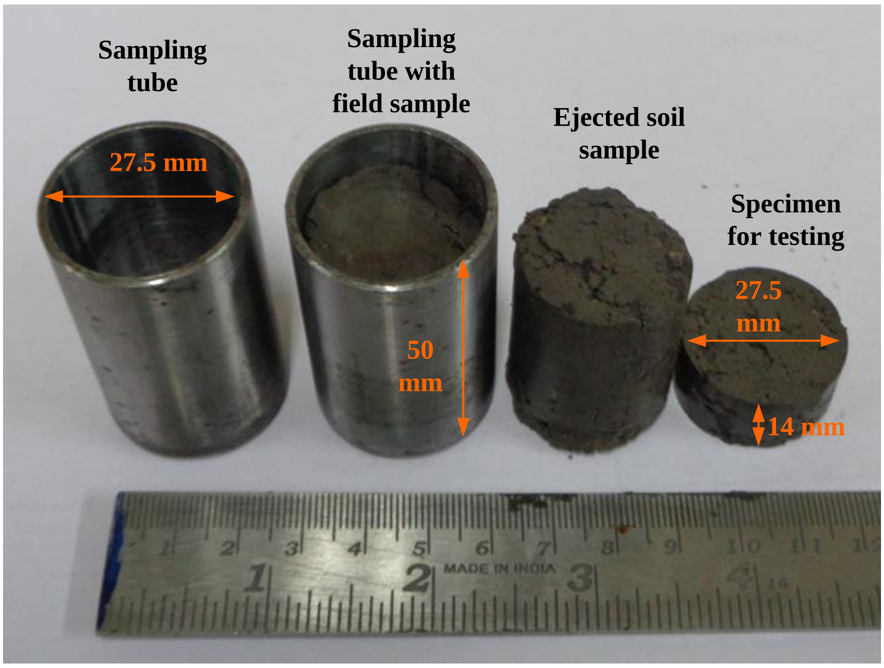

Figure 3.22: Image of sampling tube to obtain undisturbed soil samples for DSFS testing

The laboratory test results obtained from the additional field soil samples are tabulated in Table 3.6. In order to validate the proposed classification chart for identification of degree of soil expansion, the measured DSFS and corresponding desiccated volume were plotted in the proposed chart, as shown in Figure 3.23. The classification obtained from the proposed chart is matching well with swell potential classification. However, the swell potential of soil specimens collected from Chennai airport and RVNL-Sample 1 were slightly underestimated using oedometer method as the initial placement condition of samples was closer to saturation.

Table 3.6 Summary of free swell values of field soil samples obtained from different methods

Description	w_f (%)	ρ_d (Mg/m^3)	FSI (%)	Swell potential (%)	DSFS (%)	FSR
Lake clay-IITM	33	1.38	40 - L	0.6 - L	102 - M	1.4
BSB -IITM	8.8	1.7	20 - L	0.3 - L	44 - L	1.2
Vallarpadam (Kerala)	22	1.6	10 - L	0 - N	33 - N/L	1.1
Neyveli (Tamil Nadu)	30	1.34	64 - M	8.0 - H	184 - H	1.64
Chennai airport (CA)						
Sample 1	30.5	1.39	91- M	1.56 - L/M	174 - H	1.91
Sample 2	27.2	1.5	90-M	3.85 - M	190 - H	2.0
TNWML	22.8	1.6	67 - M	6.1 - H	136 - H	1.7
RVNL						
Sample at 0.5 m (S1)	39	1.27	90	3.48 - M	235 - H	1.9
Sample at 1.0 m (S2)	23.5	1.45	86	12.8 - H	186 - H	1.86
Sample at 1.5 m (S3)	28.5	1.47	82	15.3 - H	226 - H	1.82

Note: N: non-swelling, L: low swelling, M: medium swelling, H : high swelling, w_f : field water content

The data in Figure 3.23 are rearranged in Figure 3.24, where the soils were arranged from low to high degree of expansion. Figure 3.24 compares the degree of soil expansion obtained from swell potential, free swell index, free swell ratio and DSFS methods. The prediction of soil expansivity using the proposed chart is in good agreement with swell potential measurements. However, the values obtained from both FSI and FSR show slight deviation from the values obtained from standard oedometer tests. Both FSI and FSR underestimate the soil expansion. Further, the prediction of degree of soil expansion using the proposed DSFS method holds good for 6 soils with low and high degree of expansion and for remaining 4 soils, the swell potential underestimate the soil expansion.

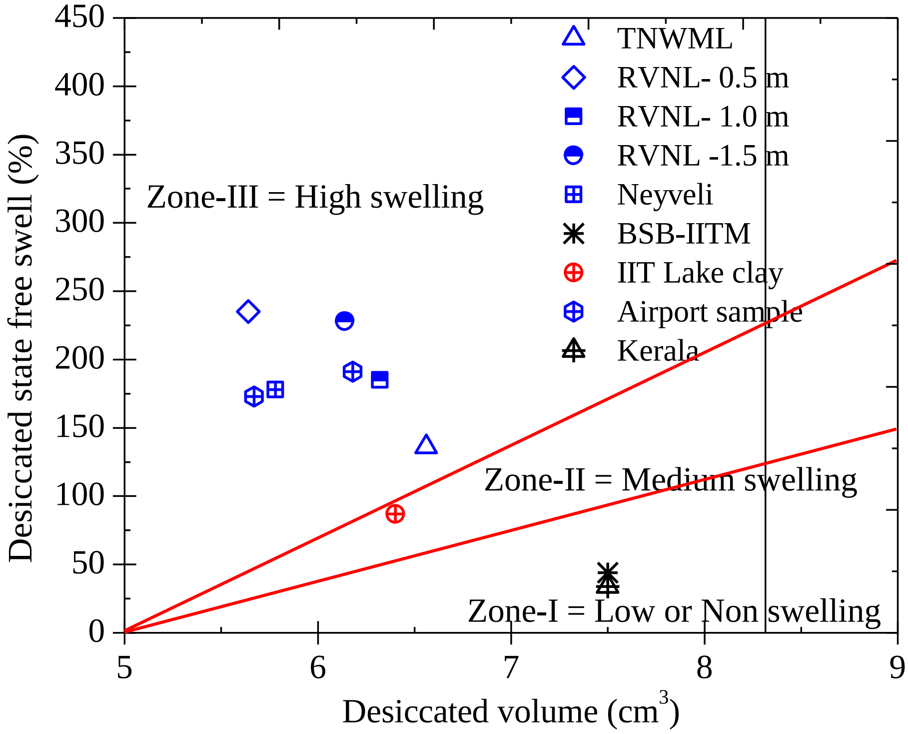

Figure 3.23: Validation of proposed chart by testing the undisturbed field soil samples

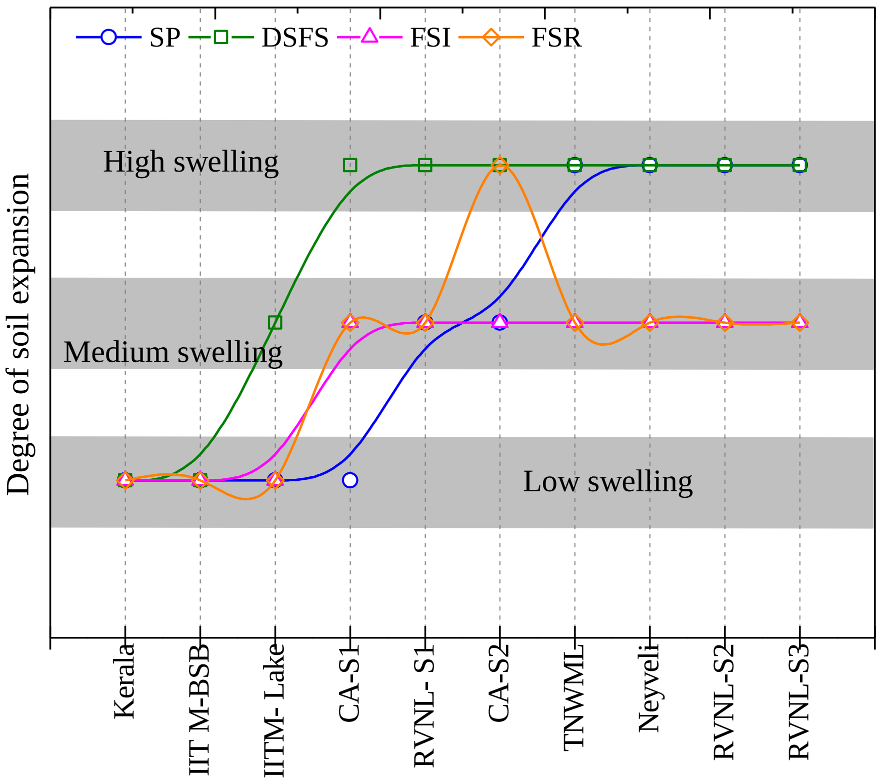

Figure 3.24: Comparison of degree of soil expansion of undisturbed field samples using different methods (soils were arranged from low to high degree of soil expansion potential)

3.5 SUMMARY AND CONCLUSIONS

In the present study, an attempt is made to include the placement conditions in the measurement of free swell using undisturbed (or compacted) soil specimens in the conventional free swell apparatus. The following conclusions are arrived based on the experimental studies conducted on twenty one remoulded specimens and ten undisturbed soil specimens collected from the field.

i. The proposed DSFS method is able to include the placement conditions such as dry density and water content in the measurement of swelling of soils. With increase in the dry density and water content, the DSFS increased owing to the use of desiccated soil specimens for testing.

ii. The DSFS increased with the increase in the percentage reduction in cross sectional area and change in void ratio.

iii. The DSFS method proved to be advantageous over the FSI method as the testing time reduced drastically from 24-48 hours to 4-12 hours. The DSFS method can be performed even in the field without the requirement of any additional equipment with minimum effort.

iv. The correlation between the proposed DSFS method and swell potential was found to be good with a R^2 value 0.96. Based on this correlation, a classification table is developed for identification and classification of soil expansivity.

v. Based on the results obtained from DSFS testing on 21 soils, a chart is proposed for the classification of degree of soil expansivity. This chart is also validated using the DSFS values obtained from the undisturbed soil specimens collected from different sites.

CHAPTER 4

ACCELERATED METHOD FOR MEASUREMENT OF SWELL POTENTIAL AND SWELL PRESSURE OF EXPANSIVE SOILS USING CONSTANT RATE OF STRAIN APPARATUS

4.1 INTRODUCTION

This chapter discuss about the measurement of swell potential and swell pressure of expansive soils using conventional oedometer apparatus and CRS apparatus. In the conventional method, the specimens are generally saturated by submerging in water under a given seating pressure. Generally, the test takes long time as the saturation process is slow due to very low permeability of expansive soils. To overcome this limitation an improved saturation method by back pressure application in a constant rate of strain (CRS) apparatus is presented here. Controlled strain loading (CSL) is adopted to bring back the swollen soil specimens to their initial thickness instead of conventional incremental loading. It is observed that the time taken to complete the test is 7 to 13 times faster compared to the conventional method. When compared to the conventional method, the swell potential and swell pressure values obtained with the back pressure saturation were found to be higher by about 19 to 34% and 6 to 28%, respectively. The reason for these higher values is attributed to the attainment of greater saturation using back pressure saturation technique. The methodology and detailed explanation of the proposed CRS method is discussed below.

4.2 EXPERIMENTAL PROGRAM

4.2.1 Materials and Sample Preparation

Four expansive soils were collected from different parts of Tamil Nadu and Telangana states of India for the present study. The basic properties of the soils were determined as per the relevant IS standards and the properties are summarized in Table 4.1. From the results of grain size analysis and Atterberg limits, all the four samples are classified as high compressible clay (CH) as per the Indian soil classification system (IS 1498-2002). As per the classification of Seed *et al.* (1962) all the four soils are classified as highly expansive soils. The air-dried soils were processed and sieved through 2 mm sieve for using them in the present study. The standard Proctor compaction tests were conducted on the processed soils as per Indian standards IS 2720 –Part 7(2002). The values of maximum dry unit weight ($(\rho_d)_{max}$) and optimum moisture content (OMC) obtained are summarised in Table 4.2.

Table 4.1 Index properties of the soils used in the present study

Sl. No.	Soil	G_s	Grain Size (%)			w_L (%)	w_P (%)	I_P (%)	w_S (%)	IS soil classification symbol
			Sand size	Silt size	Clay size					
1	Trichy soil	2.7	3	29	68	95	33	62	8.5	CH
2	Padianallur soil	2.68	12	30	58	59	28	31	9.5	CH
3	Warangal soil	2.72	22	24	54	88	24	53	8.5	CH
4	Thanjavur soil	2.75	33	17	50	92	22	70	8.0	CH

Table 4.2 Compaction and swelling properties of the soil used for the testing

Soil	Compaction characteristics		Swell potential (%)	Degree of expansivity (Seed *et al.* 1962)
	OMC (%)	$(\rho_d)_{max}$ (Mg/m^3)		
Trichy soil	30.5	1.41	9.5	High
Padianallur soil	21	1.62	6.0	High
Warangal soil	21	1.65	6.6	High
Thanjavur soil	20	1.68	10.20	High

The processed soils were mixed with the predetermined quantity of water to achieve the desired moisture content corresponding to their OMC. Then the soils were transferred to separate plastic covers, sealed and stored in desiccators for 24 hours for moisture equilibrium. Proper care was taken to maintain the constant water content between the replicate specimens. It was observed that the variation in the water content between the replicate specimens was only $\pm 0.2\%$, which is considered reasonable. Consolidation cells with the stainless steel consolidation rings of 60 mm diameter and 20 mm height were used for the present study. The inner surface of the rings was highly polished so as to reduce the side wall friction. In addition, the rings were smeared with silicone grease to further reduce the side wall friction. Predetermined quantity of the moisture equilibrated soils were placed in the consolidation rings and statically compacted to a thickness of 14 mm using a spacer of 6 mm thickness to achieve the desired maximum dry density.

4.2.2 Equipment and Testing Procedure

Conventional swell-consolidation method was adopted for the evaluation of the swell potential and swell pressure as per ASTM D4546-14 (Method C) as a control. In order to perform the tests using the conventional method, the soil specimens were set-up in the oedometer cells and assembled in the standard oedometer frame under the seating pressure of 6.25 kPa. Distilled water was then poured into the cell and allowed the specimens to swell under two way drainage condition. Swelling was continuously monitored using dial gauge of 0.002 mm till the specimen reached the equilibrium swell condition. Figure 4.1 presents the conventional fixed ring oedometer cell used for the measurement of swell parameters of expansive soil.

The swell potential (SP) is calculated as:

$$SP = \frac{\Delta H}{H} \times 100 \tag{4.1}$$

where ΔH is change in thickness (mm) at the end of swelling and H is the initial thickness of compacted specimens.

After the end of primary swelling, the swollen specimens were loaded incrementally with a load increment ratio of 1.0, till the specimens reached their initial thickness. The time-settlement data was continuously monitored during consolidation so as to evaluate the end of primary consolidation. The effective consolidation pressure required to bring the specimen back to its initial compacted thickness (initial void ratio) is recorded as the swell pressure (Hardy, 1965; Chen, 1975; Sridharan *et al.* 1986; Nelson and Miller, 1992).

In the proposed method, the specimens were saturated by the application of back pressure. Constant rate of strain (CRS) consolidation cell was used so as to facilitate the application of back pressure and measurement of pore water pressure. Figures 4.2 and 4.3 present the CRS apparatus and its components used for the present study. Back pressure of 200 kPa was applied to the top and bottom of specimens using a hydraulic pressure volume controller as per ASTM D5084-16 recommendation. Application of back pressure may cause slight compression of the soil specimens. As the applied back pressure (200 kPa) is much lower than the yield stress of compacted specimens (300-400 kPa), the compression due to back pressure application would be negligible. Further, in the initial stage of application of back pressure, both compression and swelling occurs simultaneously and it is not possible to separate the magnitudes of compression and swelling. Thus, the compression due to back pressure application is neglected. However, the compression of filter paper was accounted in the volume change data. The uplift of loading piston of the CRS cell due to the application of back pressure was compensated by placing 26 N counter weight as shown in Figure 4.2. The counter weight does not exert any additional pressure over the specimen during both saturation and consolidation phases. The loads required for the application of seating pressure of 6.25 kPa (18 N) and counter weight of 26 N were applied simultaneously, and then the back pressure was applied within about 30s. The swell was continuously monitored right from the application of back pressure using a data logger.

Figure 4.1: Components of conventional oedometer cell used for measurement of swell parameters of expansive soils under two way saturation conditions.

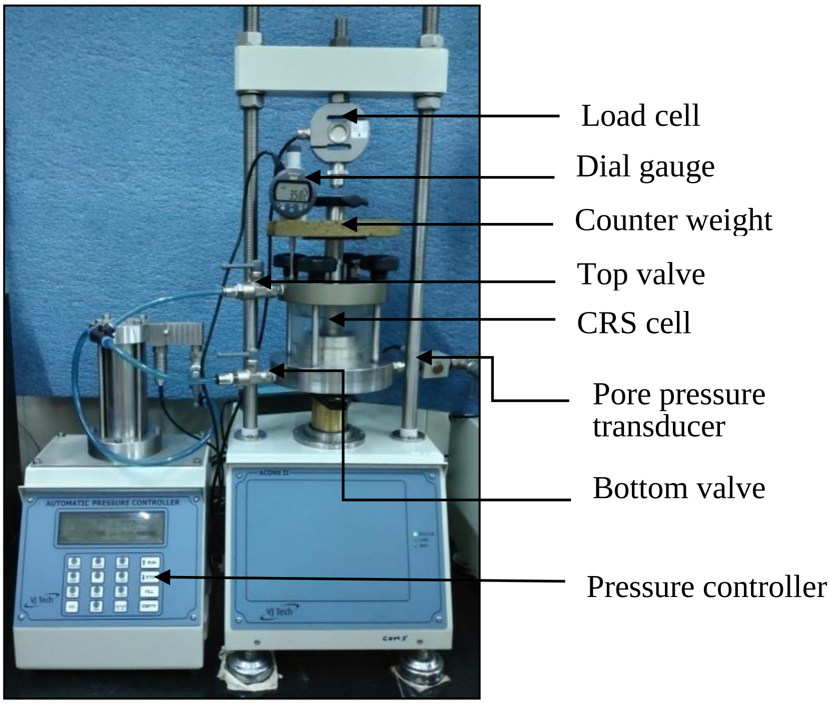

Figure 4.2: Photographic view of CRS apparatus with counter weight

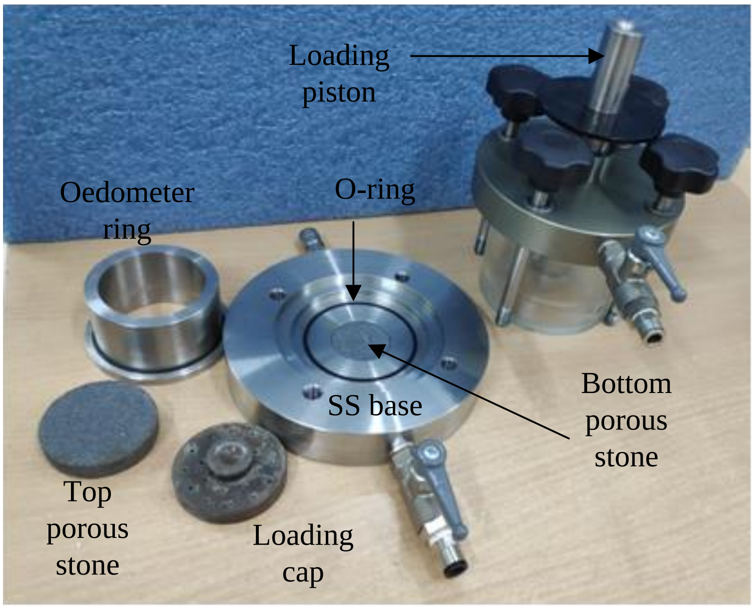

Figure 4.3: Components of CRS cell

Upon complete swelling, the loading piston was docked with the load cell for CSL testing (consolidation phase). The CSL test was performed on the specimens for obtaining the swell pressure. The bottom back pressure valve was closed so that the pore pressure develops at the base of the specimen during consolidation phase. The applied load, pore pressure developed and vertical deformation were continuously monitored. A deformation rate of 0.12 mm/hour was found to be sufficient for maintaining the allowable pore pressure ratio (i.e. the ratio of pore pressure developed (u_b) to the applied total stress (σ_v)) in the range of 3% to 15% as per ASTM D4186-12 guidelines. The average effective stress (σ'_v) on the specimens was calculated as per ASTM D4186-12 as:

$$\sigma'_v = \sigma_v - \frac{2}{3} u_b \tag{4.2}$$

4.2.3 Measurement of Water Content and Degree of Saturation

Two identical specimens were prepared for each soil, one for testing in the conventional oedometer cell and the other for testing in CRS cell. Back pressure was applied on the specimens in the CRS cell, while the other specimens were allowed to swell under the conventional soaking method under a seating pressure of 6.25 kPa. At the end of swelling, both specimens were extruded and their thickness was carefully measured before determining the water content by oven drying method. By knowing the specific gravity of soils, final thickness, mass and water content of the specimens, the degree of consolidation was calculated.

4.3 RESULTS AND DISCUSSIONS

Figures 4.4(a) to 4.4(d) compare the time-swell plots obtained from both conventional oedometer test and CRS test with back pressure saturation of all soils. As reported by Lambe and Whitman (1979), the log time-swell plot is a mirror image of log time-settlement plot in a consolidation test. Therefore, the primary and secondary swell can be identified as shown in the figures. ASTM D4546-14 also recommended a similar approach to evaluate the primary and secondary swell magnitudes. From the figures it is evident that at a given initial placement condition, the swell potential of the soil specimens determined from the CRS cell with back pressure application is higher than the swell potential determined from the conventional test.

Table 4.3 summarises the swell potential obtained from the conventional and CRS cells. Swell potential of expansive soils with back pressure saturation is found to be 19 to 34% higher than that obtained from the conventional oedoemeter cell without back pressure saturation.

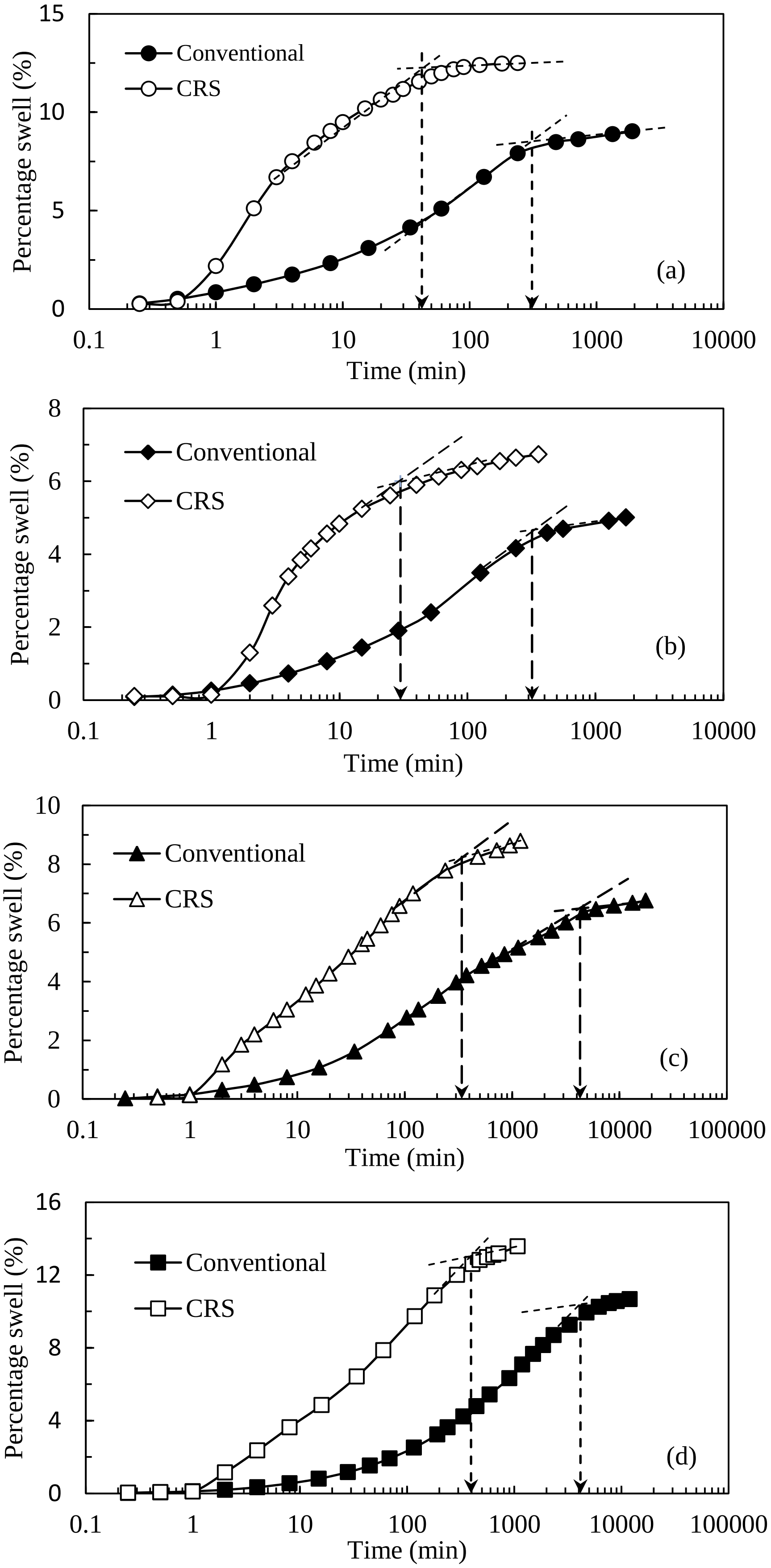

Figure 4.4: Results of swelling test for: (a) Trichy soil, (b) Padianallur soil, (c) Warangal soil and (d) Thanjavur soil

Nagaraj *et al.* (2009) also reported that the swell potential of the specimens saturated with sand drains was about 17 to 20% higher than that obtained from the conventional oedometer cell. The results are also consistent with the studies of Nelson (2016), who carried out the tests by varying the method of inundation. The increase in swell potential is attributed to the increase in saturation due to back pressure application where the diffuse double layer growth is well developed.

Vanapalli and Lu (2012) reported that the expansive soils undergo volume change till it reaches 100% saturation. The increase in swollen thickness of the specimen due to back pressure saturation is attributed to full hydration of clay particles, which leads to increase in the thickness of diffuse double layers (DDLs). Therefore, the back pressure saturation enables the specimens to attain complete saturation and high swell potentials. Figure 4.5 compares the variation in swell potential value due to change in method of inundation.

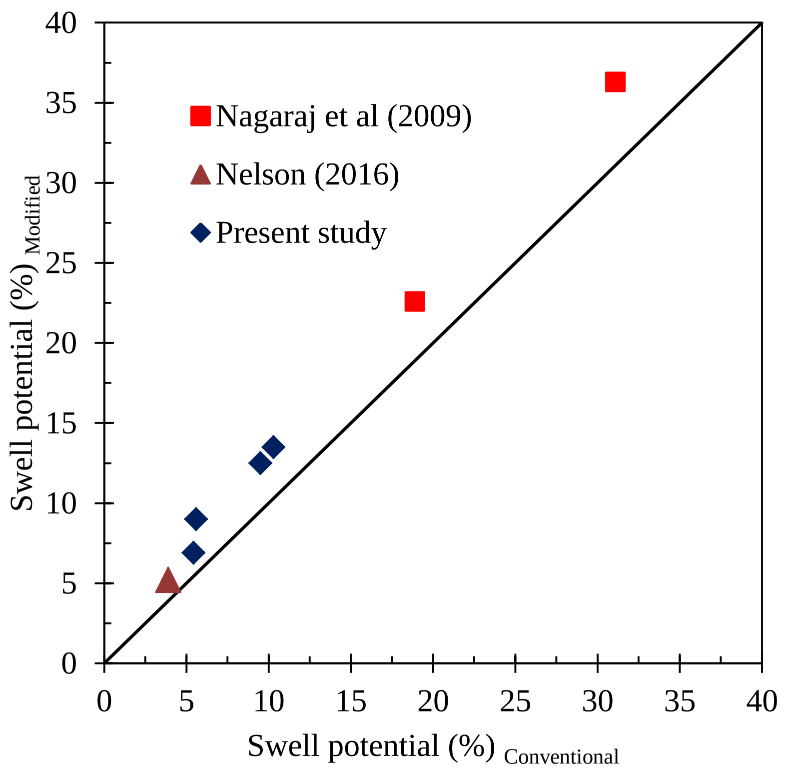

Figure 4.5: Comparison of effect of method of inundation on swell potential values obtained in the present study to the swell potential values reported in literatures

The water content and degree of saturation attained by the specimens at the end of swelling are presented in Table 4.4. The water content values of the specimens subjected to back pressure saturation are higher than the water content values of specimens tested in conventional oedometer cells, resulting in higher swelling. It is clear that the degree of saturation of the specimens tested in the CRS cells is in the range of 98 to 99%, whereas in the conventional cells, it is about 95 to 96%. It is likely that the degree of saturation of the specimens subjected to back pressure saturation would be higher and close to 100%. Upon removal of back pressure application to unload the specimens, the dissolved air might have emerged out from the saturating fluid, resulting in a slight reduction in the degree of saturation values (Head, 1998; ASTM D5084-00)

Table 4.3 Swell potential and time duration for swell measured from conventional (CON) and CRS apparatus

Soil	Primary swell (%)		Time duration for primary swell (minutes)		Ratio of time duration of primary swell for CON to CRS	Ratio of swell potential for CRS to CON
	CON	CRS	CON	CRS		
Trichy soil	8.5	12.4	310	42	7.3	1.32
Padianallur soil	4.65	6.5	320	30	10.5	1.19
Warangal soil	6.4	8.3	4300	340	12.5	1.34
Thanjavur soil	10.4	13.0	4150	395	10.5	1.29

The time taken for the completion of primary swelling is also presented in Table 4.3. Literature shows that for most of the soils the end of primary swell occurs within 24 hrs (Chen, 1975). However, some soils may take very long time for the completion of primary swelling and much more than 24 hrs. In the present study, the time required for complete primary swelling of Trichy and Padianallur soils was less than 24 hours, whereas it was greater than 24 hours for Warangal and Thanjavur soils. However, the back pressure saturation has increased the rate of primary swelling by about 7 to 12 times than that of the conventional method. The time rate of swelling in the conventional method depends on the outward movement of air voids from the soil specimens during inundation (Nelson, 2016). Whereas, the back pressure saturation method compresses the air bubbles and dissolves which leads to the enhanced rate of water flow into the specimens. This leads to the faster rate of swelling and high swell potential.

Figures 4.6(a), 4.7(a), 4.8(a) and 4.9(a) show the variation of total stress and pore pressure developed during constant rate loading after the swelling of the specimens. The results of the CSL tests are similar to that of the conventional consolidation test results. Figures 4.6(b), 4.7(b), 4.8(b) and 4.9(b) present the pore pressure ratio (ratio of pore pressure developed at the base of the specimen to the applied total stress) during the tests. The pore pressure ratio is within the permissible limits of 3 to 15% (as per ASTM D4186-12) suggesting that the rate adopted is acceptable.

Table 4.4 Water content and degree of saturation after swelling from conventional (CON) and CRS

Soil	Water content after swelling (%)		Degree of saturation after swelling (%)	
	CON	CRS	CON	CRS
Trichy soil	41.66	43.30	96.0	98.5
Padianallur soil	28.50	30.90	96.0	99.0
Warangal soil	28.50	30.20	95.5	98.0
Thanjavur soil	29.50	31.0	95.0	98.4

The vertical deformation experienced during the consolidation phase of the swell pressure tests are shown in Figures 4.6(c), 4.7(c), 4.8(c) and 4.9(c) for all the four soils used in this study. The vertical deformation data was accounted for compressibility of the apparatus, filter paper and porous stones as suggested by Fredlund (1969). The swell pressure values are summarised in Table 4.5. The swell pressure values obtained from the CSL tests are about 1.06 to 1.28 times higher than the values obtained from the conventional tests owing to the attainment of higher swell potentials due to back pressure saturation. Figure 4.10 compares the measured swell pressure due to change in method of inundation from the present study and literature.

Bolt (1956), Sridharan *et al.* (1986) and Nelson *et al.* (2006) reported that the compressibility of the montmorillonite rich soils is influenced by both mechanical and physico-chemical factors. As mentioned earlier, due to full hydration of clay particles the diffuse double layers are fully developed. Therefore, greater mechanical force is required to expel the imbibed water and compress the swollen soil specimens to their initial compacted thickness (initial void ratio). This is consistent with the conclusion of Tang *et al.* (2011) where they have measured the swell pressure at different suction levels and concluded that the soil with lesser suction value (approaching towards 100% saturation) exhibited higher swell pressure. Therefore, the conventional method yields lower swell pressure than the CRS method owing to the differences in the degree of saturation after swelling (Figure 4.6).

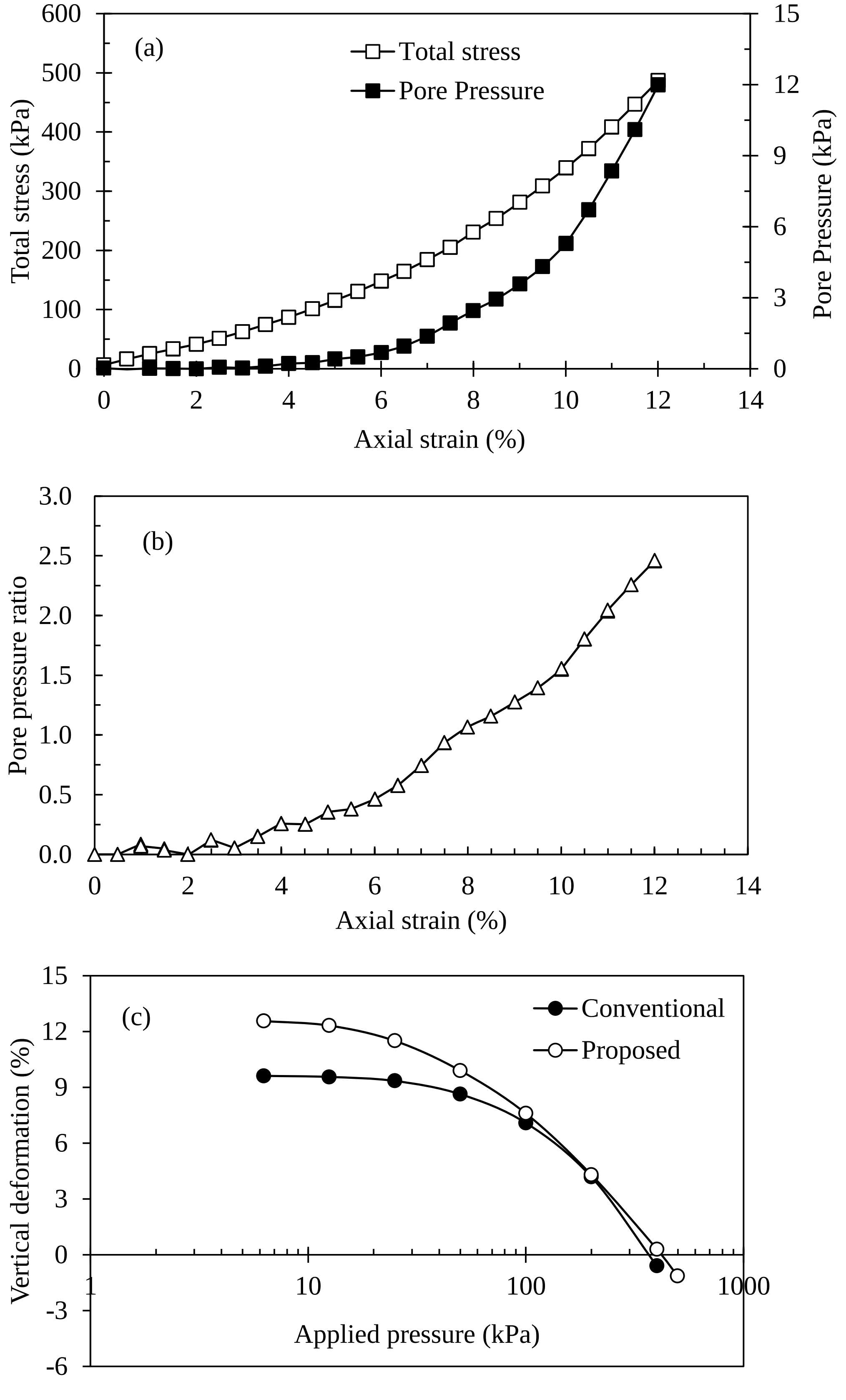

Figure 4.6: (a) Variation of axial stress and pore pressure with axial strain, (b) axial strain versus pore pressure ratio and (c) variation of vertical deformation with applied pressure for Trichy soil in the CSL test

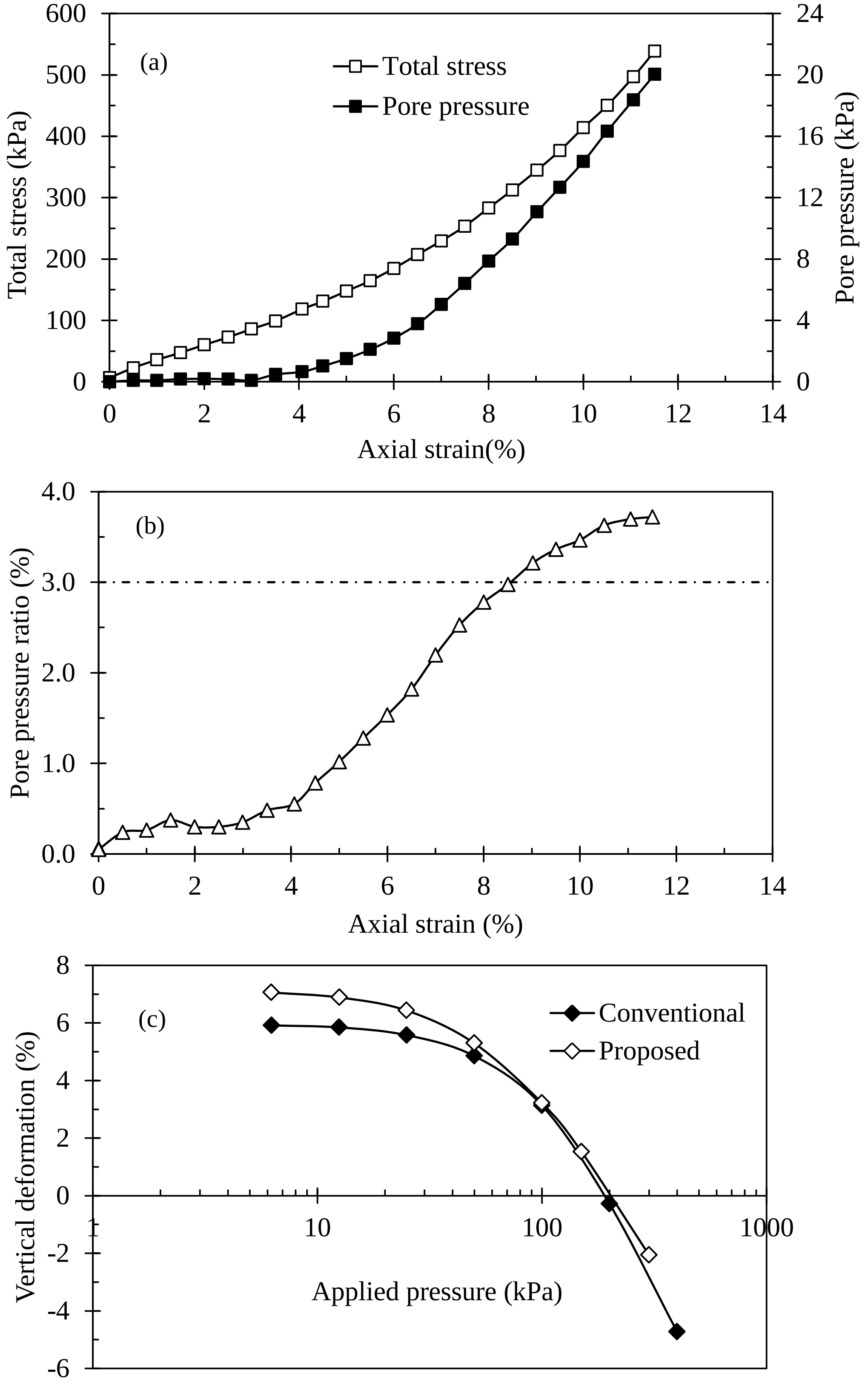

Figure 4.7: (a) Variation of axial stress and pore pressure with axial strain, (b) axial strain versus pore pressure ratio and (c) variation of vertical deformation with applied pressure for Padianallur soil in the CSL test

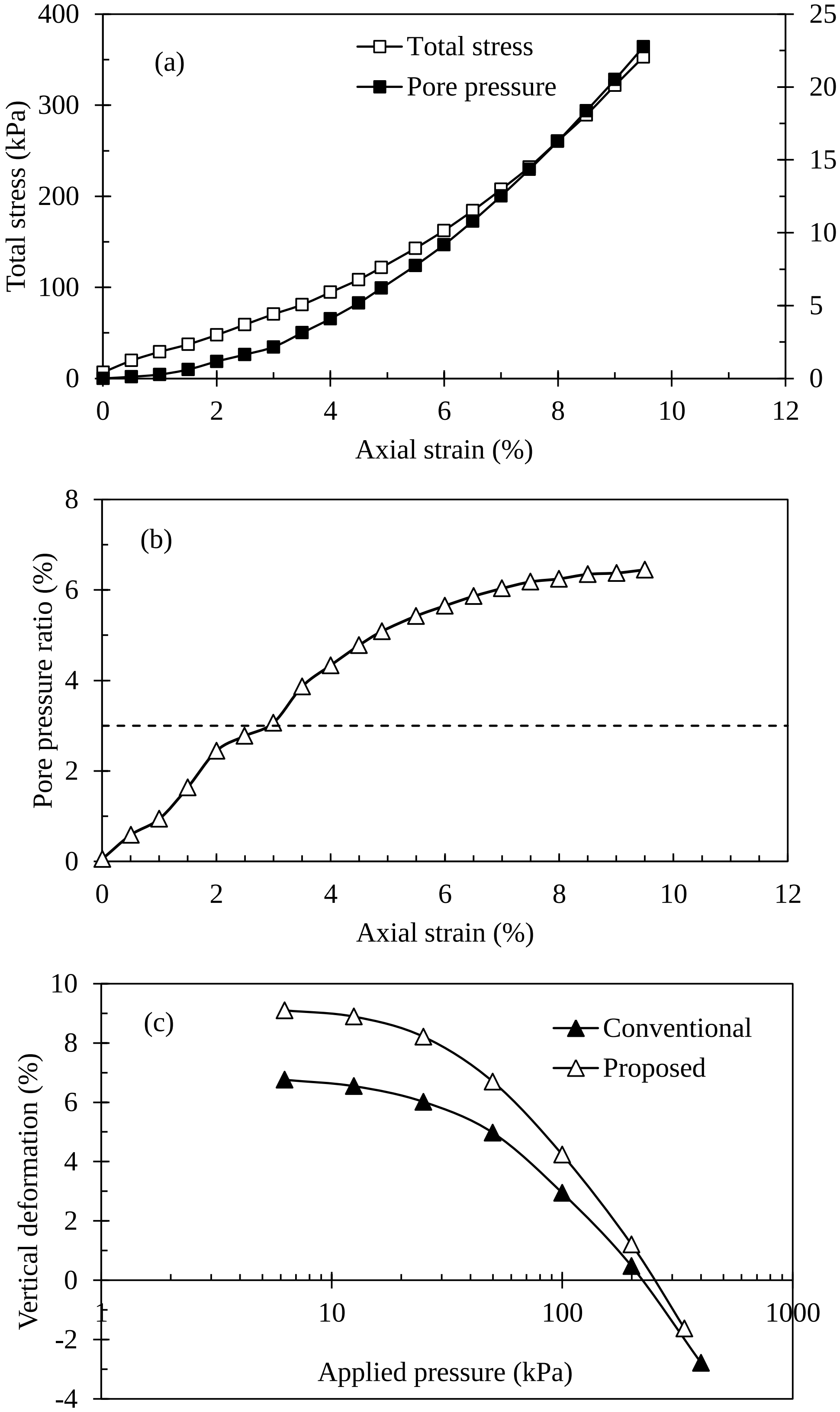

Figure 4.8: (a) Variation of axial stress and pore pressure with axial strain, (b) axial strain versus pore pressure ratio and (c) variation of vertical deformation with applied pressure for Warangal soil in the CSL test

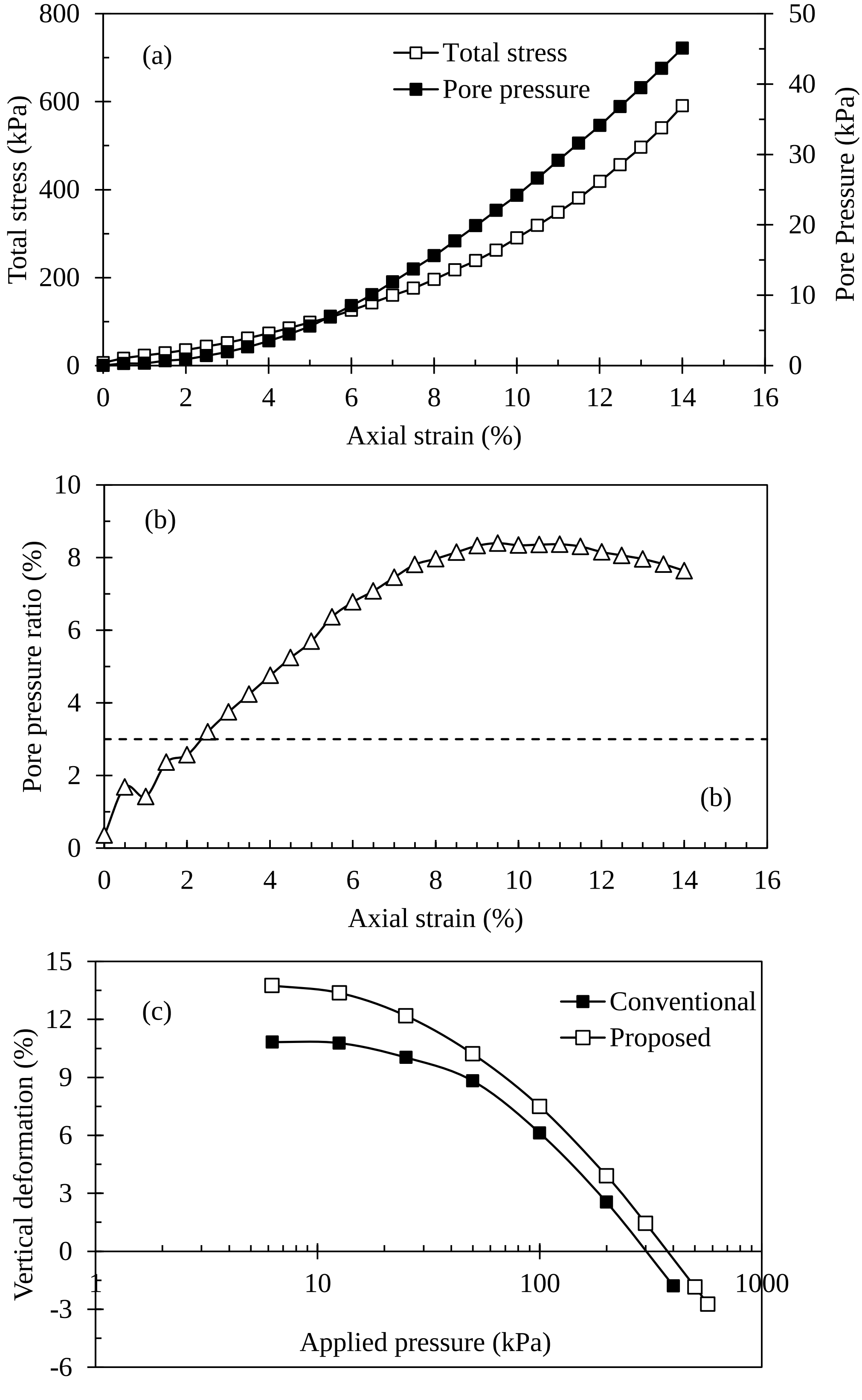

Figure 4.9: (a) Variation of axial stress and pore pressure with axial strain, (b) axial strain versus pore pressure ratio and (c) variation of vertical deformation with applied pressure for Thanjavur soil in the CSL test

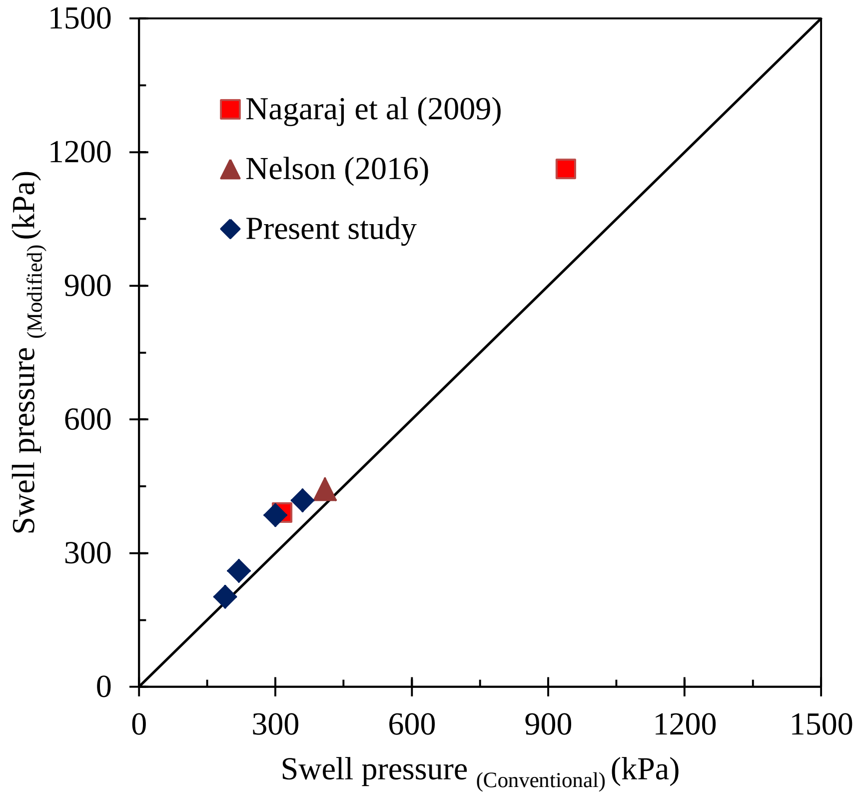

Figure 4.10: Comparison of swell pressure measurement from the present study and from the earlier literatures by varying the method of inundation

In the conventional method (IL test), sufficient time needs to be given for each load increment until the settlements stabilize. Therefore, the test duration is quite high. For example, the time required to complete the consolidation phase is 72 to 96 hours when the conventional method is adopted. However, the consolidation phase can be completed within 14 to 22 hours by adopting the CSL method. The total time required for completing the CSL test (including swelling and reconsolidation phases) is given in Table 4.5. From Table 4.5, it is evident that the proposed method with back pressure saturation is much faster by about 7 to 13 times when compared with the conventional method. The degree of saturation at the end of consolidation is also summarised in Table 4.6.

It may be noted here that both swell potential and swell pressure values obtained from the proposed method are higher owing to the greater degree of saturation after swelling. It is likely that the values obtained in the proposed method are close to the actual values due to better saturation.

Table 4.5 Swell pressures obtained from conventional (CON) and proposed (PRO) methods

Sl. No.	Description	Swell pressure, p_s (kPa)		$T_{\text{Swell+consolidation}}$ (hours)		$\frac{p_{s_{PRO}}}{p_{s_{CON}}}$	$\frac{T_{CON}}{T_{PRO}}$
		CON	PRO	CON	PRO		
1	Trichy soil	360	418	343	27	1.16	13
2	Padianallur soil	190	202	293	43	1.06	7
3	Warangal soil	220	260	432	42	1.18	10
4	Thanjavur soil	300	385	456	48	1.28	9.5

*Note: *T*-Total time required for swell and consolidation;

Table 4.6 Degree of saturation at the consolidation in conventional (CON) and (PRO) proposed method

Sl. No.	Description	Initial degree of saturation (%)	Degree of saturation after consolidation (%)	
			CON	CRS
1	Trichy soil	89	96.0	99.0
2	Padianallur soil	86	94.50	98.0
3	Warangal soil	88	95.25	98.5
4	Thanjavur soil	86	94.5	98.0

4.4 SUMMARY AND CONCLUSIONS

Swell potential and swell pressure tests were carried out on four expansive soils using conventional test method using oedometer cells and proposed test method using CRS cells with back pressure saturation. Based on the experimental results, the following conclusions are drawn:

i. The back pressure saturation technique increased the rate of primary swelling. Compared to the conventional testing method, the rate of swelling in the proposed method is about 7 to 12 times faster.

ii. The swell potential value obtained using back pressure saturation is about 19 to 34% higher than that obtained using the conventional method. This is attributed to the increased saturation and is consistent with the results reported in the literature.

iii. Similar to the swell potential, the swell pressure obtained using back pressure saturation is also higher by about 6 to 28%. This is due to the better hydration of clay particles resulting in an increase in the diffuse double layer thickness and hence the higher swell pressure.

iv. The total time required for both swell potential and swell pressure tests using the proposed method is about 7-13 times faster compared to the time required by the conventional test method. Therefore, the proposed method is a viable rapid experimental procedure for carrying out swell potential and swell pressure tests.

CHAPTER 5

DISTRESS OF AN INDUSTRIAL BUILDING CONSTRUCTED ON AN EXPANSIVE SOIL - A CASE STUDY

5.1 INTRODUCTION

This chapter presents an investigation which was carried out to find out the causes of distress of a two-storied industrial building located at Oragadam, near Chennai, India, and to recommend a suitable remediation measure. Undulations in the floors, cracks in partition walls and non-uniform heave in the pavement are some of the failure patterns noticed in and around the structure. The undisturbed soil samples were collected from the site to identify the cause of distress. From the field inspection and laboratory testing, it was found that the use of unsuitable fill material (expansive soil), followed by the ingression of water from the garden and improper location of rainwater harvesting system were the causes for the initiation of distress in the building.

5.2 DISTRESS IN THE INDUSTRIAL BUILDING

A two storied industrial building located at Oragadam, near Chennai, India, experienced distress after four years of construction. A site visit was made to identify the causes of the distress and recommend suitable remedial measure. The following are the observations.

a. The structure is a framed structure and no distress was noticed on the columns and beams.

b. All the partition walls were cracked particularly which are constructed closer to the gardening area. The maximum crack width was approximately 15 to 20 mm as shown in Figure 5.1a.

c. The glass panels were shattered.

d. Exterior floors were heaved-up and the floor tiles were found to be uneven.

e. Doors were jammed due to heaving (Figure 5.1b).

f. Alignment of the machineries in the building got disturbed.

g. Roads surrounding the building showed cracks and undulations.

h. The building is surrounded by a garden with small shrubs and plants which were continuously watered. Sufficient gradient was not available for the drainage of water.

i. Rain water harvesting arrangements were made closer to the building.

j. The area next to the building is vacant and is in low elevation. This adjacent area was stagnant with rain water due to uneven topography and improper drainage system.

k. Certain portion of the compound wall has collapsed.

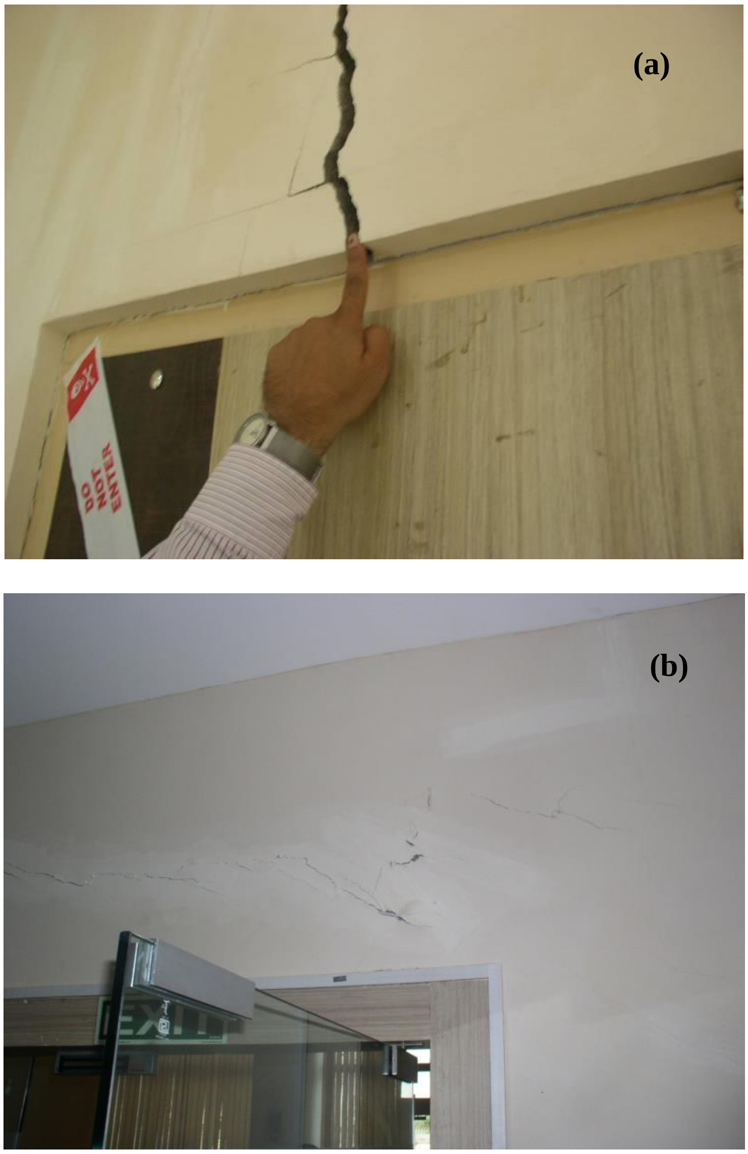

Figure: 5.1: (a) Crack in the wall and (b) Distortion of door frames

5.3 DISTRIBUTION OF EXPANSIVE SOIL IN AND AROUND CHENNAI REGION

The fill material used for the construction was collected from the nearby location of Oragadam area. So a general soil data was collected from the literature for the locations of Chennai and Oragadam region. Chennai is located along the coastline of Bay of Bengal. The major part of Chennai region is covered with a soil profile of alluvial and marine soil deposits with very low shear strength. In the Western region of Chennai, the place Anna Nagar shows the presence of medium to high expansive soil in which the soil extends up to a depth of 4.5 m (Ramaswamy and Narasimhan, 1979). Similarly, in the Southern and Northern regions, the thickness of expansive soil varies from 0 to 8 m. Further, the expansive soils are also noticed at selected locations, like pockets in places such as Sriperumbudur and Oragadam which is directed towards South-West of Chennai city. The Sriperumbudur area is covered with a thick deposit of expansive soil and its differential free swell index varies from 50 to 140%. However, the Oragadam area is identified as expansive due to the presence of weathered mudstone underlain by expansive shale (Ramaswamy and Anirudhan, 2009). Figure 5.2 shows the image of expansive shale formation at selected location in the Oragadam region.

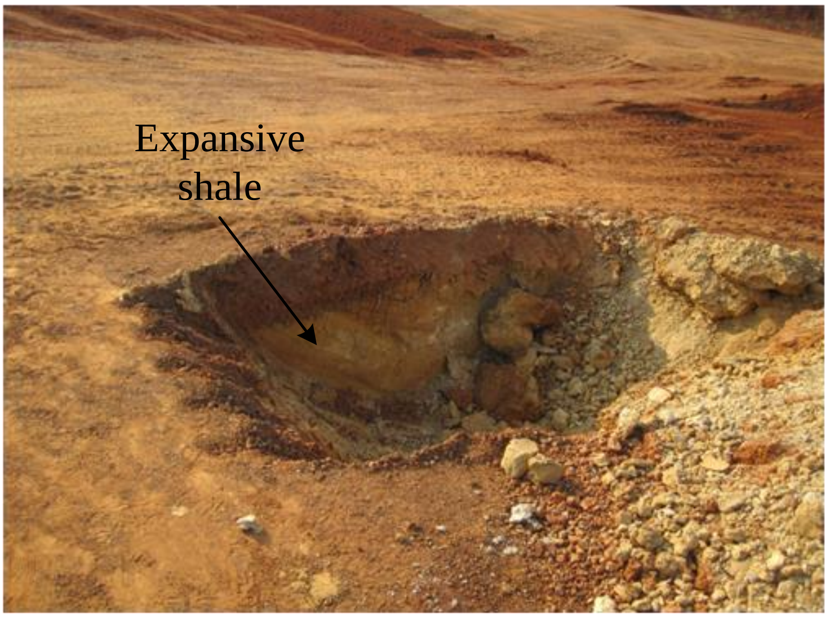

Figure 5.2: Presence of expansive shale at selected location along the stretch in the Oragadam region

5.4 REVIEW OF SOIL INVESTIGATION REPORTS

Geologically, the Oragadam area is known for shale deposits as detailed above. The groundwater table is very deep. Therefore, the presence of soft clay deposit was ruled out. The soil investigation was carried out by two agencies prior to construction. The first soil investigation agency-1 (SIA-1) performed two boreholes (BH-1 and BH-2) and carried out standard penetration test (SPT) up to 4.0 and 6.5 m depths. Disturbed samples were collected at every 1.0 m depth for laboratory testing. The variation of SPT (N) value with depth for BH-1 and BH-2 are shown in Figure 5.3. The SPT (N) values are generally high and both bearing capacity and settlement criteria are met with at a depth of 1.35 m below the existing ground level. The details of Atterberg limits and field moisture content are shown in Figure 5.4. The physical properties of soil show the presence of inorganic clay of high plasticity (CH) over the entire depth of 6.5 m as summarised in Table 5.1. In order to identify the expansive nature of the soil, differential free swell tests were carried out as per IS-2720 (Part 40): 1977. The variation of differential free swell values with depth is shown in Figure 5.5. Both soils from BH-1 and BH-2 have a differential free swell index of 67% at a depth of 2.0 m. From the results of Atterberg limits and differential free swell, the soil was identified as expansive and it was classified as medium swelling soil as per IS: 1498-1970.

Based on the investigation, the soil investigation agency (SIA-1) recommended under-reamed piles for a length of 5 m, with two bulbs as detailed in Figure 5.6 for the foundation. The under-reamed pile or belled pier is often used to resist uplift forces due to soil expansion (Chen 1975). The under reamed pile was designed based on the guidelines given in IS: 2911 (Part III)-1980.

The owner was not convinced with the recommendations of pile foundation and sought for the second opinion from the soil investigation agency-2 (SIA-2). SIA-2 reviewed the report submitted by SIA-1 and also investigated an open pit made to a depth of 1.5 m. SIA-2 recommended open foundation at a depth of 1.35 m. Both agencies were silent about the use of local material for fill. The record showed that the foundation pit was made up to a depth of 1.85 m. A layer of well-compacted quarry dust (crushed stone dust) of 0.5 m thickness was laid. The foundation was then constructed. As structural distress on the columns was not observed, it was decided that the foundation is adequate and safe.

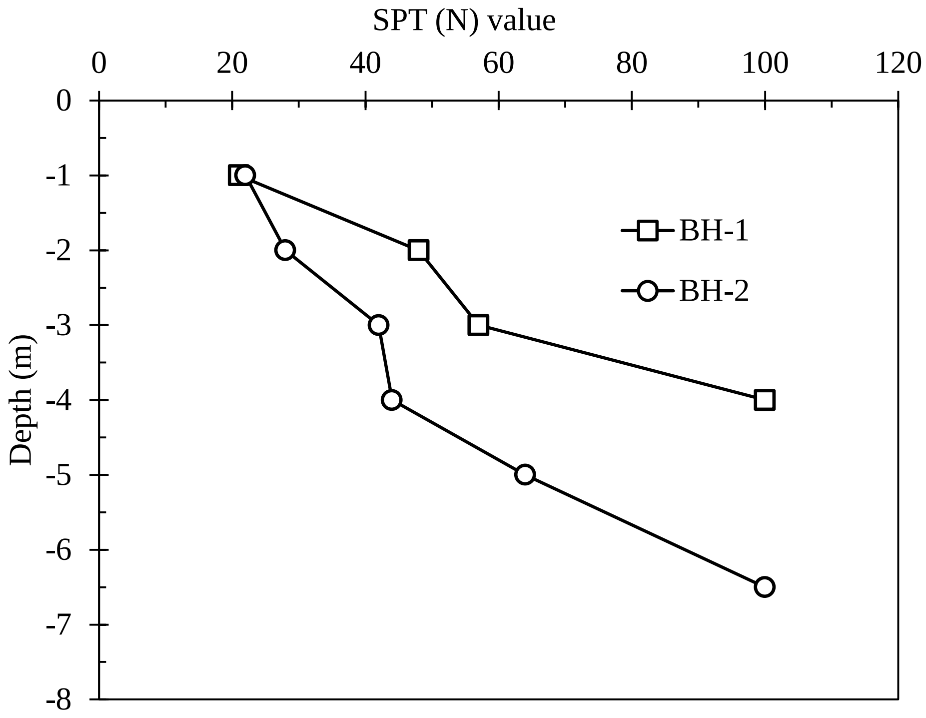

Figure 5.3: Variation of SPT (N) value with depth of soil (SIA-1)

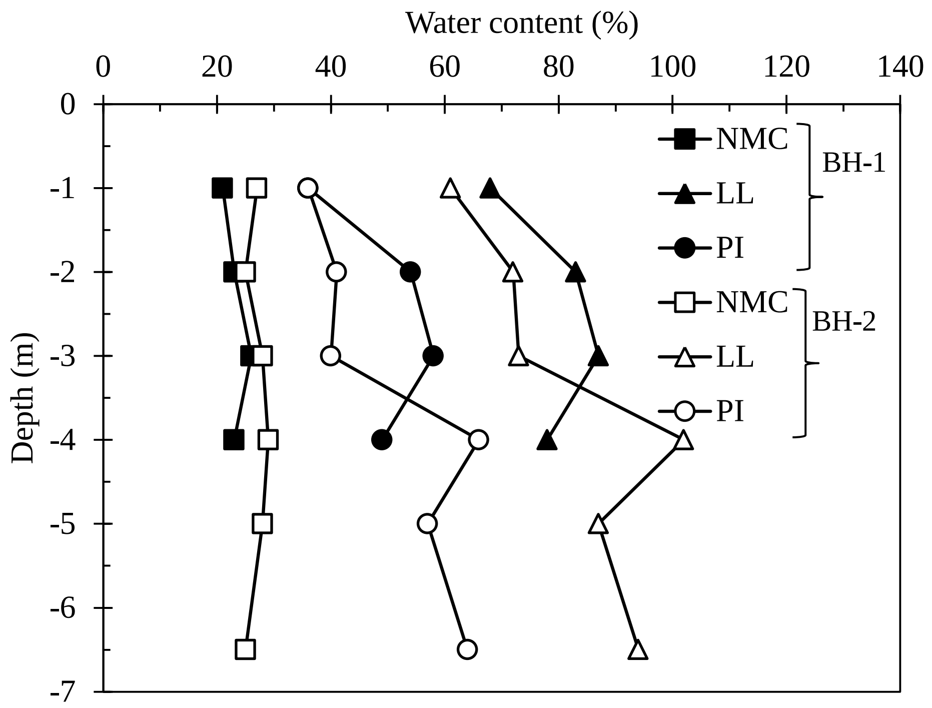

Figure 5.4: Atterberg limits and field moisture content variation with depth of soil (SIA-1) (NMC : Natural Moisture Content, LL : Liquid Limit, PI : Plasticity Index)

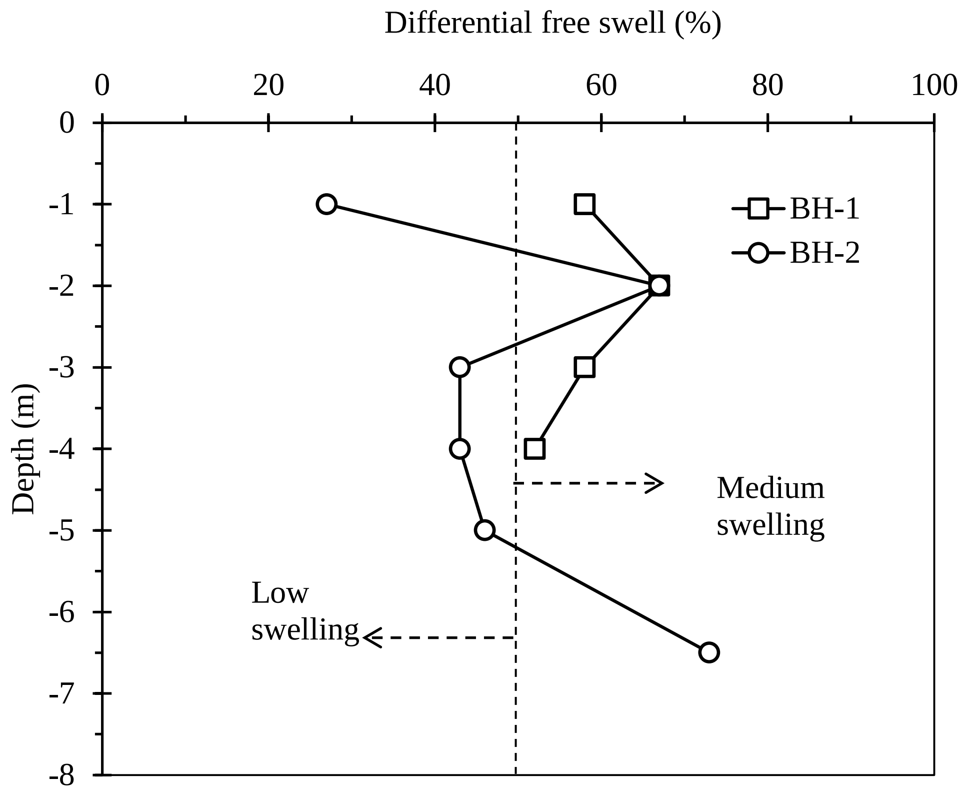

Figure 5.5: Differential free swell index profile (SIA-1)

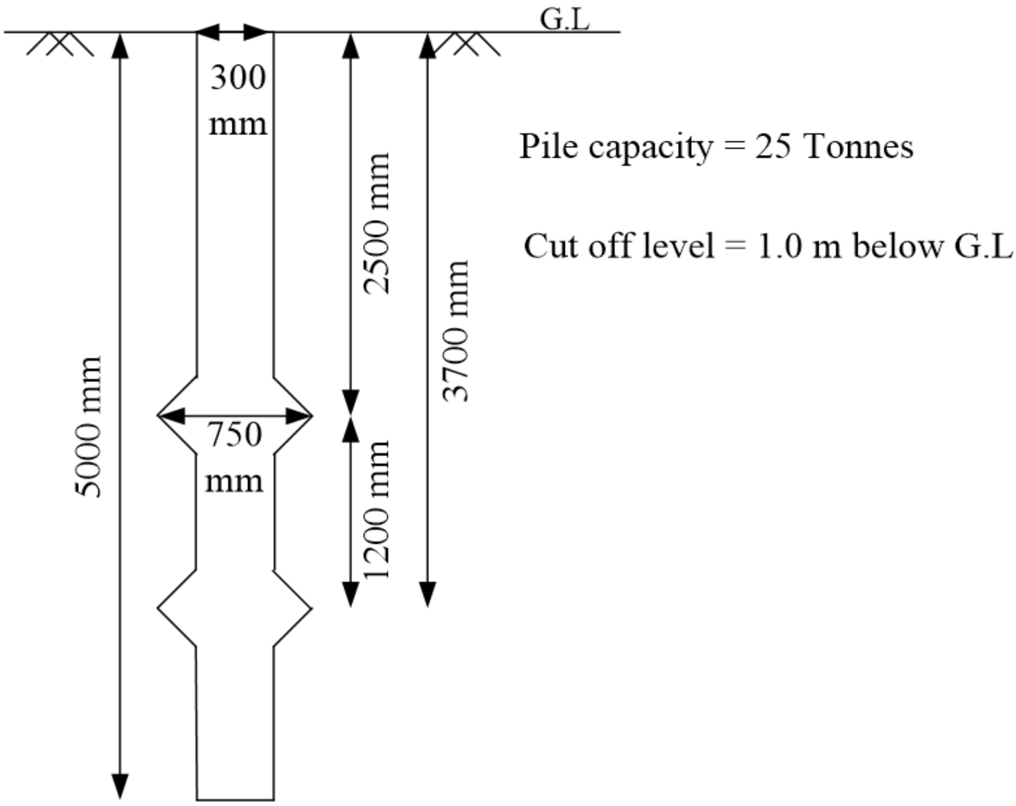

Figure 5.6: Dimensions of under reamed pile recommended by SIA -1

Table 5.1 Description of soil profile (SIA-1)

Depth (m)	Soil description
0.0 - 1.0 (B.H -1/ B.H-2)	Filled soil
1.0 - 2.0 (B.H -1/ B.H-2)	Highly compressible clay (CH), brownish and yellowish in colour
2.0 - 4.0 (B.H -1) 2.0 - 6.5 (B.H-2)	Highly compressible clay (CH), brownish and yellowish in colour

5.5 ADDITIONAL INVESTIGATION

In order to identify the causes of the distress, a borehole was augered by removing one of the slabs inside the building to a depth of 1.2 m by the authors. Soil samples were collected at different depths of 0.9, 1.05, and 1.2 m from the finished ground level. To evaluate the physical properties of the soil samples collected, Atterberg limits, grain size distribution and differential free swell index tests were performed in the laboratory. In addition, permeability test was performed on the quarry dust sample using rigid wall permeameter. Figure 5.7 presents the grain size distribution curves of soils collected from different depths. The index properties of the soil samples are shown in Table 5.2.

From the laboratory test results and field visit, it was observed that a fill was made to raise the original ground level, as shown in Figure 5.8. Layer I is of 0.6 m thick quarry dust over which the floor rests. The quarry dust is classified as poorly graded sand (SP) and it has permeability of 2.5×10^{-3} cm/s. Layer II is about 0.3 m thick and is highly plastic clay with the liquid limit of 54%. The differential free swell value is 95% which implies that soil is expansive in nature and this may create problems for lightly loaded structures. Layer III is a low plastic material with the low degree of expansion.

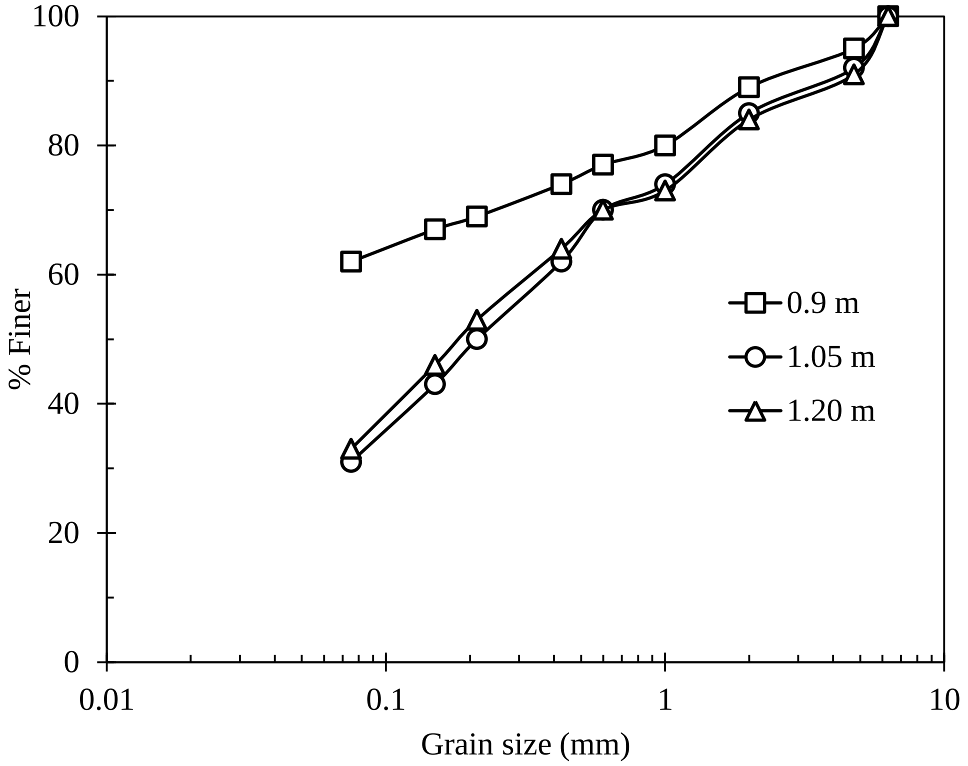

Figure 5.7: Grain size distribution curves for soil tested at 0.9, 1.05 and 1.2 m depth

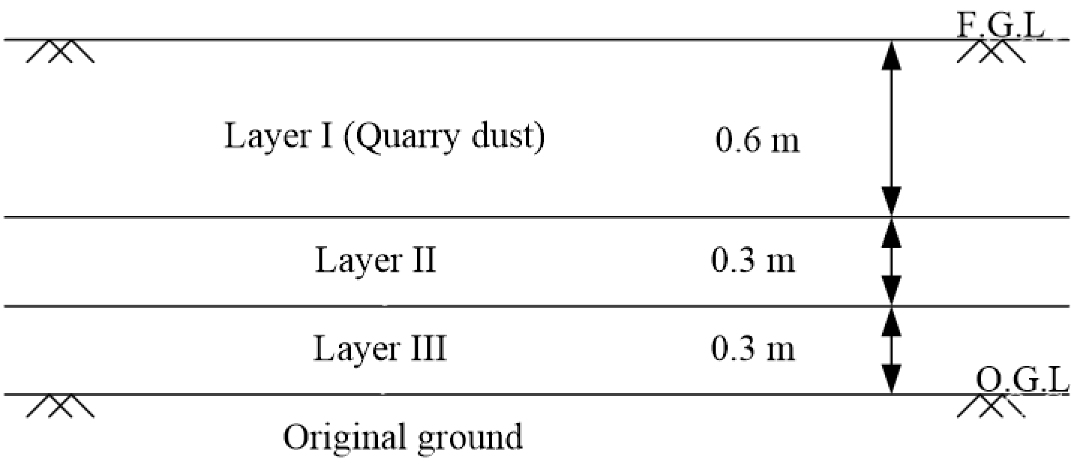

Figure 5.8: Placement of fill material and quarry dust above the original ground level (O.G.L: Original Ground Level, F.G.L: Finished Ground Level)

Table 5.2 Index properties of fill material

Property	Depth of sample collected			
	0.3-0.6 m	0.9 m	1.05 m	1.2 m
Atterberg limits				
Liquid limit (%)	-	54	34	31
Plastic limit (%)	-	22	18	17
Grain size distribution (%)				
% Gravel	1	5	8	10
% Sand	87	33	61	57
% Fines	12	62	31	33
IS soil classification	SP	CH	SC	SC
Differential free swell (%)	-	95	20	26

5.6 CAUSES OF DISTRESS

The possible causes of distress to the structure are:

i. The fill material used in the layer II is expansive in nature. The suitability of the fill material was not evaluated before using it.

ii. The natural ground is also expansive soil and was not treated.

iii. Unplanned gardening close to the structure

iv. The rainwater harvesting was made very close to the building.

v. Proper drainage arrangements for the drainage of storm water away from the building were not made.

vi. The quarry dust fill (Layer I) consists of predominantly sand-sized particles (87%), as summarised in Table 5.2 and it has a hydraulic conductivity of 2.5×10^{-3} cm/s. Therefore, the material is free draining. The water from the gardening and rains seeped through the quarry dust layer (Figure 5.9) and infiltrated into the expansive layer and activated the swelling process.

vii. The gardening work was done without considering the factors like total area of vegetation, location, number and type of trees (small trees, grasses and bushes), which will have a significant effect on moisture content variation and thus affect the safety of structures (Holtz, 1983; Keller, 2007).

viii. The seeping of water from rainwater harvesting system located close to the building enhanced the heave process.

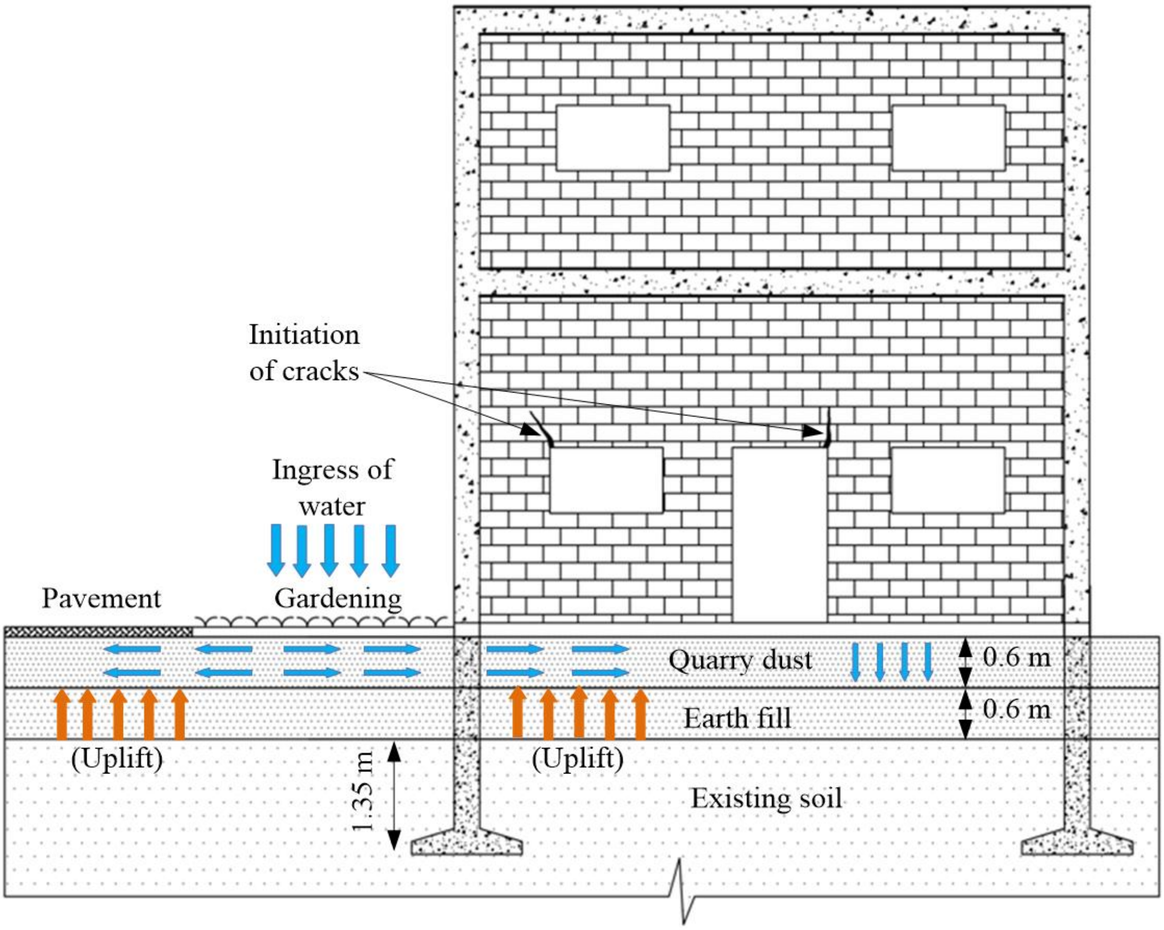

Figure 5.9: Sectional view of soil profile and foundation

5.7 RECOMMENDATIONS

The problems associated with expansive clays are well known. This study further emphasises the importance of handling expansive soil with special attention. While proper site investigation is usually carried out for heavy constructions like bridges, power plant, dams, metro projects and multi-storied buildings, less importance is given to the lightly loaded structures (Medhin, 1980). However, lightly loaded structures are mostly affected due to expansive soil. The following recommendations were made to renovate the structure.

a) Remove the soil at least to a depth of 1.2 m (including the quarry dust and fill material) below the existing floor level inside the building and replace it with a cohesive non swelling soil (CNS) as per IS 9451-1994.

b) The fill shall be appropriately compacted to at least 95% of Proctor's dry density at optimum moisture content.

c) The mid portion of the building does not require treatment at this stage and the performance shall be monitored.

d) Throughout the outer periphery of the building, proper plinth protection shall be provided to a width of at least 2.0 m.

e) Proper drainage arrangements like rain water gutter, downspout and subsurface lined drains shall be provided so that the water does not stagnate around the buildings

f) A minimum slope of 10% gradient (Nelson *et al*., 2015) shall be provided around the building to prevent the infiltration of water into the backfill and foundation soil.

g) The plants (gardening) along the perimeter of the construction area shall be removed. It is suggested to keep a minimum distance of 2 m from the construction area for plants like small shrubs and grass. For trees, it should be at least 4.5 m (Holtz, 1978).

5.8 SUMMARY AND CONCLUSIONS

Based on the field and laboratory investigations carried out in the present study the following conclusions are drawn:

i. Highly draining materials like sand or quarry dust should not be used as a fill material above the expansive soils. Such materials facilitate the flow of water to the expansive soil strata.

ii. The fill material shall be properly tested and characterised for its suitability.

iii. Gardening adjacent to the buildings founded on expansive soil shall be avoided as the roots of trees or shrubs influence the moisture variation of the subsoil. In order to avoid the influence of vegetation, the saplings (grass, shrubs and flowers) should be planted away from the buildings.

iv. Proper drainage arrangements shall be provided to avoid the stagnation of water near the buildings.

CHAPTER 6

MECHANISMS OF COMPENSATING MATERIAL IN CONTROLLING THE VOLUME CHANGE OF EXPANSIVE SOIL

6.1 INTRODUCTION

As detailed in the literature review, the soil replacement technique may be an effective option for shallow stabilization of expansive soil (Bharadwaj, 2013). A case study on the causes of distress and the remedial measures suggested for an industrial building constructed on expansive soil was discussed. As a part of retrofitting, it was suggested to use compensating material and in particular the cohesive non-swelling (CNS) soil material as per IS-9451(1994) specifications. Though utilization of compensating material is in practice for the stabilization of expansive soil, its mechanism is not clearly understood. Hence, in this chapter, a detailed laboratory study was carried out to understand the mechanisms of compensating materials in controlling the volume change of expansive soil.

6.2 EXPERIMENTAL METHODOLOGY

The testing protocol adopted to achieve the objective of the proposed study is depicted in Figure 6.1. One expansive soil and four compensating materials with different engineering properties were selected and used in the present study. A series of experiments were performed to understand the mechanism of compensating materials in controlling the volume change of expansive soil which includes swell potential and swell pressure tests, hydraulic conductivity, infiltration tests, leaching studies and wet-dry tests. These experiments were carried out as per the standard procedures detailed in IS and ASTM standards and literature.

6.2.1 Basic Characterization of Materials

The selection, collection and basic properties of expansive soil and compensating materials are discussed in this section.

i) Expansive soil

The expansive soil used in the present study was collected from Wellington Lake, near Tiruchirappalli, Tamil Nadu state. To determine the index properties, the soil was air-dried and sieved through 425 µm IS sieve. The specific gravity of expansive soil was determined using density bottle as detailed in IS 2720-3(1980). The liquid limit of expansive soil was determined using Casagrande apparatus, and it was found to be 95% (IS 2720-5 (1985)). Then the plastic limit of the soil was determined using the conventional thread rolling method. Mercury displacement method was used for obtaining the shrinkage limit of the soil, following IS 2720 – 6(1972). Based on the Atterberg limits and gradation, the soil is classified as highly compressible clay (CH). Table 6.1 summarises the index and engineering properties of expansive soil used for the study. The pH of the soil was determined as per IS 2720 – 26(1987) and electrical conductivity of the soil was determined using digital electrical conductivity meter. From the electrical conductivity determinations, the pore salinity of soil was calculated as per Todd (1980) i.e. 1 mg/l = 1.56 µSiemens.

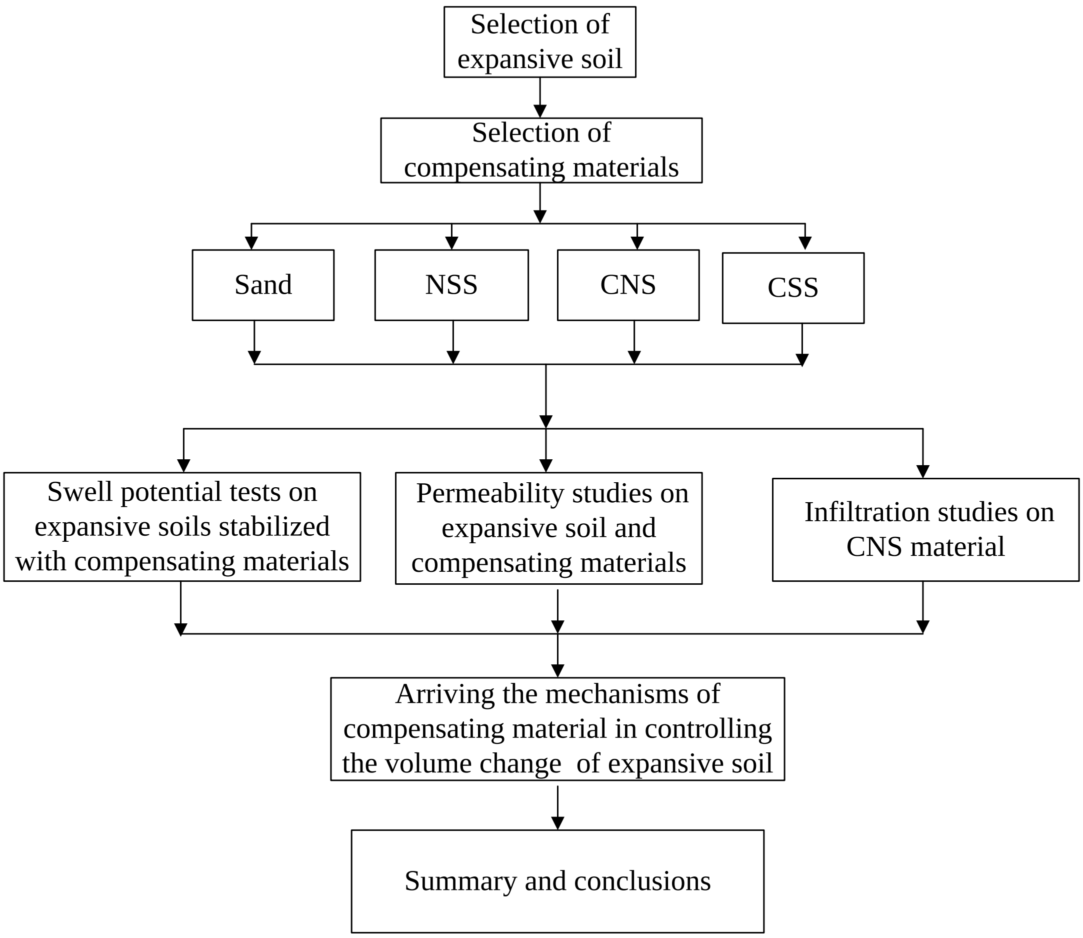

Figure 6.1: Flow chart depicting the testing program

ii) Compensating materials

a) Sand and non-swelling soil (NSS)

The river sand used for the present study was collected from the local construction site. A soil collected from the field with non-swelling characteristics and not meeting the specifications of IS 9451-1994 was selected and used for the present study. Two non-swelling soils with different physical properties were selected and used for the testing. The properties of the sand and non-swelling soil are summarised in Table 6.1. The river sand is classified as poorly graded sand (SP) and non-swelling soil-1 is classified as clayey sand (SC) and non-swelling soil-2 is classified as clayey gravel (GC).

Table 6.1 Properties of expanisve soil, CNS, NSS-1 and NSS-2 materials

Property	Expansive soil	CNS soil	Non-swelling soil - 1	Non-swelling soil - 2
Specific gravity, G_s	2.68	2.7	2.72	2.75
Atterberg limits (%)				
Liquid limit	95	41	40	28
Plastic limit	33	16	20	17
Shrinkage limit	9	15	15	16
Grain size distribution (%)				
Gravel size	-	-	-	37
Sand size	5	51	67	35
Silt size	27	31	16	16
Clay size	68	18	17	12
IS Soil Classification	CH	SC	SC	GC
Standard Proctor compaction characteristics				
OMC (%)	30.5	11.25	11.0	10.5
MDD (Mg/m^3)	1.41	1.98	1.95	2.08
Free swell index (%)	95	10	15	10
Swell potential (%)	10.5	0	0	0
UCS (kPa)	325	225	195	215

Note: OMC: Optimum Moisture Content, MDD: Maximum Dry Density, UCS: Unconfined compressive strength *c) Cohesive non-swelling soil (CNS)*

The specifications for the CNS material were already given in Table 2.7. The field soil with a proportion of CNS was not available in the nearby locations. Hence it was decided to prepare the CNS material in the laboratory environment to meet the specifications of CNS as detailed by IS 9451:1994. For that, the river sand fraction passing 4.75 mm and retained on 2 mm sieve was used for blending. And to collect the fines, a field soil was used which is dominant in kaolinite mineral and with the non-swelling property. By varying the proportions of sand and red soil, the final gradation was obtained, as shown in Figure 6.2. The physical properties are summarised in Table 6.1.

The CNS material was classified as clayey sand (SC) with 51% sand, 31% silt and 18% clay, as shown in Figure 6.2. The liquid limit and plastic limits of the soil were 41% and 16%, respectively.

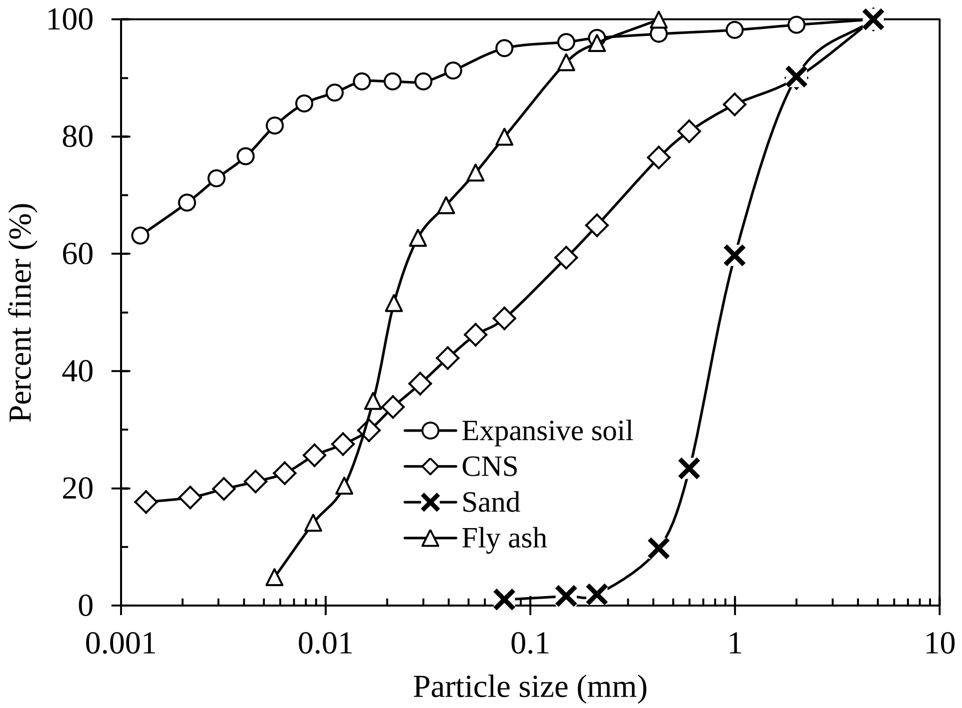

Figure 6.2: Grain size distribution curves of expansive soil (ES), CNS, sand and Class C fly ash

d) Chemically stabilized soil (CSS) cushion

Chemically stabilized soil (CSS) cushion was obtained by mixing the native expansive soil with different percentages of fly ash and lime. The following tests were performed to evaluate the CSS material: (a) index properties (b) compaction characteristics (c) unconfined compressive strength (d) swell parameters (e) hydraulic conductivity (f) and wet-dry tests on stabilized expansive soil.

e) Fly ash

The fly ash was collected form Neyveli Lignite Corporation. Since it is not a natural geo-material, the fly ash is classified based on the guidelines suggested by Prakash and Sridharan (2006). The fly ash is classified as MLN-MIN (non-plastic inorganic coarse silt sized fractions – non-plastic inorganic medium silt sized fractions) as it comprises 50% of particles' size in between 7.5 μm to 75 μm. Figure 6.2 shows the grain size distribution of Neyveli fly ash. X-ray fluorescence test was performed to determine the chemical composition of the fly ash and based on the analysis, it is classified as Class C fly ash as per ASTM C618-19. The chemical composition of Neyveli fly is given in Table 6.2.

Table 6.2 Chemical composition of expansive soil and fly ash

Constituents (%)	Expansive soil	Fly ash
SiO_2	52.19	15.86
Al_2O_3	14.87	10.30
Fe_2O_3	6.33	29.07
CaO	7.37	35
MgO	5.80	3.0
TiO_2	2.51	6.06
K_2O	1.65	0.27
Na_2O	9.27	0

f) Lime

Laboratory grade $Ca(OH)_2$ (calcium hydroxide) was used as an additive to stabilize the expansive soils. Calcium hydroxide constitutes about 86% of CaO. Further, to determine the optimum lime content of the soil, Eades and Grim (1966) procedure was followed and it was found as 4%, as shown in Figure 6.3

6.2.2 Compaction characteristics and unconfined compressive strength

Standard Proctor compaction tests were performed for determining the compaction characteristics of CNS and non-swelling soils. The tests were conducted as per the guidelines detailed in IS 2720 (Part 7) - 1980 and the compaction properties of the compensating materials are presented in Table 6.1. In addition, the tests were also conducted to study the compaction characteristics of fly ash and lime stabilized expansive soil.

For UCS tests, the specimens were prepared in 50 mm diameter and 180 mm long moulds. The predetermined quantity of water mixed soil samples were placed inside the moulds and statically compacted to the required height of 100 mm. The tests were performed using strain controlled testing frame and the compacted specimens were sheared at a deformation rate of 0.625 mm/min.

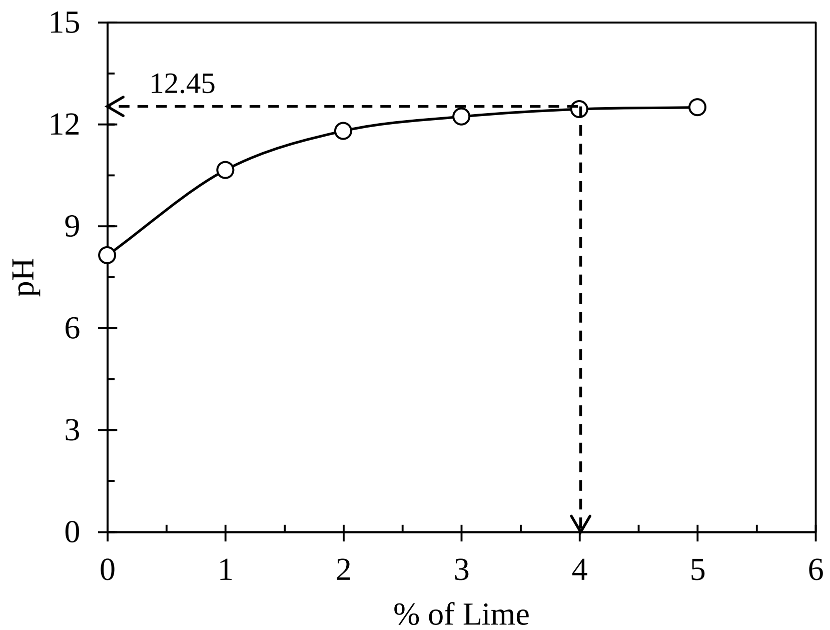

Figure 6.3: Optimum lime content of expansive soil using Eades and Grim method

6.2.3 Swell Potential Tests

a) On expansive soil

The swell potential tests were conducted as per IS 2720 -41(1997). In order to obtain a uniform soil mix, the pulverised expansive soil was thoroughly mixed with predetermined volume of distilled water. The water was sprayed on the soil using water sprayer. The water-mixed soils were then transferred to polythene covers, and sealed and stored in desiccators for 24 to 48 hrs for ensuring the moisture equilibrium. Then the soils samples were statically compacted to 20 mm thickness in oedometer rings of 75.1 mm diameter and 30 mm height. The compacted specimens were then assembled in the standard oedometer cells and setup in oedometer frames, and the swell was monitored until the vertical deformation became constant under a seating pressure of 6.25 kPa.

b) *On sand/ non-swelling soil/ CNS / CSS stabilized expansive soil*

In order to determine the volume change of two-layer soil systems, the tests were conducted in 75.1 mm diameter and 80 mm thick stainless steel rings. The compensating material was first compacted in the ring and over that the expansive clay was compacted. The expansive soil and CNS material were compacted to different thickness ratios of 0.5, 1.0 and 1.5. The thickness ratio is defined as the ratio of the thickness of CNS to the thickness of clay bed. The CNS and expansive soils were compacted to their corresponding maximum dry densities and optimum moisture contents. In addition, the swell potential tests were also conducted on the sand, non-swelling soil and CSS stabilized expansive soil. Figure 6.4 presents the schematic diagram of expansive soil stabilized with different compensating materials.

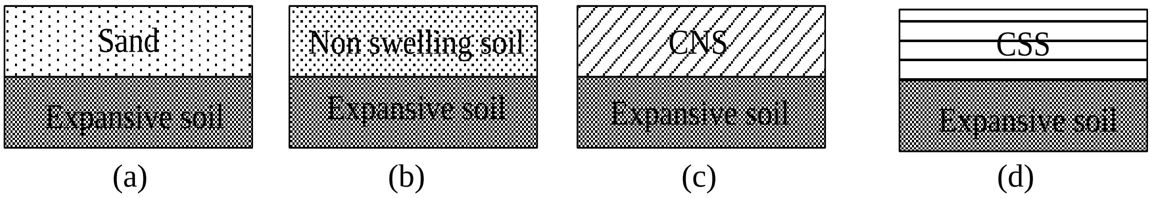

Figure 6.4: Schematic representation of expansive soil stabilized with: (a) sand (b) non-swelling soil (c) cohesive non-swelling (CNS) soil and (d) CSS

6.2.4 Swell Pressure Tests

The swell pressure of the expansive soil and CNS stabilized expansive soil was determined using both swell-consolidation and constant volume methods. In the swell-consolidation method, the compacted specimens were allowed to swell under a seating pressure of 6.25 kPa until the swell equilibrium condition was reached. Then, the swollen specimens were subjected to consolidation for compressing the specimens to their initial thickness. A load incremental ratio of 1.0 was adopted as per IS-2720-41. The pressure required to compress the swollen specimens to their initial compacted thickness is reported as swell pressure. The swell-consolidation procedure has already been discussed in detail in Chapter 4.

Figure 6.5 shows the apparatus used for the measurement of swell pressure using constant volume method. IS 272 -41(1997) suggests the use of rigid proving ring for the measurement of swell pressure. However, in the present study, a rigid load cell was used. The tests were carried out until the load cell indicator showed a constant load value with time.

6.2.5 Hydraulic Conductivity Tests

Constant head permeability tests were conducted on the expansive soil, CNS material, non-swelling soil and CSS using flexible wall permeameters (Figure 6.6). The hydraulic conductivity tests were conducted as per the procedure detailed in ASTM D5084-10. Statically compacted specimens of 70 mm diameter and 50 mm thickness were used for hydraulic conductivity testing. Before placing the specimens in the cell chamber, all the pressure lines were thoroughly checked for ensuring that no air bubbles were present in the lines. The bottom drainage line was flushed with water for removing air bubbles before assembling in the hydraulic conductivity test set-up. After placing the specimens, the top cap with two drainage lines was then placed over the porous stone. The rubber/ latex membrane was placed over the soil specimen and 'O' rings were provided on the top cap and bottom pedestal for fixing the membrane firmly over the specimens. The top drainage line is then flushed to remove the air bubbles. The specimens were allowed to saturate until the B-value of at least 0.95 was achieved. For all the soil specimens (ES/ CNS/ non-swelling/ CSS) minimum back pressure of 200 to 350 kPa was required for saturation of the specimens.

The soil specimens were then consolidated under the effective confining pressure of 50 kPa. As per ASTM D5084-10 specifications, the hydraulic gradient can range between 10 and 20 for soils with hydraulic conductivity in the range of 10^{-7} to 10^{-9} m/s. During the hydraulic conductivity testing stage, the burette readings were taken and recorded with time and the steady state condition was ensured when the outlet volume became equal to the inlet volume. ASTM D5084 suggests recording a minimum of four readings at the steady state condition for reporting the final hydraulic conductivity value.

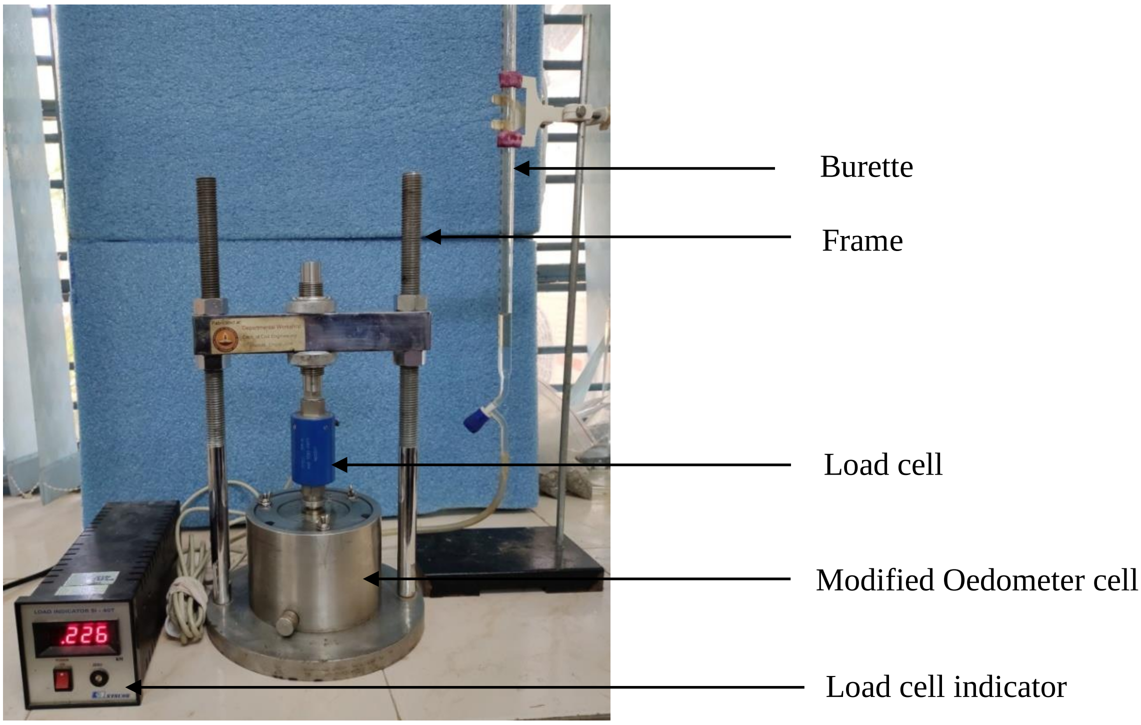

Figure 6.5: Photographic view of experimental test setup used for swell pressure measurement using constant volume method

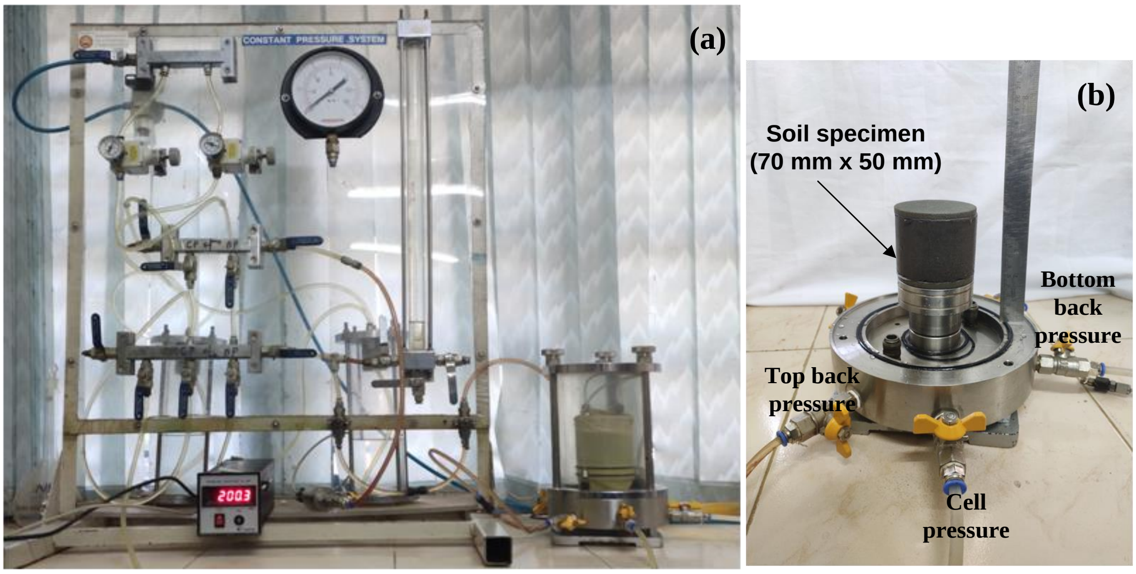

Figure 6.6: Photographic view of: (a) flexible wall permeameter apparatus for the measurement of hydraulic conductivity of compacted soil specimens, (b) close up view of permeameter cell

6.2.6 Infiltration Tests

The infiltration studies were carried out on CNS and NSS materials in oedometer-infiltration test setups. The soil specimens were compacted to their maximum dry densities at the corresponding optimum moisture content. The detailed description of this apparatus can be found in Julina (2018). Figure 6.7 shows the oedometric-infiltration test setup which was fabricated to simultaneously measure the vertical swell, inflow and outflow volumes during infiltration under a nominal surcharge pressure equivalent to 12.5 kPa and under a hydraulic gradient (*i*) of 2. The soil specimens were compacted to a thickness of 20 mm in 75.1 mm diameter and 55 mm heigh rings. The inflow volume of distilled water was monitored using an electronic weighing balance (B1) on which the Mariotte tube is placed. Also, the outflow volume was monitored using an electronic weighing balance (B2) on which a beaker was placed for collecting the effulent.

The incremental inflow or outflow infiltration rates were calculated as

$$I_{inflow}\text{ (or) }I_{outflow}\text{ (cm/s)} = \frac{Q}{A \times t} \tag{6.1}$$

where Q is the inflow (or) outflow volume (cm^3), A is the cross-sectional area of oedometer ring (cm^2) and t is time (s).

6.2.7 Leaching Studies on Stabilized Expansive Soil

Leaching study was performed in flexible wall test setups commonly used for conducting hydraulic conductivity tests. Figure 6.8(a) shows a photographic view of the apparatus used for the leaching study. After setting up the soil specimens in the cell, a cell pressure of 50 kPa was applied. Then, a back pressure of 10 kPa was applied to the specimen from the top using a burette as shown in Figure 6.8(a). The bottom back pressure valve was left open to the atmospheric pressure, and hence, no pressure was developed at the bottom of the specimen. Due to the pressure difference of 10 kPa, the water flowed from top to bottom of the specimen and the outlet effluent was collected in a small beaker at regular intervals. The distilled water was used as an infiltrating fluid for both treated and untreated specimens. The outlet effluent was analysed for the determination of possible leaching of dissolved ions using Dewpoint Potentiometer (WP4) (Figure 6.8(b)). For untreated expansive soil, the effluent has zero osmotic suction, and this was used as the control for the osmotic suction of effluent collected from the CSS stabilized expansive soil.

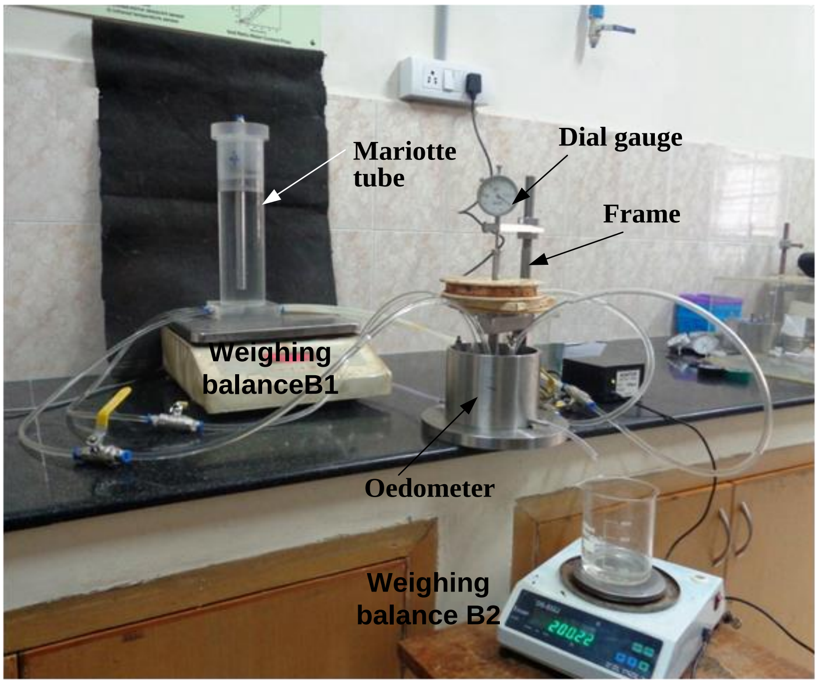

Figure 6.7: Photographic view of oedometer-infiltration setup (after Julina, 2019)

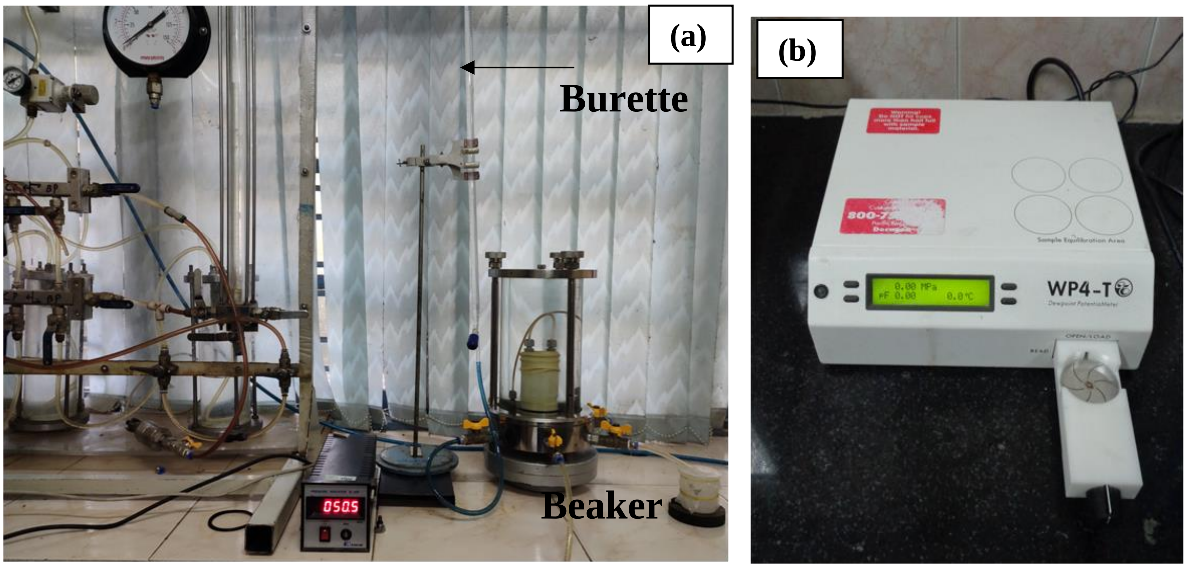

Figure 6.8: (a) Photographic view of apparatus used for leaching studies on the CSS stabilized expansive soil (b) Photographic view of Dewpoint potentiameter used for osmotic suction measurements of effluent

6.2.8 Cyclic Wet-Dry Studies

To study the effect of cyclic wetting and drying on the behaviour of untreated and stabilized expansive soil, the soils were statically compacted in the oedometer rings as discussed earlier, and allowed to swell under a seating pressure of 6.25 kPa. In order to measure the volume change during the drying process, the water in the cells was removed, and an elevated temperature of 40 ± 5˚C was adopted as suggested by Thyagaraj and Zodinsanga (2014). Figure 6.9(a) shows the apparatus used for drying the saturated soil specimens. The oedometer cells were covered with a band heater, which accelerates the drying process from the outside of the cells. The temperature of the whole system was controlled using a thermostat. The drying was carried out until the weight of the specimens became constant or till the dial gauge readings became constant. Then the second cyclic swelling cycle was carried out by the usual technique of adding water and allowed to swell. The process is repeated to the required number of wet-dry cycles for obtaining the equilibrium bandwidth. During each wet-dry cycles, the thickness and diameter of the soil specimens were measured.

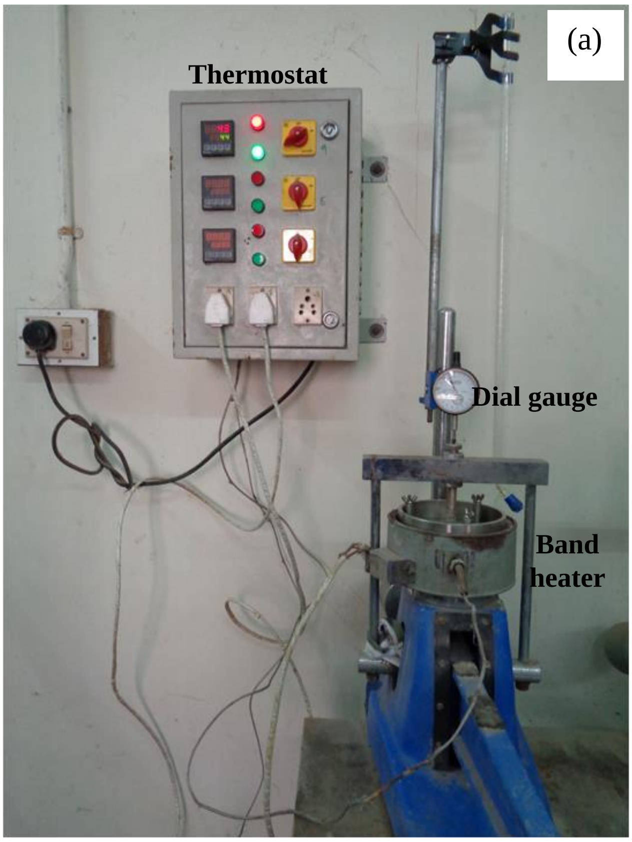

Figure 6.9: (a) Band heater arrangements for drying the soil specimens in oedometer cells under the controlled temperature of $40 \pm 5^{\circ}$ C (b) components of oedometer cell used for the wet-dry tests

6.3 RESULTS AND DISCUSSION

6.3.1 Preparation of Chemically Stabilized Soil (CSS) Cushion

The compensating materials like sand, NSS and CNS are natural materials which can be collected from the nearby sites, but in the event of unavailability, the CSS materials are prepared by blending the local soil with chemical additives. In the present work, the CSS was prepared by blending the expansive soil with fly ash and lime in different proportions. The CSS material was optimised based on the results of Atterberg limits, swell potential, swell pressure and unconfined compressive strength.

a) Physico-chemical and index properties and compaction characteristics of fly ash and lime stabilized expansive soil

The effect of fly ash on the Atterberg limits and plasticity behaviour of stabilized expansive soil is presented in Figure 6.10. The tests were performed on 28 days cured slurry soil samples. With an increase in the fly ash content, the liquid limit and plasticity index of the soil decreased. In contrast, the plastic limit and shrinkage limits increased with the fly ash content. The swelling behaviour of expansive soil can be inferred from the plasticity index. The variation in the plasticity index of fly ash stabilized soil was due to the presence of a coarser fraction of fly ash particles and available free lime (Sivapullaiah *et al*. 1996). This behaviour is comparable with the works of Cocka (2001) and Nalbantoglu (2004) where they have used Class C fly ash for expansive soil stabilization.

Table 6.3 presents the Atterberg limits, pH and pore salinity of fly ash and lime treated expansive soil. As can be seen from the Table 6.3, the addition of fly ash to expansive soil resulted in only a marginal increase in pH value, but the pore salinity values increased at rapid rate and this is because of higher pore salinity of Class C fly ash.

Figure 6.11 brings out the effect of fly ash content on optimum moisture content and maximum dry density of fly ash stabilized expansive soil. With an increase in fly ash content from 0 to 20%, the optimum moisture content increased and the maximum dry density decreased. Similar results were reported by Mir and Sridharan (2013). The reduction in the maximum dry density and increase in the optimum moisture content is attributed to the poor gradation and low specific gravity of fly ash (Mir and Sridharan, 2013).

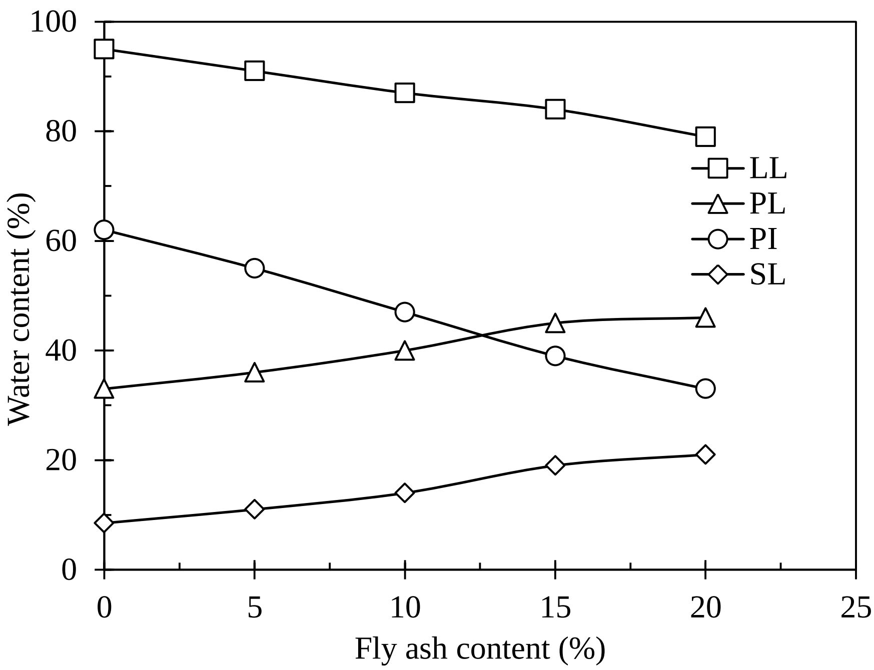

Figure 6.10: Effect of fly ash on Atterberg limits and plasticity index of expansive soil stabilized with fly ash

Table 6.3 Atterberg limits, pH and pore salinity of fly ash and lime stabilized expansive soil

Specifications	w_L (%)	w_P (%)	I_P (%)	w_S (%)	pH	Pore salinity (mg/l)
ES	95	33	62	8.5	8.0	601
ES + 5% FA	91	36	55	11	8.05	1044
ES + 10% FA	87	40	47	14	8.27	1358
ES +15% FA	84	45	39	19	8.75	1448
ES + 20% FA	79	46	33	21	9.20	1538
ES + 4% L	71.5	48	23.5	28	11.2	1346
ES + 5% FA + 2% L	73	47	26	24	10.75	1474
ES + 10% FA + 1% L	74	47	27	23.5	-	-
ES + 20% FA + 4% L	-	-	-	-	11.4	1794
FA	-	-	-	-	7.98	1057

Note : ES: expansive soil; FA: Class C fly ash; L: lime; w_L : liquid limit; w_P : plastic limit; I_P : plasticity index; w_S : shrinkage limit

In order to prepare the CSS material, expansive soil was mixed with different percentages of lime and fly ash and compaction tests were carried out on these mixtures. Figure 6.12 presents the compactions curves of lime and fly ash admixed expansive soil. The maximum increase in the optimum moisture content to 35% was observed in case of 4% lime stabilized soil. The maximum dosage of lime was limited to 4% and fly ash was limited to 20%.

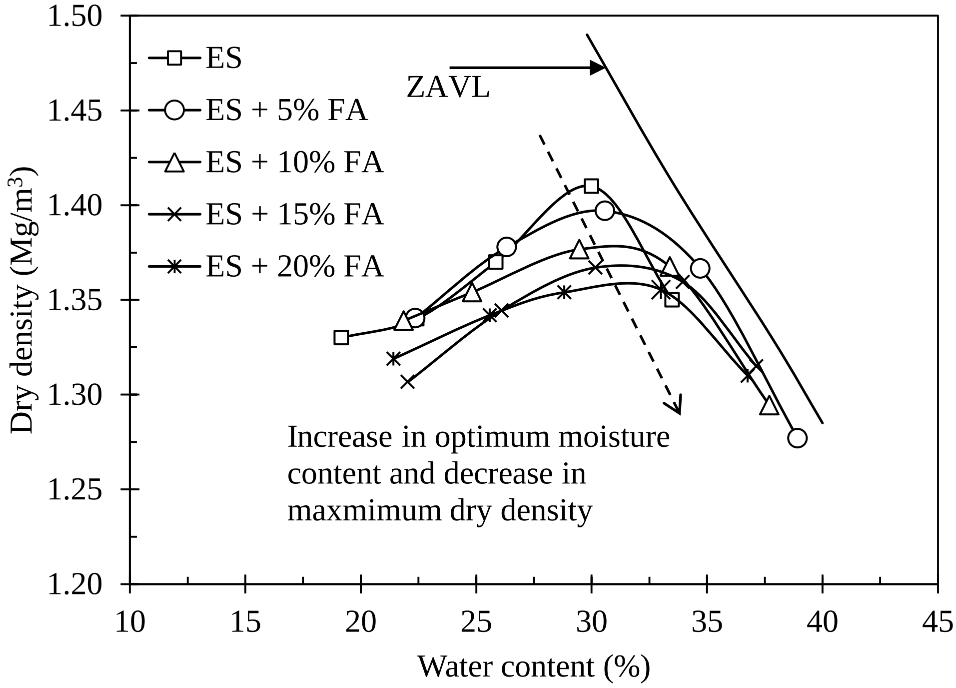

Figure 6.11: Effect of fly ash content on optimum moisture content and maximum dry density of expansive soil stabilized with fly ash (Standard Proctor compaction)

b) Swell characteristics of fly ash and lime stabilized expansive soil

Figure 6.13 compares the time-swell plots of expansive soil stabilized with different percentages of fly ash. The variation of swell potential and swell pressure with fly ash content is presented in Figure 6.14. As can seen from Figure 6.13, the swell potential of expansive soil decreases with increase in fly ash content. These specimens were tested after 28 days of curing. Addition of 20% fly ash to the expansive soil resulted in zero volume change, and it was identified as the optimum fly ash content for the stabilization of expansive soil. Similarly, the swell pressure of the expansive soils reduced from 390 kPa to 0 kPa with addition of 20% fly ash (Figure 6.14). Both swell potential and swell pressure indicate the optimum fly ash content as 20%. The swell reduction is mainly due to the addition of non-plastic silt size particles and pozzolanic reactions (Cocka, 2001; Mir and Sridharan, 2013).

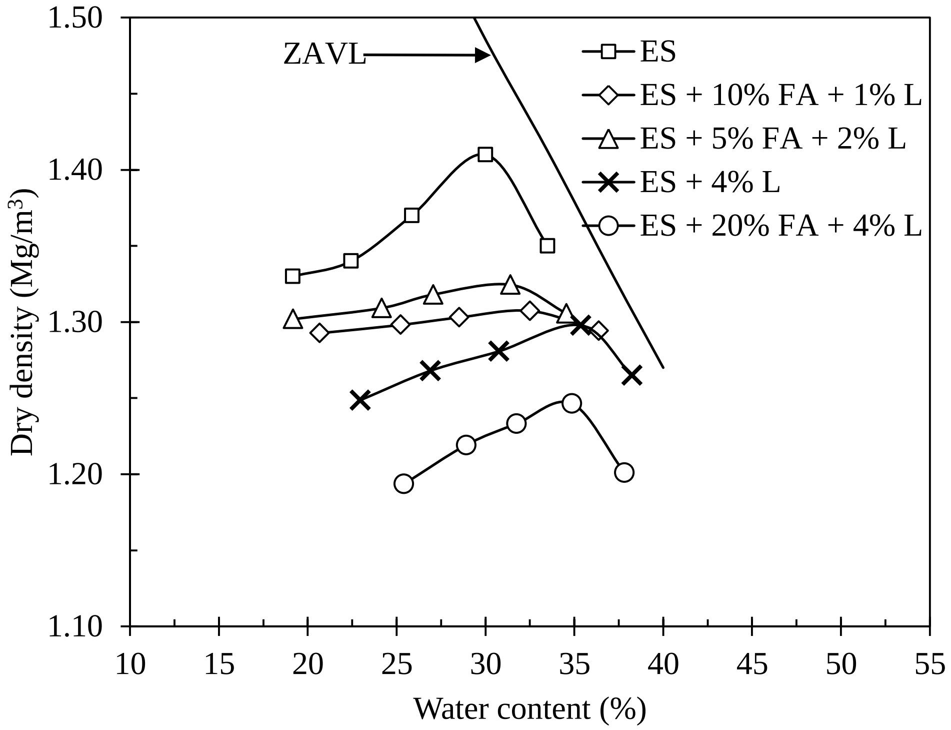

Figure 6.12: Standard Proctor compaction curves of expansive soil and stabilized expansive soil with fly ash and lime

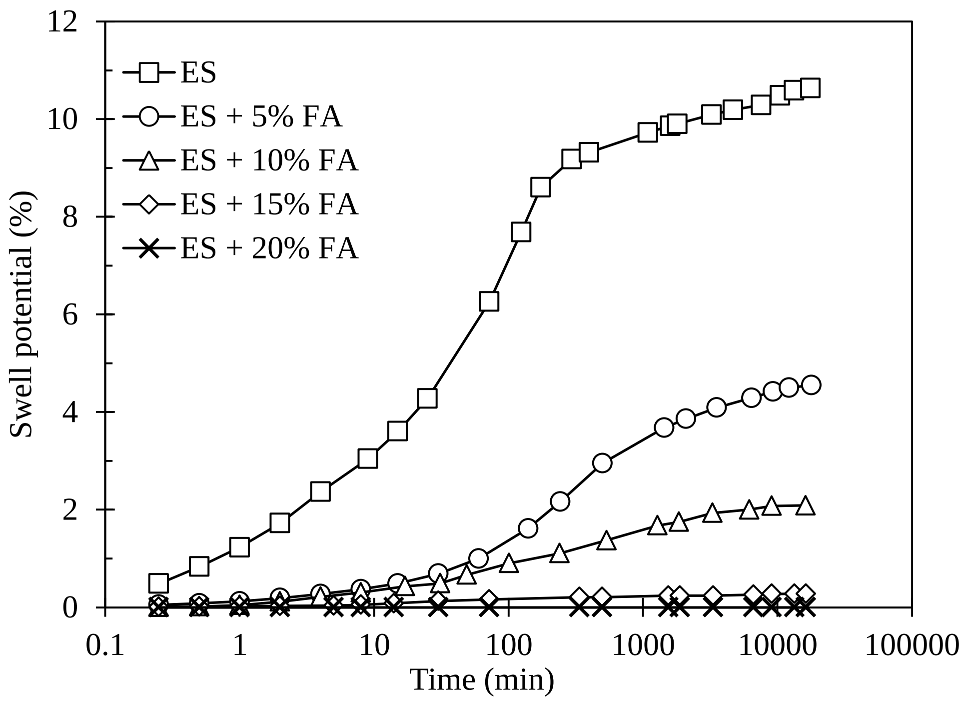

Figure 6.13: Comparison of time-swell plots of expansive soil stabilized with different percentage of fly ash

c) Unconfined compressive strength (UCS) of fly ash and lime stabilized expansive soil

Figure 6.15 brings out the effect of fly ash content on the stress-strain variation of expansive soil stabilized with fly ash. The UCS tests were conducted on 28 days cured specimens and sheared at a deformation rate of 0.625 mm/min. The UCS increased with the increase in fly ash content upto 20%. It is expected that the UCS value decreases with addition of silt size particles (fly ash) to the expansive soil, but the UCS of fly ash stabilized expansive soil increased owing to the pozzolanic reactions between the fly ash and free lime (Sridharan *et al.* 1999). The formation of cementitious compounds has dominated the influence of non-plastic silt size particles on the UCS value.

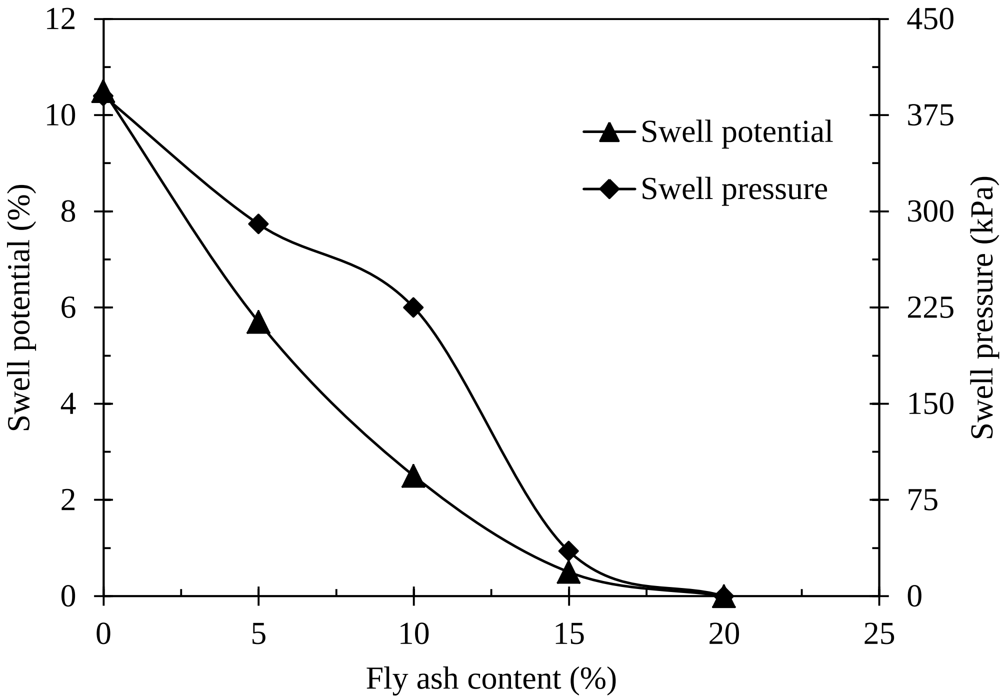

Figure 6.14: Reduction in swell potential and swell pressure of expansive soil with increase in fly ash content

Figure 6.16 brings out the combined effect of fly ash and lime on the stress-strain variation of fly ash and lime stabilized expansive soil. Expansive soil stabilized with optimum lime content of 4% lime showed an increase in UCS value of 970 kPa, and addition of 20% fly ash further increased the UCS to 1600 kPa. The UCS test was also conducted on compacted fly ash specimens at the respective optimum moisture content to maximum dry density, the UCS was found to be 3030 kPa. This is attributed to the higher percentage of CaO (35%) in the fly ash.

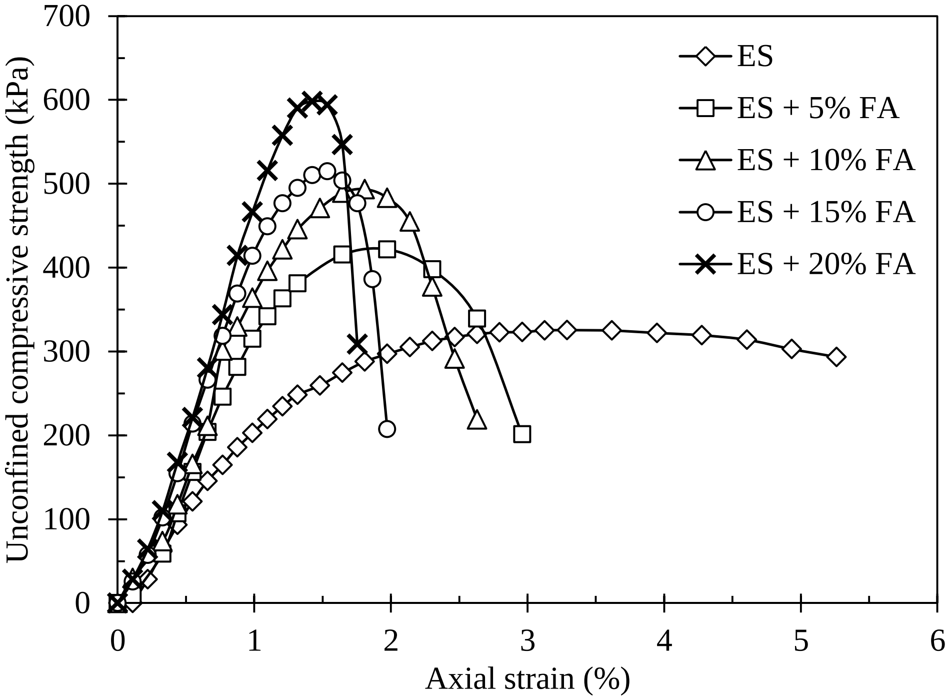

Figure 6.15: Variation in UCS value of expansive soil stabilized with different percentage of fly ash content

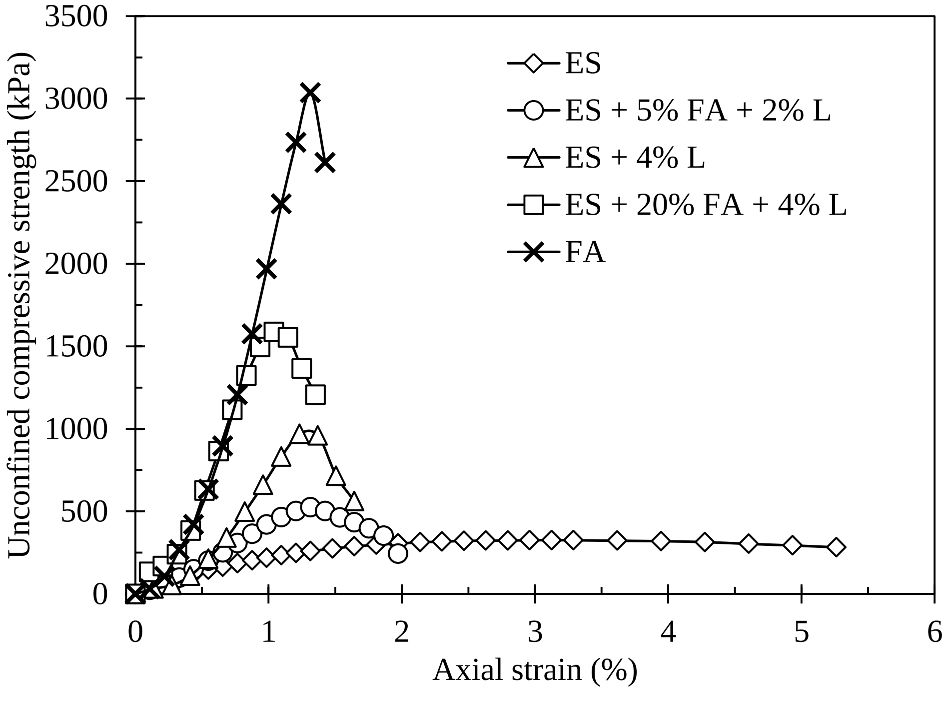

Figure 6.16: Unconfined compressive strength of fly ash and lime stabilized expansive soil cured for 28 days

Effect of wet-dry cycles on stabilized expansive soils

Figures 6.17 to 6.20 (a-d) compare the variation of vertical, lateral and volumetric deformations and water content with wet-dry cycles of expansive soil and CSS materials. During the first wetting cycle, the volume change of all the CSS materials was zero percentage and beyond this wet-dry cycle the volumetric deformations increased. The increase in volumetric deformations is due to the breakage of cementitious bonds with increase in wet-dry cycles (Rao and Shivananda 2002; Guney *et al*. 2005; Kattab *et al.* 2007). Further with increase in wet-dry cycles the water content of the stabilized soil (CSS) also increased, as shown in Figures 6.17(d) - 6.20 (d). Among the four different CSS materials tested, the CSS-4 performed better as the volumetric deformation (2.05%) was lower in comparison to the volumetric deformations of other materials (14.5%, 19.7%, and 27.6%). Hence, the CSS material prepared by blending expansive soil with 20% fly ash and 4% lime could be used a compensating material over expansive soil for long term performance. Figure 6.21 compares the desiccation cracks developed in expansive soil and fly ash and lime stabilized expansive soil subject to three wet-dry cycles. It is evident that the desiccation cracks decreased with the treatment and the fly ash and lime was found to be very effective in controlling the desiccation cracks.

6.3.2 Stabilization of Expansive Soil Using Sand as Cushion Material

The expansive soil stabilized with sand is discussed as a separate section because the nature and placement conditions are different when compared with other compensating materials like NSS, CNS and CSS.

Figure 6.22 compares the time-swell plots of expansive soil and expansive soil stabilized with sand. As can be seen in the Figure 6.22 during the initial period of inundation, slight collapse of sand was observed, and once the water reached the expansive soil, the swelling of expansive soil dominated the collapse of the sand. The decrease in the placement relative density of sand decreased the overall volume change of underlying expansive soil during inundation.

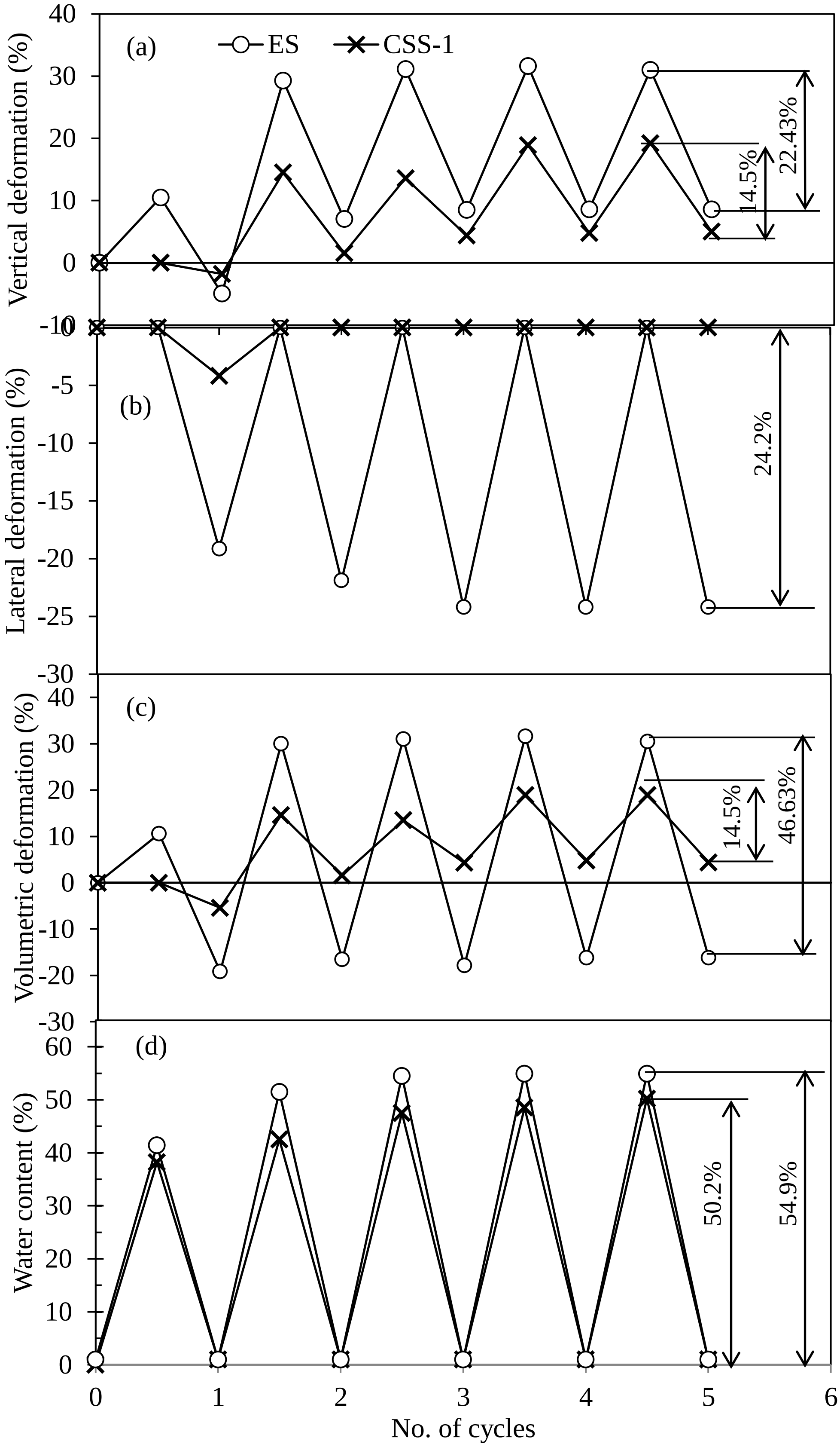

Figure 6.17: Comparison of variation of: a) vertical b) lateral and c) volumetric deformations and d) water content with wet-dry cycles of expansive soil and CSS-1 (ES + 20% FA) material

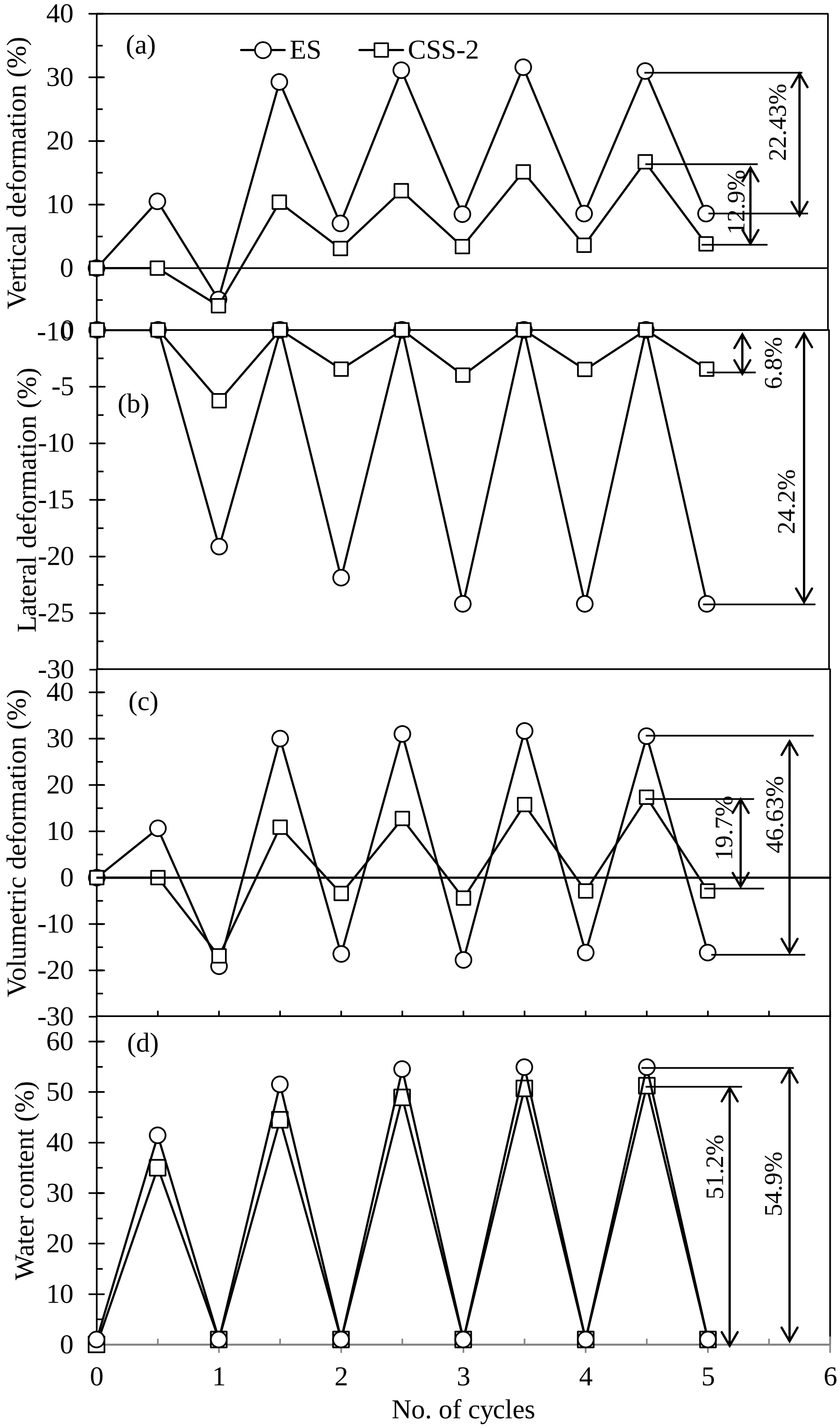

Figure 6.18: Comparison of variation of: a) vertical b) lateral and c) volumetric deformations and d) water content with wet-dry cycles of expansive soil and CSS-2 (ES + 4% L) material

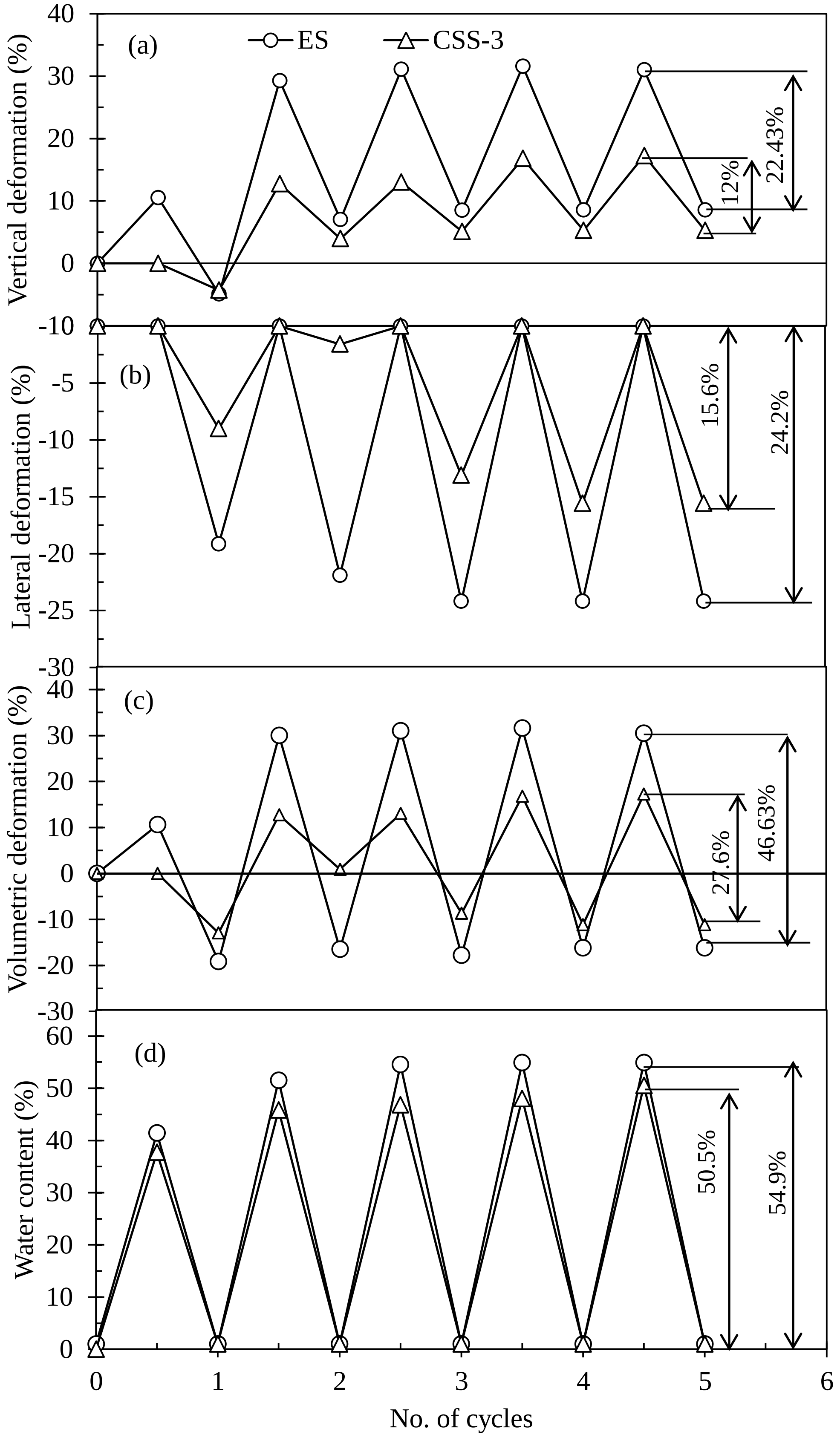

Figure 6.19: Comparison of variation of: a) vertical b) lateral and c) volumetric deformations and d) water content with wet-dry cycles of expansive soil and CSS-3 (ES + 5% FA + 2% L) material

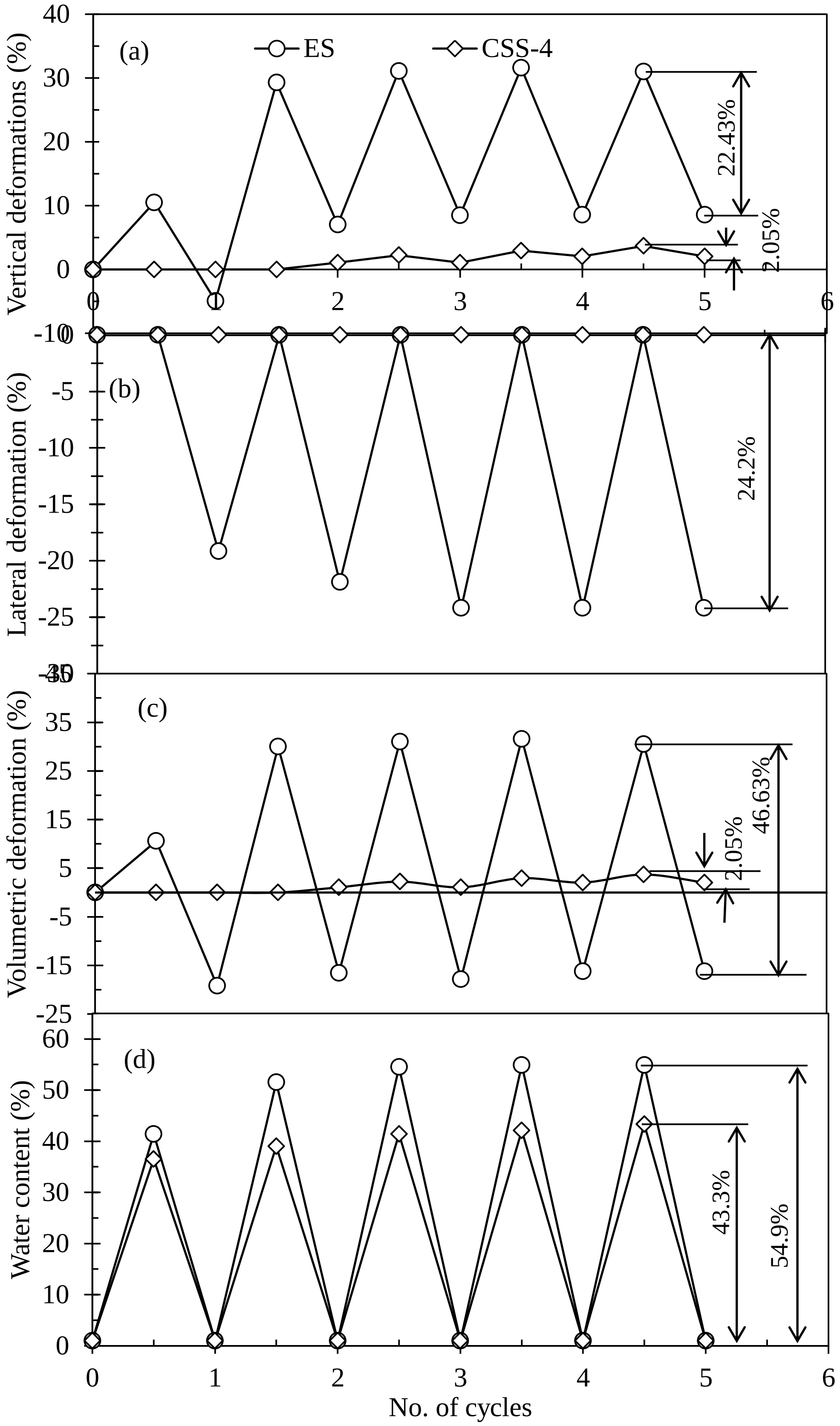

Figure 6.20: Comparison of variation of: a) vertical b) lateral and c) volumetric deformations and d) water content with wet-dry cycles of expansive soil and CSS-4 (ES + 20% FA + 4% L) material

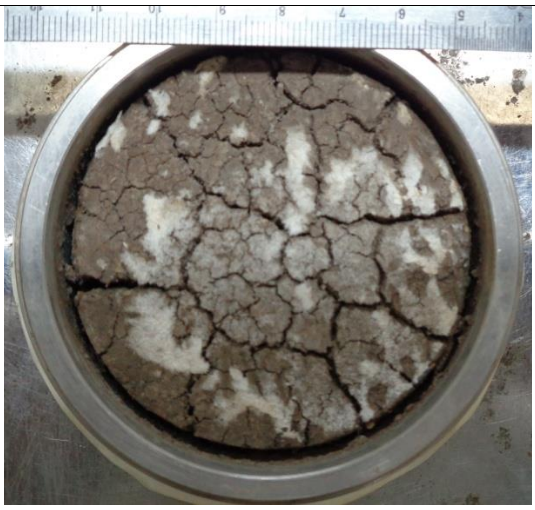	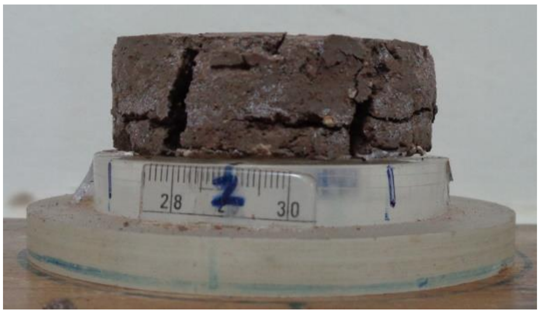
a) Surface cracks of expansive soil after three wet-dry cycles	b) Vertical cracks of expansive soil after three wet-dry cycles
	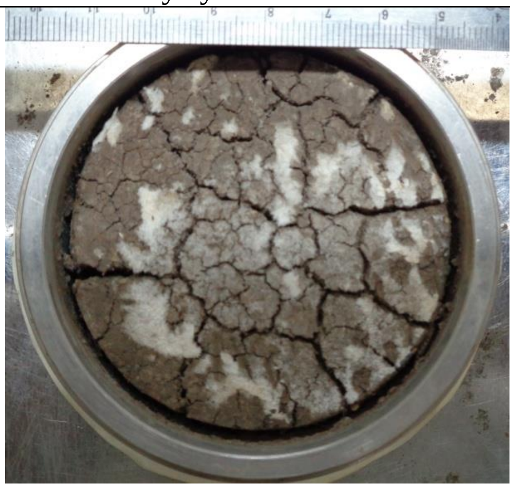
c) 20% fly ash stabilized expansive soil after three wet-dry cycles	d) 4% lime stabilized expanisve soil after three wet-dry cycles
	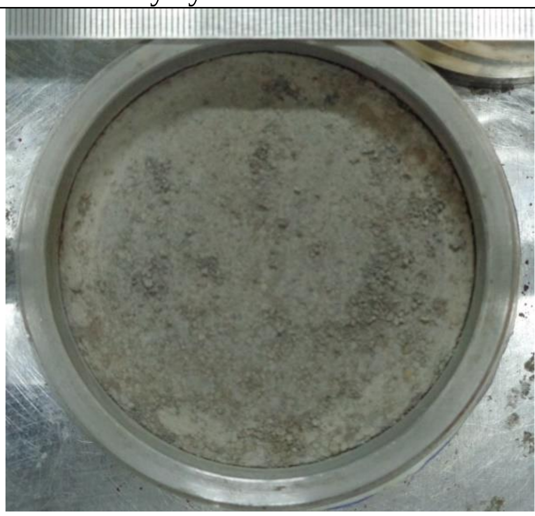
e) 5% FA+2% lime stabilized expansive soil after three wet-dry cycles	f) 20% FA + 4% lime stabilized expansive soil after three wet-dry cycles

Figure 6.21: (a,b) Images of surface and vertical cracks of ES subjected three wet-dry cycles, (c-f) Images of fly ash and lime stabilized expansive soil subjected to three wet-dry cycles

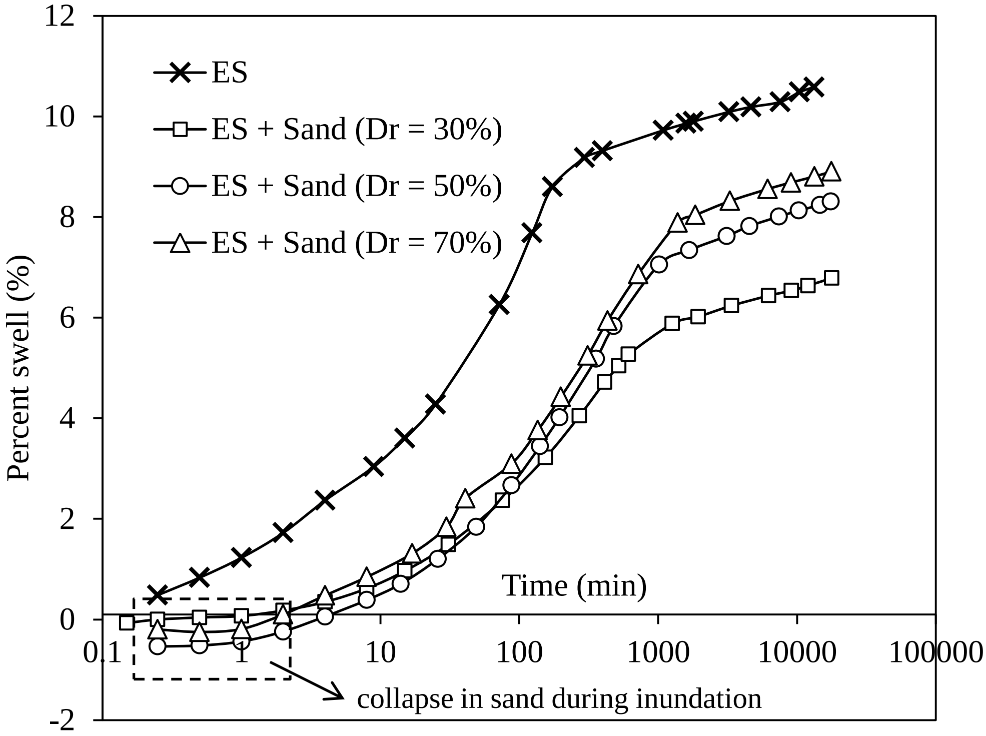

Figure 6.22: Time-swell plots of expansive soil stabilized with sand placed at different relative densities (TR = 1.0)

Earlier studies (Satyanarayana, 1969; Moussa *et al*. 1985) reported that the volume change control was due to the change in thickness of sand and loss of adhesion between the clayey particles. In the present study also, it was observed that the sand undergoes a sudden change in thickness when it is subjected to initial top saturation. However, to confirm that the swelling was controlled only due to the change in thickness of sand, additional tests were performed. An impervious plastic sheet of 1 mm thick was inserted between the expansive soil and sand to separate them. Figure 6.23 compares the sand stabilized expansive soil with and without placement of impervious sheet between sand and expansive soil. Due to the placement of impervious sheet, initially the sand collapsed and then the swell occurred with time.

Further, from Figure 6.23, it can be seen that the thickness reduction of sand during the inundation period was mostly responsible for the swell control. However, for the field applications, the placement of 1 to 1.5 m thick sand layer imposes significant overburden stress over the expansive soil. Further, comparing the swelling curve with and without plastic sheet reveals that the placement of the impervious sheet between sand and expansive soil delayed the initiation of the swelling process (Figure 6.23). Therefore, the placement of the impervious layer over the expansive soil postpones the time of initiation of swelling during inundation.

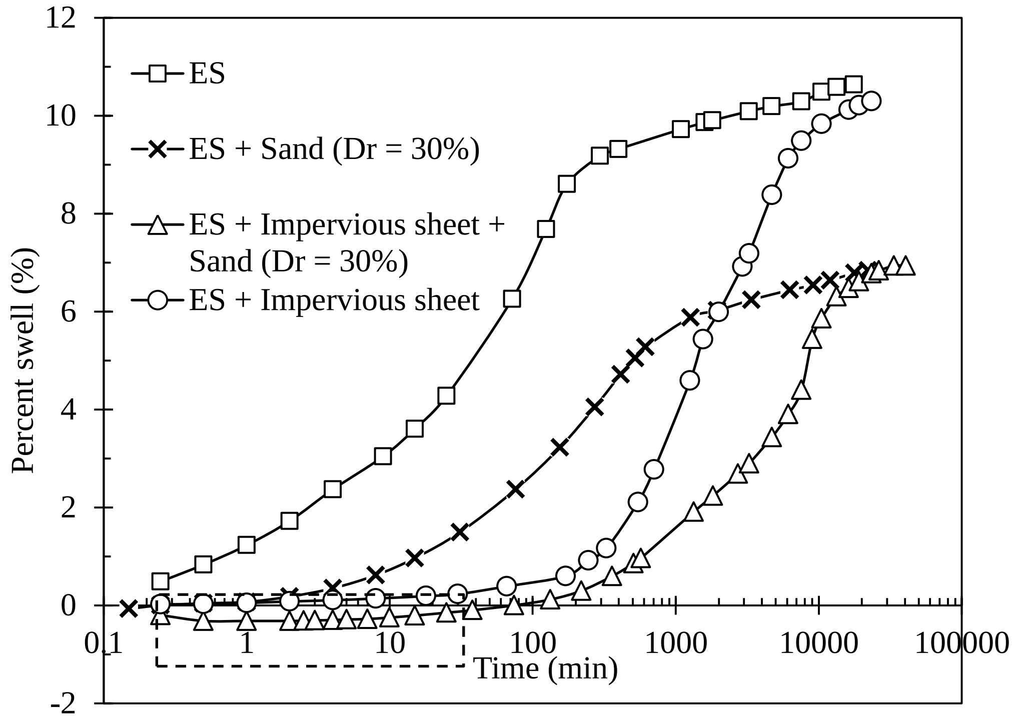

Figure 6.23: Time-swell variation of sand stabilized expansive soil with and without provision of impervious sheet

6.3.3 Stabilization of Expansive Soil Using CNS/ NSS/ CSS as a Cushion Material

This section presents the results of experiments carried out on CNS stabilized expansive soil. The tests results of NSS and CSS stabilized expansive soil are also presented for comparison. The compaction placement conditions (dry density and water content) of CSS material were already discussed in Section 6.3.1.

As observed by many researchers, the provision of CNS layer over the expansive soil has reduced the swelling capacity by 33 to 60% for the thickness ratios of 0.5 to 1.5 where CNS layer is compacted to standard Proctor placement condition, as shown in Figure 6.24. The presence of CNS material, led to a time lag in initial swelling with top saturation, and the time lag increased with increase in thickness ratio and for the thickness ratio of 1.5 for which, the time lag was found to be 2 hours. The initial time lag is mainly due to the change in the method of inundation i.e. top saturation. As explained in the methodology section, the specimen was initially saturated from the top, and once the specimen swells, the bottom valve which was connected to the burette was opened for bottom saturation as well.

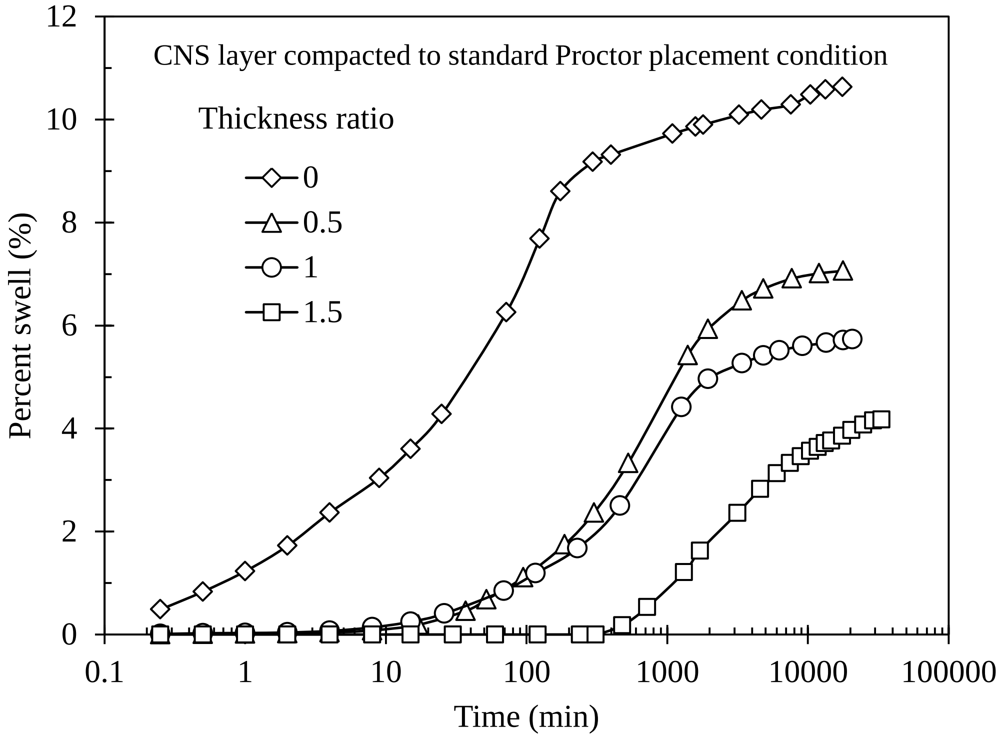

Figure 6.24: Effect of thickness ratio of CNS and expansive soil on time-swell plots of expansive soil stabilized with CNS layer compacted to standard Proctor placement condition

Figure 6.25 brings out the effect of thickness ratio on time-swell behaviour of CNS stabilized expansive soil when the CNS was compacted to modified Proctor placement condition. The swell reduction was more when the CNS was compacted to modified Proctor placement condition compared to standard Proctor placement condition. Even if the CNS stabilized soil specimen is inundated under two-way drainage conditions from the initial stage, the initial swell occurs mainly due to the bottom saturation as it takes some time for the water to reach the expansive soil from the top. However, when the specimen was allowed to saturate only from the top, the swell starts after 20 to 30 mins due to the supply of water through the side wall leakage and not through the CNS material as this test is carried out in rigid wall permeameter. Hence, during the top saturation, if the sidewall leakage is prevented, it may take more time for inundating water to reach the expansive soil from top, and this condition will simulate only the bottom saturation condition (one-way saturation). Moreover, the time lag in swell activation during the top saturation is mostly governed by the hydraulic properties of the compensating material. Nelson *et al.* (2015) reported that when the specimen is bottom saturated, the swell magnitude is higher, and it requires more time to reach the equilibrium condition when compared to the time required in the conventional method of inundation. From the above discussion, it is clear that in case of top saturation, the hydraulic conductivity of the compensating material governs the time-swell behaviour. The hydraulic properties of the compacted CNS and NSS materials are discussed in Section 6.3.6.

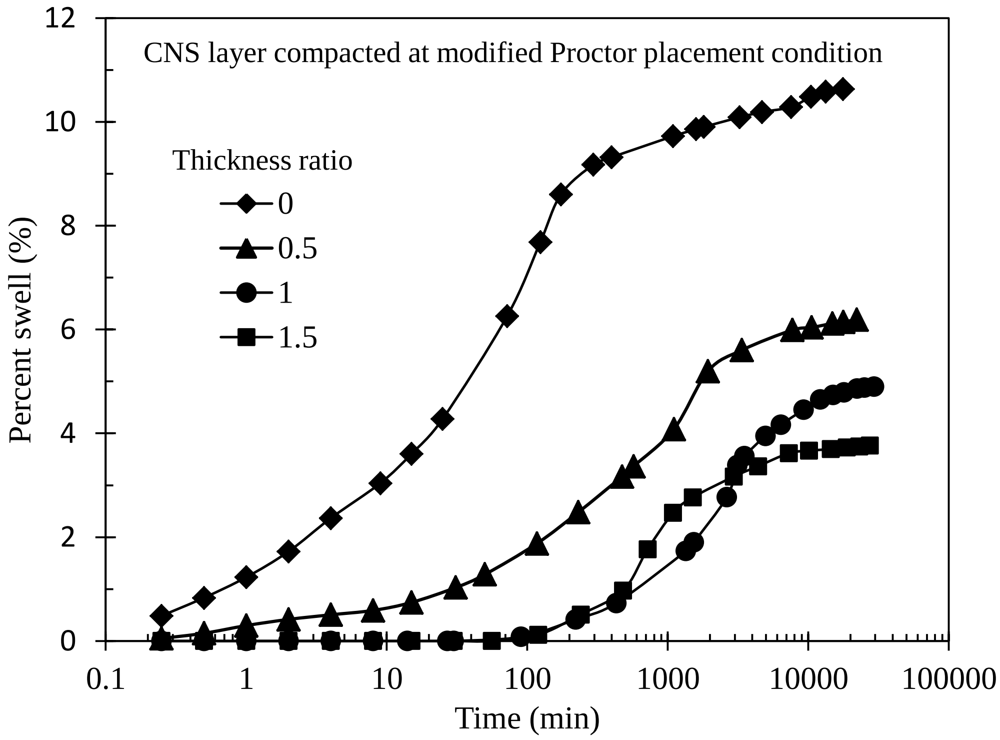

Figure 6.25: Effect of thickness ratio of CNS and expansive soil on time-swell plots of expansive soil stabilized with CNS layer compacted to modified Proctor placement condition

Figure 6.26 compares the time-swell plots of expansive soil and sand, non-swelling soil and CNS stabilized expansive soil. It is clear from Figure 6.20 that the placement of non-swelling soil (NSS) over the expansive soil reduced the swell magnitude and the reduction is slightly greater than the swell of CNS stabilized expansive soil. This finding is in line with the findings of Rao (2000). Further, Rao (2000) reported that the specifications of CNS material proposed by Katti (1978) might not be the ideal material for swell control. He also showed that the compensating materials with more percentage of clay fractions performed better than the CNS material proposed by Katti (1978).

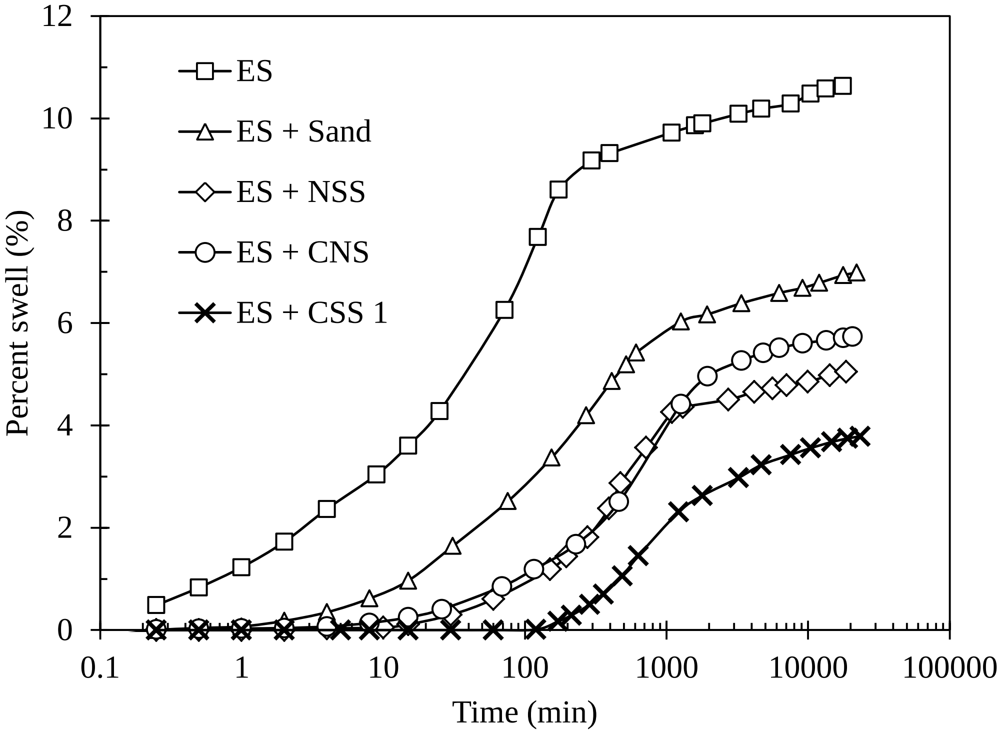

Figure 6.26: Time-swell plots of expansive soil stabilized with different compensating materials with thickness ratio of 1.0

Both CNS and NSS stabilization of expansive soil reduced the volume change of underlying expansive soil significantly. However, there is possibility that the side wall friction between CNS/ NSS and the oedometer ring might contribute to the reduction in swell. Hence, an experimental study was carried out to check the possible development of side wall friction in the CNS/ NSS stabilized soil. Different methods were tried to reduce the sidewall friction, and the results obtained using different methods are presented in Figure 6.27. In method 1, the CNS and expansive soil were compacted directly in the ring (CNS was compacted directly over the expansive soil), and no additional effort was made to minimise the friction (application of sufficient amount of silicon grease is applicable in all testing methods).

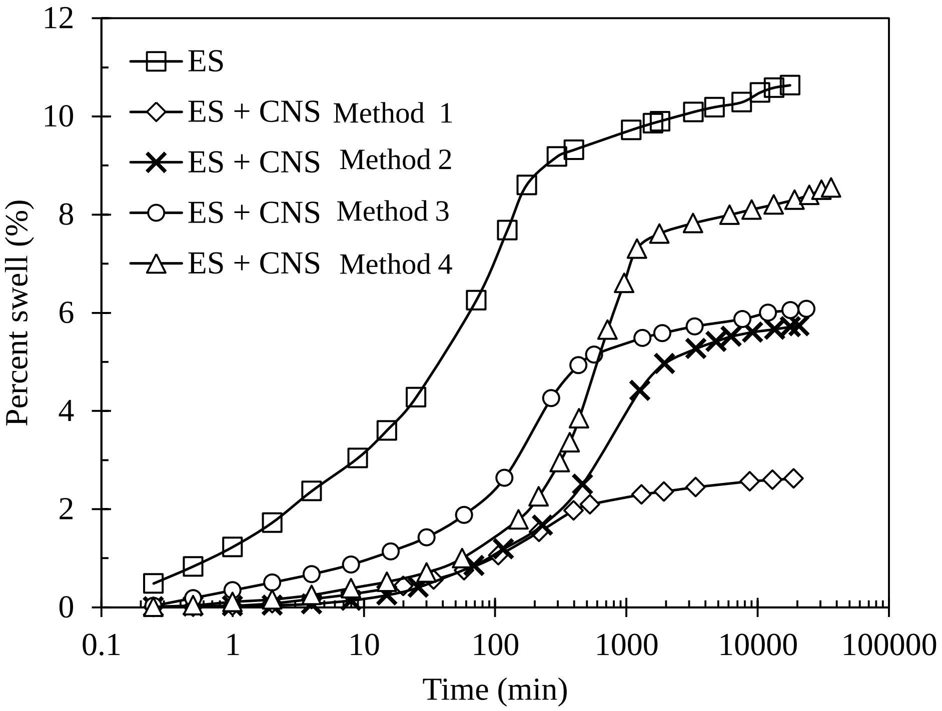

Figure 6.27: Effect of side wall friction in swell reduction of CNS stabilized expansive soil (TR =1.0)

In method 2, the oedometer ring was placed in reverse direction, the CNS layer was first compacted in the ring and over that expansive soil was compacted and then the ring was reversed and fixed in the cell. Further, in Method-3, to minimise the sidewall friction, after compacting both CNS and ES in the ring (as followed in method 2), the CNS and expansive soil were moved up and down inside the ring. A small increase in the swell was observed as a result of the movement of soil layers within the ring (Figure 6.27) was noticed. However, the swell measured from methods 2 and 3 showed a significant variation from the method 1. At the same time methods 2 and 3 did not showed much difference and the movement of soil layers within the ring leads to earlier initiation of swell (no time lag in swell activation) during inundation. The procedure adopted in method 4 is shown in Figure 6.28 to minimise the sidewall friction during the swelling process. The expansive soil was compacted in a 75.1 mm diameter ring, and over that 71 mm diameter compacted CNS was placed as shown in Figure 6.28 (b). The annular gap between the ring and soil was filled with fine sand at very loose condition to minimise the wall friction and to minimise the direct exposure of expansive soil to the inundation of water (Figure 6.28 (c)). The thickness ratio of 1.0 was used. The swell plot of expansive soil-CNS system with fine sand in the annular gap to minimise the sidewall friction and that provide easy access to water, and thus the measured swell using method 4 was higher when compared to other conditions (methods 1, 2 and 3).

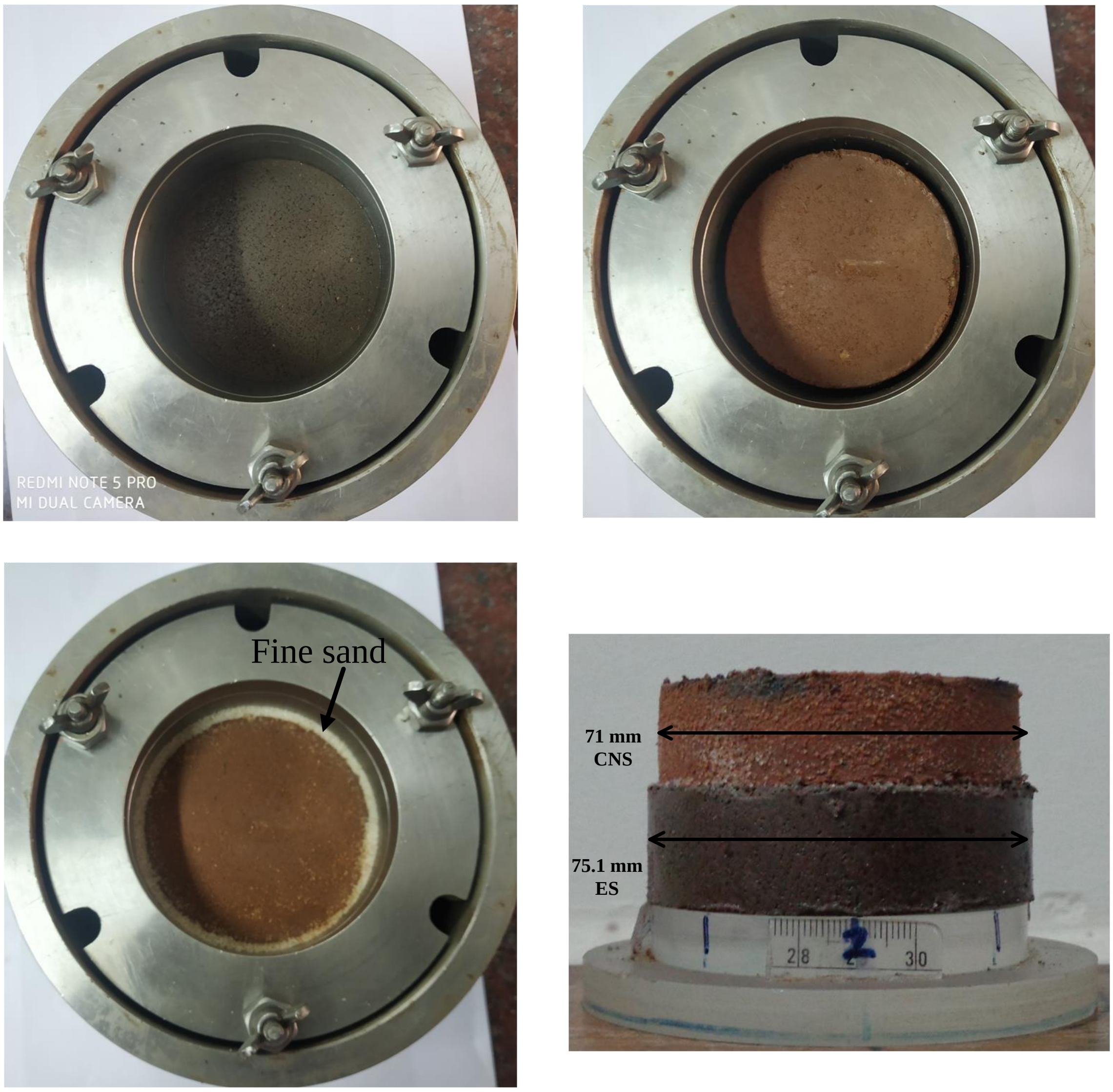

Figure 6.28: Specimen preparation and testing procedure to minimise the sidewall friction in two layer soil system: a) compacted expansive soil in ring b) placement of compacted CNS material over expansive soil c) filling of the annular gap with fine sand d) CNS and expansive soil after swelling

The swell reduction corresponding to method 1 is 75%, method 2 is 46%, method 3 is 42% and method 4 is 18%. Therefore, in the two-layer soil system, the effect of sidewall friction on swelling should be considered in the testing procedure. Further, the resistance to swelling due to sidewall friction increases with increase in the dimensions of the testing tank.

As reported in the literature, the CSS material is more effective than the natural compensating material (Katti, 1978; Murty and Praveen, 2007; Rao *et al*., 2008). In the current study also it was also observed that the CSS stabilized expansive soil showed better performance than the sand/ NSS/ CNS stabilized expansive soil. Table 6.4 presents the percent swell of sand, NSS, CNS and CSS treated expansive soil. It is further supported using the final water content of expansive soil stabilized using sand, CNS, NSS and CSS, which clearly shows that the water content of CSS stabilized expansive soil is lower than the water content of sand stabilized expansive soil.

Table 6.4 Percent swell values of sand, NSS, CNS and CSS stabilized expansive soil at the thickness ratio of 1.0

Type of compensating soil (TR = 1.0)	Percent swell (%)	Final water content of expansive soil (%)
ES	10.5	40.50
ES + Sand (D_r = 30%)	7.05	39.50
ES + NSS-1	5.05	38.50
ES + CNS	5.75	37.10
ES + CSS-1 (20% FA)	4.50	37.80
ES + CSS-2 (4% L)	4.0	36.90
ES + CSS-3(5% FA+ 2% L)	4.0	37.10
ES + CSS-4 (20% FA+4% L)	3.7	36.10

Note: FA: fly ash; L: lime

6.3.4 Effect of Surcharge Pressure on the Moisture Content Variation of CNS Stabilized Expansive Soil

The placement of compensating materials over the expansive soil also imposes a certain amount of surcharge pressure over the expansive soil. To study this effect, the volume change of expansive soil was measured under different surcharge pressures, and a similar study was also conducted on the CNS stabilized expansive soil with a thickness ratio of 1.0. Figures 6.29 and 6.30 plot the variation in the percent swell of expansive soil and CNS stabilized expansive soil under different surcharge pressure. Table 6.5 presents the final water content variation in expansive soil due to the presence of CNS material. For expansive soil, the final water content varies from 42% to 36.1% for the surcharge pressure of 6.25 kPa to 100 kPa. Whereas, for CNS stabilized expansive soil, the water contents ranged from 40.6 to 33.7% for the same surcharge pressures. The reduction in water content of CNS stabilized expansive soil is due to the additional stress or confinement resulting from frictional resistance offered by the overlying CNS material. Further, the magnitude of side wall frictional stress increases with the increase in vertical stress. The effect of side wall friction was already discussed in the previous section.

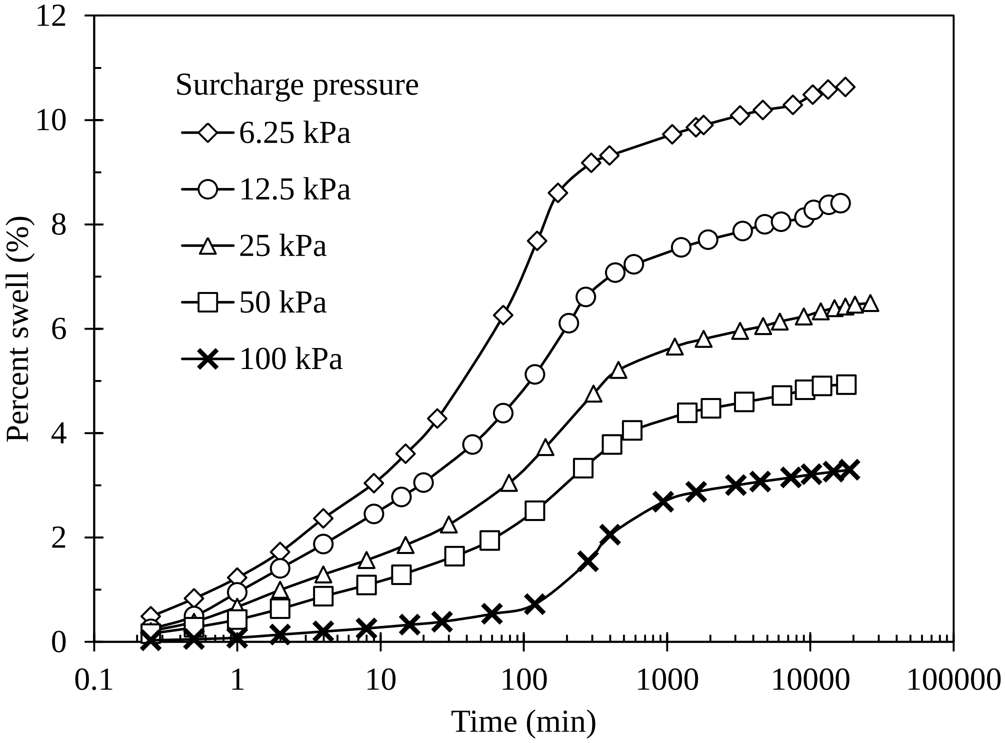

Figure 6.29: Effect of surcharge pressure on time-swell plots of expansive soil

In the earlier literature, the effect of sidewall friction in measurement of swelling in the two-layer soil system was not explored in detail. From Figure 6.29, it is clear that with an increase in surcharge pressure, the percentage swell and final water content decreased (Table 6.5).

The placement of 1 to 1.5 m thick compacted granular soil (GC or SC) in the field can impose a vertical stress of 20 to 25 kPa as the seating pressure. This stress contributes a significant resistance to the uplift during saturation in case of low to medium swelling soils. Chen (1988) reported that most of the isolated foundation system could impose stress of 50 kPa on the soil. However, this surcharge pressure is not sufficient to control the uplift pressures in high swelling soils with swelling pressures of the order of 250-400 kPa.

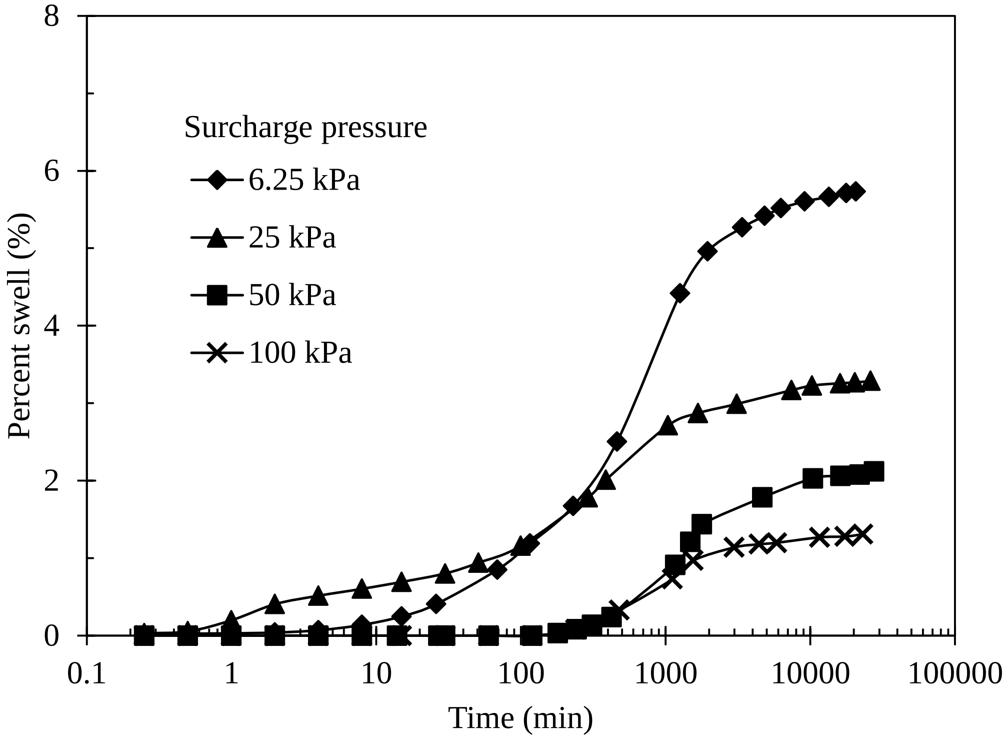

Figure 6.30: Effect of surcharge pressure on time-swell plots of CNS stabilized expansive soil

Table 6.5 Percent swell and water content variation of CNS stabilized expansive under different surcharge pressures

Surcharge pressure (kPa)	Percentage swell (%)		Final water content (%)	
	ES	ES+CNS	ES	ES+CNS
6.25	10.50	6.0	42.0	40.6
12.5	8.40	-	40.50	-
25	6.49	4.32	39.14	37.10
50	4.93	2.11	37.90	35.79
100	3.29	1.30	36.10	33.74

6.3.5 Swell Pressure of NSS, CNS and CSS Stabilized Expansive Soil

The relative efficiency of NSS, CNS and CSS in controlling the swell pressure of expansive soil using swell-consolidation and constant volume methods are explained in this section.

Figure 6.31 brings out the effect of thickness ratio on swell pressure measurement of CNS stabilized expansive soil, in which the CNS was compacted to modified Proctor placement condition using swell-consolidation method. It is evident from Figure 6.31 that the percent swell of CNS stabilized soil decreases with increase in thickness ratio, whereas the swell pressure increases with increase in thickness ratio. The swell pressure of expansive soil increased from 390 to 500 kPa in case CNS stabilized expansive soil with a thickness ratio of 1.5 (Figure 6.31). The increase in the swell pressure is due to the sidewall friction, which offers more resistance during both swelling and consolidation stages. The existence of side wall friction in the two-layer soil system was already discussed in the above section. Further, the results were also analysed by considering the factors like compressibility of apparatus, filter papers and porous stone as suggested by Fredlund (1969).

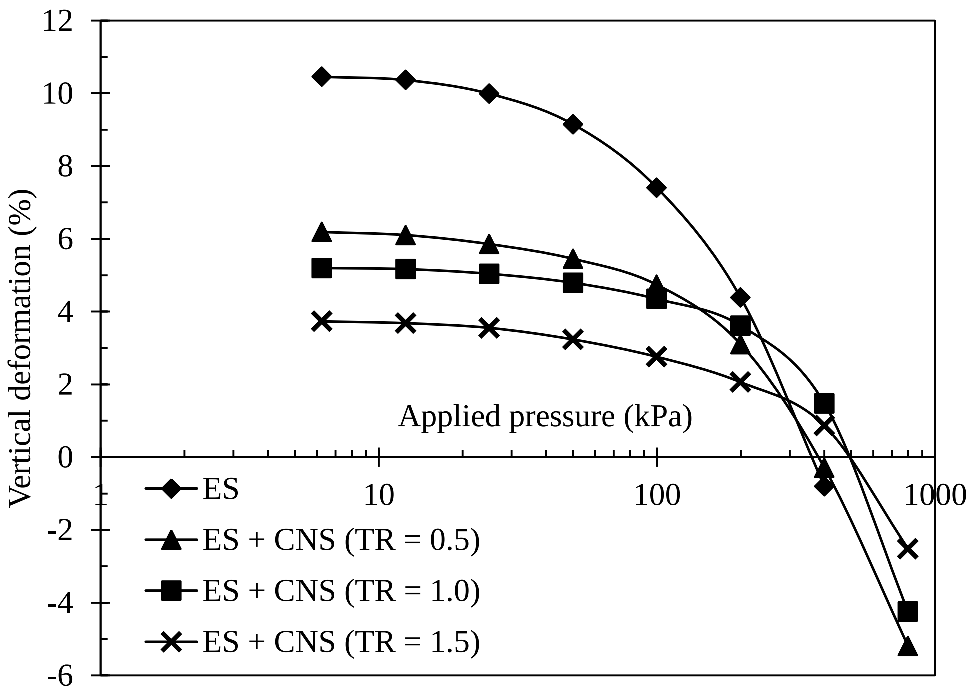

Figure 6.31: Effect of thickness ratio on swell pressure of CNS stabilized expansive soil using swell-consolidation method (CNS: compacted to modified Proctor placement condition)

Hence to minimise the error due to side wall friction, the swell pressure was determined using a constant volume (CV) method. Most of the literature on the compensating materials were based on the swell pressure measurement using the CV method (Katti, 1978; Moussa *et al*. 1985; Murty and Praveen, 2008). Moreover, it is difficult to perform the swell-consolidation test in large tanks. Figure 6.32 brings out the effect of thickness ratio on the swell pressure measured using CV method. With increase in thickness ratio, the swell pressure of CNS stabilized expansive soil decreased. The reduction in swell pressure is due to the compressibility of compensating material and possible volume change of expansive soil.

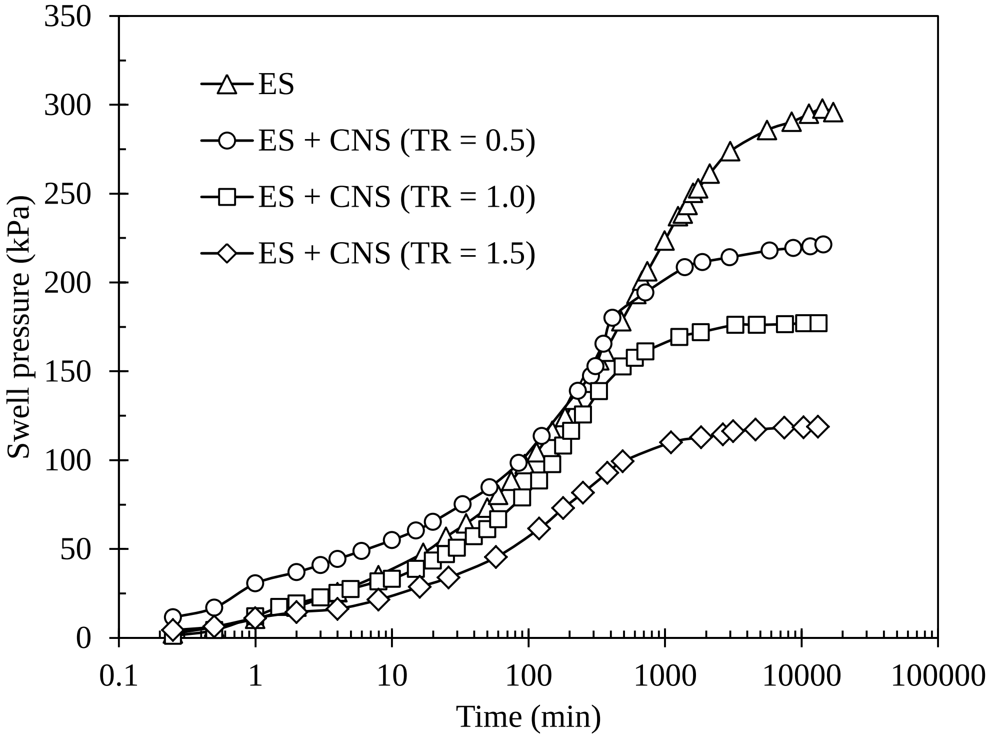

Figure 6.32: Effect of thickness ratio on swell pressure of CNS stabilized expansive soil (CNS compacted to standard Proctor placement condition) using constant volume method

In constant volume method, the specimen was not allowed to undergo volume change throughout the test because even a small amount of volume change (even 0.1 mm) during the test may reduce the swell pressure drastically (Singhal *et al*. 2011). Some experiments were also performed to minimise the randomness in the swell pressure measurement using constant volume method (Pejon and Zuquette, 2006). During the swell pressure measurement in expansive soil, the initial compacted thickness could be maintained, and it can be justified using a dial gauge, but while testing the layered soil it is not possible to maintain the initial thickness of expansive soil. Figure 6.33 (c) shows the possible change in the thickness of expansive soil and compensating material in constant volume method. The compensating material undergo compression because the bottom expansive soil exerts uplift pressure and top movement of compensating material was restricted by the load cell. And this might be the reason for more reduction in swell pressure for NSS-1 stabilized expansive soil, where NSS-1 showed more compressibility among the three compensating materials used in the study. The change in thickness or volume change of the expansive soil could be observed by determining the final water content of CNS and NSS stabilized expansive soils. The stabilized expansive soil specimens which has swollen showed an increase in final water content as shown in Figure 6.34. The swell pressure and final water content of stabilized expansive soil are summarised in Table 6.6. The CSS materials are generally less compressible, but still the CSS stabilized expansive soil showed more reduction in swell pressure, and this might be due to possible leaching of lime from the CSS material to the expansive soil.

The compressibility of compensating material and swelling of expansive soil is a simultaneous process in constant volume method. However, the same process may not happen in the field condition i.e. the compression in the compensating material might be over before the swelling starts. Hence, the constant volume method may not be an appropriate method for measuring the swell pressure of two-layer soil systems. Therefore, the placement of compensating material over the expansive soil may not affect the swell pressure where the specimens were inundated from both top and bottom. However, in case where the infiltration occurs only from top, the CNS and NSS reduces both swell potential and swell pressure owing to the restricted water supply to expansive soil.

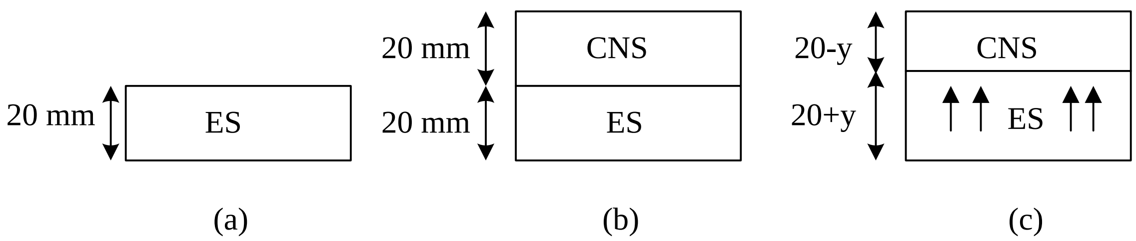

Figure 6.33: Schematic representation of possible volume change of expansive soil using constant volume method: a) expansive soil alone b) CNS stabilized expansive soil before inundation and c) CNS stabilized expansive soil after inundation

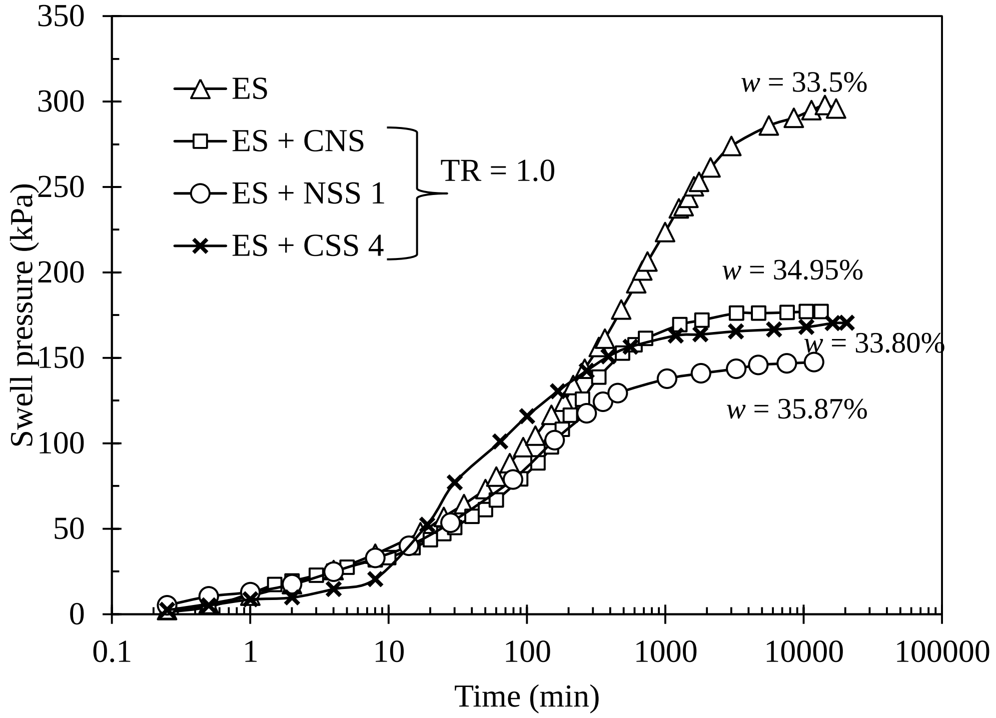

Figure 6.34: Comparison of time-swell pressure plots of expansive soil and stabilized expansive soil with CNS, NSS-1 and CSS 4

Table 6.6 Comparison of swell pressure and final water content of sand/ CNS/ NSS stabilized expansive soil

Type of compensating material	Swell pressure (kPa)	Final water content of ES (%)	% reduction in swell pressure
ES	295	33.5	-
ES + CNS (TR = 0.5)	231	35.5	21.5
ES + CNS (TR = 1.0)(ρ_d =1.98 Mg/m^3)	177	34.95	40.0
ES + CNS (TR = 1.5)	119	34.56	59.0
ES + CNS (TR = 1.0)(ρ_d =1.88 Mg/m^3)	159	36.30	46.0
ES + NSS-1(TR = 1.0)	147	35.87	50.0
ES + CSS-1(TR = 1.0)	185	34.05	37
ES + CSS-2(TR = 1.0)	182	33.50	38
ES + CSS -3(TR = 1.0)	183	34.10	38
ES + CSS-4(TR = 1.0)	170	33.80	42

6.3.6 Permeability Characteristics of Compensating Material

In the soil deposits where the expansive soils are found at the surface, inundation of water leads to water absorption and the expansive soil themselves act as a water barrier for the underlying expansive soil (Bowles, 2012). Hence the hydraulic conductivity of the compensating materials is an essential governing factor which has to be given due consideration before placing them over the expansive soils. However, in most of the works, the hydraulic property of compensating material (GC or SC) was not given due consideration in the design. Chen (1975), Nelson and Miller (1992) and Bharadwaj (2013) have highlighted that the higher hydraulic conductivity of the compensating materials leads to easy access of water to the underlying expansive soils. In general, materials like, gravel, sand and quarry dust are characterized with higher hydraulic conductivity and may act as water reservoirs over the expansive soils. Further, the guidelines regarding the selection of a range of hydraulic conductivity for the compensating materials are not available. Therefore, an attempt is made to study the hydraulic characteristics of compensating materials in order to understand the mechanism of stabilization.

In the present study, the flexible wall permeameters were used for the measurement of hydraulic conductivity of compacted CNS material and non-swelling soils. In case of river sand, the rigid wall permeameter was used. Table 6.7 summarizes the measured hydraulic conductivity values of different compensating materials used in the present study. The river sand, compacted at a relative density of 30% has a hydraulic conductivity of 7.4×10^{-3} cm/s. Similarly, for non-swelling soils, it was determined as 5.5×10^{-5} cm/s and 2.0×10^{-5} cm/s for NSS-1 and NSS-2, respectively. The hydraulic conductivity of CNS material prepared as per IS 9451 specifications was 2.5×10^{-7} cm/s and 1.5×10^{-8} cm/s when compacted to standard Proctor and modified Proctor placement conditions, respectively. Therefore, it can be said that the hydraulic conductivity could be in the range of 10^{-6} to 10^{-8} cm/s for the soils meeting the specifications of IS 9451-1994. Benson *et al.* (1994) also reported that a hydraulic conductivity of $\leq 10^{-7}$ cm/s could be obtained for the soils with liquid limit of 20%, plasticity index of 7%, activity of 0.3 (min) and clay fraction of 15% (min).

Further for clay liner application, USEPA (1993) recommended that the saturated hydraulic conductivity should be less than 10^{-7} cm/s based on the limit of percolation of 30 mm/year under unit hydraulic gradient. In general, the hydraulic conductivity of 10^{-6}

cm/s is sufficient enough to simulate the poor drainage conditions in the filed under low hydraulic gradients (Terzaghi and Peck, 1967; Lambe and Whitman, 1969; Holtz *et al.* 2011). This also confirms that the hydraulic conductivity of the compensating materials is an important governing factor for their placement over the expansive soils. Therefore, based on the above discussion, if CNS is used as a compensating material, it will act as impervious layer over layer expansive soil due to its lower hydraulic conductivity. The same behaviour may not be observed if sand or non-swelling soils are used as compensating material.

Table 6.7 Hydraulic conductivity of the compensating materials used

Compensating material	Hydraulic conductivity (cm/s)
River sand (RD = 30%)	7.4×10^{-3}
Non-swelling soil-1	5.5×10^{-5}
Non-swelling soil-2	2.0×10^{-5}
Cohesive non-swelling soil (CNS)	
At standard Proctor placement condition	2.5×10^{-7}
At modified Proctor placement condition	1.7×10^{-8}
Chemically stabilized soil (CSS)	
ES + 20% FA	4.0×10^{-6}
ES +1 0% FA + 1% L	3.5×10^{-6}
ES + 5% FA + 2% L	7.7×10^{-6}
ES + 4% L	6.9×10^{-5}
ES + 20% FA + 4% L	9.0×10^{-5}

In case of fly ash and lime stabilized expansive soils, the tests were conducted on 28 days cured compacted soil specimens. Table 6.7 also presents the hydraulic conductivity of the fly ash and lime stabilized expansive soil. It is evident from Table 6.7 that the hydraulic conductivity of all the stabilized soil specimens varies form 10^{-5} to 10^{-6} cm/s. The increase in the hydraulic conductivity is mainly attributed to the decrease in the dry density of chemically stabilized soil and the increase in percentage of non-plastic soil fractions as a result of the pozzolanic reactions (Bell, 1993). The suitability of CSS is discussed further in the following section.

Evaluation of impervious nature of CNS material through swell tests

As discussed in Section 6.9.3 that the placement of CNS layer over the expansive soil resulted in a time lag of swell activation and the time lag depended on the hydraulic conductivity of the CNS material. In order to demonstrate the impervious nature of CNS material, swell test was conducted in large diameter rigid wall oedometer cell (150 mm diameter and 170 mm height). The relative imperviousness of CNS material is brought by observing the time lag of swell activation. The ratio of CNS layer thickness to expansive soil was maintained as 1.0 (50 mm ES + 50 mm CNS) under a seating pressure of 6.25 kPa for the swell tests.

Figure 6.35 compares the time-swell plots of expansive soil and expansive soil stabilized with CNS layer. The compacted expansive soil reached equilibrium swell of 8.5 % in 25 days using top saturation only. The CNS stabilization of expansive soil reduced the swell to 4.5%. As discussed earlier, the swell reduction in the laboratory condition is attributed to sidewall friction (with an increase in diameter of the ring, the frictional resistance will also increase) and partial saturation of underlying expansive soil. However, the top saturation leads to time lag of swell activation of underlying expansive soil as the inundated water has to seep through a 50 mm thick CNS material of 2.5×10^{-7} cm/s hydraulic conductivity. The lime lag of swell activation was found to be 4 hours, and thereafter it continues to swell to reach the swell equilibrium condition (Figure 6.35).

In order to prevent the possible side wall leakage, the CNS soil nearer to the wall was removed, and the annular gap created was filled with bentonite paste. Figure 6.36 shows the filling process of bentonite paste in annular gap to prevent the side wall leakage. After providing the slurry paste, the time lag has increased from 4 hrs to 72 hours, indicating the occurrence of side wall leakage prior to using the bentonite seal in the annular gap (Figure 6.35). For the given wetting period of 25-30 days, the expansive soil and CNS stabilized soil almost reached the swell equilibrium condition, but the swelling rate of stabilized soil provided with bentonite seal was slower even after 40-50 days of inundation, and this might be due to the seepage obstruction from the low infiltration rate of compacted CNS material. The final water contents of the expansive soil and CNS stabilized expansive were presented in Table 6.8. The time lag indicates the impervious nature of CNS material. From Figure 6.35, it is also evident that the hydraulic conductivity of the compensating material in the soil replacement technique is a critical governing factor for the field performance.

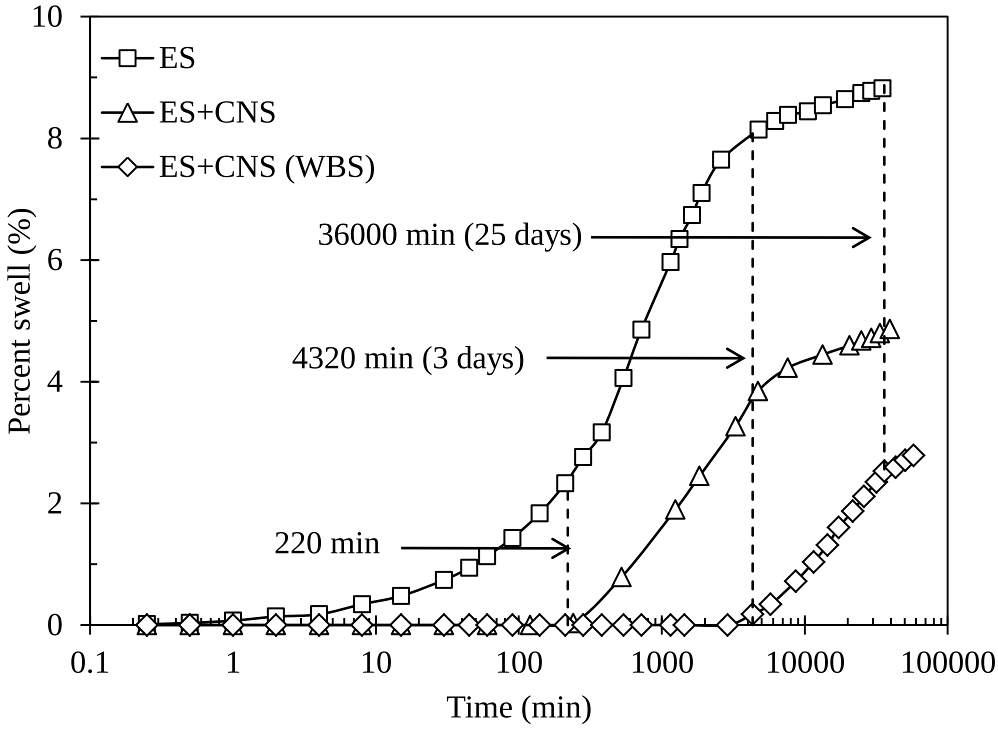

Figure 6.35: Time–swell plots of expansive soil and expansive soil stabilized with CNS depicting the time lag in swell activation using bentonite seal

6.3.7 Infiltration Characteristics of Compacted CNS Material

Infiltration tests are generally carried out to study the migration of water through the compacted material. In applications like landfill construction, these tests were performed to finalise the material for the liner or cover applications i.e. the placement material should act as a moisture barrier such that it controls the migration of leachate into the natural ground. In similar way, the present study aims at studying the infiltration characteristics of compacted CNS and NSS materials.

a) Infiltration tests on compacted CNS material

Figure 6.37 presents the variation of the inflow and outflow infiltration rates and swell with time for CNS material. From Figure 6.37, it is observed that the initial inflow was rapid due to the absorption of water by the dry porous stone placed over the compacted CNS material. Then the inflow rate reduces gradually due to the impervious nature (k = 2.5 x 10^{-7} cm/s) of high-density CNS material. The outflow volume occurred after two days but the inflow and outflow volumes were not the same. The test was further continued till the inflow and outflow volumes reached a steady state which is reported as steady-state infiltration rate. The outflow occurred after 6 days when the CNS was compacted to modified Proctor placement condition (k = 1.7 x10^{-8} cm/s) (Figure 6.38). The test was continued till the steady state condition was established (Figure 6.38). The infiltration rate of compacted CNS material was found to be 6 x 10^{-7} and 2.0 x 10^{-7} cm/s at standard and modified Proctor placement conditions, respectively. The other compensating material NNS-2 showed an infiltration rate of 2.0 x 10^{-6} cm/s under the same hydraulic gradient of 2.0 (i = 2) as shown in Figure 6.39.

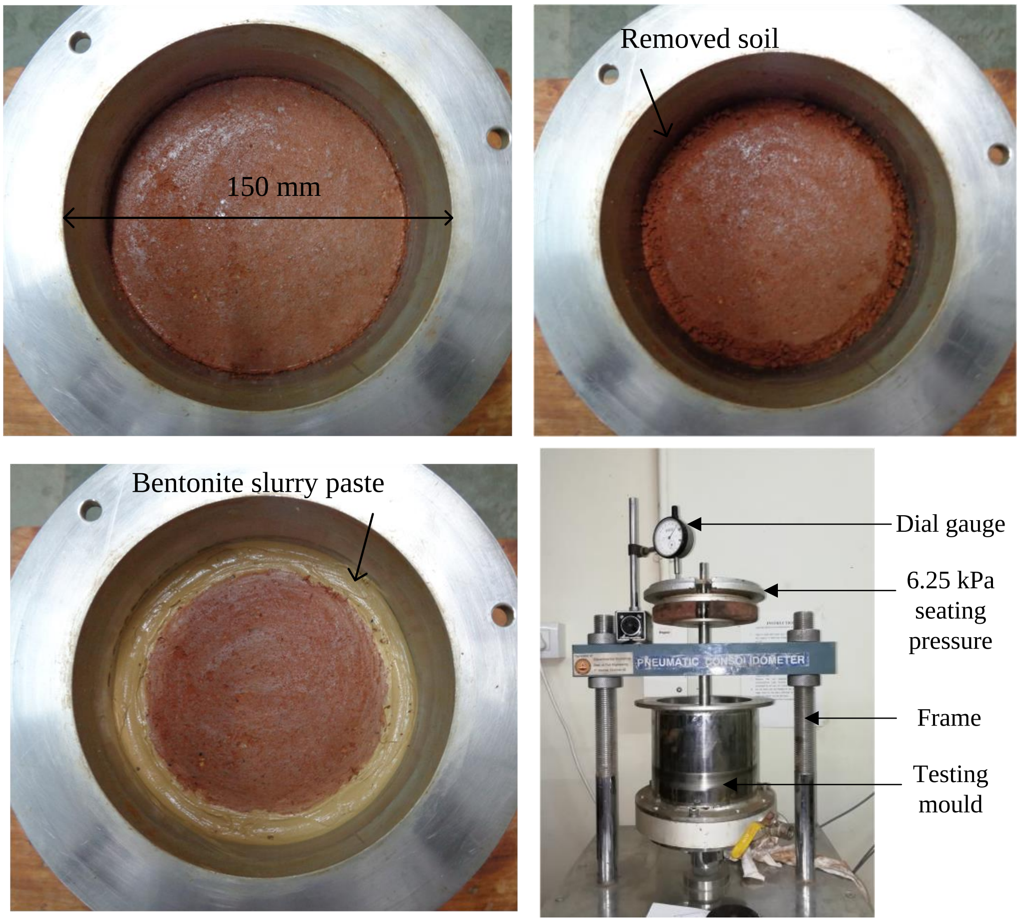

Figure 6.36: (a-c) Pictorial depiction of bentonite seal in the annular gap to prevent the side wall leakage from top saturation and d) swell measurement in large diameter mould (150 mm diameter)

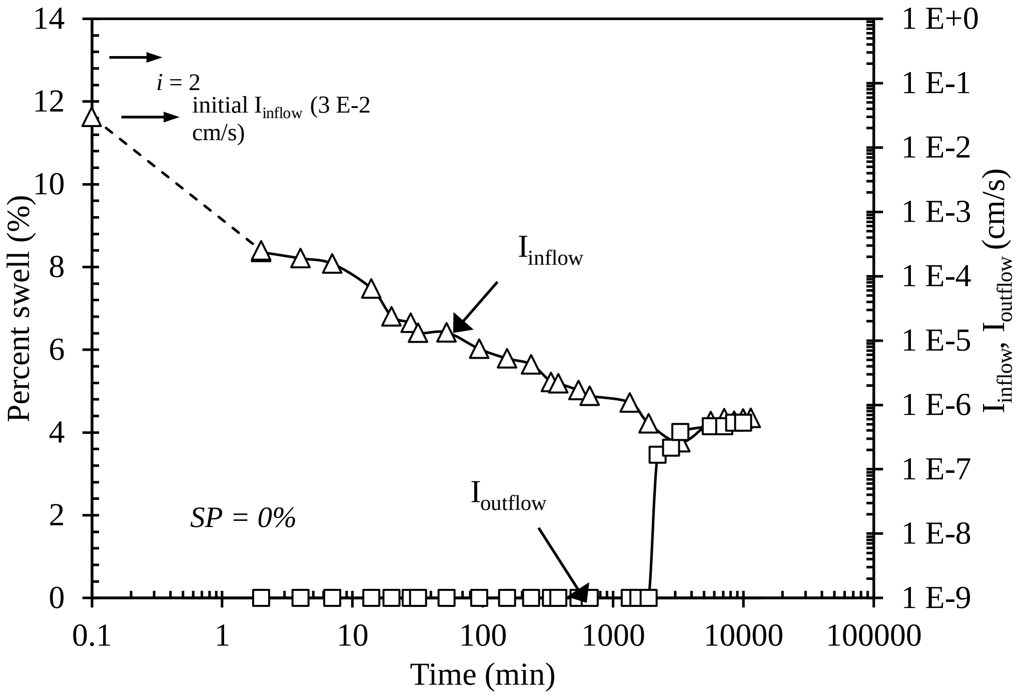

Figure 6.37: Variation of inflow and outflow and swell with time of CNS material compacted to standard Proctor placement condition

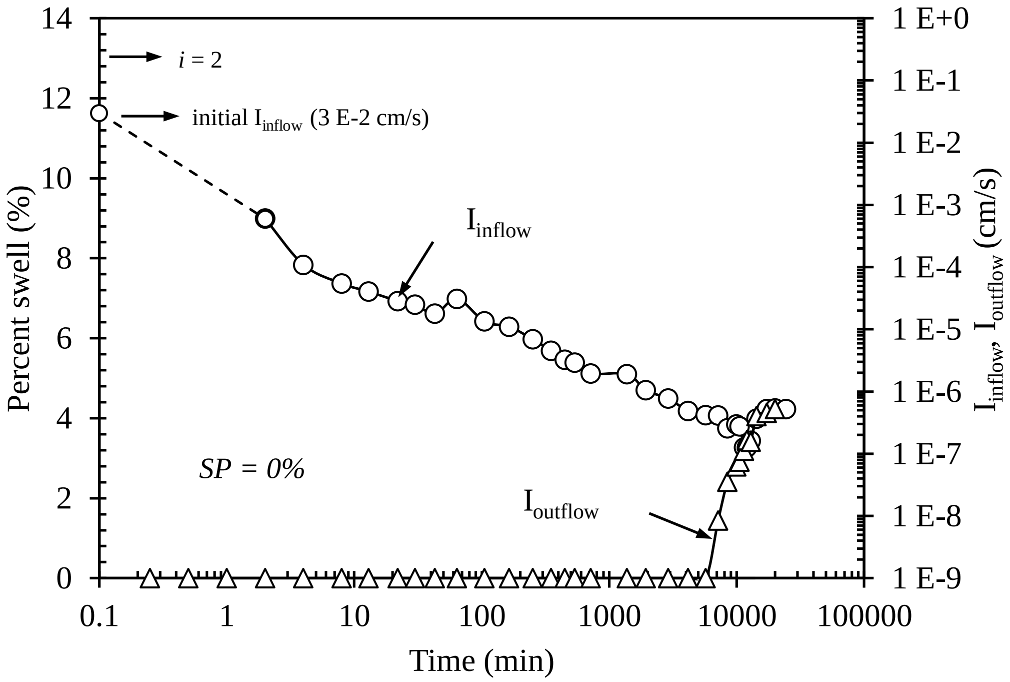

Figure 6.38: Variation of inflow and outflow and swell with time of CNS material compacted to modified Proctor placement condition.

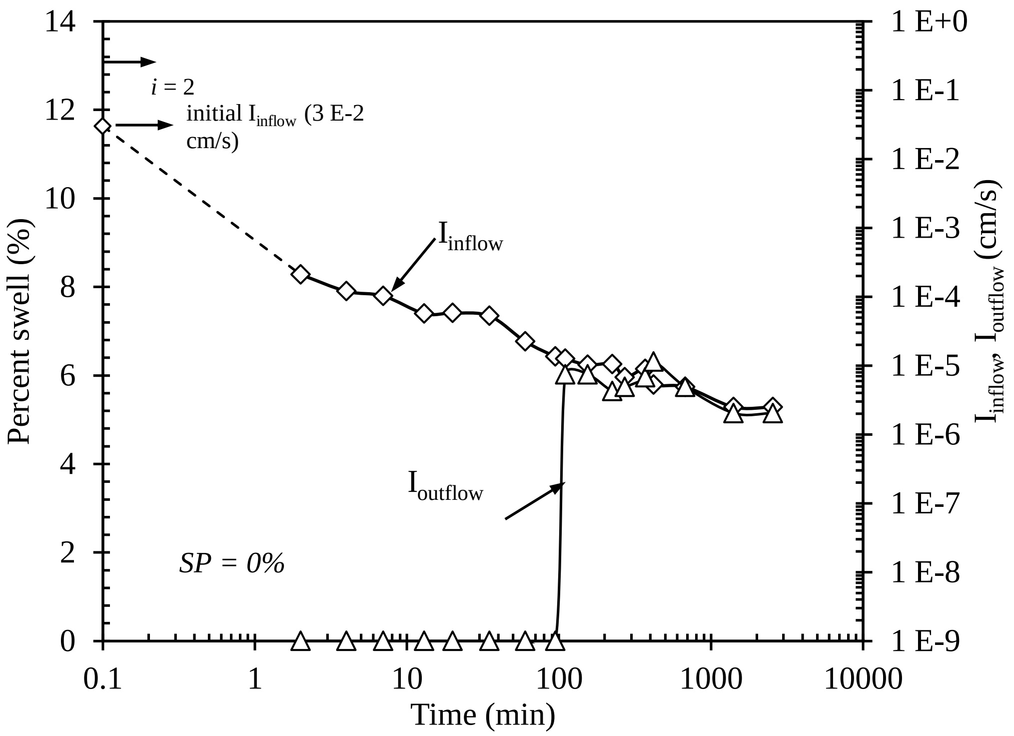

Figure 6.39: Variation of inflow, outflow and swell with time of NSS-2 material compacted to standard Proctor placement condition

Table 6.8 Water content of CNS stabilized expansive soil during top inundation

Specification	Water content (%)		
	Top layer	Middle layer	Bottom layer
ES *	40.5	39.7	40
ES + CNS *	36.8	35.50	35.0
ES + CNS (WBS)**	35.3	34.97	34.69

*inundated from top for 25 days ** inundated from top for 40 days

Albrecht and Catwright (1989) predicted the time duration for the migration of wetting front from the surface level to the determined thickness of liner material. They followed the Green Ampt approach and equation for the time prediction is given by

$$t = \left(\frac{\theta_s - \theta_i}{K_s}\right)\left(L - (h + \psi_f)\ln\left(1 + \frac{L}{h + \psi_f}\right)\right) \tag{6.2}$$

where t = time required to reach the wetting front depth, L = depth of wetting front (cm), h = ponding depth (cm), Θ_s = saturated volumetric water content, Θ_i = initial volumetric water content, K_s = saturated hydraulic conductivity (cm/s) and ψ_f = matric potential at wetting front.

The above equation was used for the prediction of time for wetting front to reach the full thickness of CNS compensating material. Figures 6.40 and 6.41 present the approximate time estimate for the migration of the wetting front for a given thickness of CNS material compacted to the standard and modified Proctor placement conditions, respectively. The depth of ponding condition varies from 10 to 40 cm, and it was optimised as 15 cm as followed by Bharadwaj (2013) in the analysis. The time for migration of maximum wetting front depth took almost 0.7 to 0.9 year for 0.9 to 1.5 m thickness of CNS compacted to standard Proctor placement condition. Similarly, for the modified Proctor placement condition, it took 4.0 to 7.5 years for 0.9 to 1.5 m thickness.

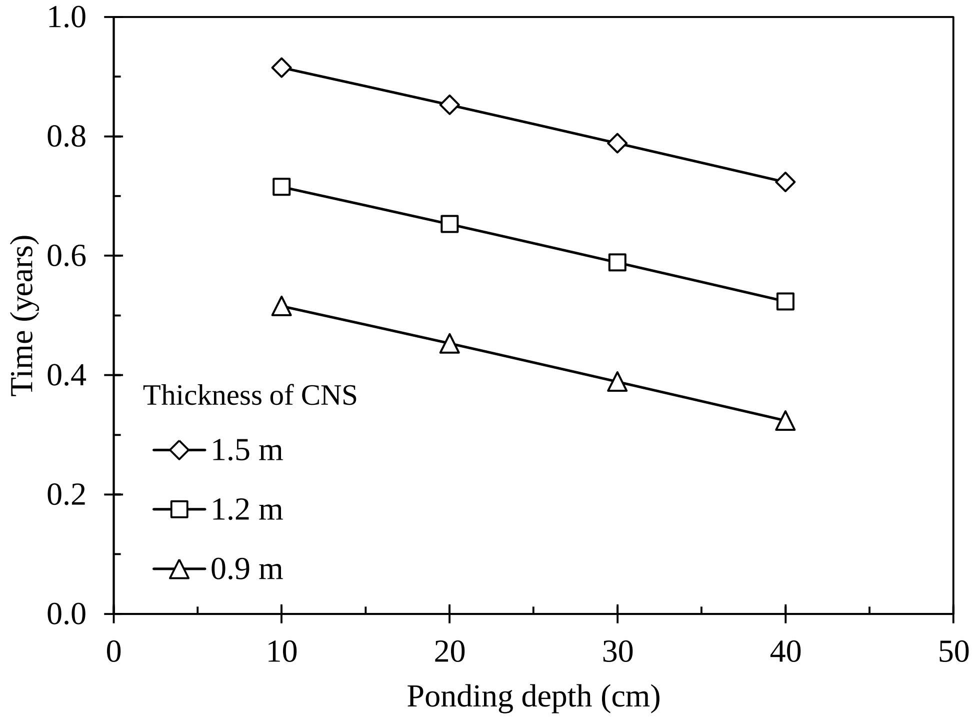

Figure 6.40: Variation of time required for migration of wetting front with ponding depth of CNS material compacted to standard Proctor placement condition

Therefore, from the results of hydraulic conductivity and infiltration studies, it can be concluded that if CNS material is used as a compensating material, it would behave as a moisture barrier during the initial phase of saturation and continuous migration of moisture could be ensured only by maintaining the constant ponding depth (constant gradient) which may not occur in the field. At the same time, if the compensating material used is characterized with higher hydraulic conductivity (1.0 x 10^{-5} cm/s), the infiltration rate becomes fast, and saturates the 0.9 to 1.5 m thick material within a month under constant ponding depth.

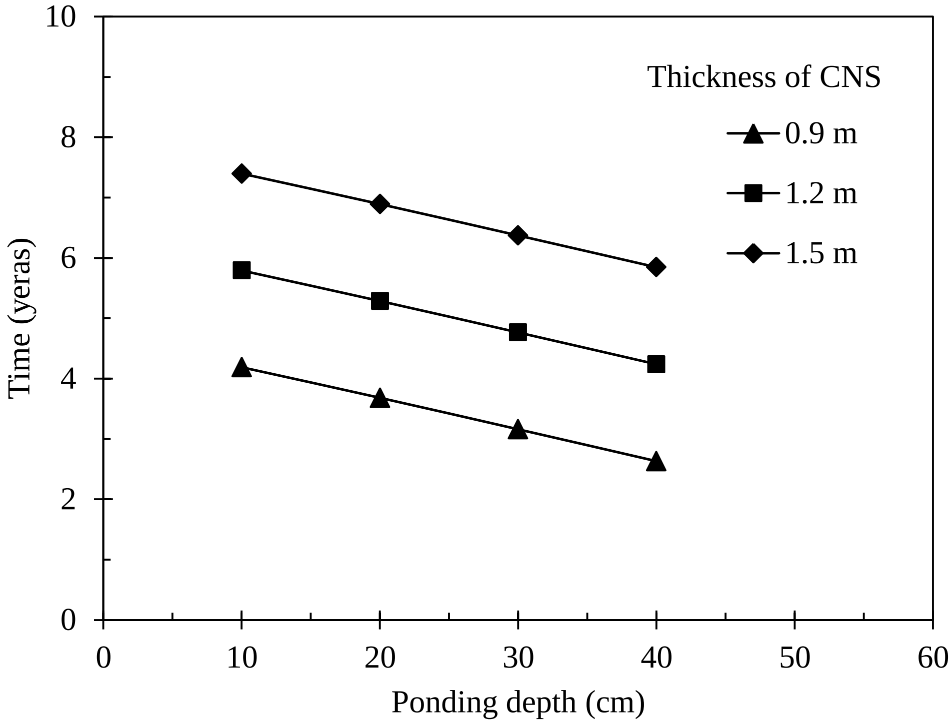

Figure 6.41: Variation of time required for migration of wetting front with ponding depth of CNS material compacted to modified Proctor placement condition

b) Migration of moisture from saturated compensating material to the underlying expansive soil

Figure 6.35 shows that the presence of CNS layer has delayed the migration of water and the time to reach the expansive soil and it was justified using the infiltration tests. Therefore a comparative study was carried out to analyse the possible variation in the water content of underlying expansive soil due to the presence of water in the saturated compensating material (i.e.) the expansive soil will not be directly inundated with water and the expansive soil swells only by drawing the water from the saturated compensating material overlying it. The tests were performed by compacting the expansive soil in the rings of 75 mm diameter and then a saturated compensating material of 71 mm diameter was carefully placed over the expansive soil and allowed to swell under a seating pressure of 6.25 kPa. It should be noted here that the non-swelling soil/ CNS material was saturated separately using back pressure application in flexible wall test setup. Then the saturated non-swelling/ CNS material was carefully removed from the flexible wall permeameter test setup and placed over the expansive soil as mentioned above. The 2 mm annular gap was filled with thick grease. Since it was difficult to place the saturated sand over the expansive soil, the sand was first placed in the ring to required relative density

(D_r = 80%) and required thickness and then the calculated amount of water pertaining to 6% was poured in to the sand layer. The diameter of CNS was taken as 71 mm to avoid the side friction as explained in the earlier sections.

Figure 6.42 compares the time-swell plots of expansive soil stabilized with different saturated compensating materials. Figure 6.42 also includes the time-swell plot of expansive soil directly inundated with water. The placement of saturated sand layer has initiated the swell as soon as the expansive soil got in contact with water from the saturated sand layer (Figure 6.42). The earlier initiation of swelling is mainly due to the higher permeability of sand layer (10^{-3} cm/s). However, with the placement of non-swelling soil (k = 10^{-5} cm/s), the swell initiation was delayed with lower swell potential. The swell was further delayed with reduced swell potential with saturated CNS material. From Figure 6.42, it is clear that the placement of impervious material (k = 10^{-7} cm/s) not only delayed the migration of water but also it delayed the rate of swelling of underlying expansive soil. This behaviour indicated that it may have a significant influence on the variation of active zone after the placement of compensating materials.

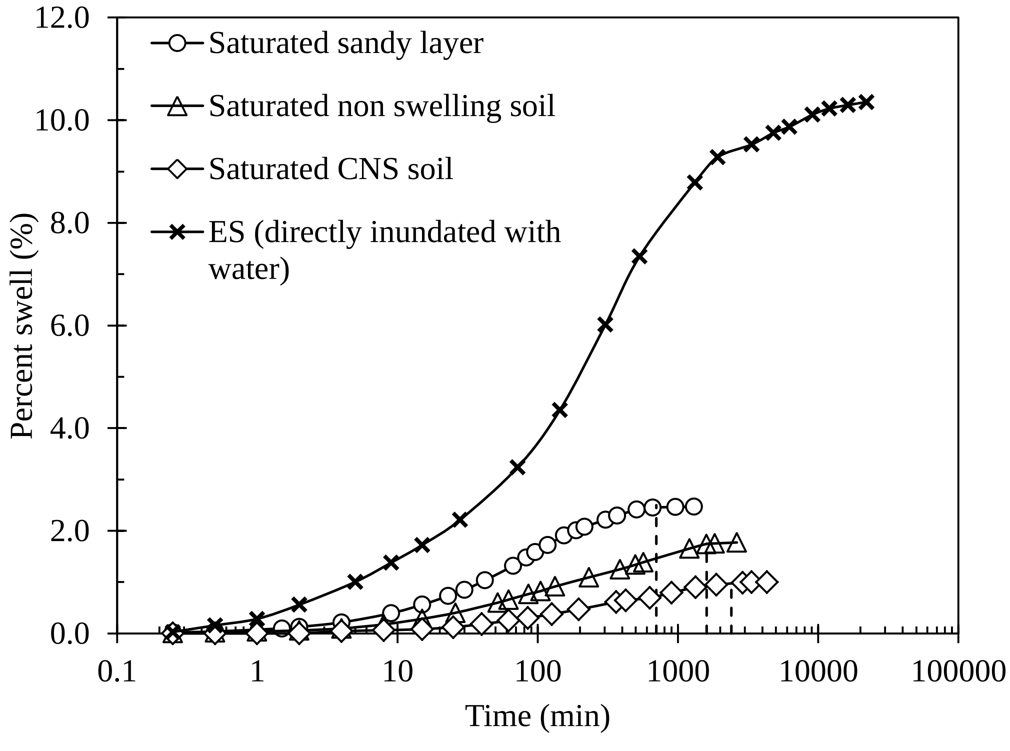

Figure 6.42: Vertical swell in the expansive soil due to the presence of water in the saturated compensating materials

6.3.8 Leaching Studies on Stabilized Expansive Soil

Previous studies, reported that the placement of CSS material over the expansive soil reduced the overall volume change. The present study aims to understanding whether the leaching of ions from the CSS is also responsible for the swell control. Further, the swell reduction was not quantified based on the leaching studies.

In the present study, the leaching of lime is evaluated using osmotic suction of respective fluid. Figure 6.43 present the variation of osmotic suction with expansive soil and stabilized expansive soil (CSS). It is clear that in untreated expansive soil, the effluent has minimum dissolved ions in the solution, and it showed a zero osmotic suction. But the effluent osmotic suction of CSS material is high and it is higher for CSS-2 (4% lime stabilized soil). It is clear that placing of stabilized soil over the expansive soil also controls the volume change through the leaching as well. Therefore, if chemically stabilized soil (CSS) cushion is used as a compensating material, other than the permeability and friction criteria (side wall friction), the leaching of stabilizer also controls the swell to some extent. For this reason the CSS performance is better than the natural CNS material.

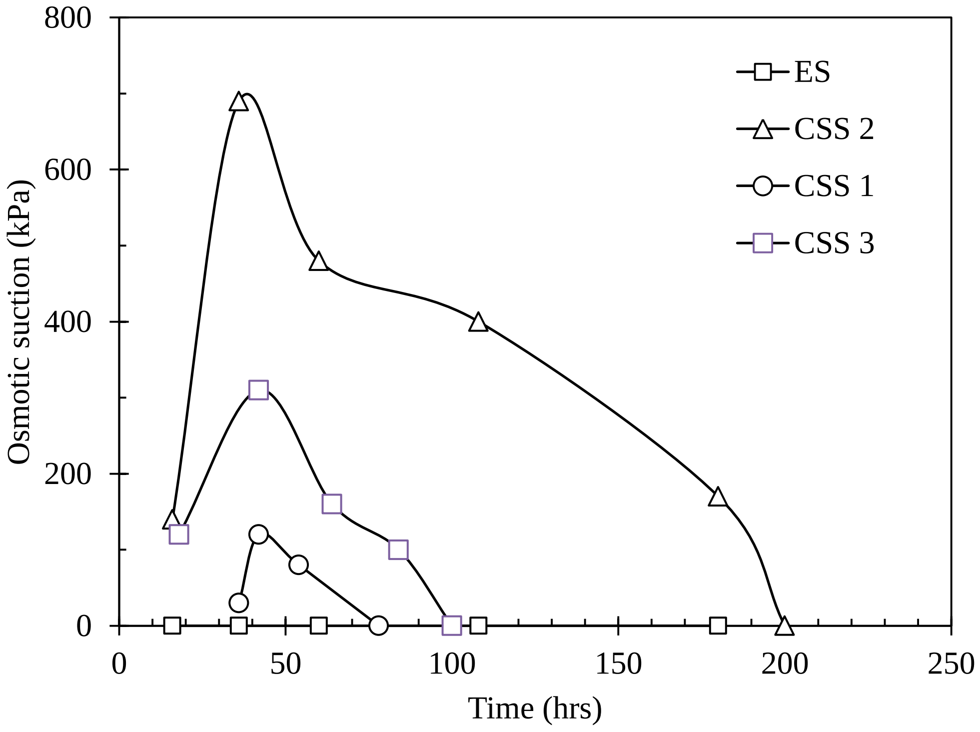

Figure 6.43: Leaching of stabilizer from stabilized expansive soil with time.

In addition to the leaching study, it was also noticed that the time elapsed for collecting the outlet volume varies from 18 to 36 hours for 50 mm thick stabilized expansive soil, whose permeability is in the range of 10^{-5} cm/s. Further, the head maintained in the study was almost equal to 100 cm. Hence, the same material may take a long time to saturate under low hydraulic gradient The test was also conducted on 50 mm thick compacted CNS material (standard Proctor placement condition) to determine the approximate elapsed time for collecting the outlet fluid, and it was closer to 9-10 days under 50 cm head of water. This study also emphasises that the permeability of the compensating material is a significant governing factor in the volume change control of underlying expansive soil.

6.3.9 Effect of wet-dry cycles on the CNS stabilized expansive soil

The effect of wet-dry cycles on volume change behaviour of CNS stabilized expansive soil is essential for understanding the long term performance of the structures founded on them. The volume change of expansive soil during wet-dry cycles could be controlled either by increasing the surcharge pressure or by altering the physico-chemical properties. Tripathy *et al.* (2002) studied the swell-shrink behaviour of compacted expansive soil and showed that the equilibrium bandwidth decreases with an increase in surcharge pressure for a given placement condition. Similarly, the expansion of diffuse double layers could be suppressed by chemical stabilisation (lime, cement, lime precipitation technique, etc.). Thyagaraj and Zodinsanga (2014) and Chittoori *et al*. (2017) reported that the chemically stabilized soil showed improved performance successive wet-dry cycles. Therefore, the behaviour of CNS stabilized expansive soil subjected to different wet-dry cycles is presented in this section.

Figure 6.44 compares the swell-shrink response of expansive soil, CNS and CNS stabilised expansive soil under a surcharge pressure of 6.25 kPa. It is clear that the swell control was maximum during the first wetting cycle and after that the effectiveness of CNS in controlling the volume change during the subsequent wetting cycles decreased. Further, the overburden stress imposed by CNS over the expansive soil is insignificant and at the same time the physico-chemical interaction are also minimum. The same is reflected in the swell behaviour as shown in Figure 6.45.

.

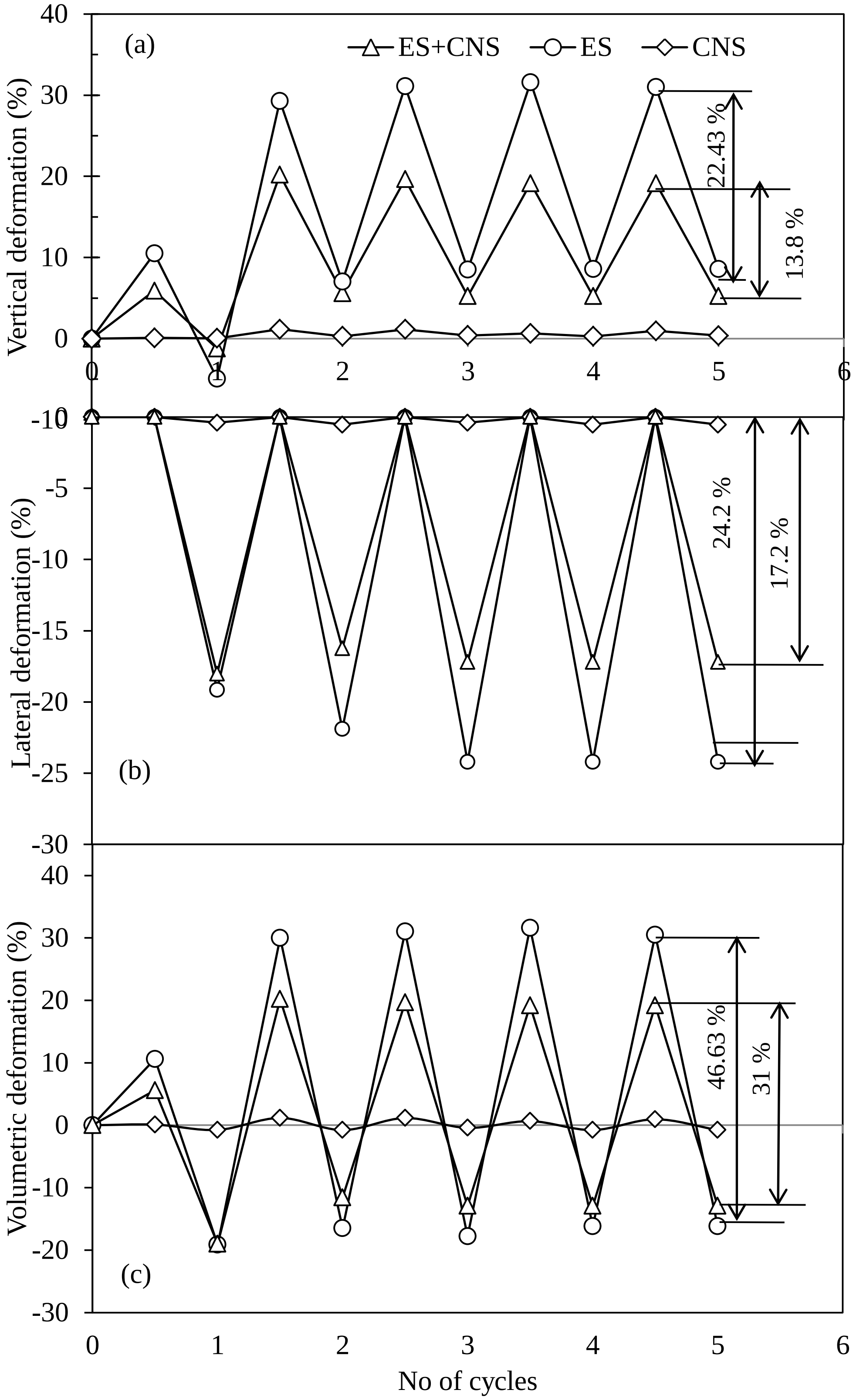

Figure 6.44: Comparison of: a) vertical b) lateral and volumetric deformations of expansive soil, CNS and CNS stabilized expansive soil during wet-dry cycles

The above section also discussed that the swell control during first wetting was mostly due to the impervious nature of the CNS material, time lag in swell activation due to saturation of specimen and side wall friction (laboratory constraint). However, the equilibrium bandwidth of volumetric deformation after five wet-dry cycles reduced to 31% against the 46.3% for expansive soil alone. The volumetric deformation is higher than the allowable limit of 3% (Keller, 2007), which suggests that the CNS layer is not effective over long term. Rao (2000) also reported that CNS was effective only during the first cycle of wetting

Figure 6.45 presents the propagation of cracks in CNS stabilized expansive soil. The development of cracks pattern in CNS stabilized expansive soil is similar to that of untreated expansive soil as reported by Julina and Thyagaraj (2018). During the first drying, the specimen experiences global shrinkage, and hence, no surface cracks were observed. However, in the subsequent drying process, both surface and vertical cracks were noticed, and there was a separation between CNS and expansive soil after the formation of cracks (Figure 6.45). It is interesting to note that no cracks were observed in the CNS material and the volume change was negligible even after five wet-dry cycles. The gap between the CNS and expansive soil due to separation may also contribute to swell reduction during measurement, as the swell during subsequent wetting occurs in this gap. Further, the formation of cracks in expansive soil also implies that the placement of CNS does not influence the intrinsic swell-shrink property of the expansive soil.

6.4 MECHANISMS OF COMPENSATING MATERIAL IN VOLUME CHANGE CONTROL OF EXPANSIVE SOIL

Based on the literature and the present experimental works, the following points are summarised on the possible mechanism of compensating materials in controlling the volume change of underlying expansive soils. The compensating materials control the swell-shrink movements of the expansive soils through the following mechanism:

a) removal and replacement of expansive soil in active zone

b) overburden stress

c) impervious nature of compensating materials

d) active depth variation due to compensating materials

e) additional mechanism in chemically stabilized soil cushion (CSS).

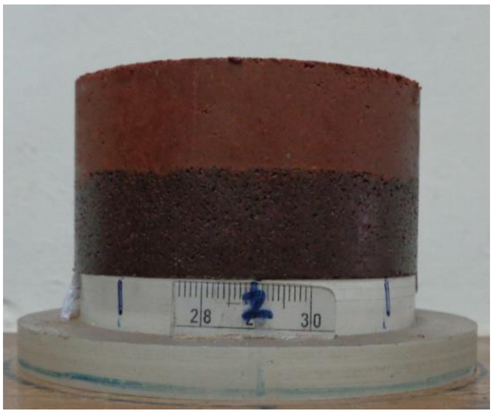

a) Compacted condition

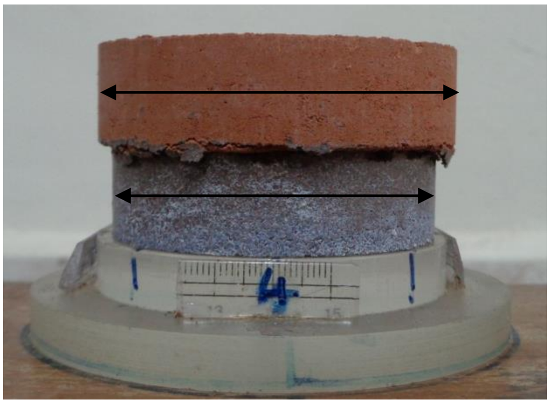

b) First drying

c) Second drying

c) Fouth drying

Figure 6.45: Images of formation of cracks in CNS stabilized expansive soil subjected to wet-dry cycles

a) Removal and replacement of expansive soil in active zone

In most of the constructions, the surface soil is removed and the depth of removal depends on the type of structures – pavement or building. Ardani (1992) discussed the method of soil replacement technique followed in Colorado state highways and showed that the depth of excavation was based on plasticity index. He reported that for the expansive soils with plasticity index greater than 50%, the maximum replacement depth of 6 ft (1.8 m) was followed. For a given soil profile, the volume change occurs only in the active zone (Chen, 1975; Nelson and Miller, 1992). However, as reported by Rao *et al*. (1988) and Fityus *et al*. (2004), about 80% volume change occurs in the top 50-60% of the active zone (Figure 6.46(a)). Yosida *et al*. (1983) and Vanapalli *et al.* (2010) also reported similar findings that the swell pressure decreases with the removal of soil in the active zone. Earlier Rao (2000) and Murty and Praveen (2008) compared the swell after placing the compensating material without the removal and replacement condition. They reported that the replacement with compensating material decreased the swelling which they have attributed to the mobilization of cohesive force in compensating material (CNS) and interaction between compensating material and expansive soil. However, it should be noted here that it is not due to interaction but due to replacement only as top layers swell more in comparison to the bottom layers and thus replacing the top layers obviously reduces the swelling.

In India, some locations in the states of Telangana, Madhya Pradesh and Maharashtra, the active zone was found to be vary from1.5 to 3.0 m. Hence, the removal and replacement itself has a significant role in the volume change control.

For a given active zone profile, the top layers swell more owing to large water content fluctuations during dry and wet seasons. As the depth increases the water content fluctuations decrease, and thus the swelling also decreases. This is further illustrated using the active zone and the variation of heave with depth in Figure 6.46 (a) and (b), respectively. As seen from Figure 6.46 (b), the heave is zero where the water content fluctuation is zero and the heave increases as the water content fluctuations increase towards the ground surface and it is maximum at the ground surface where the water content fluctuations are maximum. The placement of CNS layer has no influence on the heave till the CNS layer depth is reached as the water content fluctuates beyond the CNS depth is same as that of the case without CNS layer (Figure 6.46 d). Above the CNS layer depth, the heave does not increase as the large water content fluctuations occur in non-swelling soil. This explains that heave or swell reduction is primarily due to soil replacement, and as stated by Rao *et al.* (1988) and Fityus *et al*. (2004) 80% heave can be decreased by replacing the half of active zone with NSS or CNS.

b) Overburden stress

As reported in the literature, the suggested thickness of compensating material was in the range of 0.9 to 1.5 m. According to Chen (1988), the thickness is compensating materials is defined as the distance from the bottom of the footing to the top of the expansive soil. Terzaghi *et al.* (1996) reported that the downward weight of compensating material could counteract the partial or most of the swell pressure. However, this solution may not be a viable option for expansive soils characterized with higher swell pressures because it may require greater thickness of compensating material which may not be feasible as the overall cost of the project increases.

c) Impervious nature of compensating materials

Previous researchers used different compensating materials with varying hydraulic properties. In spite of the varying hydraulic conductivity, the compensating materials controlled the volume change primarily due to removal and replacement mechanism as discussed in the above paragraphs and also due to impervious nature which is discussed here. Further, it should be noted that materials with higher hydraulic conductivity serves as a water source for underlying expansive soil and causes swell. The subsequent drying causes the shrinkage. However, the overall swell-shrink movements will be low as the water content fluctuations also low.

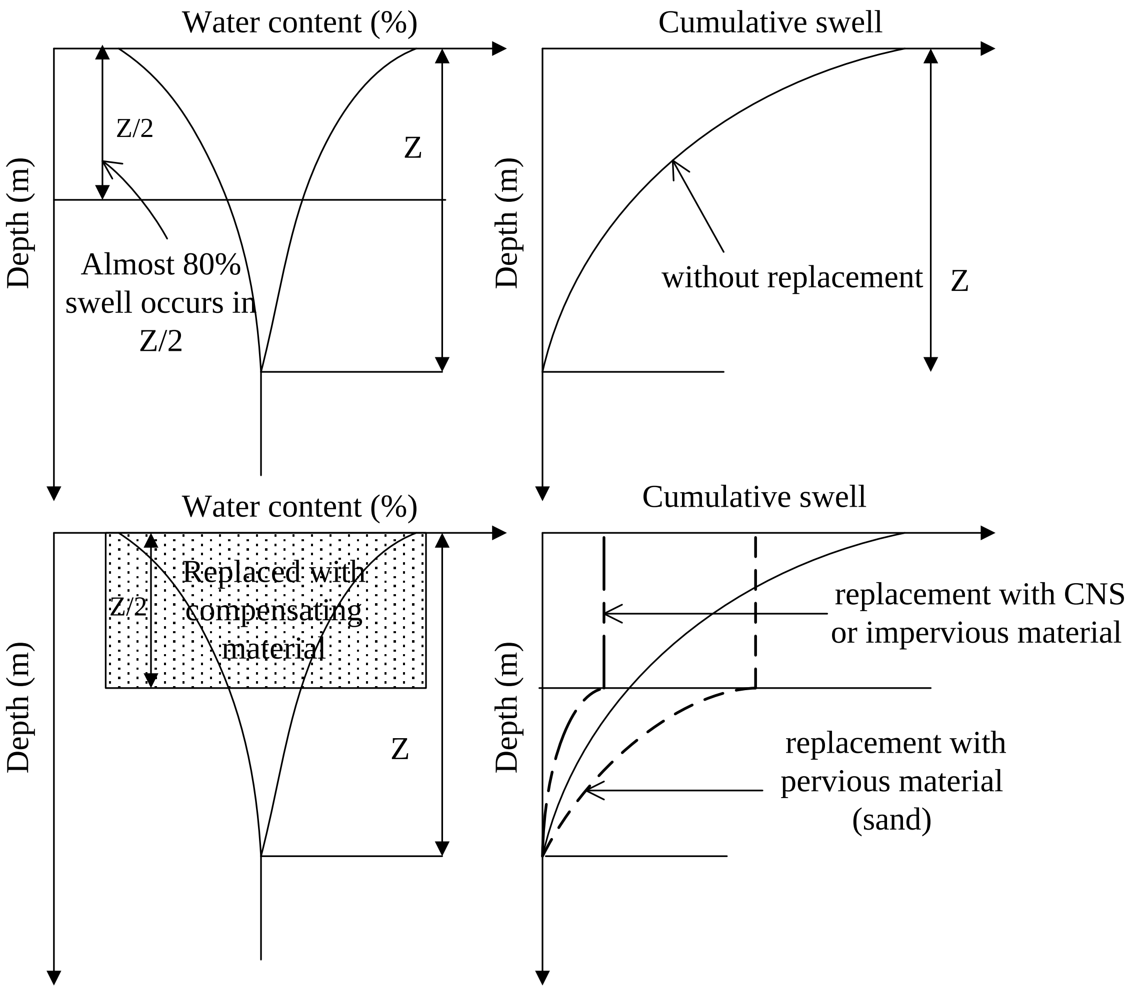

Figure 6.46: Illustration of removal of expansive soil and replacement with compensating materials: a) active zone variation b) cumulative swell before replacement c) placement of compensating in the active zone d) cumulative swell variation with placement of compensating materials.

As discussed in Chapter 5, the quarry dust was used as backfill material, which had a hydraulic conductivity of 2.5×10^{-3} cm/s. Because of its higher hydraulic conductivity, the gardening water has infiltrated through the quarry dust and reached the expansive soil (fill material). Even though the quarry dust has a higher infiltration rate, the distress was noticed after four years of construction due to the occasional supply of gardening water. However, if a backfill material is used as per the guidelines of IS 9451, it may take a long time for the gardening water to reach the expansive soil and some amount of water may drain out at the ground surface because of its lower infiltration rate capacity. The hydraulic property of the compacted CNS materials show that it is a suitable material from the mechanism of impervious barrier in controlling the swell-shrink behaviour of expansive soil.

d) Active depth variation due to compensating materials

As long as the compensating material behaves as an impervious material, the compensating material acts as a cover over the expansive soil, and it affects the cyclic infiltration and evaporation process. Also, this process has a significant role in altering the depth of active zone. In general, the provision of higher permeability material not only provides easy access to free water but also it may increase the active zone depth (Coduto, 2013). Fityus *et al*. (2004) reported that the active zone increased for the soil profile with thick vegetation, and it decreases for the soil profile covered with impervious plastic cover. Hence, the placement of compensating materials like CNS with poor drainage properties over the expansive soil may decrease the depth of active zone (Figure 6.47). In the earlier section, it was discussed that the CNS material would act as an impervious layer and hence there was a time lag for the migration of wetting front from the CNS to expansive soil. However, this variation was not explored in the literature, and hence, the field studies are essential to support this observation if CNS is used as a compensating material. Thus, the placement of a CNS layer decrease the swell-shrink movements as the depth of active zone and variation in water content fluctuations at different depths decrease.

e) Additional mechanism in chemically stabilized soil cushion (CSS)

In case of non-availability of CNS soil, the CSS materials are used as compensating material to control the volume change of expansive soils. Apart from the mechanism discussed above, the chemical stabilization mechanism also governs the volume change behaviour of expansive soils stabilized with CSS as the chemicals leach out to the underlying expansive soils and result in chemical stabilization of expansive soil to some extent.

It is very important to note that the mechanisms of stabilization of expansive soil with compensating materials in field are not simulated in the laboratory studies reported so far in the literature with respect to wetting and drying pattern, the impervious nature and variation in active zone due to compensating materials. An attempt is made in the present study to simulate the field conditions to some extent.

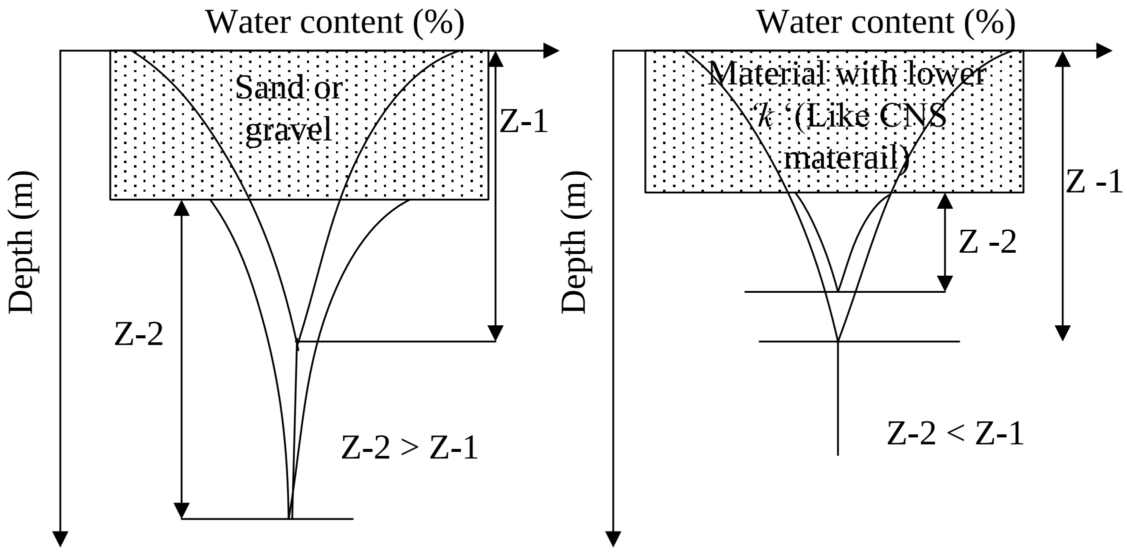

Z-1: active zone profile before soil replacement; Z-2: active zone profile after soil replacement

Figure 6.47: Possible variations in the active zone profile after placing the compensating material: (a) with higher hydraulic conductivity (Coduto, 2013) and (b) material with lower hydraulic conductivity

Table 6.9 summarizes the possible mechanisms of compensating materials which controls the swell-shrink potentials of expansive soils in the field. In Table 6.9, the mechanisms controlling the swell are rated from 1 to 4, where “1” represents that it is most effective in controlling the swell and “4” represents that it is least effective in controlling the swell. For example, as the depth of compensating material is limited to about 1.5 m (maximum), the contribution of overburden stress mechanism in controlling the swell-shrink movements of expansive soil is less and hence it is rated as 3. Further, it should be noted here that the active zone depth variation because of placement of compensating materials depends on the compensating materials used and the equilibrium of active depth occurs after few wetting and drying cycles. Hence, it is given a rating of 2 in case of CNS and 4 in case of sand, NSS and CSS. This variation is attributed to the variation of hydraulic properties of compensating materials. The primary mechanism controlling the swell-shrink potentials is attributed to removal and replacement mechanism. Impervious nature also plays a major role in case of CNS and CSS where the rating is between 2 and 3. In summary, the removal and replacement and impervious nature are the major mechanisms controlling the swell-shrink movements of expansive soil stabilized with compensating material.

Table 6.9 Mechanisms of compensating materials in controlling the swell of expansive soils

Compensating material	Mechanism of compensating material in controlling the swell				
	Removal and replacement	Overburden stress	Impervious nature	Active zone variation	Leaching of chemicals
Sand	1	3	4	4	NA
NSS	1	3	4	4	NA
CNS	1	3	2	2	NA
CSS	1	3	2/3**	3/4	2/3*

Note: 1: most responsible for swell reduction;
4: least responsible for swell reduction;
*: depends of the dosage of chemicals in CSS;
**: CSS may shows both pervious and impervious natures depending on the type and amount of additives.

6.5 SUMMARY AND CONCLUSIONS

This chapter presented a detailed laboratory study that was carried out to study the effect of different compensating materials in controlling the swell-shrink potentials of expansive soil. The following conclusions are drawn from the present laboratory studies on expansive soil stabilized with wide range of compensating materials.

i. The laboratory examination of volume change behaviour of CNS stabilized expansive soil showed that the placement of any compensating material controls the volume change of underlying expansive soil. The effect of sidewall friction and duration of inundation should be given due consideration in the laboratory measurement of volume change of the two-layer soil system.

ii. The swell pressure measurement using constant volume method showed a reduction in swell pressure of stabilized expansive soil irrespective of the compensating material used for stabilization. This reduction in swell pressure is attributed to the compression of compensating material and the corresponding volume change of underlying expansive soil. Therefore, the constant volume method is not an appropriate method for the measurement of swell pressure of the two-layered soil system.

iii. The CNS material placed over the expansive soil acts as a moisture barrier under low hydraulic gradients. The hydraulic conductivity and infiltration test results indicate the same observations in the laboratory conditions. Consequently, activation of swell occurs after a time lag during top saturation. However, the time lag reduces with the use of compensating materials of higher hydraulic conductivity than the CNS material and thus leads to earlier initiation of swell.

iv. For a given soil profile, the formation of active zone varies due to the cyclic process of precipitation and infiltration and evaporation. The presence of any impervious material at the surface affects this cyclic process, and thus decreases the active zone depth. This turn decreases the swell-shrink potentials of soils stabilized with impervious compensating materials. However, this needs further investigation through field scale study.

v. CSS material prepared using fly ash could be used as a compensating material for volume change control of expansive soil. However, its efficacy during wet-dry cycles depends on the hydraulic conductivity and leaching of the CSS material.

vi. Placement of compensating materials is controlling the volume change behaviour of expansive soils through various mechanisms – removal and replacement, overburden stress, impervious nature, active zone variation and leaching of chemicals. The effectiveness of the each mechanism varies with the type of compensating material. However for all the compensating materials the removal and replacement mechanism is the major mechanism controlling the swell-shrink movements of expansive soil. The mechanism of impervious nature of compensating material is next major contributing mechanism in case of CNS and CSS materials,

The present laboratory study reveals that the placement of compensating material is effective during the first wetting only, and its effectiveness decreased with successive wet-dry cycles. However, the testing protocol adopted for wetting and drying did not simulate the actual field conditions; wherein the two-layer system was subjected to full drying using a circumferential band heater over the oedometer cell at a constant temperature of 45°C. In contrast, in the field, desiccation of the expansive soil occurs after the desiccation compacted CNS material. Moreover, the placement of CNS material leads to partial wet-dry cycles due to the reduced variation in moisture fluctuation and reduced depth of active zone. Further, the fluctuations in moisture content are higher at the surface and it decreases with depth in the active zone. Therefore, the placement of CNS material effectively controls the volume change behaviour of expansive soil in the field even when subjected to wet-dry cycles.

CHAPTER 7

DEEP STABILIZATION OF EXPANSIVE SOIL USING LIME, FLY ASH AND LIME-FLY ASH SLURRY INJECTION

7.1 INTRODUCTION

This chapter presents the stabilization of thick expansive soil deposits in desiccated state using slurry injection technique. The study was carried out in large size laboratory tanks. Lime, fly ash and lime-fly ash slurries were used as injection additive for the treatment of expansive soil. The slurry was injected through the pre-drilled hole in the desiccated expansive soil. The volume change of the treated expansive soil was measured under a seating pressure of 6.25 kPa. Further, the long term performance of lime/ fly ash, lime-fly ash slurry treated expansive soil was brought out by subjecting the treated soil to wet-dry cycles. At the end of wet-dry cycles, the treated soil samples were cored from the test tanks for bringing out the effectiveness of treatment through evaluation of changes in physico-chemical, index and engineering properties.

7.2 EXPERIMENTAL PROGRAM

The methodology followed to achieve the proposed objective is shown in Figure 7.1. This section provides the details about the materials used, their properties, protocols adopted for compaction and desiccation of expansive soil, cyclic wetting and drying, sampling and testing of untreated and treated soils.

7.2.1 Materials and Properties

The expansive soil was collected from the Wellington lake, located near Tiruchirapalli in Tamil Nadu state. The soil was air-dried and pulverised to pass through 2 mm sieve. Standard Proctor compaction test, oedometer swell potential tests and unconfined compressive strength tests were carried out on untreated expansive soil. The soil passing the 2 mm sieve was further pulverised to pass through 425 μm sieve for the determination of index and physico-chemical properties of expansive soil. The physical and engineering properties of the expansive soil are tabulated Table 7.1.

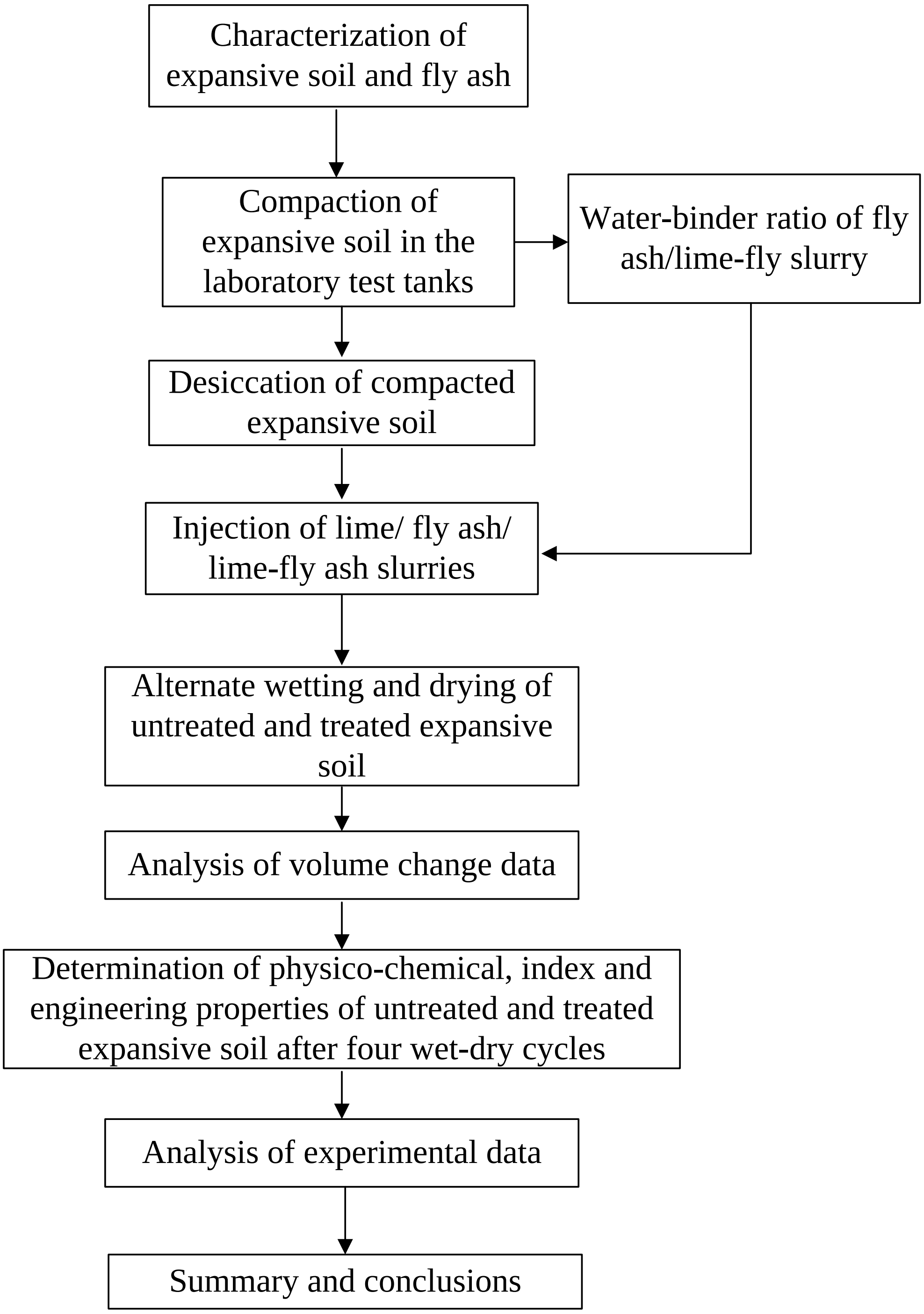

Figure 7.1: Flow chart depicting the experimental methodology adopted for deep stabilization of expansive soil in the laboratory test tanks.

The fly ash used for the present experimental studies was collected from North Chennai Thermal Power (NCTP) plant, Chennai, Tamil Nadu. Tables 7.1 and 7.2 present the physical properties and chemical compositions of fly ash obtained from X-ray fluorescence test, respectively. The fly ash comprises almost 87% of silt size particles, and it is classified as MLN (non-plastic inorganic coarse silt sized fractions) as per

Sridharan and Prakash (2007) as it comprises of 50% of silt size particles which are in the range of 20 to 75 µm size. As per ASTM C618, the fly ash used in the present study can be classified as Class F fly ash. Further the type of fly ash can also be identified based on the percentage of CaO present in it (Table 7.2). Mehta (1979) reported that the fly ash with CaO of less than 5% could be identified as low calcium fly ash.

Table 7.1 Properties of expansive soil and NCTP fly ash

Property	Expansive soil	Fly ash
pH	8.0	7.15
Specific Gravity	2.7	2.29
Gradation		
Sand size (%)	5	10
Silt size (%)	27	87
Clay size (%)	68	3
Atterberg limits (%)		
Liquid limit	95	-
Plastic limit	33	-
Shrinkage limit	8.5	-
Standars Proctor compaction characteristics		
Optimum moisture content (%)	30.5	36.2
Maximum dry density (Mg /m^3)	1.41	1.12
Classification of soil/ fly ash	CH	MLN* Class F fly ash**

***:** Sridharan and Prakash (2007); **: ASTM C618

7.2.2 Procedure for Compaction of Soil in the Test Tanks

For deep stabilization of expansive soil using lime/ fly ash/ lime-fly ash slurries, the expansive soil was compacted in cylindrical tanks of 343 mm diameter and 360 mm height. A hydraulic system based compression testing machine of 20 tonnes capacity was used for static compaction of the expansive soil to a thickness of 100 mm. The soil was compacted to 95% standard Proctor maximum dry density (1.34 Mg/m^3) at water content corresponding to 2.5% wet of optimum moisture content (33%). For the dry density of 1.34 Mg/m^3 and 100 mm thickness of compacted soil in 343 mm diameter test tank indicates that 12.38 kg of dry expansive soil mass or 16.47 kg of bulk soil mass is required for one laboratory experiment. The natural moisture content of the soil was found to be 12%. The total bulk mass of expansive soil corresponding to natural moisture content was divided into three equal fractions. Each soil fraction was thoroughly mixed with a predetermined quantity of tap water to obtain a wet soil of 33% moisture content. In order to ensure the moisture equilibrium, the water mixed soil samples were kept in plastic covers and stored in desiccators for 24 hrs. After moisture equilibration, the soil fractions were thoroughly mixed and statically compacted in the test tanks using the hydraulic reaction frame assembly in two layers. Each layer was compacted to a lift thickness of 50 mm. Further, to ensure proper bonding between the layers, the first layer was scarified before placing the soil for second layer compaction.

Table 7.2 Chemical composition of NCTP fly ash

Chemical composition	**Quantity (%)**
SiO_2	63
Al_2O_3	22.62
Fe_2O_3	6.33
CaO	3.58
MgO	-
TiO_2	2.8
K_2O	1.13
Na_2O	-

7.2.3 Determination of Water Binder Ratio for Lime, Fly ash and Lime-Fly ash slurries

In the present study, three binders namely lime, fly ash and lime-fly ash were used for the stabilization of the expansive soil. Due to the variations in the physical nature and pozzolanic property of the binder materials, the procedure adopted for determining the optimum water-binder ratio of the slurries is not the same. Therefore, the guidelines or method followed for optimization of the water binder ratio of lime slurry and lime-fly ash slurry is discussed in the following section.

Bell (1993) suggested the typical lime slurry preparation method for soil stabilization of soils by adding 1 tonne of lime to 2,500 litres of water, which yielded approximately

31% lime solution. The maximum percentage of the lime solution was limited to 40%, and beyond this value, it may lead to pumpability and slurry sprayer handling issues. Based on the above guidelines, 700 g of calcium hydroxide was mixed with 1750 ml of tap water, and this produced a 33% lime solution. The presence of 700 g of calcium hydroxide in the lime slurry solution corresponds to 5.6% of dry weight of soil in the test tank. Moreover, this percentage of lime has exceeded the initial consumption of lime (ICL) value of the soil (4%).

To determine the optimum water-binder ratio of fly ash and lime-fly ash slurry solutions, a mini-slump cone was used, which was developed by Kantro (1980). The schematic view and image of the mini-slump cone apparatus is shown in Figure 7.2. A mini-slump cone with 19 mm inner diameter at top (31.8 mm outer diameter) and 37 mm diameter at bottom with 57 mm height was used in the present study. A square-shaped glass plate was used as the base for flow testing. The slurries were prepared by mixing of lime and fly ash in dry condition and then desired quantity of water was added. The clean cone was positioned at the middle of the glass plate and then the fly ash/ lime-fly ash slurry was poured into it. After complete filling of slurry, the cone was lifted, and the slurry was allowed to spread on the glass plate as shown in Figure 7.2(c). The diameter of the slurry spread was measured using a steel ruler and the average of four measurements of the spread was reported as mini-slump spread in millimetre.

Figure 7.3 compares the variation of mini-slump cone spread with increase in water binder ratio (w/b) of fly ash and lime-fly ash slurries. For fly ash slurry, the optimum w/b ratio was found as 1.4, and beyond this ratio, the slump value remains almost constant. For fly ash slurry preparation, about 1400 gram of fly ash was mixed with 1680 ml of tap water at a water-binder ratio of 1.2. This produces 61% slurry solution and weight of fly ash used corresponds to 12% of dry weight of soil in the tank.

Wilkinson *et al*. (2010) reported different percentage of lime and fly ash combinations for lime-fly ash slurry preparation and the proportions were 33% quicklime + 66% fly ash and 43% hydrated lime + 57% fly ash. The slurry was prepared by adding one litre of water to 0.5 kg binder. Based on the above criteria, for the present study, the lime and fly ash was mixed in the proportion of 50% lime + 50% fly ash on dry weight basis. With the addition of lime to the fly ash, the slump value decreased in low range of w/b, and this happened due to the absorption of water by lime. However, the final slump value was higher than the slump value of fly ash slurry alone. In the present study, initially it was decided to select the optimum w/b ratio as the point where the slump value remains constant. However, when this condition was adopted for the soil stabilization, the volume change during the injection period itself was more, and it is evidently due to the availability of free water in the slurry. Hence, the water-binder ratio for slurry injection in expansive soil was selected as a preceding point of the optimum water-binder ratio (Figure 7.3). Even though the water-binder ratios of fly ash and lime-fly ash slurries were 1.2 and 1.6, respectively, the variation in flow value is only 10 mm for the respective water-binder ratios.

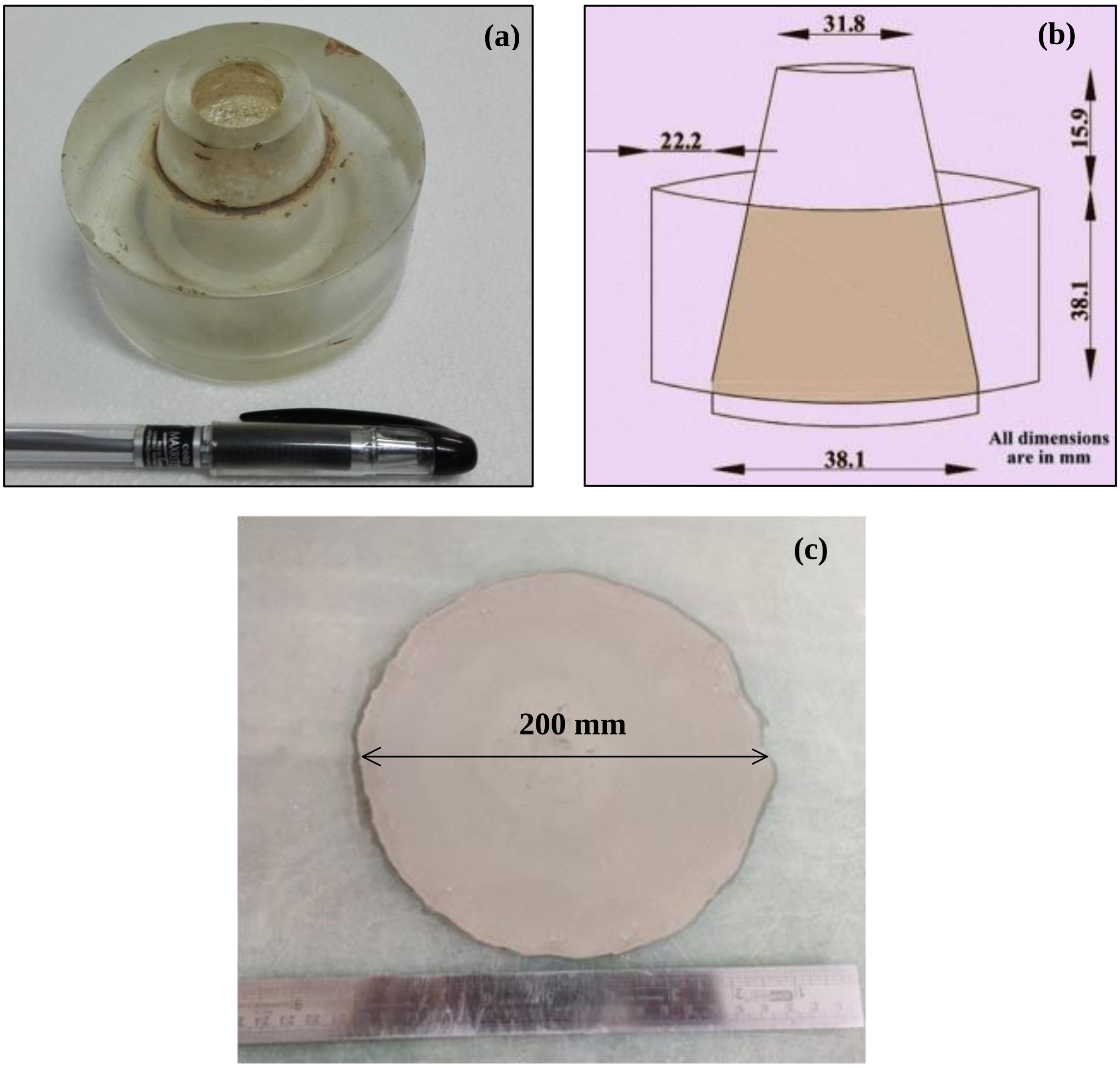

Figure 7.2: a) Schematic b) image of mini-slump cone apparatus and c) measurement of mini-slump spread

For lime-fly ash slurry stabilization, 400 g hydrated lime and 400 g of fly ash was taken and mixed in a bowl in dry condition before adding water. Then 1280 ml of tap water was taken corresponding to the w/b ratio of 1.6, and it was mixed with the binder for 5-10 minutes for ensuring the homogeneity. After mixing, the lime-fly ash slurry solution was found to be 42%. The percentage of lime with respect to the dry weight of soil is about 3.2%, which is lower than the optimum lime content of the soil (4%).

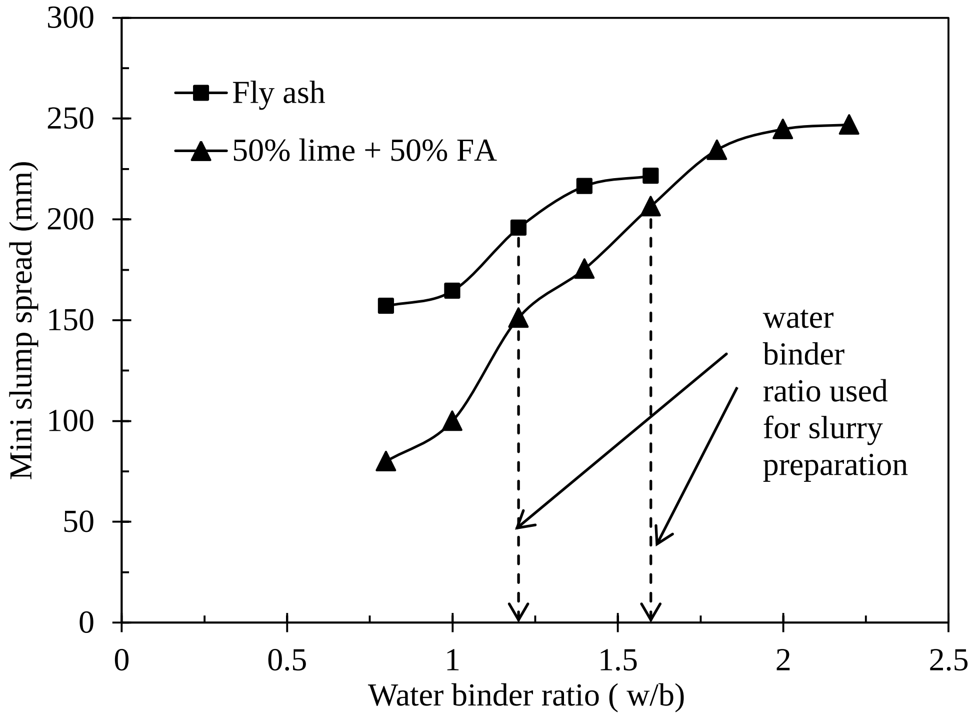

Figure 7.3: Variation of mini slump spread with w/b ratio for fly ash and lime-fly ash slurry solutions

7.2.4 Slurry Injection in the Desiccated Soil

Figure 7.4(a) shows the compacted soil specimen in the test tank before desiccation. Desiccation cracks increase the migration of lime into the expansive soil through them. Therefore, for better migration of lime solution into the expansive soil, desiccation cracks were allowed to develop in the compacted soil prior to the introduction of lime slurry or lime-fly ash slurry. The compacted soil was desiccated by exposing it to the sunlight for 10 days. The temperature in the open sunlight area varies between 34 and 36˚ C. After 10 days of drying, extensive shrinkage cracks were observed on the surface of the soil, as shown in Figure 7.4(b). The drying process was continued till the water content of 10-12% was reached which is close to the natural water content of the soil. During the drying process, the soil water content reduced from 33% to 12%, and the dry density increased from 1.34 to 1.81 Mg/m^3.

Immediately after desiccation, the lime slurry was permeated through the desiccated soil by pouring 2100 cm^3 of the lime slurry into the 75 mm diameter central hole. The injection was carried out till it reached the refusal level. About 30-40 minutes was required to fill the entire 2100 cm^3 lime solution into the desiccated soil. As expected, the lime slurry preferentially permeated through the desiccated cracks. Permeation of lime slurry closed the desiccated cracks that were developed during the desiccation of soil and lead to volume change. After the slurry injection, the treated soil was covered with wet gunny bags and cured for 28 days.

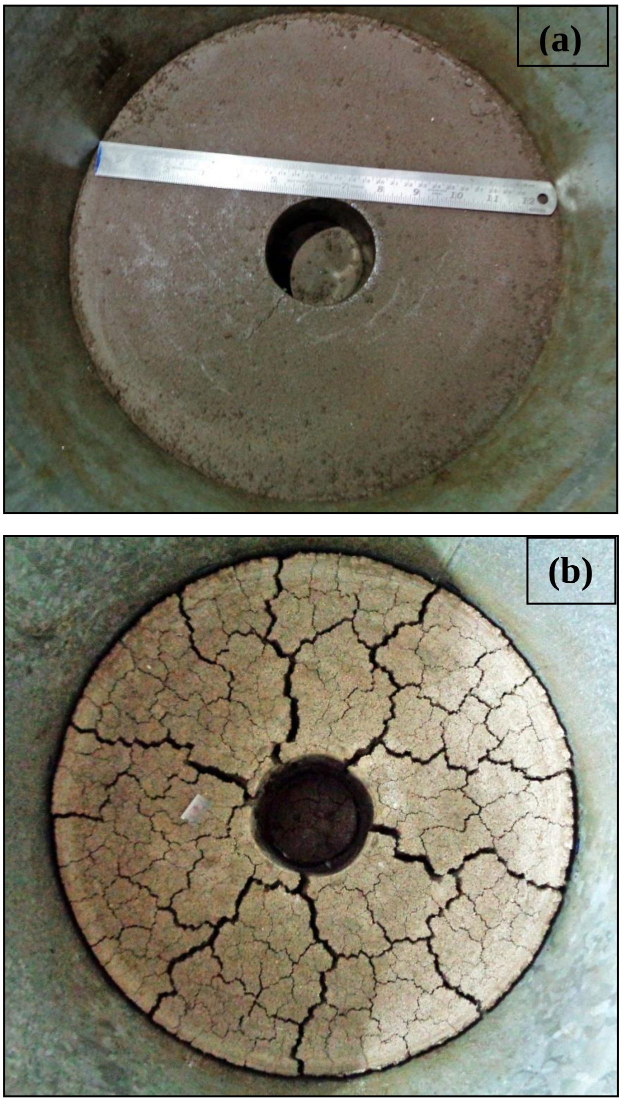

Figure 7.4: a) Compacted expansive soil in test tank and b) desiccated expansive soil

In case of lime-fly ash slurry injection, about 1900 ml of solution was injected into the desiccated soil. Similarly, for fly ash slurry injection about 2310 ml of prepared slurry solution was injected into the soil. After injection of the fly ash and lime-fly ash slurries, the treated expansive soil was cured for 28 days, similar to that of the procedure followed in case of lime slurry injected soil.

7.2.5 Cyclic Wet-Dry Tests on Treated Expansive Soil in Large Test Tanks

The schematic representation of the experimental test setup used for the volume change measurements of the untreated and treated expansive soil in the test tank is shown in Figure 7.5. After the completion of 28 days of curing in the test tank, the wet gunny bags were removed and the weight of test tanks were recorded for moisture content determination. Then the swollen thickness during the slurry injection was measured using a steel ruler. A 20 mm thick drainage layer of sand passing through 2 mm sieve (sandwiched between two non-oven geo-textiles) was provided over the expansive soil. Then the perforated electro-plated mild steel loading plate of 10 mm thickness was placed over the drainage layer. The loading plate was levelled using the spirit bubble level before placing the surcharge loads. The seating pressure of 6.25 kPa was applied using concrete cubes and steel discs. After about 60 min of application of seating load the deformation was stabilized. The soil was then inundated with tap water and the vertical deformations were measured with the aid of two 50 mm travel dial gauges of 0.01 mm least count. The soil in the test tank was allowed to swell till the swelling was negligible. Figure 7.6 illustrates the sequence of placement of drainage layer, loading plate, application of seating pressure of 6.25 kPa and arrangements for measurement of vertical deformations.

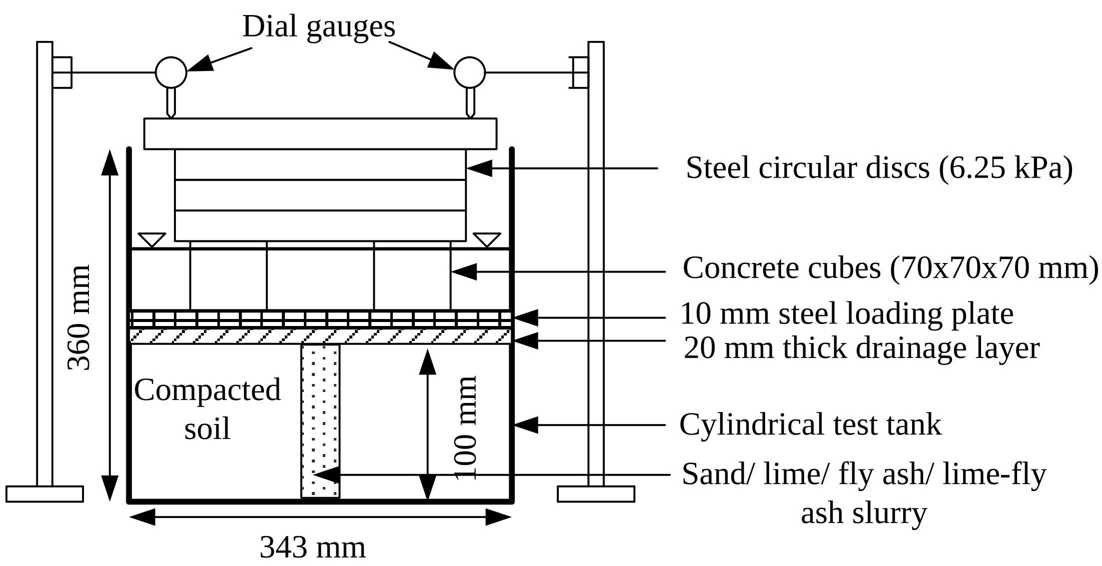

Figure 7.5: Schematic testing arrangements for swell measurement of untreated and treated expansive soils

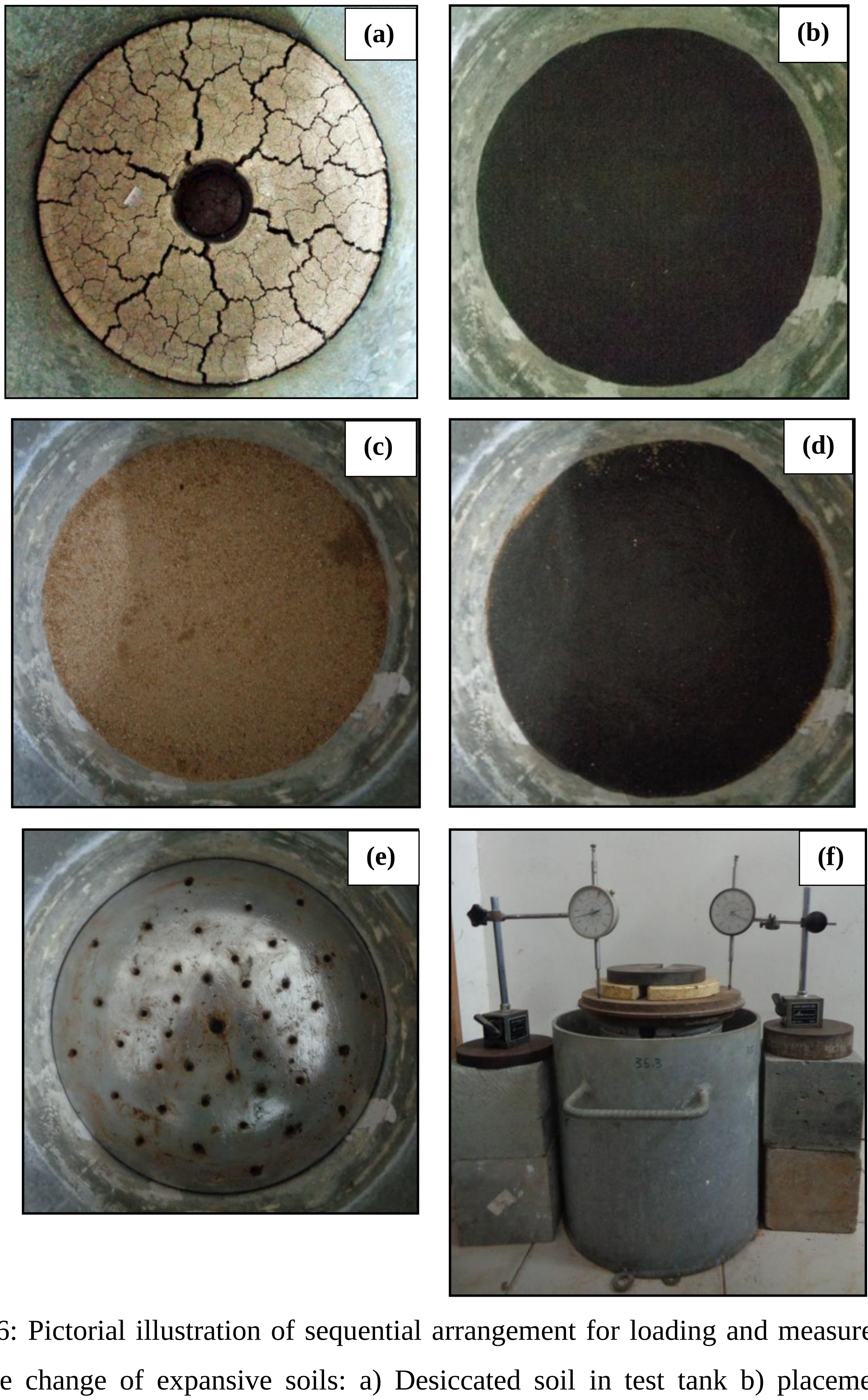

Figure 7.6: Pictorial illustration of sequential arrangement for loading and measurement of volume change of expansive soils: a) Desiccated soil in test tank b) placement of bottom geotextile layer c) placement of 20 mm thick sand layer d) placement of top geotextile layer e) placement of loading plate f) arrangements for volume change measurement after placing seating pressure of 6.25 kPa.

7.2.6 Sampling Procedure

After completion of wet-dry cycles, the soil samples were collected at radial distances of 0.9 d and 1.5 d from the centre of the slurry injection point. Figure 7.7 presents the sampling locations adopted in the present study. Sampling tubes of 38 mm diameter and 120 mm height were used for obtaining soil samples for UCS testing. Similarly, the soil samples were also collected for desiccated state free swell (DSFS) testing in 27.5 mm diameter sampling tubes. The testing procedure was already discussed in Chapter 3.

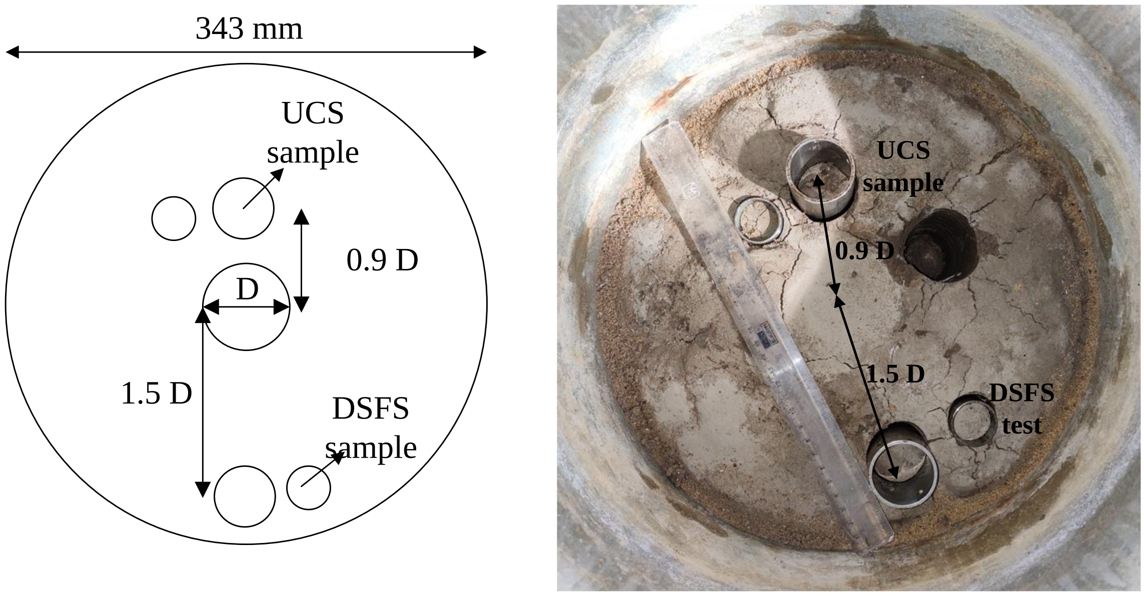

Figure 7.7: Schematic and photo image of sampling locations for UCS and DSFS samples

7.3 Results and Discussion

7.3.1 Pre-swelling of Desiccated Expansive Soil During Slurry Injection

During the process of slurry injection into the desiccated expansive soil in the test tanks through the central hole, the water content increased and the dry density decreased owing to the swelling of desiccated soil. Moreover, the slurry injection was carried out into the desiccated soil without placing any surcharge pressure over the soil. Therefore, the volume change at the surface was uneven with more volume change occurring nearer to the injection point and at the same time it may not be comparable with the volume change measured under 6.25 kPa seating pressure.

Figure 7.8 compares the amount of pre-swelling recorded in lime, fly ash and lime-fly ash slurry injected expansive soil. Further, it was observed that lime/ fly ash/ lime-fly ash slurry injected expansive soil shows almost equal amount of pre-swelling even though the water-binder ratio of slurries were different for the respective binder proportions. The present study also aimed that the measured pre-swelling of fly ash/ lime-fly ash slurry injected soil should not exceed the pre-swelling of lime slurry injected soil. For example, when water-binder ratio of 1.4 was used for fly ash slurry injection, it showed more pre-swelling with the water-binder ratio of 1.2, and the same is compared in Figure 7.8. Comparison of the pre-swelling of lime, fly ash and lime-fly ash slurry injected expansive soils reveals that the pre-swelling of fly ash slurry injected soil is higher even though the water-binder ratio was very less (1.2) and this happens mainly due to the availability of more free water in the slurry solution. Figure 7.8 also presents the water content of treated soil after slurry injection. The consequences of pre-swelling during lime slurry injection was also earlier reported by Nelson and Miller, (1992), Little (1995), Thyagaraj (2003) and Wilkinson *et al*. (2004).

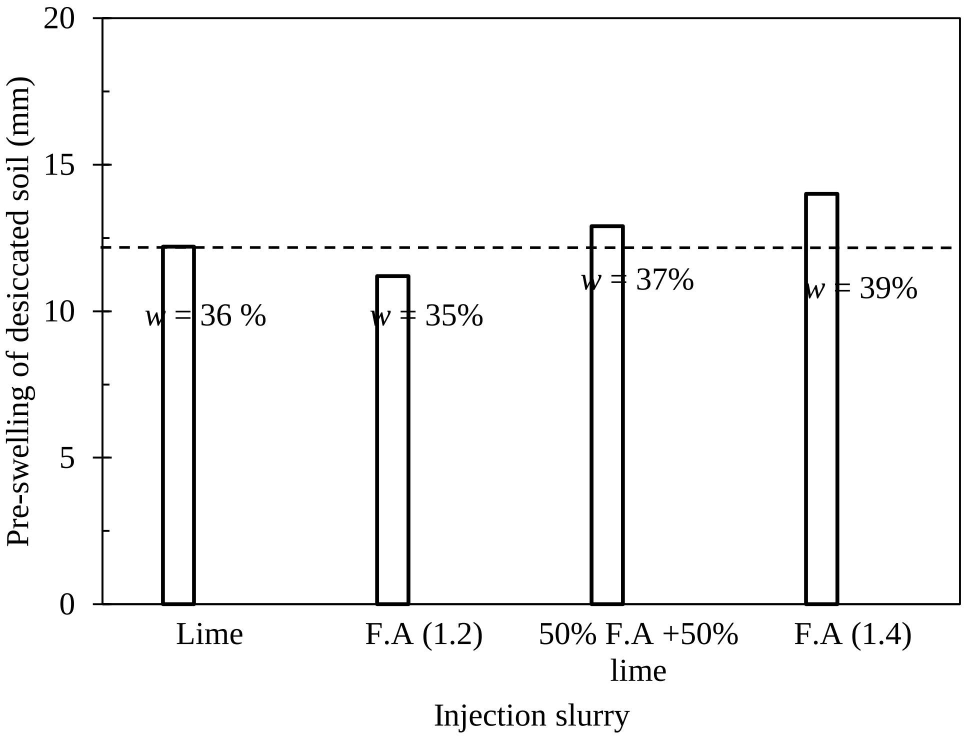

Figure 7.8: Pre-swelling of desiccated expansive soil during slurry injection (*w*: water content)

7.3.2 Effect of Wet-Dry Cycles on Untreated and Treated Expansive Soil

Figure 7.9 compares the time-swell plots of untreated and treated expansive soil during the first wetting cycle in the test tanks. Due to the volume change of expansive soil during slurry injection, the dry density of treated expansive soils decreased and it ranged between 1.24 and 1.2 Mg/m^3. Therefore for the untreated expansive soil, the volume change was measured for the compacted dry density of 1.24 Mg/m^3 instead of 1.34 Mg/m^3. The swell potential of untreated expansive soil was 6.5% (control test). For the untreated expansive soil, the central hole was filled with medium sand for better saturation and the specimen was inundated for a period of 30-40 days.

Volumetric behaviour of untreated expansive soil

During the wet-dry cycles, both vertical and lateral deformations were recorded. The wetting and drying was carried out till four cycles. Figure 7.10 presents the variation of vertical, lateral and volumetric deformations with wet-dry cycles and the equilibrium vertical, lateral and volumetric deformations were found to be 16.7%, 14% and 30.7%, respectively. The physical state of untreated expansive soil after the wet-dry cycles is presented in Figure 7.11. In is evident from Figure 7.11 that with an increase in wet-dry cycles the propagation of surface cracks also increased.

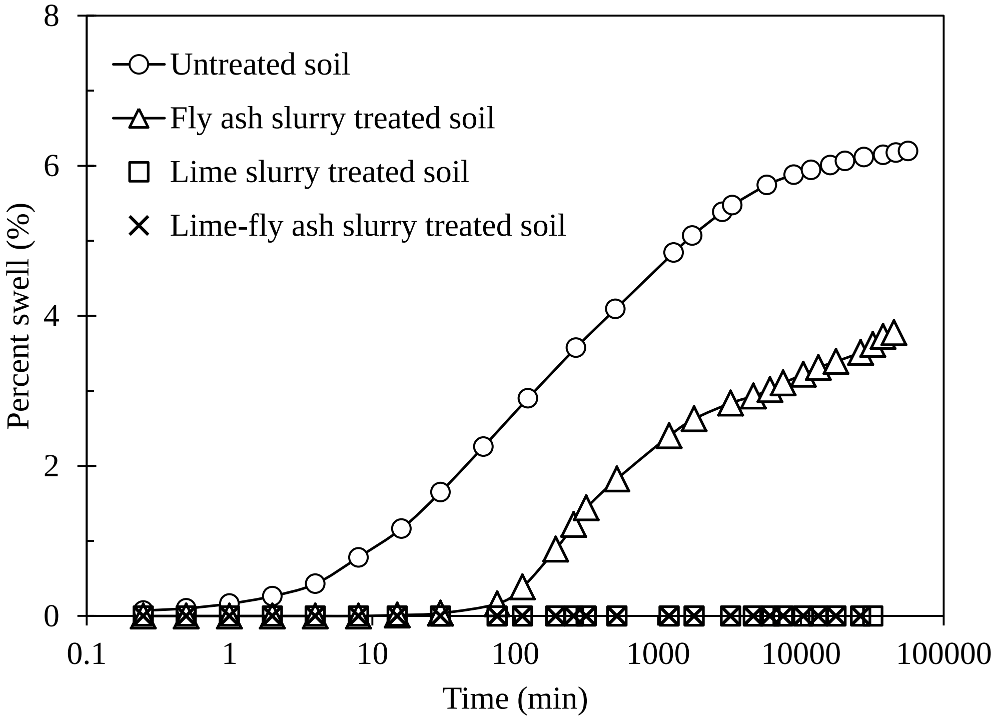

Figure 7.9: Comparison of time-swell plots of untreated and treated expansive soil with lime, fly ash and lime-fly ash slurry injection

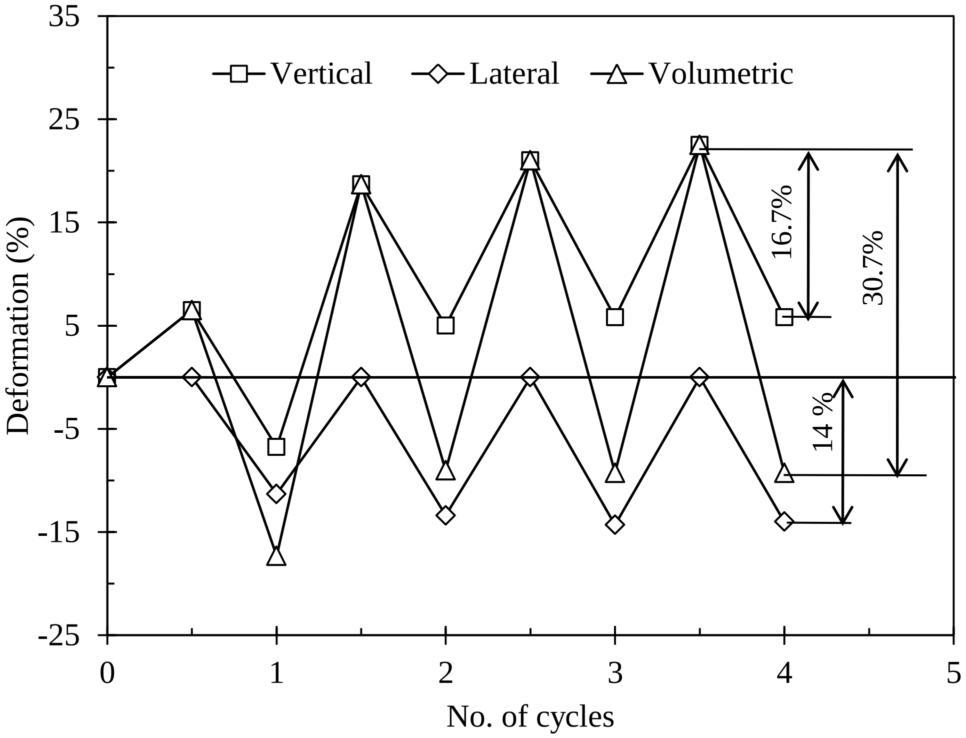

Figure 7.10: Vertical, lateral and volumetric deformations of untreated expansive soil subjected to wet-dry cycles

Volumetric behaviour of lime slurry injected expansive soil

The lime slurry injection decreased the swell potential in comparison to the swell potential of untreated expansive soil (Figure 7.9). During the lime slurry injection, the lime slurry moved through the desiccation cracks and closed the surface cracks as shown in Figure 7.12. The soil near to the injection point was more wetted when compared to the soil away from the injection point. This wetting of soil happens due to the free availability of water in the lime slurry solution. Little (1995) reported that when the lime slurry is injected into the soil, the following mechanisms may involve in the stabilization of expansive soil: a) presence of lime seams, b) pre-swelling, c) translocation and d) supernate penetration.

When the lime slurry is injected into the soil, the lime migrates and forms the slurry seams in the treated expansive soil. The presence of lime seams not only improved the strength of expansive soil but also it controlled the volume change during wetting. The lime seams also enhance the pozzolanic reactions in the adjacent soil and it makes the soil less plastic. Figure 7.12 shows the formation of seams in lime slurry treated expansive soil. The effect of pre-swelling was already discussed in the previous section.

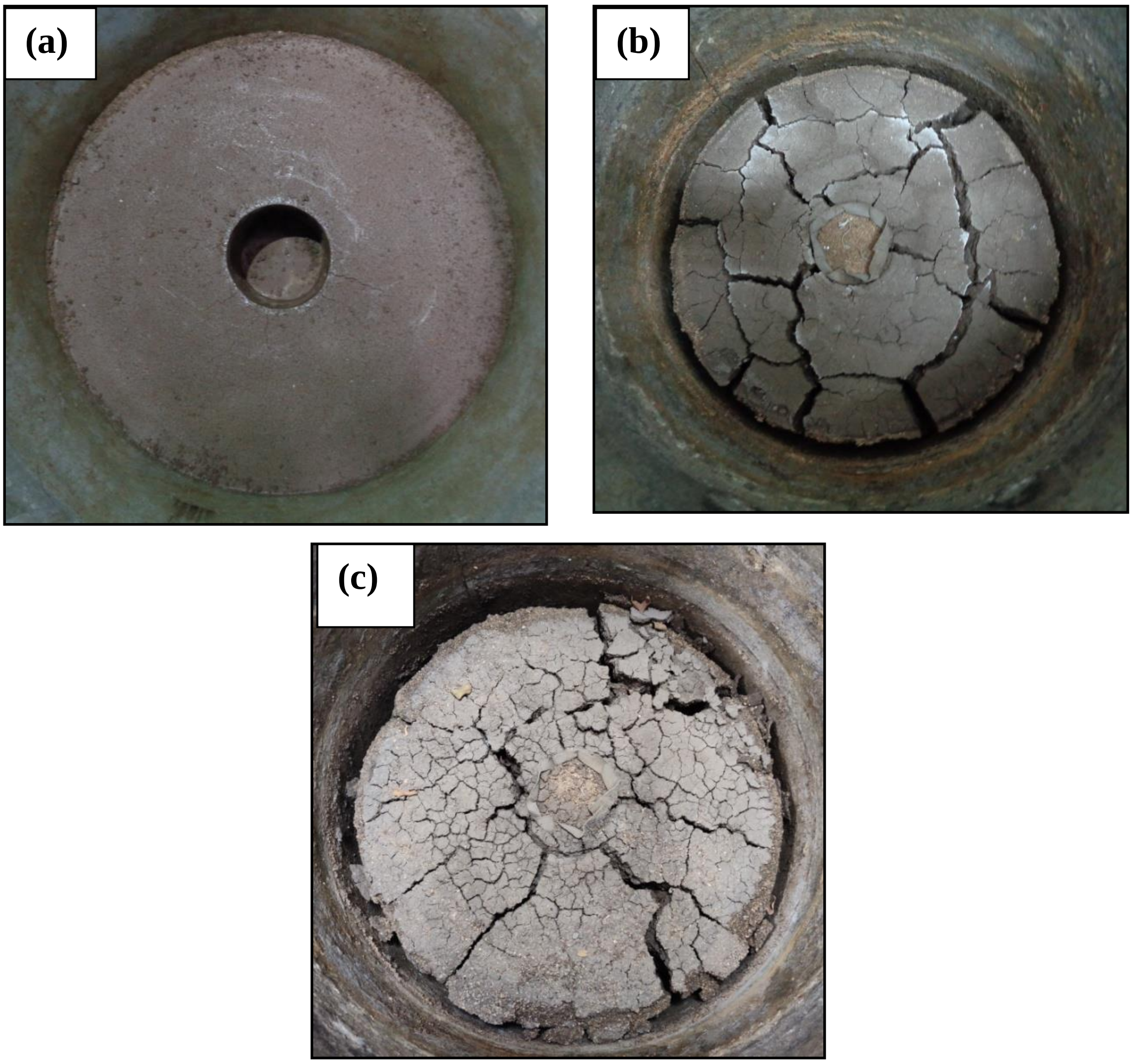

Figure 7.11: Physical state of untreated expansive soil before and after subjected to wet-dry cycles: a) compacted state b) after second drying cycle c) after third drying cycle

After the lime slurry treatment, the lime seams may migrate or translocate to the adjacent soil, and thereby, it modifies the intrinsic behaviour of the expansive soil. The continuous migration of slurry solution may form interconnected thin sheets of traces of lime and lime seams.

Table 7.2 presents the pH and pore salinity of lime slurry solution used in the present study. The lime slurry solution used for the treatment has a pH value of 12.76. Due to the high pH of the lime solution, it might be drawn into the soil either by diffusion or higher soil suction in dry condition. Petry (1980) also highlighted this mechanism.

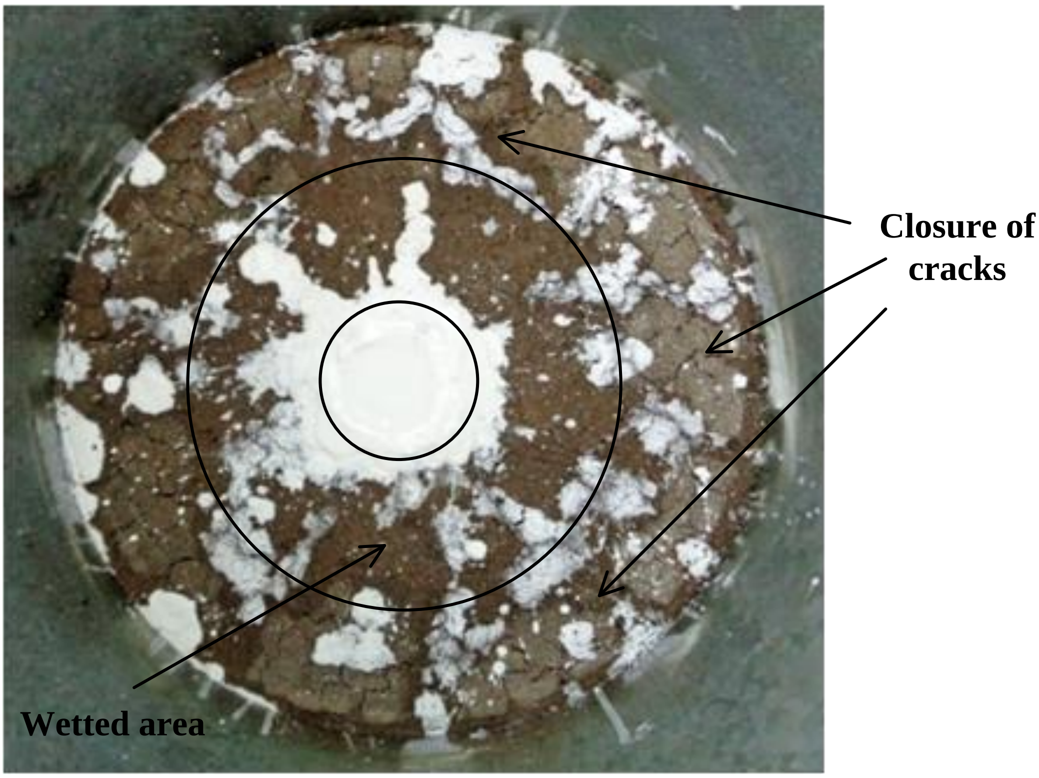

Figure 7.12: Injection of lime slurry into the desiccated expansive soil

Figure 7.13 compares the vertical, lateral and volumetric deformations of untreated and lime slurry treated expansive soil during wet-dry cycles. During the first cycle of wetting, the lime slurry treated soil showed almost zero volume change. However, with the increase in wet-dry cycles, the volume change increased as can be seen in Figure 7.13. At the end of the fourth wetting cycle, the volumetric deformation of lime slurry treated specimen increased from 0 to 10.6% and the water content also increased from 36% to 41.5%. But still, the volumetric deformation of lime slurry treated soil (10.6%) was much lower than that of untreated expansive soil (30.7%). The lateral deformation of the treated soil remains zero percentage during all the four wet-dry cycles as can be seen in Figures 7.13 and 7.14. Thus both vertical and volumetric deformations are equal during wet-dry cycles. After the first drying, the cracks were not observed at the surface, but the cracks started to appear with the increase in the drying cycles as can be seen in Figure 7.14. However, the intensity and area of cracks were much lower in comparison to the untreated expansive soil (Figures 7.11 and 7.14). This shows that the lime slurry treatment is effective in controlling the volume change to a greater extent.

Table 7.3 pH and pore salinity of expansive soil, lime, fly ash and lime-fly ash slurry solutions

Soil / slurry solution	**pH**	**Pore salinity (mg/l)**
Expansive soil	8.0	601
Lime slurry	12.76	4872
Fly ash slurry	7.50	1410
Lime-fly ash slurry	12.65	4102

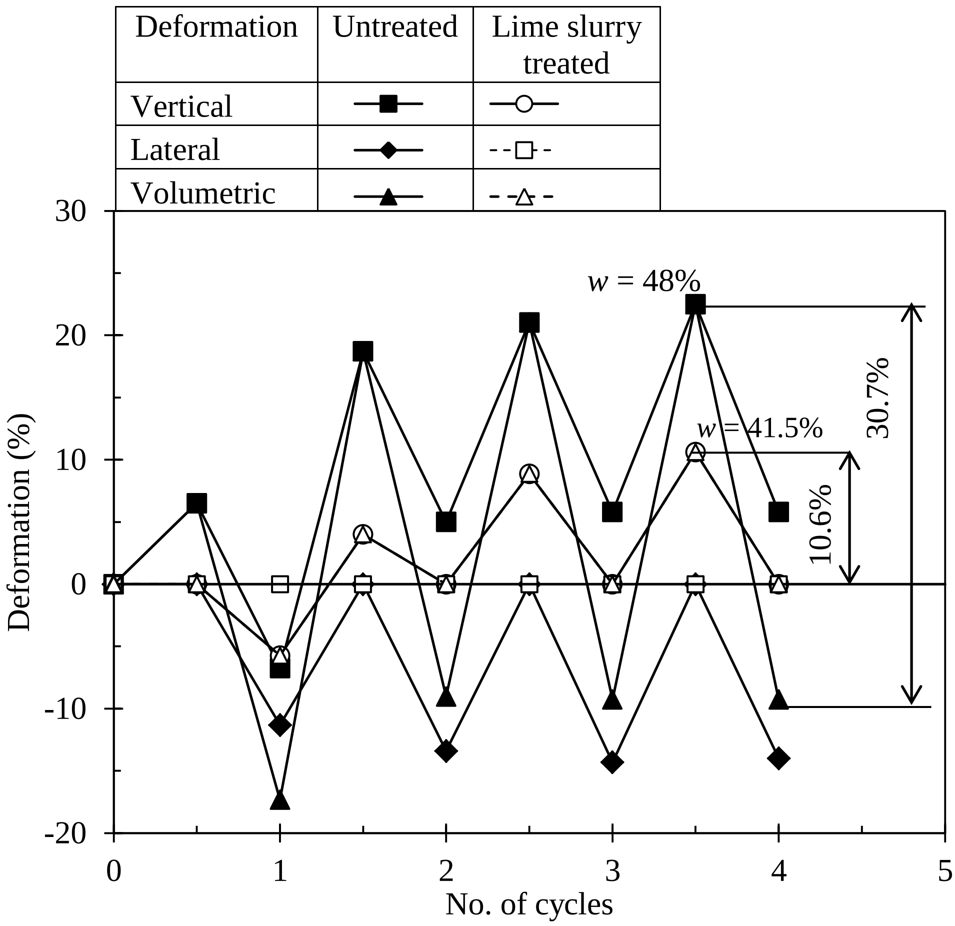

Figure 7.13: Comparison of vertical, lateral and volumetric deformations of untreated and lime slurry treated soil subjected to wet-dry cycles (*w*: water content)

Volumetric behaviour of fly ash slurry injected expansive soil

Figure 7.15 compares the vertical, lateral and volumetric deformations of untreated and fly ash slurry treated expansive soil during wet-dry cycles. Fly ash slurry treatment improved the expansive soil marginally i.e. the volumetric deformation of treated soil was 26.7% whereas for untreated soil it was 30.7%. The water content at the end of fourth wetting cycle is calculated as 46% for fly ash slurry treated soil against the untreated soil water content of 48%.

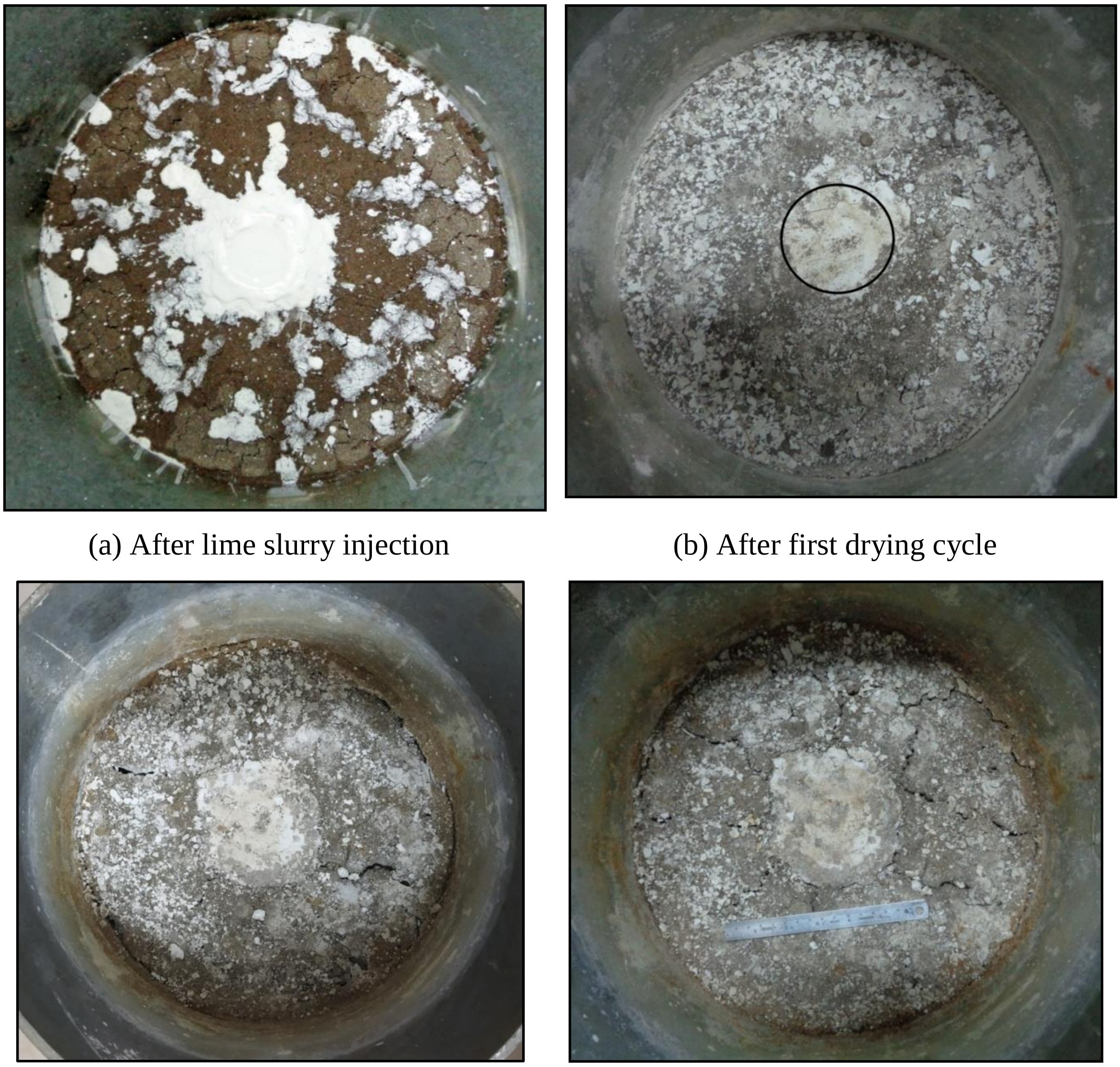

(a) After lime slurry injection (b) After first drying cycle

(c) After second drying cycle (d) After third drying cycle

Figure 7.14: Images of lime slurry treated expansive soil in test tank after different wet-dry cycles

The inefficiency of the fly ash slurry treatment is attributed to the low pH of the fly ash slurry solution (Table 7.2). Figure 7.16 presents the images of fly ash slurry treated expansive soil subjected to wet-dry cycles. The formations of cracks were similar to that of untreated soil which points out to the marginal improvement using fly ash slurry. The fly ash slurry in the desiccated cracks acted as addition of inert fine sand size particles which improves the volumetric behaviour marginally. Additionally, the low amount of lime in the class F fly ash only caused modification reactions to occur and not the pozzolanic reactions. This is also evident from the pH of fly ash slurry treated expansive soil (Table 7.3). Further, the fly ash migration into the desiccated soil was lower in comparison to the lime slurry migration owing to the relatively large size particles of fly ash. As the amount of lime in the fly ash is very low, this lime was contained within the fly ash seams and as a result it did not diffuse into the surrounding expansive soil. Furthermore, during the subsequent wetting cycles, the fly ash provides easy access to water and wets the expansive soils over a greater depth and leads to greater swelling, similar to the behaviour of untreated expansive soil.

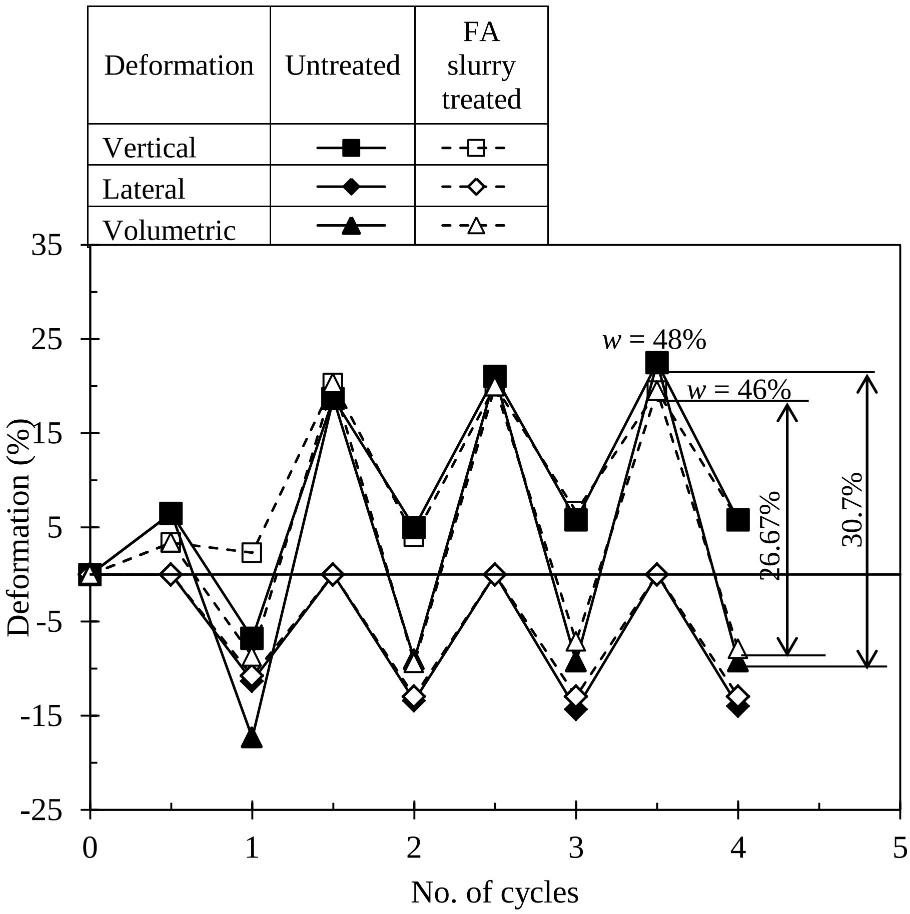

Figure 7.15: Comparison of vertical, lateral and volumetric deformations of untreated and fly ash slurry treated expansive soil (*w*: water content)

Volumetric behaviour of lime-fly ash slurry injected expansive soil

As discussed in the above section, the injection of fly ash slurry into the desiccated expansive soil was not effective in controlling the volume change and it is attributed to low amount of lime in the fly ash. This resulted in low pH of fly ash slurry, which is not conductive for pozzolanic reactions. Therefore, additional lime was added to fly ash to increase the free lime availability in the fly ash and to increase the pH to the levels which are conductive for pozzolanic reactions. Thus addition of lime increased the pH of lime-fly ash slurry. The stabilization mechanism of lime-fly ash slurry injection in stabilizing the expansive soil is similar to that of the lime slurry injection mechanics. However, the lime-fly ash slurry is advantages as it fills the macro voids (shrinkage cracks) with the cementitious lime-fly ash slurry and it is better than that occurs in the lime slurry treated expansive soil (Figures 7.12 and 7.17).

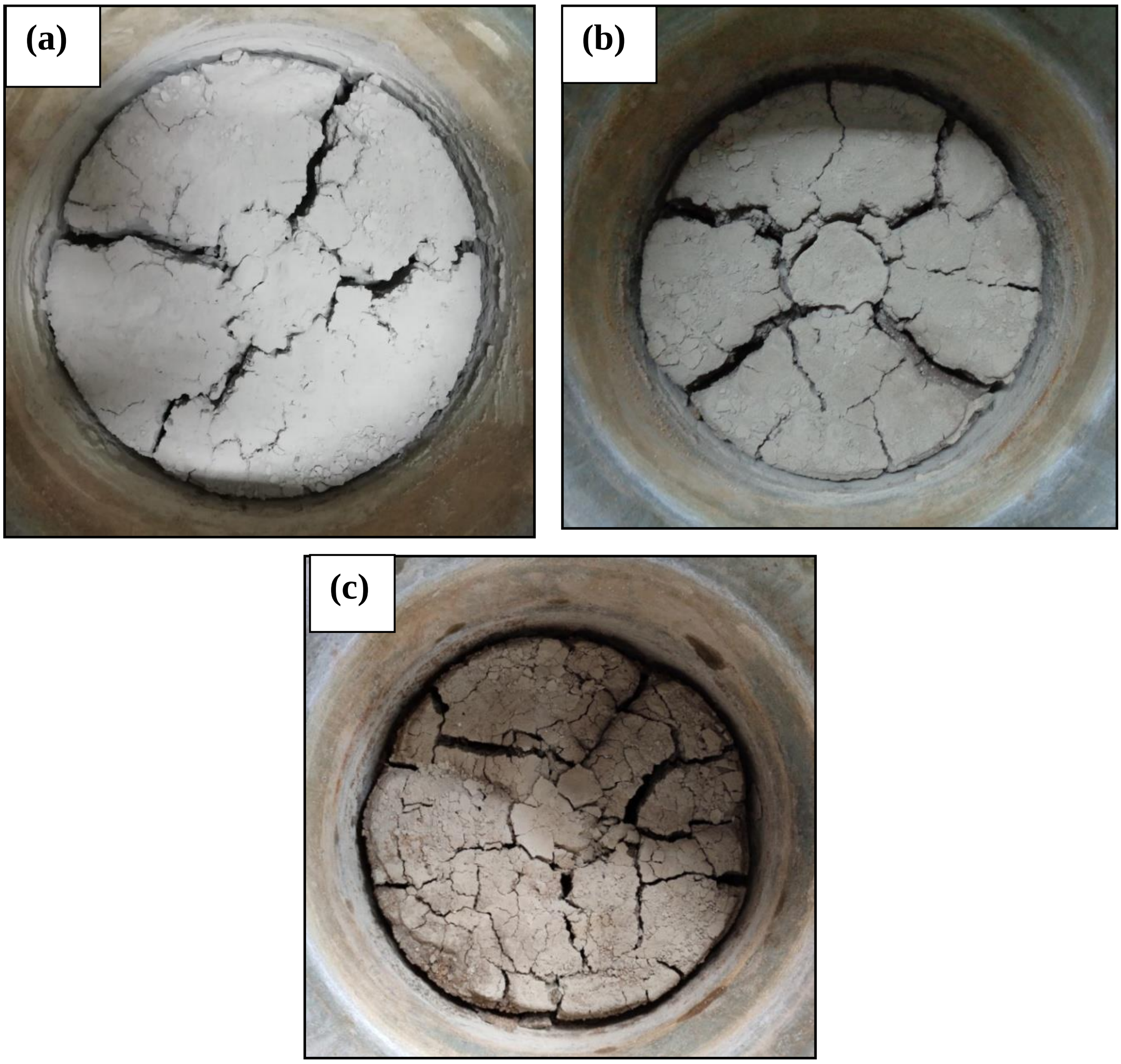

Figure 7.16: Images of fly ash slurry treated expansive soil after different wet-dry cycles: a) after first drying cycle b) after second drying cycle and c) after third drying cycle

Figure 7.17 presents the 28 days cured lime-fly ash slurry treated expansive soil where the lime-fly ash slurry seams are clearly visible. During the first cycle of wetting, the soil underwent no volume change. Earlier studies (Kayes *et al*. 2000; Wilkinson *et al*. 2010) also reported that lime-fly ash slurry treated expansive soil showed improvement in both strength and volume change characteristics.

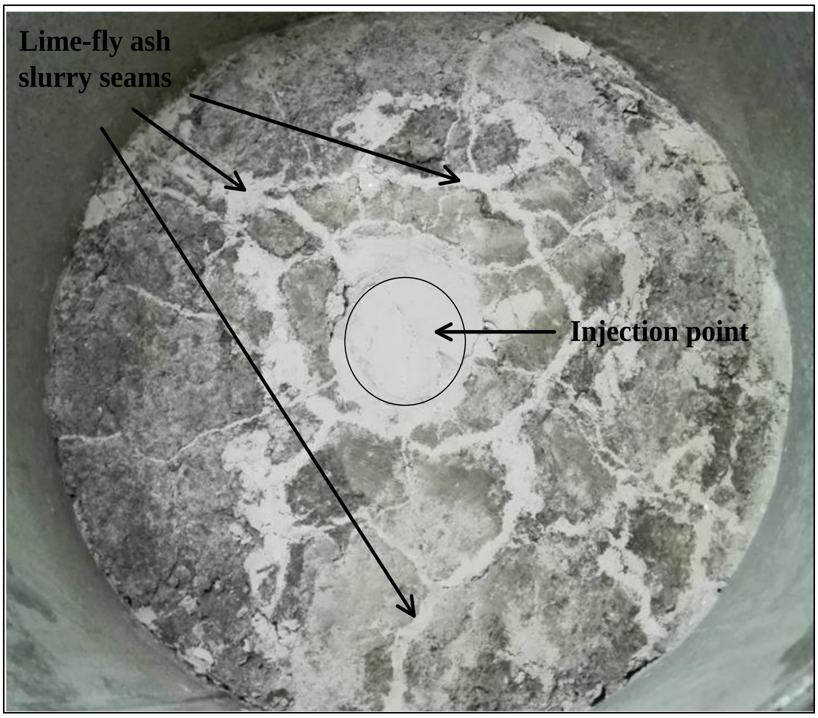

Figure 7.17: Image of lime-fly ash slurry injected expansive soil in test tank at the end of 28 days of curing

However, when the soil was subjected to wet-dry cycles, the volume change started to increase. After four cycles of wetting, the volumetric deformation was measured to be 13.64%, whereas for untreated soil, it was observed as 30.7% (Figure 7.18). Similar to the lime slurry treatment, the efficiency of lime-fly ash slurry treatment decreased with wet-dry cycles. However, the degree of improvement of lime-fly ash slurry was slightly lower in comparison to the lime slurry treatment, and the variation in treatment was mainly due to the presence of silt size particles in the lime-fly ash slurry which may not enhance the flow of slurry to a greater extent even though it was checked for its flow characteristics. The propagation of cracks in lime-fly ash slurry treated expansive soil with wet-dry cycles is shown in Figure 7.19.

Comparison of volumetric behaviour of expansive soil treated with different slurries

Figure 7.20 compares the vertical, lateral and volumetric deformations of slurry treated expansive soil with untreated expansive soil. As discussed earlier, the final degree of improvement of expansive soil is mostly governed by the pH and pore salinity of the slurry solutions used for the treatment. As can be seen from Figure 7.20, the lime slurry injection shows a significant improvement in the expansive soil which reduced the vertical deformation to 10.6% and lateral deformation to 0%. Further, the total volumetric deformation reduced to 10.6% from 30.7%, and this is equivalent to 65% reduction in the swelling capacity.

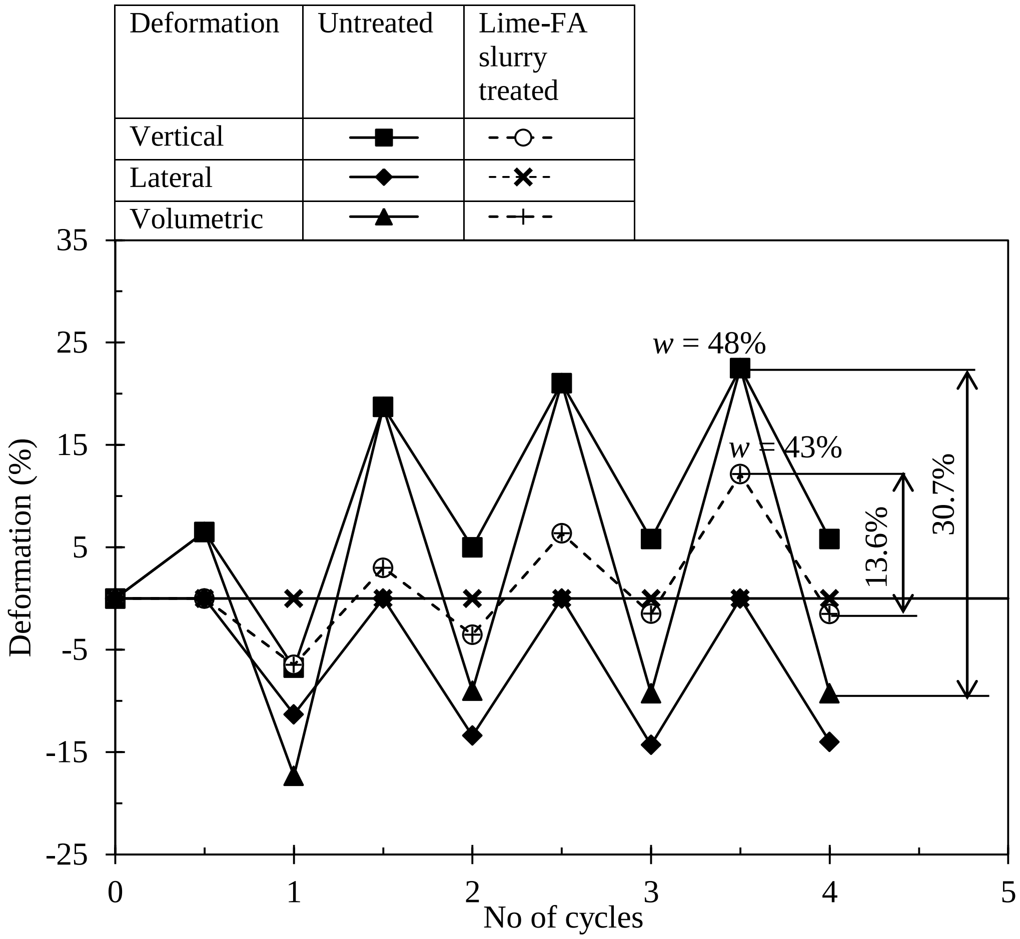

Figure 7.18: Comparison of vertical, lateral and volumetric deformations of untreated and lime-fly ash slurry treated expansive soil (*w*: water content)

The fly ash slurry injected soil showed only marginal reduction in vertical and lateral deformations. Moreover, the injection of fly ash slurry could reduce the swelling of the soil from 30.7% to 26.7% only. Whereas, the behaviour of lime-fly ash slurry treated soil was almost similar to the lime slurry treated soil (Figure 7.20). The addition of lime to fly ash has increased the pH and pore salinity of the slurry (Table 7.3) and this also resulted in the significant improvement in the treated soil. Due to lime-fly ash slurry injection, the swelling capacity of the treated soil reduced by 55.7%. Therefore, instead of lime slurry, the lime-fly ash slurry can be used as an alternate for deep stabilization of expansive soil in desiccated state. Moreover, the implementation of lime-fly ash slurry injection may reduce the consumption of lime for the soil treatment where more quantity of lime is required for mass stabilization of soil.

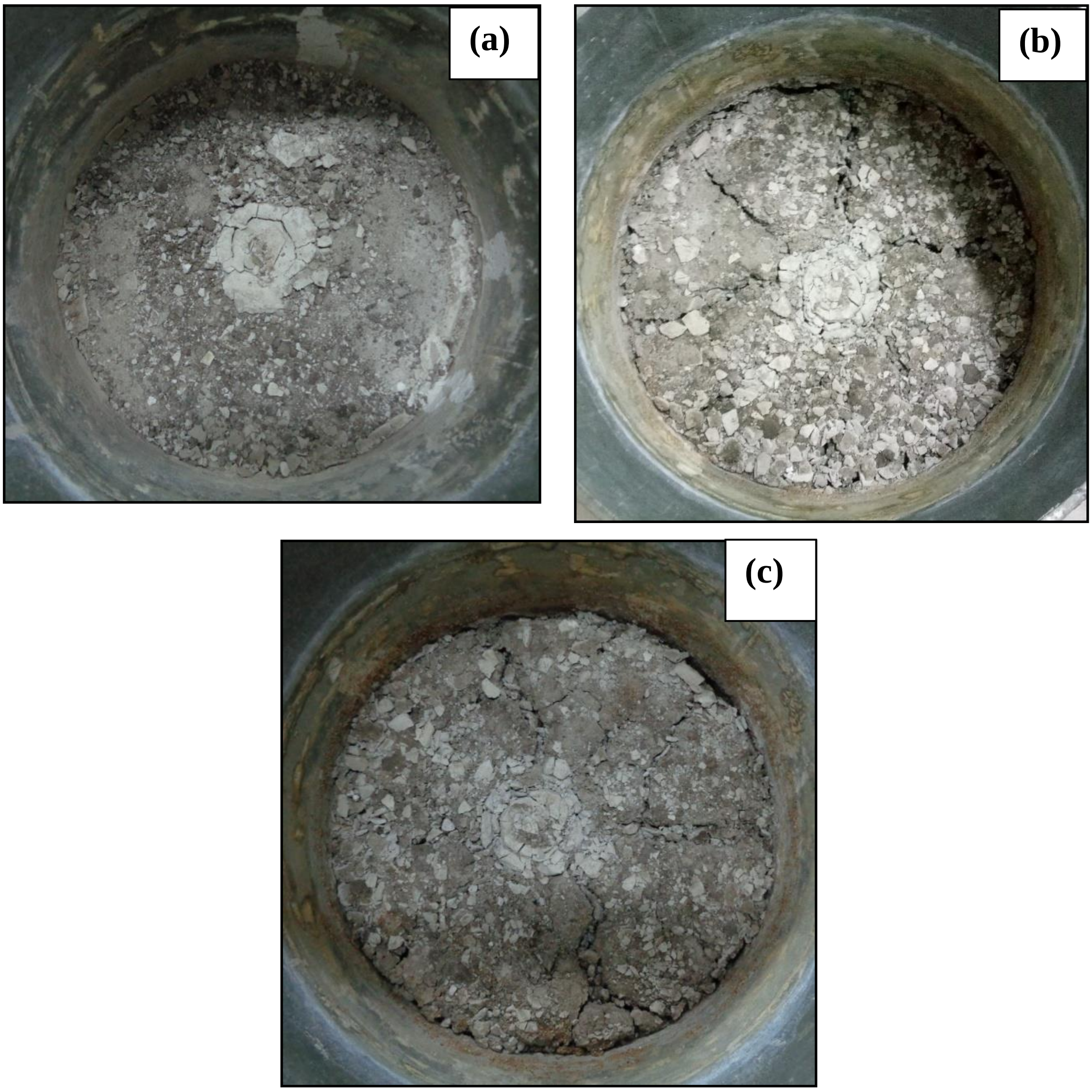

Figure 7.19: Image of lime-fly ash slurry treated expansive soil after different wet-dry cycles: (a) after first drying cycle (b) after second drying cycle and (c) after third drying cycle

Quantification of desiccation cracks of untreated and slurry treated expansive soils after different wet-dry cycles

In order to trace the propagation of desiccation cracks with increase in wet–dry cycles, the digital camera images of untreated and slurry treated expansive soils in desiccated state in the test tanks were captured at the end of drying cycles. 'ImageJ' software was used to calculate the percentage of shrinkage cracks by applying the binary image processing technique.

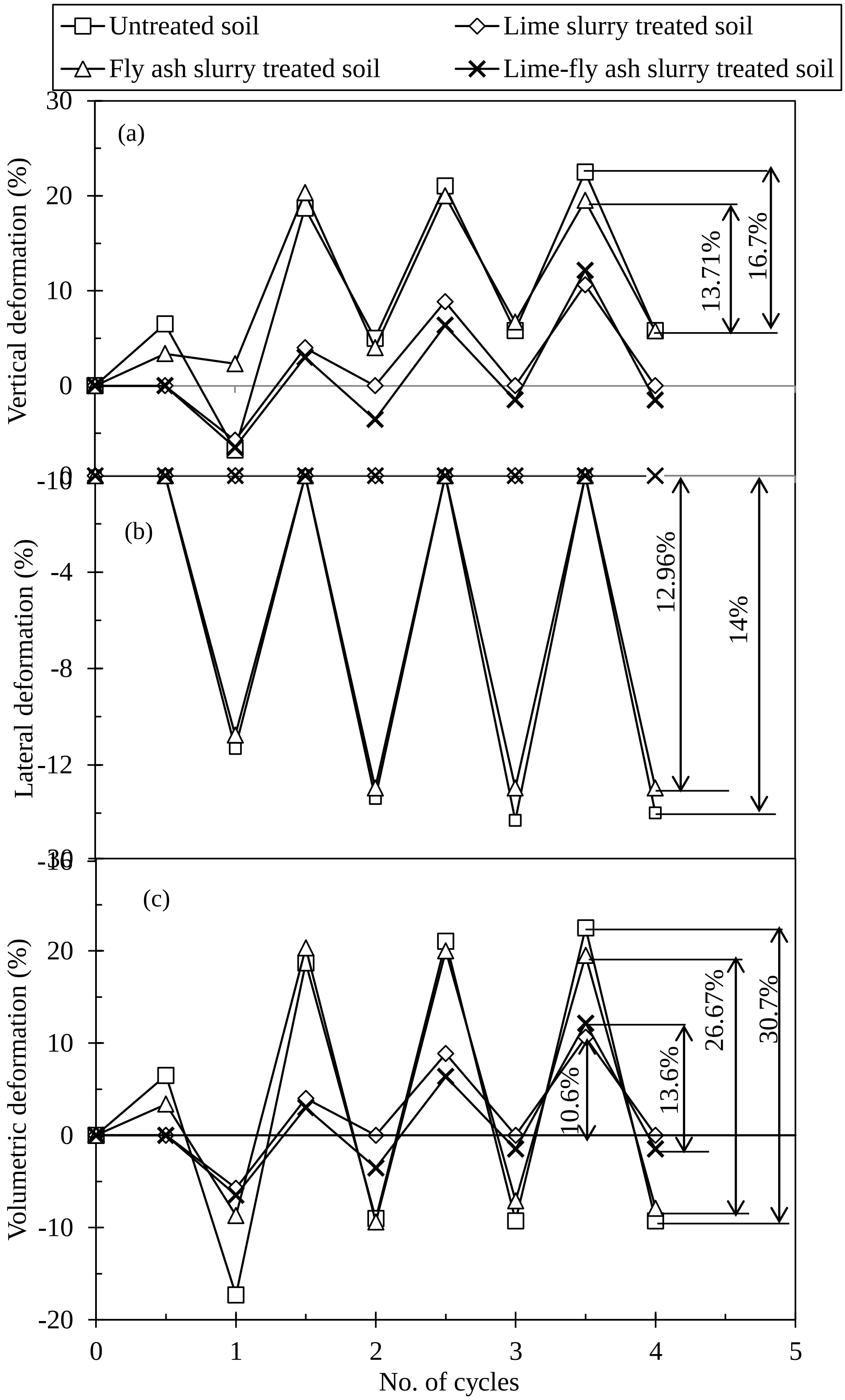

Figure 7.20: Comparison of volume change of untreated expansive with slurry treated expansive soils during wet-dry cycles: a) vertical deformation b) lateral deformation and c) volumetric deformation

The image of the untreated expansive soil (or treated expansive soil) was analyzed and the total surface area of the desiccated soil was selected with the help of circle or oval selection tool. Furthermore, the required area of interest was cropped using the cropping tool. After selecting the area of interest, the 'analyse tool' was used to calculate the total surface area of the soil specimen (A_T), and this area includes the area of cracks. Then to separate the area of the cracks from the total surface area, a threshold value of around 30 and 55 was used for the further analysis, following Julina and Thyagaraj (2018). After that, the image was converted into a black and white binary image, where the black colour represents the surface cracks, and the white colour represents the soil surface. Figures 7.21 (a) and (b) present the captured image and converted binary image of desiccated expansive soil used for the analysis, respectively. Figure 7.22 presents the binary images of untreated and slurry treated expansive soils subjected to different wet-dry cycles. By using 'Edit – selection – create selection' tool in ImajeJ, the area of soil surface excluding cracks (A_S) was found out. Then the area of the cracks (A_C) was calculated by subtracting the soil area from the total surface area. From the analysis, the percentage of cracks at soil surface after desiccation was calculated using equation (7.1)

$$\text{Percentage of cracks} = \frac{A_T - A_S}{A_T} \times 100 = \frac{A_C}{A_T} \times 100 \tag{7.1}$$

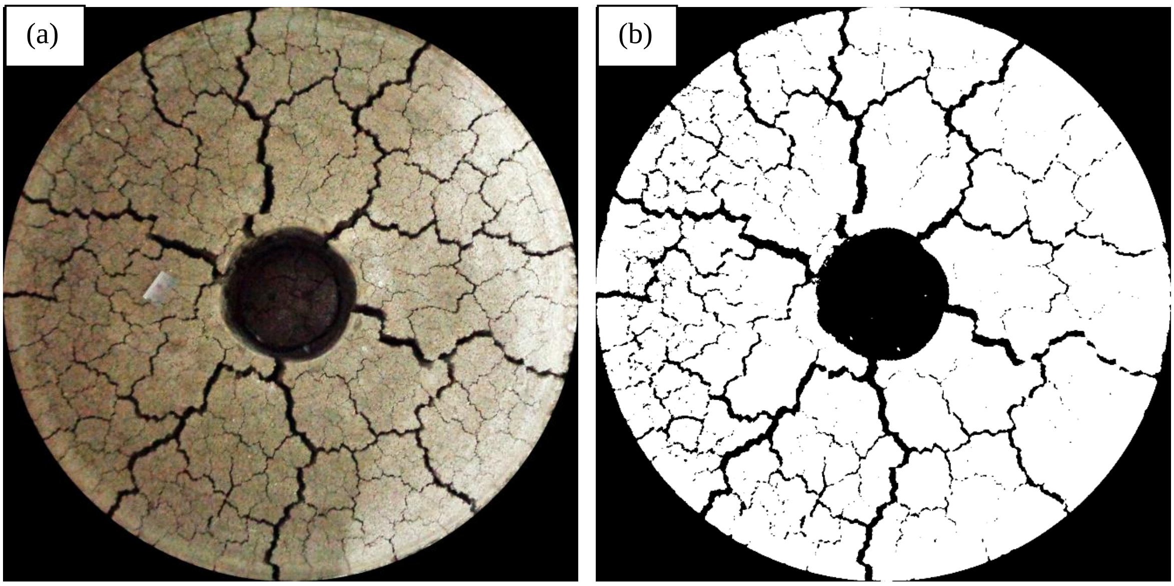

Figure 7.21: Images of: (a) desiccated expansive soil (b) converted binary image of desiccated expansive soil

	After first drying cycle	After second drying cycle	After third drying cycle
(a)	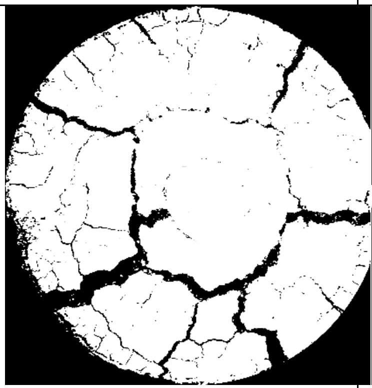	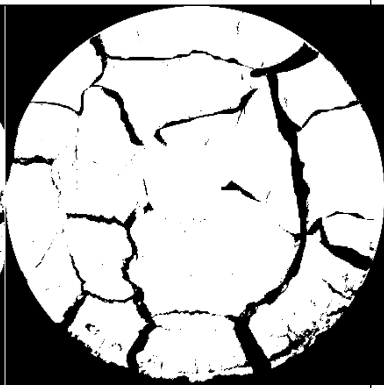	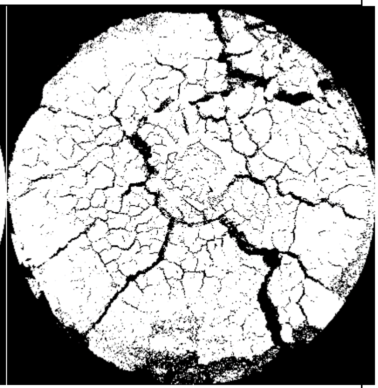
(b)	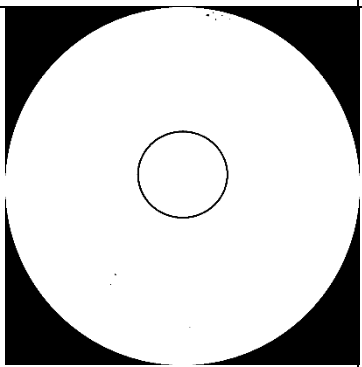	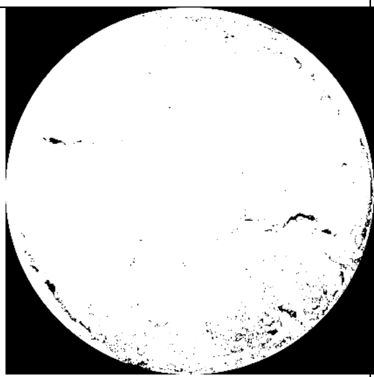	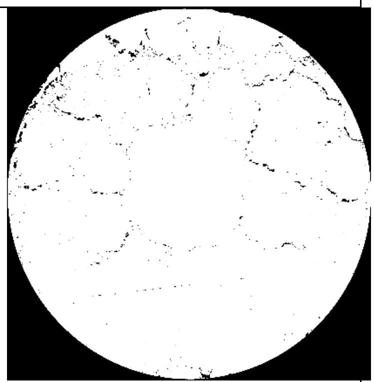
(c)	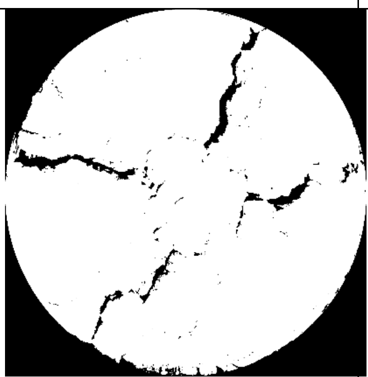	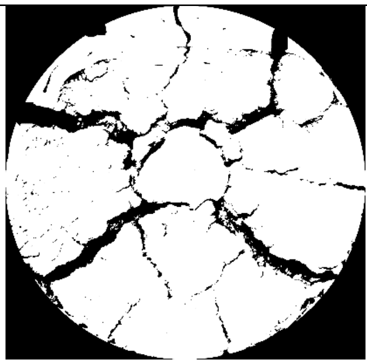	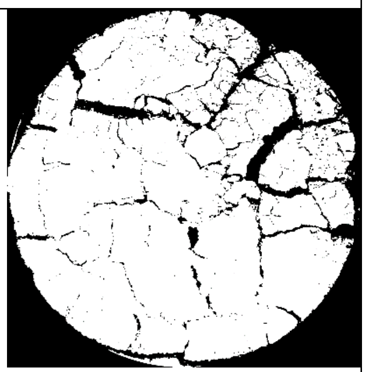
(d)	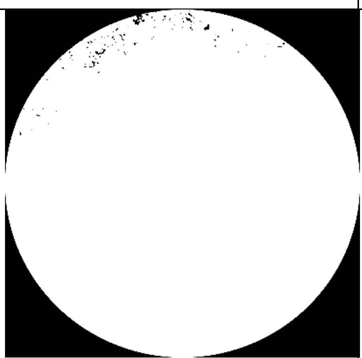	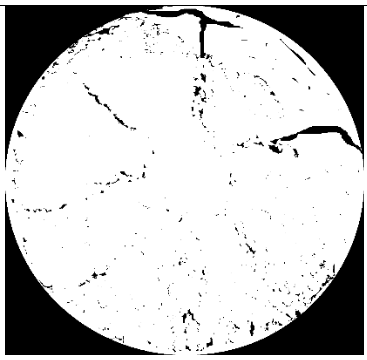	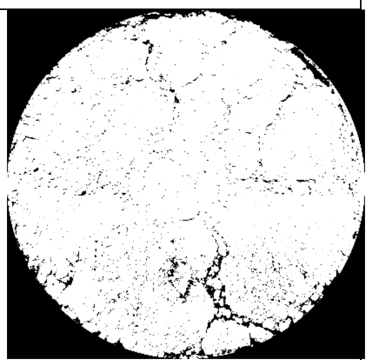

Figure 7.22 Comparison of binary images of untreated and slurry treated expansive soils: (a) untreated soil (b) lime slurry treated soil (c) fly ash slurry treated soil d) lime-fly ash slurry treated soil

Figures 7.23 shows the growth of the cracks area of untreated and slurry treated expansive soils with increase in wet-dry cycles. As can be seen in Figure 7.23, in untreated expansive soil, the percentage of cracks area at the soil surface increased with increase in wet-dry cycles. At the end of third drying cycle, the total percentage of cracks area of untreated soil was found as 31.9% (Figure 7.23c).

The slurry treatment was carried out in desiccated condition of expansive soil. At desiccated condition, the percentage of surface cracks area was calculated as 8.63% and annular gap as 7.43% (the expansive soil was desiccated from the compacted placement condition of 33% water content and 1.41 Mg/m^3 dry density). Further, after lime slurry injection, the percentage of cracks was reduced to 0.56% at the end of first drying cycle, and it slightly increased to 1.18% at the end of third drying cycle (Figure 7.23c). At the same time, the annular gap (i.e. the lateral shrinkage) disappeared with lime slurry treatment (Figure 7.23 (b)). However, these desiccation cracks were much lower than the percentage of cracks of untreated soil (31.9%).

At the end of the first drying cycle of fly ash slurry treated soil, the percentage of surface cracks was found to be 4.25% and it further increased to 12.77% at the end of the third drying cycle. Moreover, the area of annular gap of fly ash slurry treated soil was almost same as that of the annular gap developed in untreated expansive soil (Figure 7.23b). Even though the total percentage of cracks of fly ash slurry treated soil (25.70%) was lower than the untreated expansive soil (31.9%), it is much the higher than the percentage of cracks observed in lime slurry treated expansive soil (1.18%). Similarly, for the lime-fly ash slurry treated expansive soil, at the end of the first drying cycle, the total percentage of cracks was 0.28% and it increased to 5.37% at the end of third drying cycle (Figure 7.23c). As observed in lime slurry treated soil, the annular gap formation disappeard in lime-fly ash slurry treatment. The lime-fly ash slurry treated expansive soil showed a significant reduction in the traces of shrinkage cracks in comparison to the fly slurry treated soil. However, it is slightly higher than the percentage of cracks observed in lime slurry treated soil.

7.3.3 Properties of Slurry Treated Expansive Soil After Four Wet-Dry Cycles

The protocol for sampling and sampling locations of slurry treated expansive soil after four wet-dry cycles in test tank and specimen preparation for testing was already detailed in the Section 7.2.6.

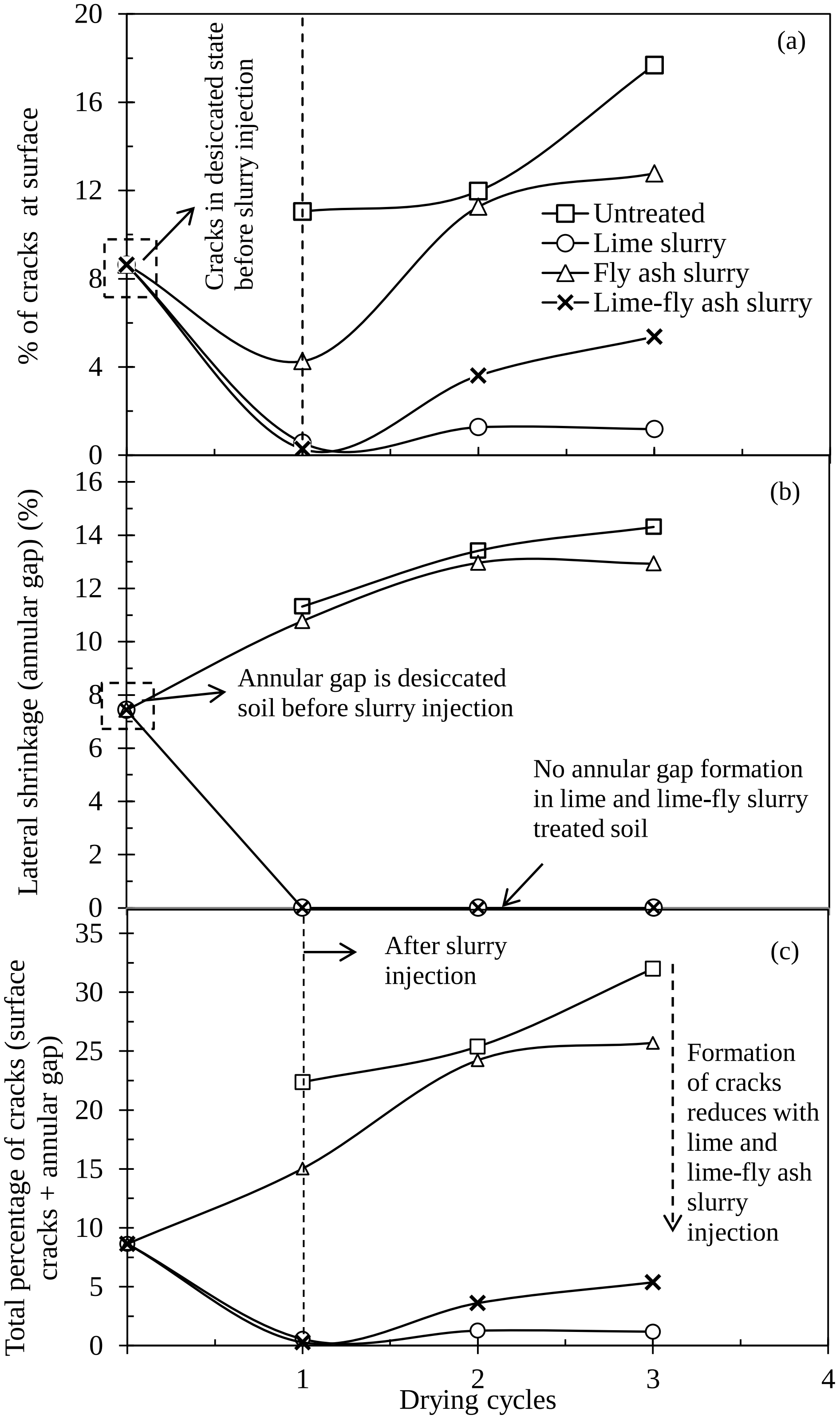

Figure 7.23: Comparison of propagation of cracks with wet-dry cycles of untreated and slurry treated expansive soils: a) percentage of surface cracks, b) annular gap (lateral shrinkage) and c) total percentage of cracks (surface cracks + annular gap)

Physico-chemical properties

The pH and pore salinity of the slurry treated expansive soil after wet-dry cycles are listed in Table 7.4. Both pH and pore salinity values of lime and lime-fly ash slurry treated soil specimens after four wet-dry cycles decreased. Moreover, the difference between the pH values of specimens collected from 0.9d and 1.5d locations is marginal. Earlier works (Rao and Thyagaraj, 2003; Thyagaraj and Suresh, 2012) reported that pH of lime slurry treated specimens increased to 11.85-12.16. However, the values reported pertain to the 10-15 days cured lime slurry treated specimens which were not subjected to wet-dry cycles.

Table 7.4 pH and pore salinity variation of the slurry treated specimens after four wet-dry cycles

Specimen condition	Sampling location	pH	Pore salinity (mg/l)
Untreated	-	8.0	601
Lime slurry injection	0.9 d	9.75	890
	1.5 d	9.34	787
Fly ash slurry injection	0.9 d	7.98	705
	1.5 d	8.01	673
Lime-fly ash slurry injection	0.9 d	9.65	923
	1.5 d	9.17	905

The lower values of pH and pore salinity in the present study are attributed to leaching of lime from the treated soil. This resulted in the increase in swelling with wet-dry cycles. The pore salinity of lime-fly ash slurry treated soil was slightly higher than the lime slurry treated soil and this might be due to the intermixing of fly ash particles with the soils where fly ash has higher pore salinity than the soil.

Index properties

Figures 7.24 (a) and (b) compare the grain size distribution curves of untreated and treated and slurry treated expansive soils collected from 0.9d and 1.5d, respectively. The slurry treated soil specimens show a significant decrease in the percentage of clay fraction with respect to the untreated specimen, and this reduction was more pronounced in lime slurry treated soil specimens. Further, the specimens collected at a radial distance of 0.9d showed greater reduction in comparison to the soil specimens collected at 1.5d radial distance.

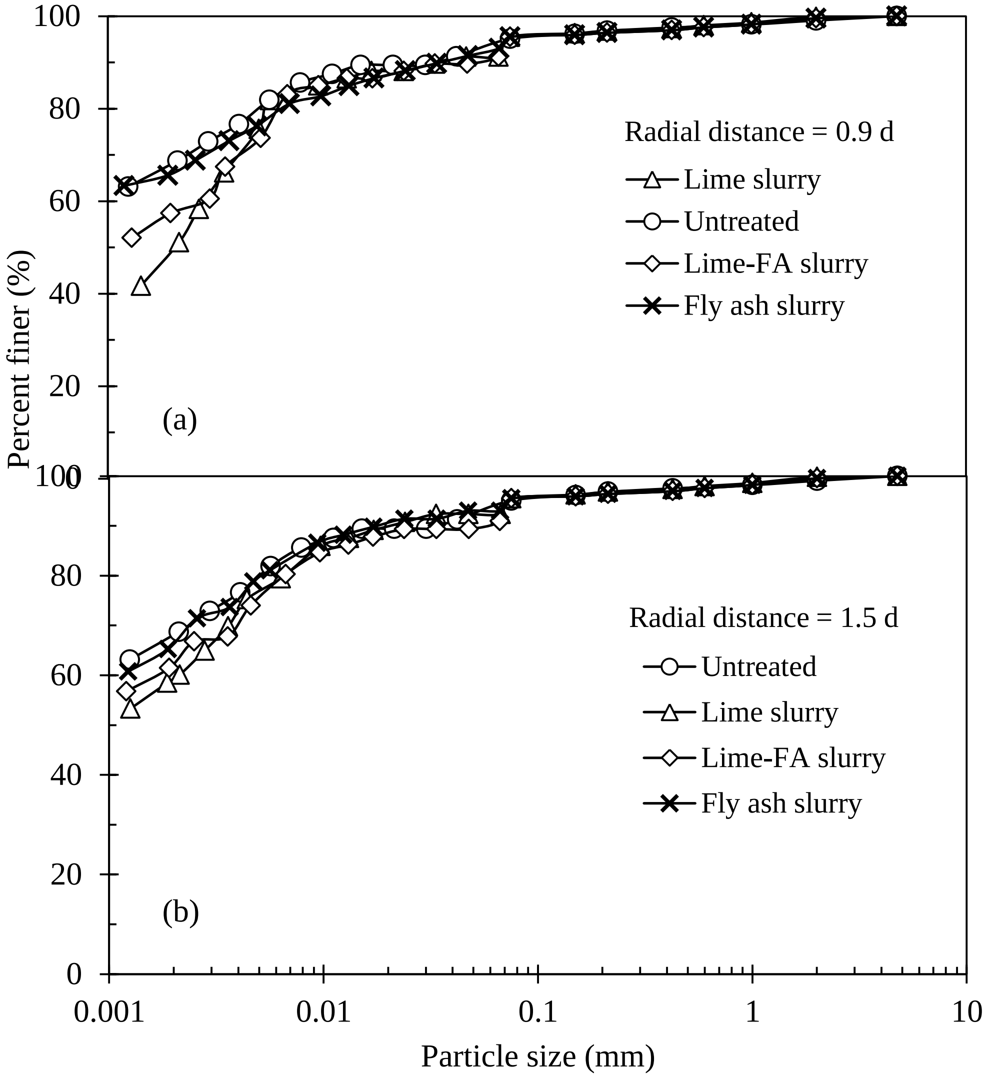

Figure 7.24: Comparison of grain size distribution curves of untreated and slurry treated expansive soil specimens cored at radial distances of: a) 0.9 d and b) 1.5 d (where d is the diameter of central injection hole).

The decrease in the clay fraction was mainly attributed to the pozzolanic reactions which alter the clay particles to coarser fraction and render them less plastic (Little, 1995; Rao *et al*. 2001; Rao and Thyagaraj, 2003). However, the wet-dry cycles might deteriorate the pozzolanic products and this may increase the clay size fractions. A similar finding was also reported by Rao *et al*. (2001), where they studied the variation in the percentage of the clay content of lime stabilized expansive soil when it was subjected to wet-dry cycles. It was reported that the reduced percentage of clay size fraction of stabilized soil has again started to increase with successive wet-dry cycles. However, it could not reach the percentage of clay content of its initial soil condition even after twenty wet-dry cycles.

The percentage reduction in clay size fraction of lime/ lime-fly ash slurry treated expansive soil was less when compared to the values reported by Rao and Thyagaraj (2003). However, in the present study, the percentage reduction of clay fraction was less due to the successive wet-dry cycles, and it is comparable with the work of Rao *et al*. (2001). Table 7.5 presents the variation in clay size fraction of lime, fly ash and lime-fly ash slurry treated expansive soil specimens.

Table 7.5 Comparison of Atterberg limits and grain size distribution of untreated expansive soil and slurry treated expansive soil specimens

Specimen condition	Sampling location	w_L (%)	w_P (%)	Ip (%)	w_S (%)	Grain size distribution (%)		
						Sand	Silt	Clay
Untreated	-	95	33	62	8.5	5	27	68
Lime slurry injected	0.9 d	76	40	36	10.5	5	46	49
	1.5 d	80	38	42	9	5	36	59
Fly ash slurry injected	0.9 d	91	35	56	8.5	5	29	66
	1.5 d	93	33	60	8.5	5	28	67
Lime-fly ash slurry injected	0.9 d	79	40	39	9.5	5	38	57
	1.5 d	84.5	36	48.5	9	5	33	62

The slurry treated expansive soil samples collected from different locations were pulverised and passed through 425 µm sieve for the determination of Atterberg limits. Table 7.5 summarises the variation in index properties of lime, fly ash and lime-fly ash slurry treated soil specimens. The liquid limit of lime slurry treated specimens reduced to 76-80%, and for lime-fly ash slurry treated specimens it reduced to 79-84.5%. The liquid limit of montmorillonite rich soil is mostly governed by diffuse double layer (DDL) thickness (Seed *et al*. 1964; Sridharan *et al*. 1986). Due to the increase in the pore salinity and lime-soil reactions, the DDL growth is suppressed, and results in a reduction in the liquid limit. However, in lime-fly ash slurry injection, the reduction in liquid limit is also influenced by the presence of non-plastic silt size fly ash particles. Similarly, the plasticity index of soil also decreased with slurry injection and it was determined as 36-42% for lime slurry and 39-48.5% for lime-fly ash slurry treated soil from the untreated plasticity index of 62%. Rao *et al*. (2001) also reported that the reduced values of liquid and plastic limits of the treated soil has again started to move towards the limits of untreated soil when subjected to wet-dry cycles.

Unconfined compressive strength

Figure 7.25 compares the stress-strain plots of untreated and treated expansive soil using lime, fly ash, and lime-fly ash slurry techniques of samples collected from a radial distance of 0.9d. For stabilized soil, it is expected to have higher strength due to the lime-soil reactions and this strength gain process continues even for a period of ten years (Little, 1995). However, in the present study the UCS values of treated soil samples remain almost closer to the values of untreated soil, and this behaviour was attributed to the loss of cementation during the wet-dry cycles. The results of pH and pore salinity also support this behaviour.

Symbol	Specimen condition	radial distance	ρ_d (Mg/m^3)	water content (%)	q_u (kPa)
—△—	Untreated	-	1.24	38.2	57
—○—	Lime	0.9 d	1.23	38.3	52
—✕—	Lime-FA	0.9 d	1.26	38	53
—◇—	FA	0.9 d	1.25	38.4	58

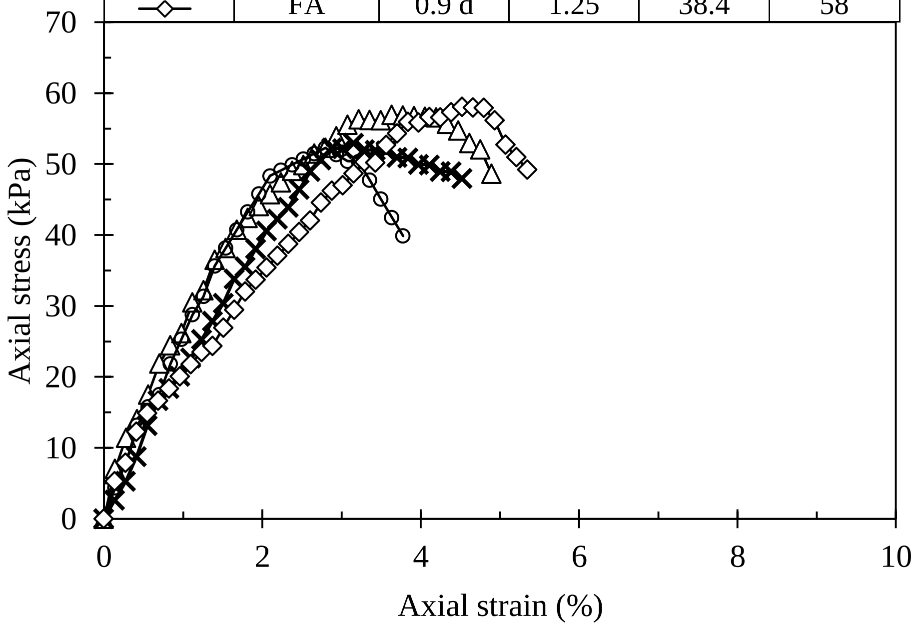

Figure 7.25: Stress-strain plots of untreated, lime, fly ash and lime-fly ash slurry treated expansive soil samples collected from a radial distance of 0.9d.

Thyagaraj and Zodinsanga (2014) showed that the UCS of lime precipitation decreases with increase in wet-dry cycles. Recently Chittori *et al*. (2017) also observed a similar variation in the lime treated soil during wet-dry cycles. However, the lime and lime-fly slurry treated soil specimen show a slight reduction in UCS value when compared to untreated soil, and this might be due to the increase in the silt content as shown in Figure 7.24. With an increase in the percentage of non-plastic silt in the native expansive soil, the UCS value may decrease (Sridharan *et al*. 1997).

Figure 7.26 shows the image where presence of lime-fly ash slurry seams in the UCS specimens after testing the soil specimen. The stress-strain plots of treated soil collected from radial distance 1.5d is shown in Figure 7.27. The behaviour is similar to the behaviour of specimens collected from 0.9d radial distance.

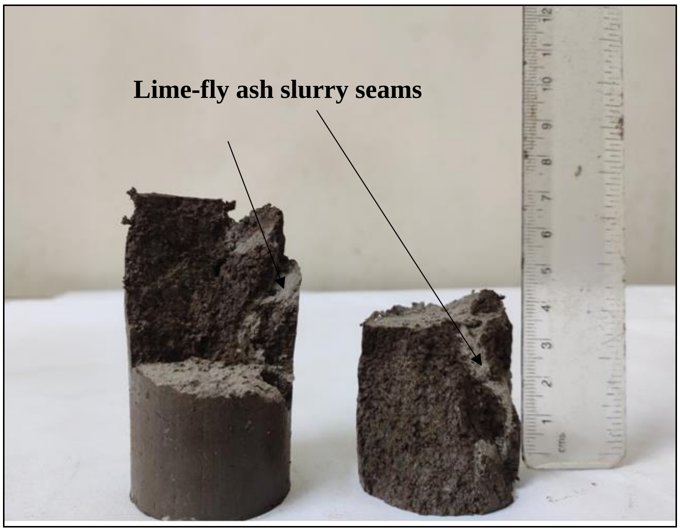

Figure 7.26: Traces of lime-fly ash slurry seams in the treated soil specimen cored at radial distance of 0.9d from the central hole in the test tank.

Free swell index and desiccated state free swell

Additional tests like free swell index (FSI) and desiccated state free swell (DSFS) were also conducted for determining the degree of soil expansion of slurry treated soils. For DSFS testing, undisturbed soil specimens were collected from the test tanks. The dry density of slurry treated soil was found to be 1.24 Mg/m^3 and water content as 38%. Table 7.6 compares the FSI and DSFS values of untreated and slurry treated soils. The degree of expansion of slurry treated soil was classified as medium swelling soil as per free swell index values. However, when DSFS is used, the slurry treated soil was classified as high swelling soil.

Symbol	Specimen condition	radial distance	ρ_d (Mg/m^3)	water content (%)	q_u (kPa)
△	Untreated	-	1.24	38.2	57
─○─	Lime	0.9 d	1.24	37.5	59
─✕─	Lime-FA	0.9 d	1.28	38.2	60
─◇─	FA	0.9 d	1.26	37.7	60

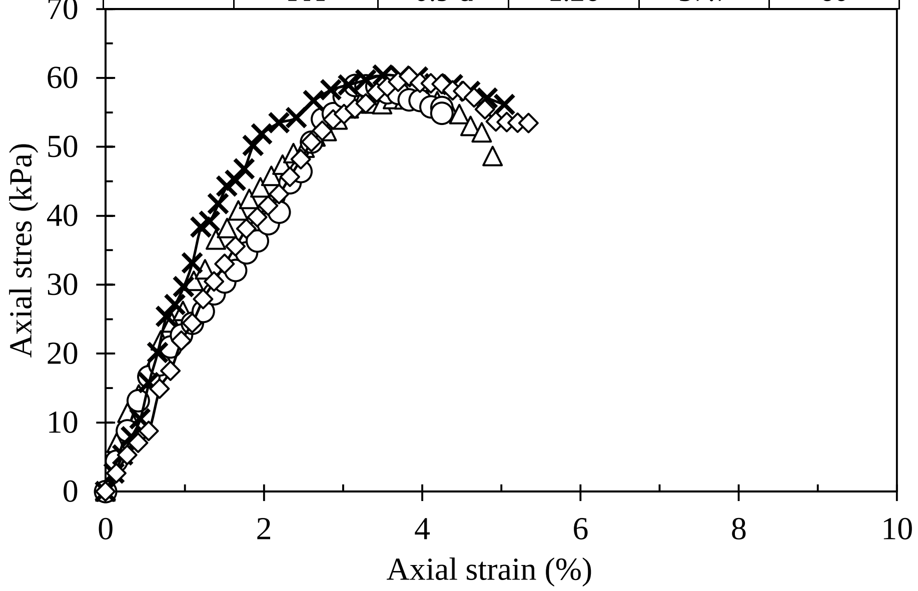

Figure 7.27: Stress-strain plots of untreated, lime, fly ash and lime-fly ash slurry treated expansive soil samples collected from a radial distance of 1.5d.

Table 7.6 FSI and DSFS tests on treated soils subjected to wet-dry cycles.

Specimen condition	Sampling location	FSI (%)	DSFS (%)	Degree of soil expansion	
				FSI	DSFS
Untreated	-	95	176	Medium	High
Lime slurry	0.9 d	61	127	Medium	High
	1.5 d	75	145	Medium	High
Fly ash slurry	0.9 d	75	171	Medium	High
	1.5 d	80	171	Medium	High
Lime -fly ash slurry	0.9 d	66	155	Medium	High
	1.5 d	70	165	Medium	High

7.4 SUMMARY AND CONCLUSIONS

A detailed laboratory study was carried out to bring out the effect of wetting and drying on the volumetric behaviour of untreated and lime, fly ash and lime-fly ash slurry treated expansive soil in large test tanks. The water-binder ratios adopted for the slurry injection were obtained from the mini-slump tests. The slump value using mini-slump cone was found to increase with increase in water-binder ratio, and beyond a particular point, the slump almost remained constant. For the present study, the water-binder ratio for fly ash and lime-fly ash slurry preparation was selected as the preceding point of the corresponding optimum water binder ratio. The following conclusions are drawn from the present study.

i. The lime and lime-fly ash slurry injection reduced the volumetric deformations during the first wetting. The reduced volumetric deformation is attributed to both modification and cementation effects of the lime/ lime-fly ash slurry which makes the soil less plastic. However, the fly ash slurry injection could not control the volume change of expansive soil as the pH of fly ash slurry was not conducive for the cementation reactions to occur.

ii. Cyclic wetting and drying of slurry treated soils increased the volumetric deformations with increase in wet-dry cycles. This is attributed to the deterioration of cementitious products with wet-dry cycles which is evidenced with the decreased pH and pore salinity values of the slurry treated expansive soils. Similar changes were observed in the liquid limit, plasticity index and grain size distribution of treated soils. The slurry treatment also resulted in significant reduction of clay content.

iii. The unconfined compressive strength of treated soils did not show much deviation from the unconfined compressive strength of untreated soil and this is attributed to the deterioration of the cementation bonds. However, the lime and lime-fly slurry treated soils showed a slight reduction in the UCS from the UCS value of untreated soil due to the increase in the silt content of the soil.

iv. Comparing the volumetric behaviour and properties of lime, fly ash and lime-fly ash slurry injection treated expansive soils, it can be concluded that the fly ash slurry treatment is not effective in controlling the volumetric behaviour owing to the low lime contents in fly ash. However, the lime-fly ash slurry treatment is as effective as lime slurry treatment in controlling the volumetric behaviour of expansive soil.

The present experimental results clearly show that both lime and lime-fly ash slurry improved the volumetric behaviour significantly during the first and second wet-dry cycles. However, the efficacy of the treatment decreased during the subsequent wet-dry cycles. It should be noted here that the slurry treated soils in the laboratory were subjected to extreme wetting and drying conditions, whereas such extreme conditions are unlikely to occur in the field after construction of the engineering structures. Therefore, in cases where the expansive soil is subjected to partial wet-dry cycles, both lime and lime-fly ash slurry injection are useful for controlling the volume change of expansive soils during wet-dry cycles as well.

Further, the effectiveness of lime and lime-fly ash slurry injection in controlling the volume change during wet-dry cycles depends on the extent of desiccation cracks developed just before the slurry injection. As the present laboratory study was carried out on compacted expansive soil just after the first drying cycle, the area of surface cracks developed in the desiccated expansive soil was limited to 8.63%. However, the present experimental results on untreated soil showed that the desiccation cracks increased with increase in wet-dry cycles, and after the third wet-dry cycle, the desiccation cracks increased to 17.7%. Thus it can be concluded that the extreme desiccation cracks occur only after third wet-dry cycle in the laboratory conditions and it would be more appropriate to carry out the lime/ lime-fly ash slurry injection after third wet-dry cycle to simulate the field conditions and to maximise the effectiveness of the slurry injection treatment as the contact volume of the expansive soil with lime/ lime-fly ash slurry increases.

CHAPTER 8

SUMMARY AND CONCLUSIONS

8.1 SUMMARY

The detrimental impact of expansive soils on lightly loaded structures is well known. In this connection, a case study was presented in the present thesis to further emphasize both the importance of characterization of expansive soils and selection of suitable ground improvement technique. In view of this, the main objective of the present thesis is to develop rapid methods of characterization for identification and classification of degree of soil expansivity and to stabilize expansive soil deposits using shallow and deep stabilization techniques.

A new method of characterization which is simple and rapid and also includes the placement conditions such as dry density and water content in the measurement of free swell was developed for the identification of expansive soils and classification of the degree of soil expansivity. The method uses the undisturbed (or compacted) soil specimens of 27.5 mm diameter and 14 mm thick so that the specimens exactly fit into 100 ml measuring jars and height corresponds to 10 cm^3 of soil volume. A total of 21 soils with a wide range of plasticity index were selected and used for the present experimental work. The correlation between the index tests such as liquid limit, plasticity index, free swell index and oedometer swell potential and the free swell measured using this method from the desiccated state was found to be good. The proposed method is termed as Desiccated State Free Swell (DSFS) method. Based on the present experimental results, a table and a chart for identification and classification of degree of soil expansivity were developed. The proposed chart of soil expansivity was validated using 10 additional undisturbed soil specimens collected from the field.

One-dimensional swell-consolidation test is a widely used test for obtaining the swell parameters as both swell potential and swell pressure can be obtained. Generally, swelling gets completed within 24 hours after inundation with water for most of the soils. However, some soils may take more than 24 hours. In order to overcome this time delay for saturation of the soil specimens, CRS cell with backpressure application was used for faster saturation during the swelling phase. Similarly, after reaching the equilibrium swell condition, the swollen soil specimens were subjected to consolidation using a constant rate of strain loading. Finally, the swell parameters obtained from this testing using CRS apparatus were compared with the swell parameters obtained from the conventional swell-consolidation method.

The shallow stabilization techniques for expansive soils are generally adopted where the active zone depth is shallow. Among the several shallow stabilization techniques, the placement of compensation materials is attractive if available in the nearby area due to their economy and ease of construction. However, the mechanisms of the compensating materials in stabilizing the expansive soils are not completely understood. Therefore, in the present study, an attempt is made to understand the mechanisms of compensating materials like sand, NSS, CNS and CSS in controlling the volume change of underlying expansive soil. The CSS was prepared by blending the expansive soil with 20% class C fly ash and 4% lime. A series of experiments were conducted to study the swell potential and swell pressure of expansive soil stabilized with compensating materials. Further to study the hydraulic properties of CNS material, the hydraulic conductivity tests using flexible wall permeameters and infiltration tests were carried out. Based on the experimental results obtained from the present study, an effort is made to understand the possible mechanisms of compensating materials in soil replacement technique.

For deep expansive soil deposits, lime pile, lime columns and lime slurry injection techniques are being used for stabilization of expansive soils. In order to understand the slurry injection technique in stabilizing the expansive soil during wet-dry cycles, a series of laboratory experiments were carried out using lime, fly ash and lime-fly ash slurries in desiccated state. These tests were performed in cylindrical tanks of 343 mm diameter and 360 mm height. A mini-slump cone apparatus was used to determine the water-binder ratio of the fly ash and lime-fly ash slurries. The slurries were injected through a central hole into the desiccated expansive soil and cured for 28 days. Then the slurry treated soils were subjected to wet-dry cycles in the test tanks under a seating pressure of 6.25 kPa to bring out the efficacy of stabilization. Further, after four wet-dry cycles, the soil specimens were collected from the test tank and the physico-chemical and index properties and unconfined compressive strength of treated soils was evaluated.

8.2 CONCLUSIONS

The main conclusions derived from the current research are summarised below:

8.2.1 Distress of an industrial building constructed on an expansive soil – a case study

1. Based on the field visit and laboratory study, it was found that the use of expansive soil as fill material in the construction was responsible for the distress in the building. In addition, water from the gardening and rainwater harvesting pits seeped through the quarry dust layer and infiltrated into the expansive layer and activated the swelling process.

2. It was suggested to remove the backfill soil at least to a depth of 1.2 m below the current floor level inside the building and replace it with a compensating material with the specification detailed in IS 9451-1994. The material should be compacted to a minimum of 95% of standard Proctor density.
3. To control the infiltration of water into the fill material and foundation soil, a minimum slope of 10% gradient shall be provided around the building. Further proper plinth protection could be ensured at least for a width of 2.0 m
4. To control the moisture fluctuations in the soil profiles, it was suggested to plant the saplings away from the periphery of the building. A minimum distance of 2.0 m for small shrubs and grass and 4.5 m for trees.

8.2.2 Development of rapid method for characterization of expansive soils

1. The proposed DSFS method is able to include the placement conditions such as dry density and water content in the measurement of swelling of soils. With increase in the dry density and water content, the DSFS increased owing to the use of desiccated soil specimens for testing.

2. The DSFS method proved to be advantageous over the FSI method as the testing time reduced drastically from 24-48 hours to 4-12 hours. The DSFS method can be performed even in the field without the requirement of any additional equipment with minimum effort.

3. The correlation between the proposed DSFS method and swell potential was found to be good with a R^2 value 0.96. Based on this correlation, a classification table is developed for the identification and classification of soil expansivity as given below.

Desiccated State Free Swell (%)	Degree of Soil Expansion
< 75	Low swelling
75-125	Medium swelling
125 - 400	High swelling
> 400	Very high swelling

4. Based on the results obtained from DSFS testing on 21 soils, a chart is proposed for the classification of degree of soil expansivity, presented below. This chart is also validated using the DSFS values obtained from the undisturbed soil specimens collected from different sites.

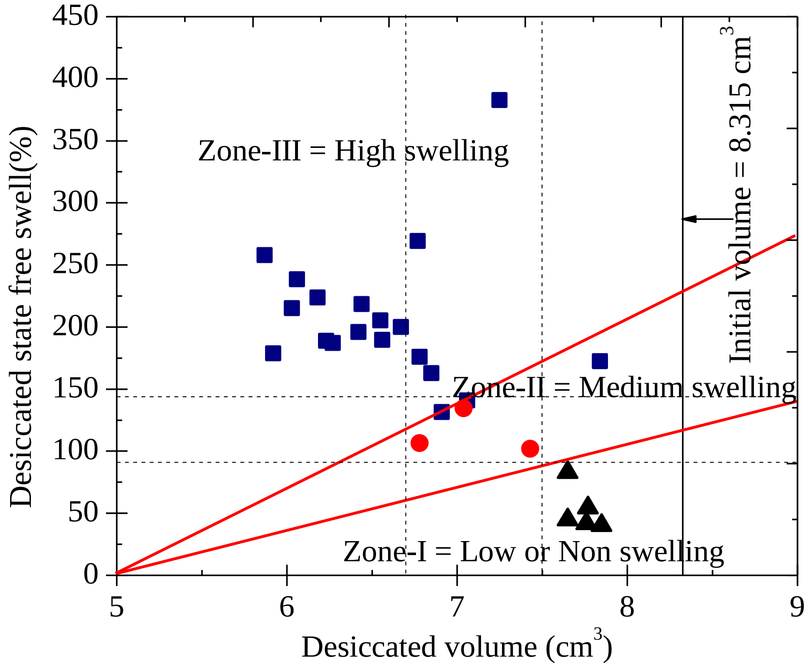

8.2.3 Accelerated method for measurement of swell potential and swell pressure of expansive soil using constant rate of strain apparatus

1. The magnitude of swell potential from CRS test method is about 19 to 34% higher than the swell potential values obtained from the conventional test method. The increase in the swell potential is due to better saturation due to the back pressure

application. Further, the time duration for the measurement of swell potential in the CRS test method is about 7 to 12 times faster than the time duration in the conventional test method, which involves incremental load application.

2. The swell pressure from the CRS test method is 6 to 24 % higher than the swell pressure from the conventional test method. The increase in swell pressure is attributed to the increase in the swell potential value resulted from better saturation. Further, the consolidation phase could be completed within 12 to 22 hrs, whereas in the conventional test method it took 72 - 96 hrs.

3. Overall the time duration for the measurement of swell potential and swell pressure is reduced to 7-13 times in the proposed CRS test method.

8.2.4 Mechanisms of compensating material in volume change control of underlying expansive soil

1. The swell pressure measurement using constant volume method showed a reduction in swell pressure of stabilized expansive soil irrespective of the compensating material used for stabilization. The reason for this reduction in swell pressure is attributed to the compression of compensating material and the corresponding volume change of underlying expansive soil. Therefore, the constant volume method may not be an appropriate method for the measurement of swell pressure of the two-layered soil system.

2. The CNS material placed over the expansive soil acts as a moisture barrier under low hydraulic gradients. The hydraulic conductivity and infiltration test results indicate the same observations in the laboratory conditions. Consequently, activation of swell occurs after a time lag during top saturation. However, the time lag reduces with the use of compensating materials with higher hydraulic conductivity than the CNS material and thus leading to early initiation of swell.

3. For a given soil profile, the formation of active zone varies due to the cyclic process of precipitation and infiltration and evaporation. The presence of any impervious material at the surface affects this cyclic process, and thus decreases the active zone depth. This in turn decreases the swell-shrink potentials of soils stabilized with impervious compensating materials. However, this needs further investigation through field scale study.

4. Placement of compensating materials control the volume change behaviour of expansive soils through various mechanisms such as removal and replacement, overburden stress, impervious nature, active zone variation and leaching of chemicals. The effectiveness of the each mechanism varies with the type of compensating material. However, for all the compensating materials the removal and replacement mechanism is the major mechanism controlling the swell-shrink movements of expansive soil. The mechanism of impervious nature of compensating material is next major contributing mechanism in case of CNS and CSS materials.

The present laboratory study reveals that the placement of compensating material is effective during the first wetting only, and its effectiveness decreased with successive wet-dry cycles. However, the testing protocol adopted for wetting and drying in the laboratory did not simulate the actual field conditions; wherein the two-layer system was subjected to full drying using a circumferential band heater over the oedometer cell at a constant temperature of 45°C. In contrast, in the field, desiccation of the expansive soil occurs after the desiccation of compacted CNS material. Moreover, the placement of CNS material leads to partial wet-dry cycles due to the reduced variation in moisture fluctuation and reduced depth of active zone. Further, the fluctuations in moisture content are higher at the surface and it decreases with depth in the active zone. Therefore, the placement of CNS material effectively controls the volume change behaviour of expansive soil in the field even when subjected to wet-dry cycles.

8.2.5 Deep stabilization of expansive soil using lime, fly ash and lime-fly ash slurry injection

1. The lime and lime-fly ash slurry injection reduced the volumetric deformations during the first wetting. The reduced volumetric deformation is attributed to both modification and cementation effects of the lime/ lime-fly ash slurry which makes the soil less plastic. However, the fly ash slurry injection could not control the volume change of expansive soil as the pH of fly ash slurry was not conducive for the cementation reactions to occur.
2. Cyclic wetting and drying of slurry treated soils increased the volumetric deformations with increase in wet-dry cycles. This is attributed to the deterioration of cementitious products with wet-dry cycles which is evidenced with the

decreased pH and pore salinity values of the slurry treated expansive soils. Similar changes were observed in the liquid limit, plasticity index and grain size distribution of treated soils. The slurry treatment also resulted in significant reduction of clay content.

3. The unconfined compressive strength of treated soils did not show much deviation from the unconfined compressive strength of untreated soil and this is attributed to the deterioration of the cementation bonds. However, the lime and lime-fly ash slurry treated soils showed a slight reduction in the UCS from the UCS value of untreated soil due to the increase in the silt content of the soil.

The present experimental results clearly show that both lime and lime-fly ash slurry injection improved the volumetric behaviour significantly during the first and second wet-dry cycles. However, the efficacy of the treatment decreased during the subsequent wet-dry cycles. It should be noted here that the slurry treated soils in the laboratory were subjected to extreme wetting and drying conditions, whereas such extreme conditions are unlikely to occur in the field after construction of the engineering structures. Therefore, in cases where the expansive soil is subjected to partial wet-dry cycles, both lime and lime-fly ash slurry injection may be useful for controlling the volume change of expansive soils during wet-dry cycles as well.

Further, the effectiveness of lime and lime-fly ash slurry injection in controlling the volume change during wet-dry cycles depends on the extent of desiccation cracks developed before the slurry injection. As the present laboratory study was carried out on compacted expansive soil just after the first drying cycle, the area of surface cracks developed in the desiccated expansive soil was limited to only 8.63%. However, the present experimental results on untreated soil showed that the desiccation cracks increased with increase in wet-dry cycles, and after the third wet-dry cycle, the desiccation cracks increased to 17.7%. Thus it can be concluded that the extreme desiccation cracks occur only after third wet-dry cycle in the laboratory conditions and it would be more appropriate to carry out the lime/ lime-fly ash slurry injection after third wet-dry cycle to simulate the field conditions and to maximise the effectiveness of the slurry injection treatment as the contact volume of the expansive soil with lime/ lime-fly ash slurry increases.

8.3 SCOPE FOR FUTURE STUDY

The present experimental work on stabilization of expansive soils using compensating materials was carried out in large diameter oedometers where the wetting was carried out from both top and bottom of the two-layer system. Further, the side wall leakage in the rigid wall oedometers provides easy access of water to the underlying expansive soil. Consequently, the swell-shrink potentials measured for the two-layered systems using different compensating materials were high. However, the infiltration occurs only from the top surface in the field condition. Therefore, the future studies can focus on designing the experimental test setup which eliminates the above drawbacks of side wall leakage and bottom saturation and the test setups should also simulate the field conditions as closely as possible. Further, pilot scale field studies can be carried out using proper instrumentation.

From the present study and the literature, it was found that the compensating materials stabilize the expansive soils through the following mechanisms, namely, removal and replacement, overburden stress, impervious nature, active zone variation and leaching of chemicals. Most of the above mechanisms are related to the alteration of active depth due to placement of compensating material. However, the variation in active depth due to placement of compensating materials cannot be simulated in the laboratory conditions using model studies owing to the scale of the problem and such information from the field studies is also not available. Therefore, future studies can be focused on bringing out the variations in active depth through field studies. These studies are expected to provide better understanding of the mechanisms of compensating materials in stabilizing the expansive soils and also improve the confidence levels when using the compensating materials.

REFERENCES

1. **AASHTO T 307-99** (2003). Standard method of test for determining the resilient modulus of soils and aggregate materials. AASHTO TS-1a.
2. **Ardani, A.** (1992) Expansive soil treatment methods in Colorado. Colorado Department of Transportation, Colorado, US.
3. **Ahnberg, H.,** and **S.E. Johansson** (2005) Increase in Strength with Time in Soils Stabilized with Different Types of Binder in Relation to the Type and Amount of Reaction Products. International Conference on Deep Mixing Best Practice and Recent Advances, Deep Mixing, May 23 – 25, Stockholm, Sweden, 195-202.
4. **Aitchison, G.D.** and **J.W. Holmes** (1953) Aspects of swelling in the soil profile. *Australian Journal of Applied Science*, **4**, 244-259.
5. **Al-Mukhtar, M., A. Lasledj** and **J.F. Alcover** (2010). Behaviour and minerology changes in lime treated expansive soil at 50˚ C. *Applied clay science*, **50**, 199 – 203.
6. **Al-Hamoud, A.S., A.A. Basma, A.I.H. Malkawi,** and **M.A. Al-Bashabsheh** (1995) Cyclic swelling behaviour of clays. *Journal of Geotechnical Engineering*, ASCE, **121(7)**, 562-565.
7. **Albrecht, K.A.** and **K. Cartwright** (1989) Infiltration and hydraulic conductivity of a compacted earthen liner. *Ground Water*, **27(1)**, 14-19.
8. **American Coal Ash Association** (1998) State Solid Waste Regulations governing the use of coal combustion products, ACCA, Alexandria, Virginia.
9. **ASTM C618-19**, Standard Specification for Coal Fly Ash and Raw or Calcined Natural Pozzolan for Use in Concrete, ASTM International, West Conshohocken, PA.
10. **ASTM D4546-12**, Standard Test Methods for One-Dimensional Swell or Collapse of Soils, ASTM International, West Conshohocken, PA.
11. **ASTM D4186-12**, Standard Test Method for One-Dimensional Consolidation Properties of Saturated Cohesive Soils Using Controlled-Strain Loading, ASTM International, West Conshohocken, PA.
12. **ASTM D5084-16**, Standard Test Methods for Measurement of Hydraulic Conductivity of Saturated Porous Materials Using a Flexible Wall Permeameter, ASTM International, West Conshohocken, PA.
13. **BS 13755-**5 (1990) Method of tests for soils for engineering purposes. Compressibility, permeability and durability tests. British Standards Institution, London.
14. **Bell, F. G.** (1976). The influence of the mineral content of clays on their stabilization by cement. *Bull AssocEngGeol*,**13(4)**, 267-278.

15. **Bell, F. G.** (1988) Stabilisation and treatment of clay soils with lime, Part 2 – Some applications. *Ground Engineering*, **21(2)**, 25-29.

16. **Bell, F. G.** (1993) Engineering Treatment of Soils. E & FN Spon, London.

17. **Benson, C.H., H. Zhai** and **X. Wang** (1994) Estimation of hydraulic conductivity of compacted clay liners. *Journal of Geotechnical and Geoenvironmental Engineering*, ASCE, **120(2)**, 366-387.

18. **Bharadwaj, A** (2013) Effect of soil replacement option on surface deflection for expansive clay profiles. *Ph.D. Dissertation*, Arizona state university.

19. **Bhuvaneshwari, S., R.G. Robinson,** and **S.R. Gandhi** (2019). Resilient modulus of lime treated expansive soil. *Geotechnical and Geological Engineering*, **37(1)**, 305-315.

20. **Boardman, D. I., Glendinning, S.** and **Rogers, C. D. F.** (2001). Development of stabilization and solidification in lime-clay mixes. *Geotechnique*, **50(6)**, 533-543.

21. **Bolt, G. H.,** (1956) Physico-chemical analysis of the compressibility of pure clays. *Geotechnique*, **6(2)**, 86-93,

22. **Bowles, L. E.** (2012). *Foundation analysis and design. McGraw-hill.*

23. **Briaud, J. L., X. Zhang,** and **S. Moon** (2003) Shrink test–water content method for shrink and swell predictions. *Journal of Geotechnical and Geoenvironmental Engineering*,ASCE, **129(7)**, 590-600.

24. **Broms, B. B., and P. Boman** (1979). Lime columns-a new foundation method. *Journal of Geotechnical Engineering*, **105(4)**, 539-556.

25. **Bushra, I.,** and **R.G. Robinson** (2013) Effect of fly ash on cement admixture for a low plasticity marine soil. *Advances in Civil Engineering Materials*, **2(1)**, 608-621.

26. **Central Electricity Board** (2017) Report on fly ash generation at coal/ lignite based thermal power stations and its utilization in the country. New Delhi, India.

27. **Chen, F.H.** (1965) The use of piers to prevent the uplifting of lightly loaded structures founded on expansive soil. Concluding Proc. Eng. Effects of Moisture changes in soil, Int. Res. Eng. Conf. Expansive Clay Soils, supplementing the symposium in Print, Texas A&M Press, 152-171.

28. **Chen, F.H.** (1975) *Foundations on expansive soils*. Elsevier Scientific Publishing Company, New York.

29. **Chen, F. H.** (1988) *Foundations on expansive soils*. Elsevier, New York.

30. **Chew, H., H. Takeda, K. Ichikawa** and **T. Hosoi** (1993) Chemico lime pile soil improvement used for soft clay ground. *Eleventh South East Asian Geotechnical Conference*, Singapore, 19-324

31. **Chittoori, B. C., A.J. Puppala,** and **A. Pedarla (2017).** Addressing clay mineralogy effects on performance of chemically stabilized expansive soils

subjected to seasonal wetting and drying. *Journal of Geotechnical and Geoenvironmental Engineering*, ASCE, **144(1)**, 04017097.

32. **Coduto, D.P.** (2013) Foundation Design: Principles and Practices. Pearson education.

33. **Cokca, E. (2001)** Use of Class C fly ashes for the stabilization of an Expansive soil. Journal of Geotechnical and Geoenvironmental Engineering. ASCE, 127, 568-573

34. **Croft, J. B.** (1967) The influence of soil mineralogical composition on cement stabilization. *Geotechnique*, **17(2)**, 119-135.

35. **Cuisinier, O.** and **D. Deneele (2008)** Long-term behaviour of lime-treated expansive soil subjected to wetting and drying. Unsaturated soils: Advances in Geo-Engineering. Taylor and Francis Group, London.

36. **Das, S. K.,** and **Yudhbir. (2005).** Geotechnical characterization of some Indian fly ashes. *Journal of Materials in Civil Engineering*, **17(5)**, 544-552.

37. **Day, R.W.** (1994) Swell-shrink behaviour of compacted clay. Journal of Geotechnical Engineering, **120(3)**, 618-623.

38. **Davidson, L.K., T. Demirel** and **R.L, Handy** (1965) Soil Pulverization and soil lime stabilization. *Highway Research Record*, **92**, 103-125.

39. **Dif, A.F.** and **W.F. Bluemel (1991)** Expansive soils under cyclic drying and wetting. *Geotechnical Testing Journal*, **14(1)**, 96-102.

40. **Dhowian, A. W. (1990)** Heave prediction techniques and design consideration on expansive soils. *Journal of King Saud University, Engineering Science,* **2 (2)**, 355-376.

41. **Drumm, E. C., Y. Boateng-Poku,** and **T.P. Johnson** (1990). Estimation of subgrade resilient modulus from standard tests. *Journal of Geotechnical Engineering*, **116(5)**, 774-789.

42. **Durkee, D.B** (2000) Active zone and edge moisture variation distance in expansive soils. *Ph.D Dissertation.* Colorado State University, Fort Collins Colorado.

43. **Edil, T.B., H.A. Acosta** and **C.H. Benson** (2006). Stabilizing soft fine grained soils with fly ash. *Journal of Materials in Civil engineering*, **18(2)**, 283-294.

44. **Estabragh, A. R., M.R.S. Pereshkafti, B. Parsaei** and **A.A. Javadi** (2013). Stabilised expansive soil behaviour during wetting and drying. *International Journal of Pavement Engineering*, **14(4)**, 418-427.

45. **Fityus, S. G., D.W. Smith** and **M.A. Allman** (2004). Expansive soil test site near Newcastle. *Journal of Geotechnical and Geoenvironmental Engineering*, ASCE, **130(7)**, 686-695.

46. **Fityus, S. G., D.A. Cameron** and **P.F. Walsh** (2005). The shrink swell test. *Geotechnical Testing Journal*, **28(1)**, 92-101.

47. **Fredlund, D. G.** (1969). Consolidometer test procedural factors affecting swell properties. *In Proceedings of the Second International Conference on Expansive Clay Soils*, Texas A & M Press, College Station, TX, 435-456**.**

48. **Fredlund, D. G.,** and **H. Rahardjo** (1993). Soil mechanics for unsaturated soils. John Wiley & Sons.

49. **Freeman, T.J., R.M. Driscoll R.M** and **G.S. Little** (2002) Has Your House Got Cracks? A Homeowner's Guide to Subsidence and Heave Damage. Thomas Telford Ltd. London, UK.

50. **Glendinning, S.** and **C.D.F. Rogers** (1996). Deep stabilisation using lime. Lime Stabilisation. London: Thomas Telford, 127-136

51. **Guney, Y., D. Sari, M. Cetin** and **M. Tuncan** (2007) Impact of cyclic wetting – drying on swelling behavior of lime stabilized soil. *Building and Environment*, **42**, 681-688.

52. **Hameed, R.A (1991)** *Characterization of expansive soils in the eastern province of Saudi arabia.* Master of science, Thesis, King Fahd University of Petroleum and Minerals. Dhahran, Saudi Arabia

53. **Harrison, H. G,** and **Davidson, D. T.** (1960). Lime fixation in clayey soils. *Highway Research Board Bulletin*, **262**, 20-32.

54. **Hardy, R. M.,** (1965) Identification and performance of swelling soil types. *Canadian Geotechnical Journal*, **2(2)**, 141-153.

55. **Head, K. H.,** (1998) Manual of soil laboratory testing - Effective stress tests (Vol 3). John Wiley and Sons Ltd. England.

56. **Herrin, M.** and **H. Mitchell (1961)** Lime-soil mixtures.Highway Research Board Bulletin, **304**, 99-138.

57. **Hewayde, E., E.H. Naggar** and **N. Khorshid** (2005). Reinforced lime columns: a new technique for heave control. *Ground Improvement*, **9(2)**, 79-87.

58. **Holtz, W. G.** and **H.J. Gibbs** (1956) Engineering Properties of Expansive Clays. Trans. ASCE, **121(1)**, 641–663.

59. **Holtz, W.G.** (1959). Expansive clays- properties and problems. Quat. Colorado School Mines, **54(4)**, 448-468.

60. **Holtz, W. G.** (1969) Volume change in expansive soils and control by lime treatment. *Proceedings of the Second International Conference on Expansive soils*, Texas, 157-174.

61. **Holtz, W.G.** and **S.S. Hart** (1978) Home construction on shrinking and swelling soils. National Science Foundation, Washington DC. Denver: Colorado Geological Survey.

62. **Holtz, W.G.** (1983) The influence of vegetation on the swelling and shrinkage of clays in the United States of America. *Geotechnique,* **33(2)**, 159-163.

63. **Holtz, R. D., W.D. Kovacs** and **T.C. Sheahan** (2011) An introduction to geotechnical engineering. Pearson Education.

64. **IS 2720-3** (1980) Indian standard method of test for soils: Determination of specific gravity of fine-grained soils. Bureau of Indian Standards, New Delhi, India

65. **IS 2720-5** (1985) Indian standard method of test for soils: Determination of liquid limit and plastic limit. Bureau of Indian Standards, New Delhi, India.

66. **IS 2720-6** (1972) Indian standard method of test for soils: Determination of shrinkage factors. Bureau of Indian Standards, New Delhi, India.

67. **IS 2720-7 (1980)** Indian standard method of test for soils: Determination of water content-dry density relation using light compaction. Bureau of Indian Standards, New Delhi, India.

68. **IS 2720-26** (1987) Indian standard method of test for soils: Determination of pH value. Bureau of Indian Standards, New Delhi, India.

69. **IS 2720–40** (1977) Indian standard method of test for soils Determination of free swell index of soils. Bureau of Indian standards, New Delhi, India.

70. **IS 2720-41**(1997) Indian standard method of test for soils Measurement of swelling pressure of soils. Bureau of Indian standards, New Delhi, India.

71. **IS 9451** (1994) Guidelines for lining of canals in expansive clay. Bureau of Indian Standards, New Delhi.

72. **IS 1498** (1970) Classification and identification of soils for general engineering purposes. Bureau of Indian Standards, New Delhi.

73. **IS 1892** (1979) Code of practice for subsurface investigation for foundations. Bureau of Indian Standards, New Delhi.

74. IS 2911-III (1985) Code of practice for design and construction of pile foundations. Bureau of Indian Standards, New Delhi.

75. **Ingles, O.G. and J.B. Metcalf** (1972) Soil stabilization. Butterworth, Sydney, Australia.

76. **Julina, M.** (2018) Effect of wet-dry cycles and interacting fluid on volume change and hydraulic behaviour of compacted clay liners. *Ph.D. Dissertation.* Indian Institute of Technology –Madras, Chennai, India.

77. **Julina, M.,** and **T. Thyagaraj** (2018). Determination of volumetric shrinkage of an expansive soil using digital camera images. *International Journal of Geotechnical Engineering*, 1-9.

78. **Justo, J. L., A. Delgado** and **J. Luiz** (1984) The influence of stress-path in the collapse-swelling of soils at the laboratory, *Proceedings of Fifth International conference on expansive soils*, Adelaide, Australia, 67–71.

79. **Kumar, B.R.,** and **R.S. Sharma** (2004) Effect of fly ash on engineering properties of expansive soils. *Journal of Geotechnical and Geoenvironmental Engineering*.

ASCE, **130(7)**, 74-767

80. **Kantro, D.L**. (1980) Influence of water-reducing admixtures on properties of cement paste – a miniature slump test. *Cement concrete and Aggregates*, **2(2)**, 95–102.

81. **Katti, R.K.** (1978) Search for solutions to problem in Black cotton soil. *Indian Geotechnical Journal*, **9**, 1-88.

82. **Katti, R.K.** and **A.R. Katti** (1994) Behaviour of saturated expansive soil and control methods. Central Board of Irrigation and Power. New Delhi.

83. **Katti, R.K.., H.B. Laad, S.K. Kulkarni** and **R.K. Lal** (1969) Studies on mechanics of expansive soil media and its application to certain field problems. *Proceedings of symposium on Characteristics of and construction Techniques in Black cotton Soil*, Poona, India, 49-61.

84. **Katti, R. K.** and **J.M. Kate** (1975) Role of micro particles in interaction between CNS layer and underlying expansive soil media. *Proceedings of the Fifth Asian Regional Conference on Soil Mechanics and Foundation Engineering*, Bangalore, India. 15–18**.**

85. **Kayes, I., D. Nissen** and **J. Adamson** (2000). Stabilisation of Rail Track Formation and Embankments, CORE2000 conference, RTSA, Glenelg, S.A.

86. **Keller, E.A.,** (2007) Introduction to environmental geology. Prentice Hall, Englewood Cliffs, NJ, USA.

87. **Khattabb, S.A.A., M. Al-Mukhtar** and **J.M. Fleureau** (2007) Long-term stability characteristics of a lime-treated plastic soil. *Journal of Materials in Civil Engineering*, **19(4)**, 358-366.

88. **Kitsugi, K.** and **R.H. Azakami** (1982) Lime column techniques for the improvement ofclay ground. *Symposium on Recent Development in Ground Improvement Techniques*, Bangkok, 105-115.

89. **Lambe, T. W.,** and **R.V. Whitman** (1979) Soil mechanics. John Wiley & Sons. New York**.**

90. **Lee, D.J.** and **J. Ian** (2012) Expansive Soils. *ICE Manual of Geotechnical Engineering*, Thomas Telford Ltd. UK,

91. **Lee, W., N.C. Bohra, A.G. Altschaeffl,** and **T.D. White** (1997). Resilient modulus of cohesive soils. *Journal of Geotechnical and Geoenvironmental Engineering*, ASCE, **123(2)**, 131-136.

92. **Li, D.,** and **E.T. Selig** (1994). Resilient modulus for fine-grained subgrade soils. *Journal of geotechnical engineering*, ASCE, **120(6)**, 939-957.

93. **Little, D. N. (1995)** Stabilization of pavement subgrades and base courses with lime. National Lime Association, USA**.**

94. **Madhyannapu, R.S., Puppala, A.J., S. Nazarian, S.**, and **D. Yuan,** (2010) Quality Assessment and quality control of deep soil mixing construction for stabilizing expansive subsoils. *Journal of Geotechnical and Geoenvironmental Engineering*, ASCE, **136(1)** , 119-128

95. **Mathew, K. P.,** and **S.N. Rao** (1997) Effect of lime on cation exchange capacity of marine clay. *Journal of Geotechnical and Geoenvironmental Engineering*, ASCE. 123, 183-185.

96. **Medhin, B.W** (1980) Swelling characteristics of expansive soils. *Ph.D Dissertation*, University of Washington, United States.

97. **Mehta, P. K.** (1983). Pozzolanic and cementitious byproducts as mineral admixtures for concrete-a critical review. Special Publication, **79**, 1-46.

98. **Mishra, A. K.,** and **A. Sridharan** (2017). A critical study on shrinkage behaviour of clays. *International Journal of Geotechnical Engineering*, 1-11.

99. **Mir, B.A.** and **A. Sridharan** (2013) Physical and compaction behaviour of clayey soil-fly ash mixtures. *Geotech. Geol. Eng*. **31(4)**, 1059-1072.

100. **Mitchell, J. K.,** and **K. Soga** (2005) Fundamentals of soil behavior. John Wiley & Sons.

101. **Miura, N., S. Horpibulsuk,** and **T.S. Nagaraj** (2001**).** Engineering behavior of cement stabilized clay at high water content**.** *Soils and Foundations***, 41(5),** 33-45**.**

102. **Mohammad, L. N., B. Huang, A.J. Puppala,** and **A. Allen** (1999). Regression model for resilient modulus of subgrade soils. *Transportation Research Record,* **1687(1)**, 47-54.

103. **Moseley, M.P.** and **K. Kirsch** (2004) Ground Improvement. Spon Press, Taylor and Francis.

104. **Moussa, A. A., Abd-el-Meguid, M. A., Okdah, S. M.,** and **Heikal, A. H.** (1985). Effect of sand cushion on swelling and swelling pressure of expansive silty clay. Proceedings of the eleventh international conference on soil mechanics and foundation engineering, San Francisco.

105. **Murthy, R.V**. and **G.V. Praveen** (2008) Use of chemically stabilized soil as cushion material below light weight structures founded on expansive soils. *Journal of materials in civil engineering*, ASCE, **20(5)**, 392 – 400.

106. **Nagaraj, H. B., M.M. Munnas** and **A. Sridharan (2009)** Critical evaluation of determining swelling pressure by swell-load method and constant volume method. *Geotechnical Testing Journal*, **32(4)**, 305-314.

107. **Nalbantoğlu, Z.** (2004). Effectiveness of class C fly ash as an expansive soil stabilizer. *Construction and Building Materials*, **18(6)**, 377-381.

108. **Nalbontaglu, N.**, and **E.R. Tuncer** (2001) Compressibility and Hydraulic Conductivity of Chemically treated expansive clay. *Canadian Geotechnical*

journal. **38**, 154-160.

109. **Nelson, J. D., K.C. Chao, D.D. Overton,** and **E.J. Nelson** (2015). Foundation engineering for expansive soils. John Wiley & Sons.

110. **Nelson, J.D.,** and **D.J. Miller** (1992) Expansive soils: Problems and Practise in Foundation and Pavement Engineering. John Wiley & sons.

111. **Nelson, J.D., D. Overton** and **Durkee D.** (2001) Depth of wetting and the Active Zone. Expansive clay soils and vegetative influence on shallow foundations, ASCE, 95-109

112. **Nelson, J. D., D.K. Reichler,** and **J.M. Cumbers** (2006) Parameters for heave prediction by oedometer tests. *Proceedings of Fourth International conference on unsaturated soils*. Arizona, United states, 951-961.

113. **Nelson, J.D.,** (2016) Time dependence of swelling in oedometer tests on expansive soil, *Proceedings of the fifteenth Asian regional conference on soil mechanics and geotechnical engineering*, Fukuoka, Kyushu, Japan. 490-493.

114. **Pandey, V. C.**, and **N. Singh** (2010) Impact of fly ash incorporation in soil systems. *Agriculture, ecosystems & environment*, **136(1)**, 16-27.

115. **Patil, N. G., P. Tiwary, D.K. Pal, T. Bhattacharyya, D. Sarkar, C. Mandal,** and **M. Lokhande** (2012). Soil water retention characteristics of black soils of India and pedotransfer functions using different approaches. *Journal of Irrigation and Drainage Engineering*, ASCE, **139(4)**, 313-324.

116. **Pejon, O. J.,** and **L.V. Zuquette,** (2006). Effects of strain on the swelling pressure of mudrocks. *International Journal of Rock Mechanics and Mining Sciences*, **5(43)**, 817-825.

117. **Porbaha, A.** (1998) State-of-the-art in Deep Mixing Technology, Part I: Basic Concepts and Overview of Technology. *Ground Improvement*, **2(2)**, 81-92.

118. **Prakash, K., A. Sridharan,** and **S.M. Rao** (1989). Lime addition and curing effects on the index and compaction characteristics of a montmorrillonitic soil. *Geotechnical Engineering*, **20(1)**, 39-47.

119. **Puppala, A. J., T. Manosuthikij,** and **B.C. Chittoori** (2013). Swell and shrinkage characterizations of unsaturated expansive clays from Texas. *Engineering Geology*, **164**, 187-194.

120. **Puppala, A. J., L.N. Mohammad,** and **A. Allen** (1996). Engineering behavior of lime-treated Louisiana subgrade soil. *Transportation Research Record*, **1546(1)**, 24-31.

121. **Puppala, A. J., E. Wattanasanticharoen,** and **K. Punthutaecha,** (2003) Experimental evaluations of stabilisation methods for sulphate-rich expansive soils. *Ground Improvement*, **7(1)**, 25-35.

122. **Puppala, A. J., R.S. Madhyannapu, S. Nazarian, D. Yuan** and **L. Hoyos** (2008) Deep soil mixing technology for mitigation of pavement roughness. Technical Report No. FHWA/TX-08/0-5179-1, Submitted to Texas Department of Transportation Research and Technology Implementation Office, The University of Texas at Arlington, Arlington, Texas.

123. **Rajasekaran, G.** and **S.N. Rao** (1996). Lime column technique for the improvement of soft marine clay. Grouting and deep mixing, Yonekura, 443-446.

124. **Rajasekaran, G.** and **S.N. Rao** (1997) Lime stabilisation technique for the improvement of marine clays. *Soils and Foundations*, **37**, 97-104.

125. **Raman, V.** (1967) Identification of expansive soils from plasticity index and shrinkage index data. *Indian Engineering*, Culcutta, India.

126. **Ramaswamy, S.V.** and **S.L. Narasimhan** (1979) Behaviour of buildings on expansive soils—some case histories. *Institution of Engineers (India)*, **58**, 141–46

127. **Ramaswamy, S. V.,** and **I.V. Anirudhan** (2009). Experience with expansive soils and shales in and around chennai. *Indian Geotechnical Society*, **2(7)**, 873-881.

128. **Rao, K.S.S** (2000). Swell-shrink behaviour of expansive soils-geotechnical challenges. *Indian Geotechnical Journal*, **30(1)**, 1-68.

129. **Rao, A.S.,** and **M.R. Rao** (2010) Behaviour of expansive soils under stabilized fly ash cushions during cyclic wetting and drying. *International Journal of Geotechnical Engineering*, **4(1)**, 111-118.

130. **Rao, K. S., S.M. Rao** and **S. Gangadhara** (2000). Swelling behavior of a desiccated clay. *Geotechnical Testing Journal*, **23(2)**, 193-198.

131. **Rao, M. R., A.S. Rao** and **R.D. Babu** (2008). Efficacy of cement-stabilized fly Ash cushion in arresting heave of expansive soils. *Geotechnical and Geological Engineering*, **26(2)**, 189-197.

132. **Rao, R. R., H. Rahardjo,** and **D.G. Fredlund** (1988). Closed-form heave solutions for expansive soils. *Journal of geotechnical engineering*, ASCE, **114(5)**, 573-588.

133. **Rao, S. N., G. Rajasekaran** and **C.V. Prasad** (1993). Lime column method of stabilization in a marine clay. *Eleventh South East Asian Geotechnical Conference*, 397-402.

134. **Rao, S. M., B.V.V. Reddy,** and **M. Muttharam** (2001). Effect of cyclic wetting and drying on the index properties of a lime-stabilised expansive soil. *Ground Improvement*, **5(3)**, 107-110.

135. **Rao, S. M.** and **P. Shivananda** (2002). Swelling behaviour of lime stabilized specimens subjected to wetting – drying cycles. Chemo Mechanical Coupling in Clays: From Nano Scale to Engineering Applications, 95-103.

136. **Rao, K. S.S., P.V. Sivapullaiah** and **J.V. Gurumurthy** (1994) An appraisal of CNS material as a cushion to reduce swelling potential. *Proceedings of the Indian*

Geotechnical Conference on Developments in Geotechnical Engineering, Warangal,**1**, 1 57–60**.**

137. **Rao, S. M.,** and **T. Thyagaraj** (2003). Lime slurry stabilisation of an expansive soil. *Geotechnical Engineering*, **156(3)**, 139-146.

138. **Rao, S. M.** and **B. Venkataswamy** (2002). Lime pile treatment of black cotton soils. *Ground Improvement*, **6(2)**, 85-93

139. **Robnett, Q. L.** and **M.R. Thompson** (1976) Effect of lime treatment on the resilient behavior of fine-grained soils. *Transportation Research Record*, **560**,11-20.

140. **Sahoo, J. P.** and **P.K. Pradhan** (2010). Effect of lime stabilized soil cushion on strength behaviour of expansive soil. *Geotechnical and Geological Engineering***, 28(6),** 889-897.

141. **Sahoo, J., P. Pradhan** and **K. Rao** (2008). Behavior of stabilized soil cushions under cyclic wetting and drying. *International Journal of Geotechnical Engineering*, **2(2)**, 89-102.

142. **Satyanarayana, B.** (1969). Behavior of expansive soil treated or cushioned with sand. *Proceedings of Second International Conference on Expansive Soils*, Texas, 308-316.

143. **Seed, H. B., R.J. Woodward and R. Lundgren** (1962) Prediction of swelling potential for compacted clays, *Journal of the soil mechanics and foundations*, ASCE, **88(3)**, 53-88.

144. **Shuai, F. (1996)** Simulation of swelling pressure measurements on expansive soils. *Doctoral dissertation*, University of Saskatchewan, Canada.

145. **Singhal, S., S.L. Houston,** and **W.N. Houston** (2011) Effects of testing procedures on the laboratory determination of swell pressure of expansive soils. *Geotechnical Testing Journal*, **34(5)**, 476-488.

146. **Sivapullaiah, P.V., J.P. Prasanth,** and **A. Sridharan** (1996) Effect of fly ash on index properties of black cotton soil. *Soils and Foundations*, **36**, 97-103.

147. **Sivapullaiah, P.V.** and **P.H.P. Reddy** (2009) Fly ash to control alkali-induced volume change in soils. Ground Improvement**, 162(4),** 167-173.

148. **Sivapullaiah, P.V., K.S.S. Rao,** and **J.V. Gurumurthy** (2004) Stabilisation of rice husk ash for use as cushion below foundations on expansive clay. *Ground Improvement*, **8(4)**,137-149.

149. **Sivapullaiah, P.V., T.G. Sitharam,** and **K.S.S. Rao** (1987) Modified free swell index for Clays. *Geotechnical Testing Journal*, **10(2)**, 80-85.

150. **Sivapullaiah, P. V., A. Sridharan** and **V.K. Stalin** (1996) Swelling behaviour of soil bentonite mixtures. *Canadian Geotechnical Journal*, **33(5)**, 808-814.

151. **Sivapullaiah, P.V., A. Sridharan** and **B.K.V Raju** (2000). Role of amount and type of clay in the lime stabilization of soils. *Ground Improvement,* **4(1)**, 37-45.

152. **Skempton, A.W.** (1953) The colloidal activity of clay. *Proceedings of Third International Conference of Soil Mechanics and Foundation Engineering*, Switzerland.

153. **Soundara, B.** and **R.G. Robinson** (2009) Influence of test method on swelling pressure of compacted clay. *International Journal of Geotechnical Engineering*, **3(3)**, 439-444.

154. **Soni K.M.** (2009) Construction on expansive soils. Building and construction, NBM and CW, Athena Information solutions Pvt. Ltd, New Delhi.

155. **Sridharan, A.** and **Y. Gurtug** (2004) Swelling behaviour of compacted fine-grained soils. *Engineering geology*, **72(1-2)**, 9-18.

156. **Sridharan, A.** and **K. Prakash** (1998). Mechanism controlling the shrinkage limit of soils. *Geotechnical Testing Journal,* **21(3)**, 240-250.

157. **Sridharan, A.** and **K. Prakash** (2000) Classification procedures for expansive soils. *Geotechnical Engineering*. **143(4)**, 235- 240.

158. **Sridharan, A.** and **K. Prakash** (2007) Geotechnical engineering and characterisation of coal ashes. CBS Publications and Distributors, New Delhi.

159. **Sridharan A.** and **S.M. Rao** (1988) A scientific basis for the use of index tests in identification of expansive soils. *Geotechnical Testing Journal,* **11(3)**, 208-212.

160. **Sridharan, A., S.M. Rao** and **S. Joshi** (1990) Classification of expansive soils by Sediment volume method. *Geotechnical Testing Journal*, **13(4)**, 375-380.

161. **Sridharan, A., A.S. Rao,** and **P.V. Sivapullaiah** (1986) Swelling pressure of clays. *Geotechnical Testing Journal*, **9(1)**, 24-33.

162. **Sridharan, A., S.M. Rao,** and **N.S. Murthy** (1985) Free swell index of soils: a need for redefinition. *Indian Geotechnical Journal*, **15(2)**, 94–99.

163. **Sridharan, A., J. P. Prashanth** and **P.V. Sivapullaiah,** (1997). Effect of fly ash on the unconfined compressive strength of black cotton soil. *Ground Improvement,* **1(3)**, 169-175.

164. **Tang, C. S., A.M. Tang, Y.J. Cui, P. Delage, C. Schroeder** and **E. De Laure** (2011) Investigating the swelling pressure of compacted crushed-Callovo-Oxfordian claystone. *Physics and Chemistry of the Earth,* **36 (17-18)**, 1857-1866

165. **Terashi, M**. (2002a). Development of deep mixing machine in Japan, Proceedings of Deep Mixing Workshop 2002 in Tokyo, Port and Airport Research Institute and Coastal Development Institute of Technology.

166. **Terzaghi, K., R.B. Peck** and **G. Mesri** (1996). Soil mechanics in engineering practice. John Wiley & Sons.

167. **Thompson, M.R.,** and **Q.L. Robnett** (1979). Resilient properties of subgrade soils. *Journal of Transportation Engineering*, ASCE, **105(1)**, 71–89.

168. **Thyagaraj, T** (2001). Laboratory studies on in-situ chemical stabilization of black cotton soil. *MSc. Dissertation*, Indian Institute of science, Bangalore, India

169. **Thyagaraj, T.** and **S.P. Suresh** (2012) In-situ Stabilization of an expansive soil in desiccated state. *International Journal of Geotechnical Engineering*, **6(3)**, 287-296.

170. **Thyagaraj, T**. and **S. Zodinsanga** (2014). Swell–shrink behaviour of lime precipitation treated soil. *Ground Improvement,* **167(4)**, 260-273.

171. **Townsend, F. C.,** and **E.E. Chisolm,** (1976). Plastic and resilient properties of heavy clay under repetitive loading (No. WES-TR-S-76-16). Army engineer waterways experiment station vicksburg miss.

172. **Todd, D.K.** (1980) Ground Water Hydrology. Wiley, New York,USA

173. **Tripathy, S., K.S. Rao** and **D.G. Fredlund** (2002). Water content-void ratio swell-shrink paths of compacted expansive soils. *Canadian Geotechnical Journal*, **39(4)**, 938-959.

174. **Tsytovich, N. A., M. Abelev** and **I.G. Takhirov** (1971) Compacting saturated loess by means of lime pile. *Proceedings Fourth International Conference on Soil Mechanics and Foundation Engineering*, Budapest, 837-842.

175. **Tu. H.** (2015) Prediction of the variation of swelling pressure and 1-D heave of expansive soils with respect to suction. *MSc. Dissertation*, University of Ottawa, Canada.

176. **Van der Merwe, D. H.**, **A.P. Steyn** and **F. Hugo** (1980) The pre-treatment of clay soils for road construction. Int. conf. Expansive Soils, ASCE, 361-382.

177. **Vanapalli, S.** and **L. Lu** (2012) A state-of-the art review of 1-D heave prediction methods for expansive soils. *International Journal of Geotechnical Engineering*, **6 (1)**, 15-41.

178. **Vanapalli, S.K., Lu Lu** and **W.T. Oh** (2010). Estimation of swelling pressure and 1-D heave in expansive soils. *Proceedings of the* 5_{th} *International Conference on Unsaturated Soils.*

179. **Villar, M. V.** and **A. Lloret** (2008) Influence of dry density and water content on the swelling of a compacted Bentonite. *Applied Clay Science*, **39 (1-2)**, 38-49.

180. **Wilkinson, A., A. Haque, J. Kodikara, D. Christie** and **J. Adamson** (2004) Stabilization of reactive subgrades by cementitious slurry injection–a review. *Australian Geomechanics Journal,* **39(4)**, 81-93.

181. **Wilkinson, A., A. Haque, J. Kodikara, J. Adamson** and **D. Christile** (2010). Improvement of Problematic soils by lime slurry pressure injection: case study. *Journal of Geotechnical and Geoenvironmental Engineering*, ASCE, **136(10)**, 1459-1468.

182. **Wilson, B. E., S.M. Sargand, G.A. Hazen,** and **R. Green** (1990). Multiaxial testing of subgrade. *Transportation Research Record*, 91-95

183. **Witczak, M.W.,** and **J. Uzan** (1988). The Universal Airport Design System, Report I of IV: Granular material characterization. Department of Civil Engineering, University of Maryland, College park.

184. **Yoshida, R. T., D.G. Fredlund** and **J.J. Hamilton** (1983). The prediction of total heave of a slab-on-grade floor on Regina clay. *Canadian Geotechnical Journal*, **20(1)**, 69-81.

185. **Yong, R.Y.,** and **B.P. Warkentin** (1966) Introduction to Soil Behaviour. The Macmillian Company, New York, US.

LIST OF PUBLICATIONS

I. REFEREED JOURNALS ON THE BASIS OF THIS THESIS

1. **Ashok Kumar, T., R.G. Robinson** and **T. Thyagaraj** (2018) Distress of an industrial building constructed on an expansive soil - a case study from India, *ICE Proceedings -Forensic Engineering*, **171(3)**, 121-126.
2. **Ashok Kumar, T., M.Raheena., R.G. Robinson** and **T.Thyagaraj** (2018) A rapid method of determination of swell potential and swell pressure of expansive soils using constant rate of strain apparatus. *Geotechnical Testing Journal* (Under Review).

II. PRESENTATIONS IN CONFERENCES (outside of thesis)

1. **Ashok Kumar, T., T. Thyagaraj,** and **R.G Robinson** (2018) Stabilization of swelling soils at higher water content using deep soil mixing method. *Proceedings of the Conference on Next frontiers in civil engineering: sustainable and resilient infrastructure,* IIT Bombay.77-78
2. **Ashok Kumar, T., T. Thyagaraj,** and **R.G Robinson** (2019) Effect of lime treatment on expansive soils at higher initial water content. *Proceedings of the 7th young geotechnical engineering conference*, NIT Silchar, Assam.